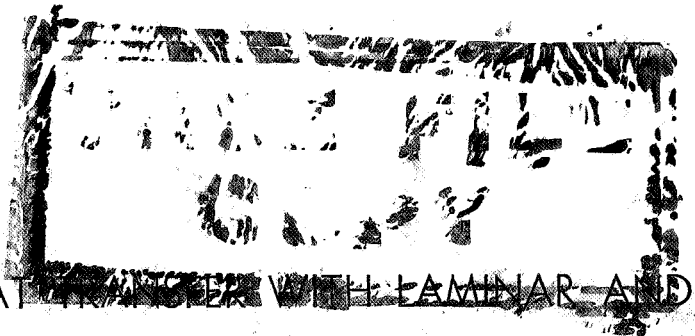

HEAT TRANSFER WITH LAMINAR AND TURBULENT FLOW BETWEEN PARALLEL PLANES WITH CONSTANT AND VARIABLE WALL TEMPERATURE AND HEAT FLUX

BY

P. A. McCUEN, W. M. KAYS, AND W. C. REYNOLDS

PREPARED UNDER GRANT NSG-52-60
FOR
THE NATIONAL AERONAUTICS AND SPACE ADMINISTRATION

REPORT NO. AHT-3

THERMOSCIENCES DIVISION
DEPARTMENT OF MECHANICAL ENGINEERING
STANFORD UNIVERSITY
STANFORD, CALIFORNIA

APRIL 12, 1962

HEAT TRANSFER WITH LAMINAR AND TURBULENT FLOW BETWEEN PARALLEL PLANES WITH CONSTANT AND VARIABLE WALL TEMPERATURE AND HEAT FLUX

By

P. A. McCuen, W. M. Kays, and W. C. Reynolds

Report No. AHT-3

Prepared Under Grant NSG 52-60

for

The National Aeronautics and Space Administration

Thermosciences Division
Department of Mechanical Engineering
Stanford University
Stanford, California

April 12, 1962

ACKNOWLEDGEMENTS

This report arises from a continuing project to which several persons have contributed substantially. The authors would like to acknowledge the contributions of each of them.

Raymond E. Lundberg has worked closely with us in the design and construction of the experiments and has contributed greatly to the solution of the general mathematical problem. Howard S. Heaton and Edward Y. W. Leung have performed valuable service in the design and construction of various parts of the experimental apparatus.

The authors gratefully recognize the National Aeronautics and Space Administration for their financial support of the program.

The construction of substantial portions of the test apparatus was very ably performed by Messrs. Frank McKinley, George Yoshida, and Tots Ikebe, and their efforts are greatly appreciated.

For his assistance in the conduct of the tests and the development of computer programs, sincere thanks are extended to Mr. Peter Donnelly. In this latter regard, the excellent services of the Stanford University Computation Center are also gratefully recognized.

Others who have contributed to the program include Messrs. Donald Flood, Percy Maung, Kwong Tack Dang, Frederick Test, Bruce Lazier, and Mum Bun Chan.

Finally, the authors would like to express their sincere thanks to Mrs. Virginia Blazer at Vidya, Inc. for her outstanding job of typing the manuscript.

ABSTRACT

The general problem treated is that of convective heat transfer in a parallel plane passage with both laminar and turbulent hydrodynamically fully established flow. With the assumptions that the fluid has constant properties and negligible viscous dissipation, internal energy generation, and axial conduction, the governing differential energy equation is solved for several basic wall boundary conditions. The resulting fundamental solutions can be superimposed to satisfy any wall temperature or heat flux boundary condition.

The fundamental boundary condition sets, or cases, are four in number. In each case the fluid and walls initially have a uniform zero temperature; then, at the "thermal entry," one of the following steps occurs:

1. The temperature at one wall is increased to unity, that at the other wall being held at zero;
2. The heat flux at one wall is increased to a non-zero constant, that at the other wall being held at zero;
3. The temperature at one wall is increased to unity, the heat flux at the other wall being held at zero;
4. The heat flux at one wall is increased to a non-zero constant, the temperature at the other wall being held at zero.

The solution of the four cases results in dimensionless wall temperatures, wall heat fluxes, and fluid mean temperatures; these are called "fundamental solutions," and their use in solving problems with arbitrary wall boundary conditions is described. These fundamental solutions are presented in tabular and graphical form for laminar flow, and for turbulent flow with $Pr = 0.70$ and

Re = 20,000, 30,000, and 50,000. The case of Pr = 0.01 is also considered for the fully developed temperature profile region.

The governing energy equation is reduced to two ordinary differential equations by separation of variables. One of these equations, together with its boundary conditions, constitutes a problem of the Sturm-Liouville type, and is solved by direct numerical integration. The resulting lower eigenvalues and constants are presented in tabular form. The higher eigenvalues and constants are determined by the WKBJ approximate solution and are also presented. An integral solution is set forth for use in the immediate vicinity of the thermal entry.

A facility for the experimental study of heat transfer between air and a non-isothermal parallel plane passage is described. Turbulent flow data gathered with the facility are presented for several wall boundary conditions and are compared with the theory predictions.

TABLE OF CONTENTS

INDEX TO THE FIGURES

INDEX TO THE TABLES

NOMENCLATURE

English letter symbols

A^+	a constant in the eddy diffusivity for momentum transfer expression, herein taken to be 26
c_p	specific heat at constant pressure, Btu/lb-^oF
C	a constant, defined where used
C_n	eigenconstant
D_h	hydraulic diameter, here $4y_o$, ft
f	a function, defined where used
f	friction factor, defined by (IV.B.9)
$g(\bar{y})$	function used in the WKBJ approximation
g_c^{-1}	constant of proportionality in Newton's Second Law, $(\text{lb-ft/\#-sec}^2)^{-1}$
G,H	arbitrary constants
h	convective heat-transfer coefficient, Btu/sec-ft^2-^oF
$h(\bar{y})$	variable used in the turbulent WKBJ approximation and Appendix A, defined by (IV.G.3)
I	incomplete gamma function
J	Bessel function of the first kind
k	thermal conductivity, Btu/sec-ft^2-^oF/ft
K	a constant in the eddy diffusivity for momentum transfer expression, herein taken to be 0.4
K_n	normalizing factor used in the Berry and de Prima iterations
$\dot{m}$	mass flow rate, lb/sec
n	outward normal coordinate from a wall, ft

Nu	Nusselt number, $\frac{hD_h}{k}$
Pr	Prandtl number, $\frac{\mu c_p}{k}$
q"	heat flux, Btu/sec-ft^2 (Note: q_w'' is positive when energy flows <u>from</u> the wall <u>to</u> the fluid.)
r	radial length coordinate, ft
r_o	circular tube radius, ft
r_o^+	normalized circular tube radius
Re	Reynolds number, $\frac{u_m D_h}{\nu}$
$S(\bar{y})$	a temperature shape profile, see (IV.B.27)
t	temperature, ^oF
u	velocity in the x direction, ft/sec
u_m	mean fluid velocity, ft/sec
$\bar{u}$	normalized velocity in the x direction, $\frac{u}{u_m}$
u^+	normalized velocity in the x direction, defined by (IV.B.16)
$w(\bar{y})$	weight function in the Sturm-Liouville equation
x	axial length coordinate, ft
$\bar{x}$	normalized axial length coordinate, $\frac{x}{D_h RePr}$
$X(\bar{x})$	function used in the separation of variables
y	transverse length coordinate, ft
y_o	parallel plane passage half-width, ft
$\bar{y}$	normalized transverse length coordinate, $\frac{y}{y_o}$

y^+ normalized transverse length coordinate, defined by (IV.B.8)

y_o^+ normalized parallel plane passage half-width, defined by (IV.B.8)

$Y_n(\bar{y})$ eigenfunction, used in the separation of variables

z normalized transverse length coordinate with origin at the lower wall, $1 + \bar{y}$

Greek letter symbols

α thermal diffusivity, $\frac{k}{\rho c_p}$, ft^2/sec

α a distance parameter, used in Appendix E only

γ parameter used in the turbulent WKBJ approximation, defined by (IV.G.19)

Γ gamma function

δ denotes incremental step of wall boundary condition

δ parameter used in the turbulent WKBJ approximation, defined by (IV.G.15)

ϵ_H eddy diffusivity for heat transfer, ft^2/sec

ϵ_M eddy diffusivity for momentum transfer, ft^2/sec

ζ normalized transverse length coordinate with origin at the upper wall, $1 - \bar{y}$

η normalized transverse length coordinate with origin at the lower wall, $1 + \bar{y}$

$\bar{\eta}$ normalized transverse length coordinate with origin at the upper wall, $1 - \bar{y}$

θ normalized temperature, defined for the four fundamental cases by (II.B.10, 11, 12, 13)

$\bar{\theta}$ normalized temperature, $\theta - \theta_{fd}$

λ_n eigenvalue

μ viscosity, lb/sec-ft

ν kinematic viscosity, $\frac{\mu}{\rho}$, ft^2/sec

ξ dummy normalized axial length coordinate

ξ similarity solution variable

ρ density, lb/ft^3

σ dummy variable

τ shear stress, $\#/ft^2$

τ_o wall shear stress, $\#/ft^2$

Φ normalized heat flux, defined for the four fundamental cases by (II.B.10, 11, 12, 13)

ϕ phase shift in the WKBJ solutions

ψ similarity solution function

ω dummy variable, defined by (E.4)

Subscripts

e thermal entrance, $\bar{x} = 0$

fd fully developed

i inner wall

m mixed mean

m summation index

n summation index

o outer wall

w wall, $\bar{y} = \pm 1$

I. INTRODUCTION

I. A. The Problem

The parallel planes geometry studied in this work is a mathematical idealization of an often-encountered heat-transfer surface geometry. It consists of two parallel planes of arbitrary finite spacing, arbitrary length, and infinite breadth, between which fluid flows in the lengthwise direction. The problem is a two-dimensional one, the physical occurrences in each imaginary plane normal to the breadth being identical.

The geometry is the limiting case of the circular annular passage as the radius ratio approaches unity, and of the rectangular passage as the aspect ratio becomes large. It is because it represents a mathematically simple approximation of these two physically realizable and practically important geometries that the parallel planes configuration is worthy of study.

Examples of heat-transfer systems that often can be represented by parallel planes include the nuclear power reactor with parallel plate fuel elements and the parallel fin extended surface heat exchanger. In the former case one normally wishes to compute surface temperatures from surface heat fluxes, while in the latter the reverse is true. Often the thermal "boundary conditions" will differ in magnitude at the two plates, and even vary in the flow direction. Indeed, it is not difficult to envision a situation in which the heat flux is known at one plate while the temperature is specified at the other. Thus it is seen that there are many possible heat-transfer problems pertinent to the parallel planes geometry.

I. B. Objective

The objective herein is to develop a simple and unified calculation technique and numerical values for the design

engineer to solve parallel plane steady-state convective heat-transfer problems of a wide variety of wall boundary conditions for the case in which the fluid has constant properties, a fully established velocity profile, and negligible viscous dissipation, internal energy generation, and axial conduction.

I. C. Summary

The general technique for solving parallel planes convective heat-transfer problems is developed in Section II. Use is made of the "fundamental solution" concept proposed by the author together with Reynolds, Lundberg, et al.[48] Numerical values of these fundamental solutions are calculated in Section III for laminar flow, and in Section IV for turbulent flow.

In Section V is reported experimental work conducted to verify certain assumptions inherent in the turbulent flow analysis.

Finally, conclusions are drawn from the analysis and some suggested areas for further study are outlined in Section VI.

Numerical examples of the use of the methods developed herein are to be found in Appendix D.

II. GENERAL FORMULATION OF THE PROBLEM AND THE CONCEPT OF THE FUNDAMENTAL SOLUTIONS

II. A. Discussion of the Problem

As set forth in the Introduction, it is the purpose of this study to develop solutions to problems of convective heat transfer between a fluid and a parallel planes passage for a wide variety of wall boundary conditions. Fortunately, the differential equation describing the temperature profile in the fluid is linear and homogeneous so it is quite unnecessary to solve the problem in detail for each possible boundary condition; indeed, this would be an impossible task since the number of possible boundary conditions is infinite. Rather, it is necessary only to restrict attention to the minimum number of boundary conditions required to construct all other boundary conditions by superposition. For the symmetric geometry of the parallel planes this minimum number is four. These four "building block" problems will be solved in detail in Sections III and IV and their solutions will be called "fundamental solutions."

The remainder of this section will be devoted to the development of the form of these fundamental solutions and to a discussion of the superposition technique by which these solutions can be used to solve the arbitrary wall boundary condition problem.

II. B. The Mathematical Formulation

The energy equation for flow between parallel planes is:

$$\frac{\partial}{\partial y}\left[\left(\alpha + \epsilon_H\right)\frac{\partial t}{\partial y}\right] = u\,\frac{\partial t}{\partial x} \qquad \text{(II.B.1)}$$

when the following restrictions are applied:

1. The velocity profile is fully established.

2. The fluid transport properties and density are constant.
3. Axial heat conduction, both molecular and eddy, is negligible.
4. Viscous energy dissipation is negligible.
5. Internal fluid energy generation is negligible.
6. Conditions are invariant with time.

Nondimensionalizing, the following definitions are used:

$$\bar{y} \triangleq \frac{y}{y_o} \quad \text{(see Fig. II.B.1)} \qquad \text{(II.B.2)}$$

$$\bar{x} \triangleq \frac{x}{D_h RePr} \quad (D_h = 4y_o \text{ for the parallel planes geometry}) \qquad \text{(II.B.3)}$$

$$\theta \triangleq \text{a suitably normalized temperature to be defined later} \qquad \text{(II.B.4)}$$

The coordinate system employed is defined in the figure below.

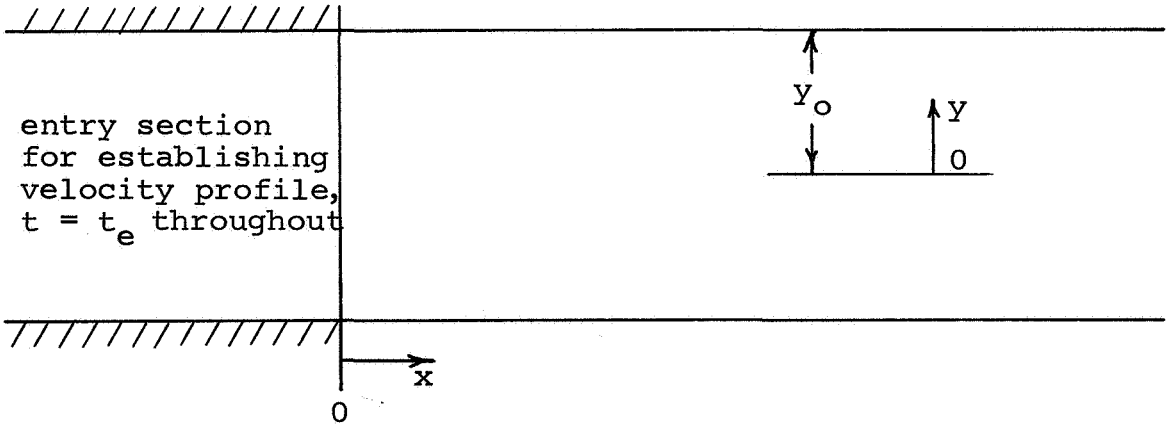

Figure II.B.1. Parallel Planes Coordinate System

Equation (II.B.1) then becomes

$$\frac{\partial}{\partial \bar{y}}\left[\left(1+\frac{\epsilon_H}{\nu}\,\mathrm{Pr}\right)\frac{\partial\theta}{\partial\bar{y}}\right]=\frac{u}{16u_m}\frac{\partial\theta}{\partial\bar{x}} \qquad \text{(II.B.5)}$$

where u_m is the mean fluid velocity, defined as

$$u_m \triangleq \frac{1}{2}\int_{-1}^{+1} u\, d\bar{y}$$

As stated in the Introduction, attention is to be focused on three general types of wall boundary conditions, namely: (1) temperature specified at each wall, (2) heat flux specified at each wall, and (3) temperature specified at one wall and heat flux specified at the other. With this aim in mind, the simplified boundary conditions listed below will be dealt with first.

Case 1	Case 2	
$t(0,\bar{y}) = t_e$	$t(0,\bar{y}) = t_e$	
$t(\bar{x},1) = t_w$	$q''(\bar{x},1) = q''_w$	(II.B.6,7)
$t(\bar{x},-1) = t_e$	$q''(\bar{x},-1) = 0$	

Case 3	Case 4	
$t(0,\bar{y}) = t_e$	$t(0,\bar{y}) = t_e$	
$t(\bar{x},1) = t_w$	$q''(\bar{x},1) = q''_w$	(II.B.8,9)
$q''(\bar{x},-1) = 0$	$t(\bar{x},-1) = t_e$	

Here t_w, q''_w, and t_e are not functions of distance. A dimensionless temperature and temperature derivative in the transverse direction will now be defined for each of the four cases.

Case 1

$$\theta^{(1)} \triangleq \frac{t - t_e}{t_w - t_e} \qquad \Phi^{(1)} \triangleq - D_h \frac{\partial \theta^{(1)}}{\partial n}$$

Case 2

$$\theta^{(2)} \triangleq \frac{t - t_e}{q''_w \frac{D_h}{k}} \qquad \Phi^{(2)} \triangleq - D_h \frac{\partial \theta^{(2)}}{\partial n} \qquad \text{(II.B.10,11)}$$

Case 3

$$\theta^{(3)} \triangleq \frac{t - t_e}{t_w - t_e} \qquad \Phi^{(3)} \triangleq - D_h \frac{\partial \theta^{(3)}}{\partial n}$$

Case 4

$$\theta^{(4)} \triangleq \frac{t - t_e}{q''_w \frac{D_h}{k}} \qquad \Phi^{(4)} \triangleq - D_h \frac{\partial \theta^{(4)}}{\partial n} \qquad \text{(II.B.12,13)}$$

Here n denotes the outward normal from the nearest wall. Note that n is not dimensionless, but has the units of length, like y. Recognizing that $q''_w = - k(\partial t/\partial n)$ the above boundary conditions and definitions can be combined to give the following conditions. (It should be noted that throughout this study q'' is taken as positive at a wall when the heat transfer is from the wall to the fluid, regardless of the wall under consideration.)

Case 1

$$\theta^{(1)}(0,\bar{y}) = 0$$

$$\theta^{(1)}(\bar{x},1) = 1$$

$$\theta^{(1)}(\bar{x},-1) = 0$$

Case 2

$$\theta^{(2)}(0,\bar{y}) = 0$$

$$\Phi^{(2)}(\bar{x},1) = 1 = 4 \frac{\partial \theta^{(2)}}{\partial \bar{y}} \qquad \text{(II.B. 14,15)}$$

$$\Phi^{(2)}(\bar{x},-1) = 0 = -4 \frac{\partial \theta^{(2)}}{\partial \bar{y}}$$

Case 3

$$\theta^{(3)}(0,\bar{y}) = 0$$

$$\theta^{(3)}(\bar{x},1) = 1$$

$$\Phi^{(3)}(\bar{x},-1) = 0 = -4\frac{\partial\theta^{(3)}}{\partial\bar{y}}$$

Case 4

$$\theta^{(4)}(0,\bar{y}) = 0$$

$$\Phi^{(4)}(\bar{x},1) = 1 = 4\frac{\partial\theta^{(4)}}{\partial\bar{y}} \qquad \text{(II.B. 16,17)}$$

$$\theta^{(4)}(\bar{x},-1) = 0$$

II. C. The Fundamental Solutions

The differential Equation (II.B.5) taken with each of the four sets of boundary conditions listed above specifies the four fundamental problems or cases to be solved. One is usually interested in the θ's or Φ's (the temperatures or heat fluxes) at a wall, and so the θ's and Φ's evaluated there will be referred to as fundamental solutions. In fact, a double subscript notation will be employed to specify these fundamental solutions, the first subscript denoting the wall at which the solution applies and the second denoting the wall at which the nonzero boundary condition applies. For example, $\theta_{io}^{(2)}$ will denote the non-dimensionalized temperature at the inner wall for the fundamental case of the second kind with the nonzero boundary condition specified at the outer wall. The inner wall-outer wall notation is used here to be consistent with that employed in the treatment of annular passages. Where applicable, in the development to follow the outer wall will be that at $\bar{y} = +1$.

The mixed-mean fluid temperatures are also of interest, and they will be denoted by the subscript m. For example, $\theta_{mo}^{(2)}$ will denote the non-dimensionalized mixed-mean fluid temperature for the fundamental case of the second kind with the nonzero boundary condition specified at the outer wall. These mean temperatures will also be called

fundamental solutions. From energy considerations, the mixed-mean temperature is given by

$$\theta_{mj}^{(k)} = \frac{1}{2u_m} \int_{-1}^{+1} \theta_j^{(k)} \, u \, d\bar{y} \qquad \text{(II.C.1)}$$

where k refers to the fundamental case, and j to the wall at which the nonzero boundary condition is applied. Actually, for the parallel planes geometry $\theta_{mo} = \theta_{mi}$ for all four fundamental cases. Throughout this study when only one i or o subscript is used it refers to the wall at which the nonzero boundary condition is applied.

The fundamental solutions to be sought are listed below. Note that the laminar flow solutions will differ from those for turbulent flow since the differential Equation (II.B.5) assumes a different form.

Fundamental solutions of the first kind

$$\Phi_{ii}^{(1)} = \Phi_{oo}^{(1)}$$

$$\Phi_{oi}^{(1)} = \Phi_{io}^{(1)}$$

$$\theta_{mi}^{(1)} = \theta_{mo}^{(1)}$$

Note: $\theta_{ii}^{(1)} = \theta_{oo}^{(1)} = 1$

$\theta_{io}^{(1)} = \theta_{oi}^{(1)} = 0$

Fundamental solutions of the second kind

$$\theta_{ii}^{(2)} = \theta_{oo}^{(2)}$$

$$\theta_{oi}^{(2)} = \theta_{io}^{(2)}$$

$$\theta_{mi}^{(2)} = \theta_{mo}^{(2)}$$

Note: $\Phi_{ii}^{(2)} = \Phi_{oo}^{(2)} = 1$

$\Phi_{io}^{(2)} = \Phi_{oi}^{(2)} = 0$

Fundamental solutions of the third kind

$$\Phi^{(3)}_{ii} = \Phi^{(3)}_{oo}$$

$$\theta^{(3)}_{oi} = \theta^{(3)}_{io}$$

$$\theta^{(3)}_{mi} = \theta^{(3)}_{mo}$$

Note: $\theta^{(3)}_{ii} = \theta^{(3)}_{oo} = 1$

$\Phi^{(3)}_{oi} = \Phi^{(3)}_{io} = 0$

Fundamental solutions of the fourth kind

$$\theta^{(4)}_{ii} = \theta^{(4)}_{oo}$$

$$\Phi^{(4)}_{oi} = \Phi^{(4)}_{io}$$

$$\theta^{(4)}_{mi} = \theta^{(4)}_{mo}$$

Note: $\Phi^{(4)}_{ii} = \Phi^{(4)}_{oo} = 1$

$\theta^{(4)}_{oi} = \theta^{(4)}_{io} = 0$

II. D. The Use of the Fundamental Solutions

In the body of this study the above fundamental solutions are determined for both laminar and turbulent flow. In this section it will be assumed that they are already in hand and their use will be demonstrated first for uniform wall boundary conditions, and then for axially varying wall boundary conditions.

1. Uniform wall boundary conditions

a. Temperature specified at each wall

Here the boundary conditions are

$$\begin{aligned} t(0,\bar{y}) &= t_e \\ t(\bar{x},1) &= t_{wo} \\ t(\bar{x},-1) &= t_{wi} \end{aligned} \qquad \text{(II.D.1)}$$

It is asserted that the solution to the problem specified by the differential Equation (II.B.1) together with the above boundary conditions is

$$t(\bar{x},\bar{y}) = \theta_o^{(1)}(\bar{x},\bar{y})\left(t_{wo} - t_e\right) + \theta_i^{(1)}(\bar{x},\bar{y})\left(t_{wi} - t_e\right) + t_e \qquad \text{(II.D.2)}$$

From Equations (II.B.1, 10, 14) and (II.D.1) it is seen that Equation (II.D.2) satisfies both the differential equation and the boundary conditions, and so must indeed be a solution of the problem.

It would normally be of interest to determine the wall heat fluxes and mean fluid temperature, and this can be done with the following equations:

$$q''_{wo}(\bar{x}) = \frac{k}{D_h}\left[\Phi_{oo}^{(1)}(\bar{x})\left(t_{wo} - t_e\right) + \Phi_{oi}^{(1)}(\bar{x})\left(t_{wi} - t_e\right)\right] \qquad \text{(II.D.3)}$$

$$q''_{wi}(\bar{x}) = \frac{k}{D_h}\left[\Phi_{io}^{(1)}(\bar{x})\left(t_{wo} - t_e\right) + \Phi_{ii}^{(1)}(\bar{x})\left(t_{wi} - t_e\right)\right] \qquad \text{(II.D.4)}$$

$$t_m(\bar{x}) = \theta_{mo}^{(1)}(\bar{x})\left(t_{wo} - t_e\right) + \theta_{mi}^{(1)}(\bar{x})\left(t_{wi} - t_e\right) + t_e \qquad \text{(II.D.5)}$$

These follow from Equations (II.B.10), (II.C.1), and (II.D.2).

b. Heat flux specified at each wall

Here the boundary conditions are

$$\begin{aligned} t(0,\bar{y}) &= t_e \\ q''(\bar{x},1) &= q''_{wo} \\ q''(\bar{x},-1) &= q''_{wi} \end{aligned} \qquad \text{(II.D.6)}$$

and, as in the preceding case, it can be seen that the following expression is a solution of the problem.

$$t(\bar{x},\bar{y}) = \frac{D_h}{k}\left[\theta_o^{(2)}(\bar{x},\bar{y})q''_{wo} + \theta_i^{(2)}(\bar{x},\bar{y})q''_{wi}\right] + t_e \quad \text{(II.D.7)}$$

Also

$$t_{wo}(\bar{x}) = \frac{D_h}{k}\left[\theta_{oo}^{(2)}(\bar{x})q''_{wo} + \theta_{oi}^{(2)}(\bar{x})q''_{wi}\right] + t_e \quad \text{(II.D.8)}$$

$$t_{wi}(\bar{x}) = \frac{D_h}{k}\left[\theta_{io}^{(2)}(\bar{x})q''_{wo} + \theta_{ii}^{(2)}(\bar{x})q''_{wi}\right] + t_e \quad \text{(II.D.9)}$$

$$t_m(\bar{x}) = \frac{D_h}{k}\left[\theta_{mo}^{(2)}(\bar{x})q''_{wo} + \theta_{mi}^{(2)}(\bar{x})q''_{wi}\right] + t_e \quad \text{(II.D.10)}$$

c. Temperature specified at one wall and heat flux specified at the other

It will be assumed that the temperature is specified at the "outer" wall. Then the boundary conditions are

$$\begin{aligned} t(0,\bar{y}) &= t_e \\ t(\bar{x},1) &= t_{wo} \\ q''(\bar{x},-1) &= q''_{wi} \end{aligned} \quad \text{(II.D.11)}$$

Here the fluid temperature is given by a combination of the third and fourth fundamental cases.

$$t(\bar{x},\bar{y}) = \theta_o^{(3)}(\bar{x},\bar{y})\left(t_{wo}-t_e\right) + \theta_i^{(4)}(\bar{x},\bar{y})q''_{wi}\frac{D_h}{k} + t_e \quad \text{(II.D.12)}$$

and

$$q''_{wo}(\bar{x}) = \Phi_{oo}^{(3)}(\bar{x})\frac{k}{D_h}\left(t_{wo} - t_e\right) + \Phi_{oi}^{(4)}(\bar{x})q''_{wi} \quad \text{(II.D.13)}$$

$$t_{wi}(\bar{x}) = \theta_{io}^{(s)}(\bar{x})\left(t_{wo} - t_e\right) + \theta_{ii}^{(4)}(\bar{x})\,\frac{D_h}{k}\,q''_{wi} + t_e \qquad \text{(II.D.14)}$$

$$t_m(\bar{x}) = \theta_{mo}^{(s)}(\bar{x})\left(t_{wo} - t_e\right) + \theta_{mi}^{(4)}(\bar{x})\,\frac{D_h}{k}\,q''_{wi} + t_e \qquad \text{(II.D.15)}$$

2. Axially varying wall boundary conditions

To illustrate the rationale behind the form of the solutions for axially varying wall boundary conditions, attention will be directed to the particular case of $t_{wi} = t_e$ and t_{wo} varying with $\bar{x}$ in a stepwise fashion (see Fig. II.D.1). Suppose now that one wished to evaluate the fluid temperature at some position $\bar{x}_1$. From (II.D.2) it appears that

$$\begin{aligned} t(\bar{x}_1,\bar{y}) = {} & \left[\theta_o^{(1)}(\bar{x}_1-\xi_1,\bar{y})\right]\delta t_{wo}(\xi_1) + \left[\theta_o^{(1)}(\bar{x}_1-\xi_2,\bar{y})\right]\delta t_{wo}(\xi_2) \\ & + \left[\theta_o^{(1)}(\bar{x}_1-\xi_3,\bar{y})\right]\delta t_{wo}(\xi_3) + \left[\theta_o^{(1)}(\bar{x}_1-\xi_4,\bar{y})\right]\delta t_{wo}(\xi_4) \\ & + t_e \qquad \text{(II.D.16)} \end{aligned}$$

In fact (II.D.16) does give the temperature distribution for the posed problem since the equation satisfies both the governing differential equation and the specified boundary conditions. (Note that $\theta_{oo}^{(1)} = 1$ and all fundamental solutions with negative $\bar{x}$ arguments are zero by definition.) The above equation can be written more simply as

$$t(\bar{x}_1,\bar{y}) = \sum_{n=1}^{4}\left[\theta_o^{(1)}(\bar{x}_1 - \xi_n,\bar{y})\right]\delta t_{wo}(\xi_n) + t_e \qquad \text{(II.D.17)}$$

and it can be seen that at any $\bar{x}$

$$t(\bar{x},\bar{y}) = \sum_{\substack{\text{all steps}\\ \text{before } \bar{x}}}\left[\theta_o^{(1)}(\bar{x} - \xi_n,\bar{y})\right]\delta t_{wo}(\xi_n) + t_e \qquad \text{(II.D.18)}$$

Now suppose one is confronted with a similar problem except that the temperature at the outer wall is a continuous function of $\bar{x}$ (or of the dummy variable ξ). One could approximate $t_{wo}(\xi)$ by a series of small steps such as depicted in Figure II.D.2; then $t(\bar{x},\bar{y})$ would be given by (II.D.18). And now, if the steps are made smaller and more numerous, in the limit the sum becomes an integral.

$$t(\bar{x},\bar{y}) = \int_{\xi=0}^{\xi=\bar{x}} \left[\theta_o^{(1)}(\bar{x} - \xi,\bar{y})\right] dt_{wo}(\xi) + t_e \qquad \text{(II.D.19)}$$

And now, to handle a wall temperature distribution made up of continuous curves and steps one simply evaluates the integral in (II.D.19) in the Stieltjes sense rather than in the ordinary Riemann sense; that is, one breaks the integral up into sums and integrals.*

The varying wall heat flux case is handled in a similar fashion. For the case of an adiabatic inner wall there results

$$t(\bar{x},\bar{y}) = \frac{D_h}{k}\int_{\xi=0}^{\xi=\bar{x}} \left[\theta_o^{(2)}(\bar{x} - \xi,\bar{y})\right] dq''_{wo}(\xi) + t_e \qquad \text{(II.D.20)}$$

It will be noted that this solution satisfies the governing differential equation and the specified boundary conditions.

The equations of interest for the three types of wall boundary conditions are set forth below in the same format as that employed for the uniform wall boundary conditions. Note that all integrals appearing must be evaluated in the Stieltjes sense.

---

*The reader is referred to References 21 and 30 for discussion of these methods as applied to the circular tube and the flat plate boundary layer.

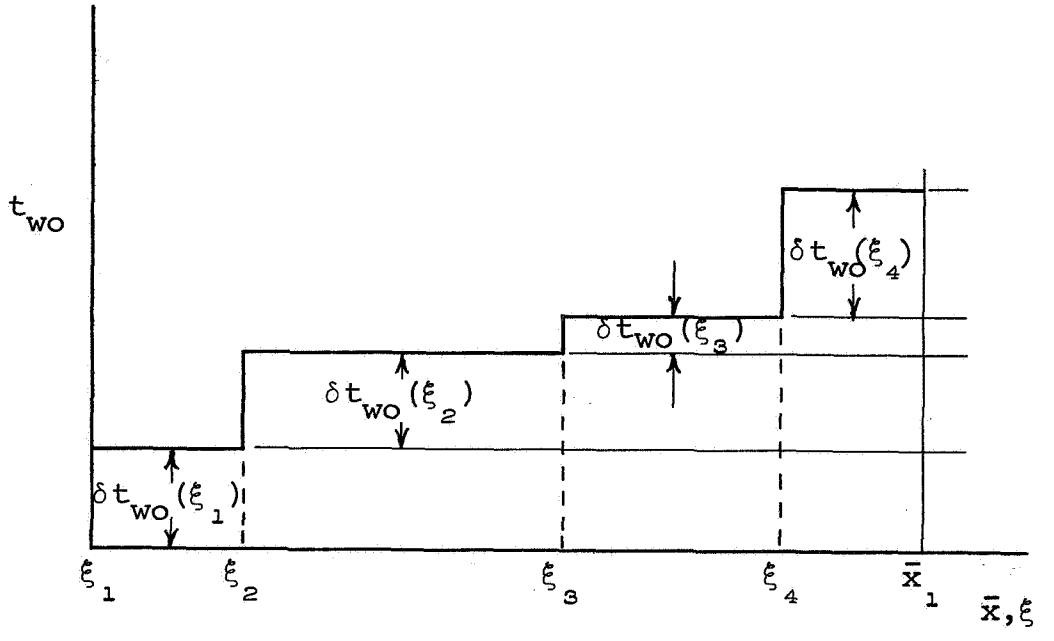

Figure II.D.1. Illustration of a Step Wall Temperature Distribution

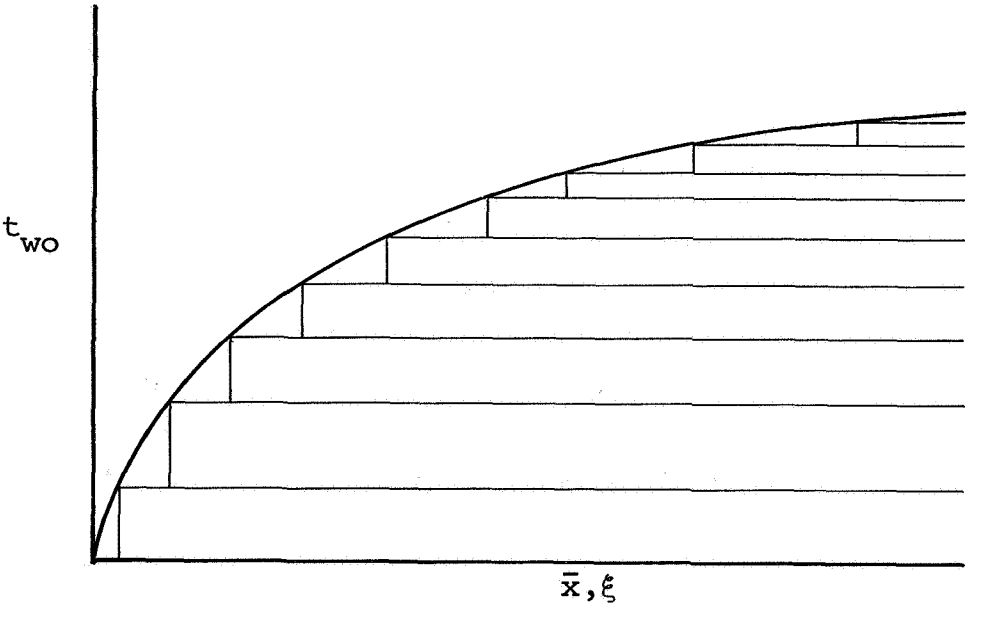

Figure II.D.2. Illustration of an Arbitrary Wall Temperature Distribution

a. Temperature specified at each wall

Here the boundary conditions are

$$t(0,\bar{y}) = t_e$$

$$t(\bar{x},1) = t_{wo}(\bar{x}) \qquad \text{(II.D.21)}$$

$$t(\bar{x},-1) = t_{wi}(\bar{x})$$

and the solutions are

$$t(\bar{x},\bar{y}) = \int_{\xi=o}^{\xi=\bar{x}} \left[\theta_o^{(1)}(\bar{x}-\xi,\bar{y})\right] dt_{wo}(\xi) + \int_{\xi=o}^{\xi=\bar{x}} \left[\theta_i^{(1)}(\bar{x}-\xi,\bar{y})\right] dt_{wi}(\xi) + t_e \qquad \text{(II.D.22)}$$

$$q''_{wo}(\bar{x}) = \frac{k}{D_h}\left\{ \int_{\xi=o}^{\xi=\bar{x}} \left[\Phi_{oo}^{(1)}(\bar{x}-\xi)\right] dt_{wo}(\xi) + \int_{\xi=o}^{\xi=\bar{x}} \left[\Phi_{oi}^{(1)}(\bar{x}-\xi)\right] dt_{wi}(\xi)\right\} \qquad \text{(II.D.23)}$$

$$q''_{wi}(\bar{x}) = \frac{k}{D_h}\left\{ \int_{\xi=o}^{\xi=\bar{x}} \left[\Phi_{io}^{(1)}(\bar{x}-\xi)\right] dt_{wo}(\xi) + \int_{\xi=o}^{\xi=\bar{x}} \left[\Phi_{ii}^{(1)}(\bar{x}-\xi)\right] dt_{wi}(\xi)\right\} \qquad \text{(II.D.24)}$$

$$t_m(\bar{x}) = \int_{\xi=o}^{\xi=\bar{x}} \left[\theta_{mo}^{(1)}(\bar{x} - \xi)\right] dt_{wo}(\xi)$$

$$+ \int_{\xi=o}^{\xi=\bar{x}} \left[\theta_{mi}^{(1)}(\bar{x} - \xi)\right] dt_{wi}(\xi) + t_e \qquad \text{(II.D.25)}$$

b. Heat flux specified at each wall

Here the boundary conditions are

$$t(0,\bar{y}) = t_e$$

$$q''(\bar{x},1) = q''_{wo}(\bar{x}) \qquad \text{(II.D.26)}$$

$$q''(\bar{x},-1) = q''_{wi}(\bar{x})$$

and the solutions are

$$t(\bar{x},\bar{y}) = \frac{D_h}{k}\left\{\int_{\xi=o}^{\xi=\bar{x}} \left[\theta_o^{(2)}(\bar{x} - \xi,\bar{y})\right] dq''_{wo}(\xi)\right.$$

$$\left. + \int_{\xi=o}^{\xi=\bar{x}} \left[\theta_i^{(2)}(\bar{x} - \xi,\bar{y})\right] dq''_{wi}(\xi)\right\} + t_e \qquad \text{(II.D.27)}$$

$$t_{wo}(\bar{x}) = \frac{D_h}{k}\left\{\int_{\xi=o}^{\xi=\bar{x}} \left[\theta_{oo}^{(2)}(\bar{x} - \xi)\right] dq''_{wo}(\xi)\right.$$

$$\left. + \int_{\xi=o}^{\xi=\bar{x}} \left[\theta_{oi}^{(2)}(\bar{x} - \xi)\right] dq''_{wi}(\xi)\right\} + t_e \qquad \text{(II.D.28)}$$

$$t_{wi}(\bar{x}) = \frac{D_h}{k}\left\{\int_{\xi=o}^{\xi=\bar{x}}\left[\theta_{io}^{(2)}(\bar{x}-\xi)\right]\,dq''_{wo}(\xi)\right.$$

$$\left.+\int_{\xi=o}^{\xi=\bar{x}}\left[\theta_{ii}^{(2)}(\bar{x}-\xi)\right]\,dq''_{wi}(\xi)\right\}+t_e \qquad \text{(II.D.29)}$$

$$t_m(\bar{x}) = \frac{D_h}{k}\left\{\int_{\xi=o}^{\xi=\bar{x}}\left[\theta_{mo}^{(2)}(\bar{x}-\xi)\right]\,dq''_{wo}(\xi)\right.$$

$$\left.+\int_{\xi=o}^{\xi=\bar{x}}\left[\theta_{mi}^{(2)}(\bar{x}-\xi)\right]\,dq''_{wi}(\xi)\right\}+t_e \qquad \text{(II.D.30)}$$

c. <u>Temperature specified at one wall and heat flux specified at the other</u>

Hwer the boundary conditions are

$$\begin{aligned} t(0,\bar{y}) &= t_e \\ t(\bar{x},1) &= t_{wo}(\bar{x}) \qquad \text{(II.D.31)} \\ q''(\bar{x},-1) &= q''_{wi}(\xi) \end{aligned}$$

and the solutions are

$$t(\bar{x},\bar{y}) = \int_{\xi=o}^{\xi=\bar{x}}\left[\theta_o^{(3)}(\bar{x}-\xi,\bar{y})\right]\,dt_{wo}(\xi)$$

$$+\frac{D_h}{k}\int_{\xi=o}^{\xi=\bar{x}}\left[\theta_i^{(4)}(\bar{x}-\xi,\bar{y})\right]\,dq''_{wi}(\xi)+t_e \qquad \text{(II.D.32)}$$

$$q''_{wo}(\bar{x}) = \frac{k}{D_h}\int_{\xi=o}^{\xi=\bar{x}} \left[\Phi_{oo}^{(3)}(\bar{x} - \xi)\right] dt_{wo}(\xi)$$

$$+ \int_{\xi=o}^{\xi=\bar{x}} \left[\Phi_{oi}^{(4)}(x - \xi)\right] dq''_{wi}(\xi) \qquad \text{(II.D.33)}$$

$$t_{wi}(\bar{x}) = \int_{\xi=o}^{\xi=\bar{x}} \left[\theta_{io}^{(3)}(\bar{x} - \xi)\right] dt_{wo}(\xi)$$

$$+ \frac{D_h}{k}\int_{\xi=o}^{\xi=\bar{x}} \left[\theta_{ii}^{(4)}(\bar{x} - \xi)\right] dq''_{wi}(\xi) + t_e \qquad \text{(II.D.34)}$$

$$t_m(\bar{x}) = \int_{\xi=o}^{\xi=\bar{x}} \left[\theta_{mo}^{(3)}(\bar{x} - \xi)\right] dt_{wo}(\xi)$$

$$+ \frac{D_h}{k}\int_{\xi=o}^{\xi=\bar{x}} \left[\theta_{mi}^{(4)}(\bar{x} - \xi)\right] dq''_{wi}(\xi) + t_e \qquad \text{(II.D.35)}$$

II. E. The General Nusselt Number Relations

It was brought out previously that the familiar Nusselt number is not emphasized in this work since it acquires the utility of the fundamental solutions only in several special cases of the wall boundary conditions. This fact will be demonstrated in the present section in which are derived the Nusselt number relations in terms of fundamental solutions for the four wall boundary condition cases. It is hoped that the reader who is experienced in working with the Nusselt modulus for problems of the type treated here will find this section useful for relating his experience to the fundamental solution results.

Uniform wall boundary condition Nusselt numbers will be derived for the four problem cases treated previously. In each case the wall denoted by the subscript "o" will be treated. For the parallel planes geometry, of course, identical results would be obtained for the wall referred to by the subscript "i."

By definition

$$Nu_o \triangleq \frac{h_o D_h}{k} \tag{II.E.1}$$

and

$$h_o \triangleq \frac{q''_{wo}}{t_{wo} - t_m} \tag{II.E.2}$$

Hence

$$Nu_o = \frac{D_h}{k}\left(\frac{q''_{wo}}{t_{wo} - t_m}\right) \tag{II.E.3}$$

1. Case one

Here the Nusselt number will be found for the case of a uniform temperature specified at each wall. Combining (II.D.3), (II.D.5), and (II.E.3) one obtains

$$Nu_o = \frac{\Phi_{oo}^{(1)}\left(t_{wo} - t_e\right) + \Phi_{oi}^{(1)}\left(t_{wi} - t_e\right)}{t_{wo} - t_e - \theta_{mo}^{(1)}\left(t_{wo} - t_e\right) - \theta_{mi}^{(1)}\left(t_{wi} - t_e\right)} \tag{II.E.4}$$

Hence

$$Nu_o = \frac{\Phi_{oo}^{(1)} + \Phi_{oi}^{(1)}\left(\frac{t_{wi} - t_e}{t_{wo} - t_e}\right)}{1 - \theta_{mo}^{(1)}\left[1 + \left(\frac{t_{wi} - t_e}{t_{wo} - t_e}\right)\right]} \tag{II.E.5}$$

2. Case two

For the case of a uniform heat flux specified at each wall, the Nusselt number is found by combining (II.D.8), (II.D.10), and (II.E.3).

$$Nu_o = \frac{q''_{wo}}{\theta^{(2)}_{oo} q''_{wo} + \theta^{(2)}_{oi} q''_{wi} - \theta^{(2)}_{mo} q''_{wo} - \theta^{(2)}_{mi} q''_{wi}} \qquad \text{(II.E.6)}$$

or

$$Nu_o = \frac{1}{\theta^{(2)}_{oo} + \theta^{(2)}_{oi} \left(\frac{q''_{wi}}{q''_{wo}}\right) - \theta^{(2)}_{mo} \left(1 + \frac{q''_{wi}}{q''_{wo}}\right)} \qquad \text{(II.E.7)}$$

3. Case three

Here the Nusselt number will be found at the wall at which a uniform temperature is specified, a uniform heat flux being specified at the other wall. From (II.D.13), (II.D.15), and (II.E.3)

$$Nu_o = \frac{\Phi^{(3)}_{oo} \left(t_{wo} - t_e\right) + \Phi^{(4)}_{oi} q''_{wi} \frac{D_h}{k}}{t_{wo} - t_e - \theta^{(3)}_{mo} \left(t_{wo} - t_e\right) - \theta^{(4)}_{mi} q''_{wi} \frac{D_h}{k}} \qquad \text{(II.E.8)}$$

or

$$Nu_o = \frac{\Phi^{(3)}_{oo} + \Phi^{(4)}_{oi} \left(\frac{q''_{wi} \frac{D_h}{k}}{t_{wo} - t_e}\right)}{1 - \theta^{(3)}_{mo} - \theta^{(4)}_{mi} \left(\frac{q''_{wi} \frac{D_h}{k}}{t_{wo} - t_e}\right)} \qquad \text{(II.E.9)}$$

4. Case four

In this case the Nusselt number will be set forth for the wall at which a uniform heat flux is specified, a uniform temperature being specified at the other wall. From (II.D.14), (II.D.15), and (II.E.3) one obtains

$$Nu_o = \frac{q''_{wo}\,\frac{D_h}{k}}{\theta_{oi}^{(3)}\left(t_{wi}-t_e\right)+\theta_{oo}^{(4)}q''_{wo}\,\frac{D_h}{k}-\theta_{mi}^{(3)}\left(t_{wi}-t_e\right)-\theta_{mo}^{(4)}q''_{wo}\,\frac{D_h}{k}} \qquad \text{(II.E.10)}$$

or

$$Nu_o = \frac{1}{\theta_{oo}^{(4)}-\theta_{mo}^{(4)}+\left(\theta_{oi}^{(3)}-\theta_{mi}^{(3)}\right)\left(\frac{t_{wi}-t_e}{q''_{wo}\,\frac{D_h}{k}}\right)} \qquad \text{(II.E.11)}$$

It can be seen from the relations for the four cases that the Nusselt number is a function of the relative magnitudes of the fluxes or temperatures at the walls. Hence, an infinite number of Nusselt numbers can exist for each fundamental case, whereas the number of fundamental solutions is finite - five for each of the four cases.

III. LAMINAR FLOW

III. A. Survey of Previous Studies

The first published study of heat transfer in a closed conduit was that of Graetz[22] in 1885. Graetz considered flow in a circular tube with uniform wall temperature, and was able to obtain the first three terms of an infinite series solution for the local Nusselt number. Graetz's series approach is the one most commonly employed by succeeding investigators; unless otherwise specified, it is the approach used by all the authors mentioned in this summary. Graetz's work is available in Jacob's book, "Heat Transfer."[26]

In 1923 Nusselt[40] presented what appears to be the first study of heat transfer in laminar flow between parallel planes. He treated the case of uniform and equal wall temperatures and used an attack similar to that of Graetz. His solution also has the same shortcoming as Graetz's in that the series for the local Nusselt number converges very slowly near the thermal entry, and the effort involved in the computation of more than the first three terms was prohibitively great. Leveque[35] alleviated this difficulty in 1928 with his approximate integral-type solution valid near the thermal entry. Leveque also presented the first solution for a nonuniform wall temperature case. His work is available in a heat-transfer review by Drew.[19]

In 1940 Norris and Streid[39] published an independent verification of Nusselt's results. This was done again by Purday[47] in 1949, and by Prins, Mulder, and Schenk,[46] and Yih and Cermak[65] in 1951. Thus, by 1951 the first three terms of the series solution for the local Nusselt number were very well established for the case of uniform and equal wall temperatures.

Yih and Cermak, in the same 1951 paper, continued on to generalize their uniform and equal wall temperature solution to the case of variable (but equal) wall temperatures using a superposition method. They then treated the insulated walls case, the case of uniform and unequal wall temperatures, and the case of variable and unequal wall temperatures. In the same paper they also solved the circular tube problem for variable wall temperature and for an insulated wall, and they treated the finite wall resistance case. This paper seems to be the first published proposal of the superposition method for handling the variable wall temperature problem in internal flow, although the method had previously been used in certain external flow problems by Rubesin.[49] Unfortunately, Yih and Cermak's work did not receive wide circulation, so the method was not in general use until it was outlined by Klein and Tribus[30] in 1953.

van der Does de Bye and Schenk[18] solved the case of finite wall resistance with equal wall temperatures in 1953. Berry[4] and Schenk[51] also treated this problem in the same year. In 1954 Schenk and Beckers[52] dealt with the case of finite wall resistance and nonuniform inlet temperature profile, and Butler and Plewes[8] treated the case of one wall at a uniform temperature and the other wall insulated. Schenk[50] solved this problem again in 1955 and also dealt with the case of the uninsulated wall having a finite resistance. Bodnarescu[6] solved again the constant and equal wall temperature problem, and also considered the effects of axial conduction. In 1956 Dennis and Poots[17] used the Rayleigh approximate method to solve the problem treated earlier by van der Does de Bye and Schenk.

Sellars, Tribus, and Klein[57] made a significant contribution in 1956 by showing that the WKBJ approximation (after Wentzel, Kramers, Brillouin and Jefferies), often used for obtaining solutions of the wave equation, can

fruitfully be applied to the internal entry length problem in conduits. They derived asymptotic expressions for the eigenvalues and eigenconstants occurring in the uniform and equal wall-temperature problem, and observed that these expressions gave excellent results for values higher than the second or third. They also solved the uniform and equal wall heat-flux problem by an inversion method.

More recently Cess and Shaffer[12,13] solved the uniform-equal and uniform-unequal wall heat-flux problems by a direct attack using the procedure suggested by Siegel, Sparrow, and Hallman.[58] Dzung[20] treated the case of arbitrary but equal wall heat fluxes. In another paper Cess and Shaffer[14] list the eigenvalues and eigenconstants occurring in the uniform and unequal wall temperature problem. Pahor and Strnad[43] calculated the uniform and equal wall temperature Nusselt number employing the properties of the confluent hypergeometric function, and Brown[7] reports the first ten eigenvalues and constants for this problem with eleven figure accuracy.

Several methods differing from the Graetz series approach have been proposed for the solution of thermal extrance length problems. Levy[36] presents an approximate solution based on the problem of heat conduction through a composite slab. Singh[59] suggested expanding the fluid temperature in a series of Bessel functions. Agrawal[1] employed an infinite Fourier sine series, and Gupta[23] and Sparrow and Siegel[62] applied variational methods.

Stein[63] has considered flow between parallel planes with a fully developed temperature and velocity profile. He derived the fully established Nusselt number for constant and unequal wall heat fluxes.

Finally, two mathematical papers appear in the literature which are helpful in the treatment of thermal entrance length problems. The first is by Lauwerier,[33] who presents

some useful properties of confluent hypergeometric functions, and the second is by Berry and de Prima,[5] who propose an iterative method for the determination of eigenvalues.

It is apparent that the eigenvalues and eigenconstants necessary for computing the fundamental solutions of the first and second kinds have already been reported at least once in the literature. For completeness they are also calculated herein, together with those required for the solutions of the third and fourth kind.

III. B. Mathematical Formulation and Method of Solution

In this section the four sets of fundamental solutions will be developed for laminar flow between parallel planes. It will be seen that the solution of the differential equation together with the appropriate boundary conditions leads to an eigenvalue problem. The bulk of the labor involved in finding the fundamental solutions is that of calculating the necessary eigenfunctions, eigenvalues, and constants.

1. The differential equations and boundary conditions

For laminar flow the eddy diffusivity of heat, ϵ_H, is zero, and (II.B.5) reduces to

$$\frac{\partial^2\theta}{\partial\bar{y}^2} = \frac{u}{16u_m}\frac{\partial\theta}{\partial\bar{x}} \qquad \text{(III.B.1)}$$

For laminar flow between parallel planes

$$\frac{u}{u_m} = \frac{3}{2}\left(1 - \bar{y}^2\right) \qquad \text{(III.B.2)}$$

so (III.B.1) becomes

$$\frac{\partial^2\theta}{\partial\bar{y}^2} = \frac{3}{32}\left(1 - \bar{y}^2\right)\frac{\partial\theta}{\partial\bar{x}} \qquad \text{(III.B.3)}$$

This is the differential equation to be solved.

The boundary conditions on the equation for each of the four fundamental cases are given by (II.B.14, 15, 16, and 17).

Case 1	Case 2	
$\theta^{(1)}(0,\bar{y}) = 0$	$\theta^{(2)}(0,\bar{y}) = 0$	
$\theta^{(1)}(\bar{x},1) = 1$	$\frac{\partial\theta^{(2)}}{\partial\bar{y}}(\bar{x},1) = \frac{1}{4}$	(III.B.4,5)
$\theta^{(1)}(\bar{x},-1) = 0$	$\frac{\partial\theta^{(2)}}{\partial\bar{y}}(\bar{x},-1) = 0$	

Case 3	Case 4	
$\theta^{(3)}(0,\bar{y}) = 0$	$\theta^{(4)}(0,\bar{y}) = 0$	
$\theta^{(3)}(\bar{x},1) = 1$	$\frac{\partial\theta^{(4)}}{\partial\bar{y}}(\bar{x},1) = \frac{1}{4}$	(III.B.6,7)
$\frac{\partial\theta^{(3)}}{\partial\bar{y}}(\bar{x},-1) = 0$	$\theta^{(4)}(\bar{x},-1) = 0$	

It will be found that the solution of (III.B.3) requires that the boundary conditions at the walls be homogeneous. This is not yet the case, but a simple transformation of the dependent variable, θ, will bring this about. Far downstream of the entry the temperature profile becomes fully developed; this fully developed temperature will be denoted by θ_{fd}. A new temperature profile, $\bar{\theta}$, is obtained by subtracting off the fully developed profile, θ_{fd}, from the temperature profile at any axial location, θ. This transformation was first employed by Sparrow, et al.[61]

$$\bar{\theta} \triangleq \theta - \theta_{fd} \qquad \text{(III.B.8)}$$

Since (III.B.3) is linear, and is satisfied by both θ and θ_{fd}, it is also satisfied by $\bar{\theta}$.

$$\frac{\partial^2\bar{\theta}}{\partial\bar{y}^2} = \frac{3}{32}\left(1 - \bar{y}^2\right)\frac{\partial\bar{\theta}}{\partial\bar{x}} \qquad \text{(III.B.9)}$$

And now, since both θ and θ_{fd} satisfy the identical boundary conditions at the wall for each of the fundamental cases, the boundary conditions on $\bar{\theta}$ become

Case 1	Case 2	
$\bar{\theta}^{(1)}(0,\bar{y}) = -\theta_{fd}^{(1)}$	$\bar{\theta}^{(2)}(0,\bar{y}) = -\theta_{fd}^{(2)}$	
$\bar{\theta}^{(1)}(\bar{x},1) = 0$	$\frac{\partial\bar{\theta}^{(2)}}{\partial\bar{y}}(\bar{x},1) = 0$	(III.B.10,11)
$\bar{\theta}^{(1)}(\bar{x},-1) = 0$	$\frac{\partial\bar{\theta}^{(2)}}{\partial\bar{y}}(\bar{x},-1) = 0$	

Case 3	Case 4	
$\bar{\theta}^{(3)}(0,\bar{y}) = -\theta_{fd}^{(3)}$	$\bar{\theta}^{(4)}(0,\bar{y}) = -\theta_{fd}^{(4)}$	
$\bar{\theta}^{(3)}(\bar{x},1) = 0$	$\frac{\partial\bar{\theta}^{(4)}}{\partial\bar{y}}(\bar{x},1) = 0$	(III.B.12,13)
$\frac{\partial\bar{\theta}^{(3)}}{\partial\bar{y}}(\bar{x},-1) = 0$	$\bar{\theta}^{(4)}(\bar{x},-1) = 0$	

The fully developed temperature profiles are determined in Section III.B.3. For the moment they will be assumed known.

The differential equation and the homogeneous boundary conditions are now in hand; the solution of the problems so specified follows in the succeeding section.

2. Solution of the four fundamental problems - general considerations

Equation (III.B.9) yields to the method of separation of variables. Let

$$\bar{\theta}(\bar{x},\bar{y}) = X(\bar{x}) \cdot Y(\bar{y}) \qquad \text{(III.B.14)}$$

Then

$$\frac{1}{1-\bar{y}^2}\,\frac{Y''}{Y} = \frac{3}{32}\,\frac{X'}{X} = -\lambda^2$$

where λ is a constant. Thus the following two ordinary differential equations are obtained

$$X' + \frac{32}{3}\lambda^2 X = 0 \qquad \text{(III.B.15)}$$

$$Y'' + \lambda^2\left(1 - \bar{y}^2\right) Y = 0 \qquad \text{(III.B.16)}$$

A solution of (III.B.15) is

$$X = e^{-\frac{32}{3}\lambda^2\bar{x}} \qquad \text{(III.B.17)}$$

It will be recognized that (III.B.16) is a differential equation of the Sturm-Liouville type, where λ is the eigenvalue and $1 - \bar{y}^2$ is the weight function. Thus, if the boundary conditions on Y are homogeneous, and it will be shown in a moment that they are, then the equation together with the boundary conditions form a Sturm-Liouville problem and there are an infinite number of possible eigenvalues, λ_n, and eigenfunctions, Y_n. Thus, from (III.B.14), (III.B.16), and (III.B.17), a solution of (III.B.9) is

$$e^{-\frac{32}{3}\lambda^2\bar{x}}\, Y$$

This satisfies the differential equation, but in order to satisfy the boundary condition at $\bar{x} = 0$ all the possible eigenfunctions must be superimposed. This is permissible since (III.B.9) is both linear and homogeneous.

$$\bar{\theta}(x,y) = \sum_{n=0}^{\infty} C_n Y_n(\bar{y}) e^{-\frac{32}{3}\lambda^2\bar{x}} \qquad \text{(III.B.18)}$$

The C_n's are eigenconstants determined by the boundary condition at $\bar{x} = 0$ in the following manner. From (III.B.18) and (III.B.10, 11, 12, 13) one obtains for all four fundamental cases

$$- \theta_{fd}(\bar{y}) = \sum_{n=o}^{\infty} C_n Y_n(\bar{y}) \qquad \text{(III.B.19)}$$

Making use of the orthogonality property of a Sturm-Liouville function

$$\int_{-1}^{+1} \left(1 - \bar{y}^2\right) Y_n \cdot Y_m \, d\bar{y} = 0 \qquad n \neq m \qquad \text{(III.B.20)}$$

one obtains

$$- \int_{-1}^{+1} \theta_{fd} \left(1 - \bar{y}^2\right) Y_n \, d\bar{y} = C_n \int_{-1}^{+1} \left(1 - \bar{y}^2\right) Y_n^2 \, d\bar{y} \qquad \text{(III.B.21)}$$

Thus

$$C_n = \frac{- \int_{-1}^{+1} \theta_{fd} \left(1 - \bar{y}^2\right) Y_n \, d\bar{y}}{\int_{-1}^{+1} \left(1 - \bar{y}^2\right) Y_n^2 \, d\bar{y}} \qquad \text{(III.B.22)}$$

Once the eigenfunctions and the fully developed temperature profiles are in hand for the four fundamental cases, the corresponding eigenconstants can be calculated from (III.B.22). It should be noted that it is actually θ_{fd} evaluated at $\bar{x} = 0$ that appears in this equation; this has significance for case two where it will be shown that θ_{fd} is a function of $\bar{x}$.

It can be seen that in order for (III.B.18) to satisfy the boundary conditions at the wall (III.B.10, 11, 12, 13) the following boundary conditions must be imposed on Y.

Case 1	Case 2	
$Y(1) = 0$	$Y'(1) = 0$	(III.B.23,24)
$Y(-1) = 0$	$Y'(-1) = 0$	

Case 3	Case 4	
$Y(1) = 0$	$Y'(1) = 0$	(III.B.25,26)
$Y'(-1) = 0$	$Y(-1) = 0$	

Since these boundary conditions are homogeneous, the differential Equation (III.B.16) together with these conditions do indeed form problems of the Sturm-Liouville type. The solutions to this particular problem can be represented in terms of confluent hypergeometric functions, as noted by Lauwerier.[33] However, these functions are as yet only incompletely tabulated in the literature and it was found necessary to solve the equation directly for this study.

The methods used for calculating the eigenfunctions and eigenvalues for the four fundamental cases will be described in Section III.G.

3. The fully developed temperature profiles

In Section III.B.1 the fully developed temperature profile was introduced, and was defined as the temperature profile occurring far downstream of the thermal entry. In this section the fully developed temperature profile for each of the four fundamental cases will be presented. It will be seen that these profiles are invariant with $\bar{x}$ for cases one, three, and four; furthermore, for these cases the profiles can be discovered from physical reasoning alone, without solving the governing differential equation.

a. Case one

From (III.B.4) it is seen that the wall boundary conditions here are

$$\theta^{(1)}(\bar{x},1) = 1$$

$$\theta^{(1)}(\bar{x},-1) = 0$$

Since the flow is laminar, the temperature profile approaches a straight line from 0 at $\bar{y} = -1$ to 1 at $\bar{y} = +1$. The development of this profile appears something like that shown in the following sketch.

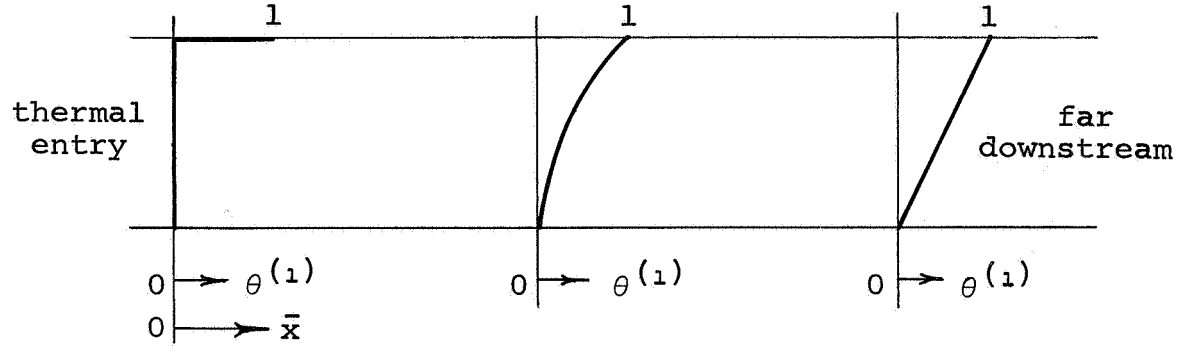

It can be seen from the sketch that the equation for the fully developed profile is

$$\theta_{fd}^{(1)} = \frac{1}{2}\left(1 + \bar{y}\right) \qquad \text{(III.B.27)}$$

This result could also have been obtained by solving the governing differential equation. Since the heat transfer to the fluid at $\bar{y} = 1$ is conducted right through and out again at $\bar{y} = -1$, the fluid temperature does not change with $\bar{x}$ in the fully developed region. Hence (III.B.3) reduces to

$$\frac{d^2\theta_{fd}^{(1)}}{d\bar{y}^2} = 0$$

Thus

$$\theta_{fd}^{(1)} = C_1 \bar{y} + C_2$$

where C_1 and C_2 are the constants of integration. Applying the boundary conditions at $\bar{y} = +1$ and -1, respectively

$$1 = C_1 + C_2$$

$$0 = - C_1 + C_2$$

Hence

$$C_1 = C_2 = \frac{1}{2}$$

and

$$\theta_{fd}^{(1)} = \frac{1}{2}\left(1 + \bar{y}\right)$$

which agrees with the result obtained from physical reasoning.

b. Case two

From (III.B.5) the wall boundary conditions are

$$\frac{\partial \theta^{(2)}}{\partial \bar{y}} (\bar{x},1) = \frac{1}{4}$$

$$\frac{\partial \theta^{(2)}}{\partial \bar{y}} (\bar{x},-1) = 0$$

In this case the equation for the fully developed temperature profile is not obvious from physical reasoning alone since it is not a straight line; however, it can readily be found from (III.B.3). The following sketch shows the manner in which the temperature profile develops.

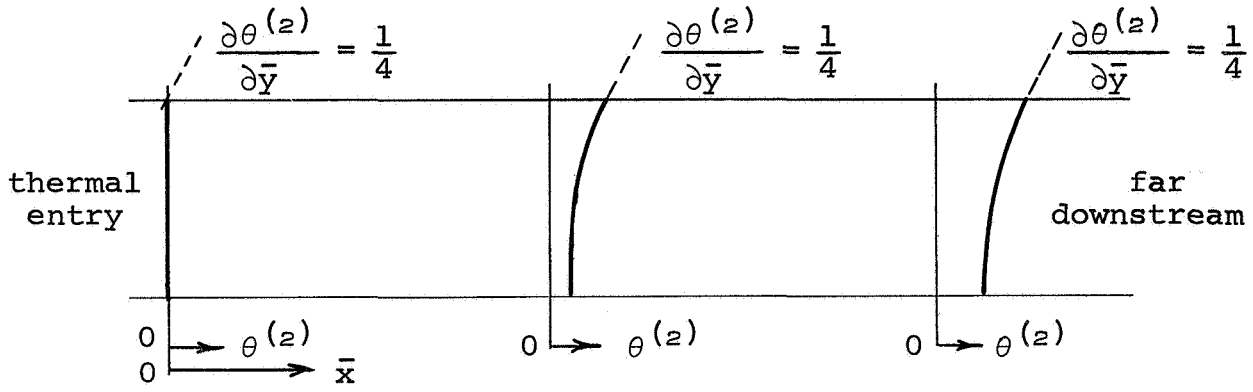

Equation (III.B.3) and the boundary conditions (III.B.5) are reproduced here for convenience.

$$\frac{\partial^2\theta^{(2)}_{fd}}{\partial\bar{y}^2} = \frac{3}{32}\left(1 - \bar{y}^2\right)\frac{\partial\theta^{(2)}_{fd}}{\partial\bar{x}} \qquad \text{(III.B.28)}$$

$$\frac{\partial\theta^{(2)}_{fd}}{\partial\bar{y}}(\bar{x},1) = \frac{1}{4} \qquad \text{(III.B.29)}$$

$$\frac{\partial\theta^{(2)}_{fd}}{\partial\bar{y}}(\bar{x},-1) = 0 \qquad \text{(III.B.30)}$$

Since the wall heat flux is uniform, energy balance considerations dictate that

$$\theta^{(2)}_{m_{fd}} = 2\bar{x} \qquad \text{(III.B.31)}$$

and

$$\frac{\partial\theta^{(2)}_{m_{fd}}}{\partial\bar{x}} = 2 \qquad \text{(III.B.32)}$$

Furthermore, since the temperature profile is fully developed

$$\frac{\partial \theta_{fd}^{(2)}}{\partial \bar{x}} = \frac{\partial \theta_{m_{fd}}^{(2)}}{\partial \bar{x}} = 2 \qquad \text{(III.B.33)}$$

Hence (III.B.28) becomes

$$\frac{\partial^2 \theta_{fd}^{(2)}}{\partial \bar{y}^2} = \frac{3}{16}\left(1 - \bar{y}^2\right) \qquad \text{(III.B.34)}$$

Integrating with respect to $\bar{y}$

$$\frac{\partial \theta_{fd}^{(2)}}{\partial \bar{y}} = \frac{3}{16}\left(\bar{y} - \frac{1}{3}\bar{y}^3\right) + f_1(\bar{x})$$

Applying the boundary condition at $\bar{y} = -1$

$$0 = \frac{3}{16}\left(-1 + \frac{1}{3}\right) + f_1(\bar{x})$$

$$f_1(\bar{x}) = \frac{1}{8}$$

Hence

$$\frac{\partial \theta_{fd}^{(2)}}{\partial \bar{y}} = \frac{3}{16}\left(\bar{y} - \frac{1}{3}\bar{y}^3\right) + \frac{1}{8}$$

Integrating with respect to $\bar{y}$

$$\theta_{fd}^{(2)} = \frac{3}{16}\left(\frac{1}{2}\bar{y}^2 - \frac{1}{12}\bar{y}^4\right) + \frac{1}{8}\bar{y} + f_2(\bar{x}) \qquad \text{(III.B.35)}$$

Combining (II.C.1), (III.B.2), and (III.B.35)

$$\theta_{m_{fd}}^{(2)} = \frac{3}{4}\int_{-1}^{+1}\left\{\left[\frac{3}{16}\left(\frac{1}{2}\bar{y}^2 - \frac{1}{12}\bar{y}^4\right) + \frac{1}{8}\bar{y} + f_2(\bar{x})\right]\left(1 - \bar{y}^2\right)\right\} d\bar{y} \qquad \text{(III.B.36)}$$

Performing the integration, one obtains

$$\theta^{(2)}_{m_{fd}} = f_2(\bar{x}) + \frac{39}{2240} \qquad \text{(III.B.37)}$$

Combining (III.B.31) and (III.B.37)

$$f_2(\bar{x}) = 2\bar{x} - \frac{39}{2240} \qquad \text{(III.B.38)}$$

Hence, inserting in (III.B.35)

$$\theta^{(2)}_{fd} = \frac{3}{16}\left(\frac{1}{2}\bar{y}^2 - \frac{1}{12}\bar{y}^4\right) + \frac{1}{8}\bar{y} + 2\bar{x} - \frac{39}{2240} \qquad \text{(III.B.39)}$$

Finally

$$\theta^{(2)}_{fd} = \frac{1}{8}\left(16\bar{x} - \frac{39}{280} + \bar{y} + \frac{3}{4}\bar{y}^2 - \frac{1}{8}\bar{y}^4\right) \qquad \text{(III.B.40)}$$

The fully developed temperature profile for case two continually changes with $\bar{x}$, but its dependence on $\bar{y}$ becomes invariant.

c. Case three

From (III.B.6) the wall boundary conditions for this case are

$$\theta^{(3)}(\bar{x},1) = 1$$

$$\frac{\partial\theta^{(3)}}{\partial\bar{y}}(\bar{x},-1) = 0$$

And here the development of the temperature profile appears as follows.

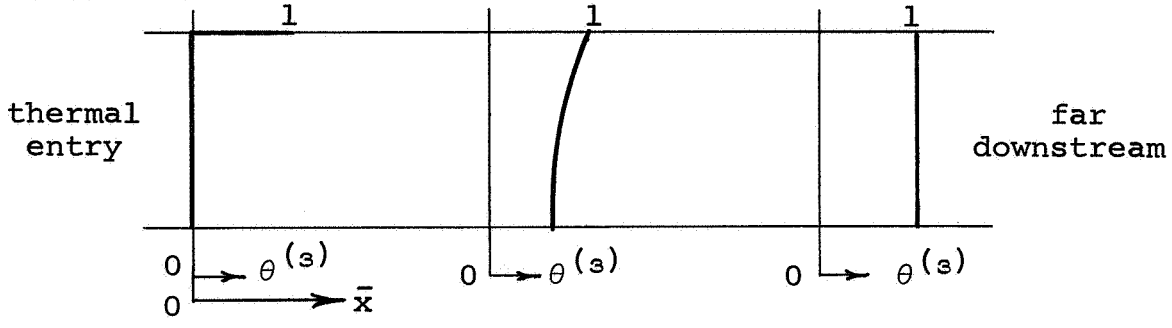

It can be seen from the sketch that the equation for the fully developed profile is

$$\theta_{fd}^{(3)} = 1 \qquad \text{(III.B.41)}$$

d. Case four

From (III.B.7) the wall boundary conditions are

$$\frac{\partial \theta^{(4)}}{\partial \bar{y}} (\bar{x},1) = \frac{1}{4}$$

$$\theta^{(4)} (\bar{x},-1) = 0$$

And physical reasoning shows the temperature profile to develop as shown in the sketch below.

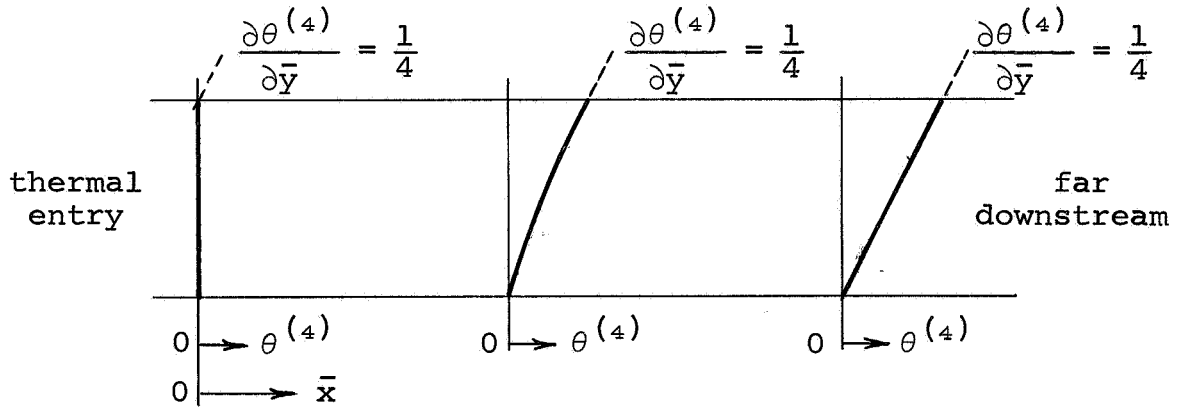

The equation for the fully developed profile is

$$\theta_{fd}^{(4)} = \frac{1}{4} (1 + \bar{y}) \qquad \text{(III.B.42)}$$

III. C. The Four Fundamental Solutions

From (III.B.8) and (III.B.18) it can be seen that for the four fundamental cases the temperature profile is given by

$$\theta = \theta_{fd} + \sum_{n=o}^{\infty} C_n Y_n e^{-\frac{32}{3}\lambda_n^2 \bar{x}} \qquad \text{(III.C.1)}$$

In this section the above equation will be combined with the fully developed temperature profiles found in Section III.B.3 to yield the fundamental solutions for each of the four cases. Numerical values of these solutions are presented in tabular and graphical form, the computational details being provided in Section III.G and Appendix B.

1. Case one

Combining (III.B.27) and (III.C.1) one obtains for the case one temperature profile

$$\theta^{(1)} = \frac{1}{2}(1 + \bar{y}) + \sum_{n=o}^{\infty} C_n Y_n e^{-\frac{32}{3}\lambda_n^2 \bar{x}} \qquad \text{(III.C.2)}$$

This profile holds throughout the entire flow field. At the walls, by definition, the above becomes

$$\theta_{oo}^{(1)} = \theta_{ii}^{(1)} = 1$$

$$\theta_{oi}^{(1)} = \theta_{io}^{(1)} = 0$$

Differentiating (III.C.2) and employing the definition (II.B.10)

$$\Phi_{oo}^{(1)} = \Phi_{ii}^{(1)} = 4\left(\frac{\partial\theta^{(1)}}{\partial\bar{y}}\right)_{\bar{y}=1} = 2 + 4\sum_{n=o}^{\infty} C_n Y_n'(1) e^{-\frac{32}{3}\lambda_n^2 \bar{x}}$$

(III.C.3)

(It is understood that the proper case superscript goes with C_n and Y_n.)

and

$$\Phi_{oi}^{(1)} = \Phi_{io}^{(1)} = -4\left(\frac{\partial\theta^{(1)}}{\partial\bar{y}}\right)_{\bar{y}=-1} = -2 - 4\sum_{n=0}^{\infty} C_n Y_n'(-1) e^{-\frac{32}{3}\lambda_n^2\bar{x}} \qquad \text{(III.C.3)}$$

Now, from energy balance considerations

$$\theta_m^{(1)} = 2\int_0^{\bar{x}} \left(\Phi_{oo}^{(1)} + \Phi_{io}^{(1)}\right) d\bar{x} \qquad \text{(III.C.4)}$$

Performing the indicated integration yields

$$\theta_m^{(1)} = \frac{3}{4}\sum_{n=0}^{\infty}\left[\frac{C_n}{\lambda_n^2}\left(Y_n'(-1) - Y_n'(1)\right)\left(e^{-\frac{32}{3}\lambda_n^2\bar{x}} - 1\right)\right] \qquad \text{(III.C.5)}$$

But as $\bar{x} \to \infty$, $e^{-\frac{32}{3}\lambda_n^2\bar{x}} \to 0$, and also, from the considerations discussed in Section III.B.3, $\theta_m^{(1)} \to \frac{1}{2}$. Hence

$$\frac{1}{2} = -\frac{3}{4}\sum_{n=0}^{\infty}\left[\frac{C_n}{\lambda_n^2}\left(Y_n'(-1) - Y_n'(1)\right)\right] \qquad \text{(III.C.6)}$$

Combining (III.C.5) and (III.C.6) yields

$$\theta_m^{(1)} = \frac{1}{2} + \frac{3}{4}\sum_{n=0}^{\infty}\left[\frac{C_n}{\lambda_n^2}\left(Y_n'(-1) - Y_n'(1)\right) e^{-\frac{32}{3}\lambda_n^2\bar{x}}\right] \qquad \text{(III.C.7)}$$

The fundamental solutions of the first kind are summarized below.

$$\theta_{oo}^{(1)} = \theta_{ii}^{(1)} = 1$$

$$\theta_{oi}^{(1)} = \theta_{io}^{(1)} = 0$$

$$\Phi_{oo}^{(1)} = \Phi_{ii}^{(1)} = 2 + 4 \sum_{n=o}^{\infty} C_n Y_n'(1) e^{-\frac{32}{3}\lambda_n^2 \bar{x}}$$

$$\Phi_{oi}^{(1)} = \Phi_{io}^{(1)} = -2 - 4 \sum_{n=o}^{\infty} C_n Y_n'(-1) e^{-\frac{32}{3}\lambda_n^2 \bar{x}}$$

$$\theta_{mo}^{(1)} = \theta_{mi}^{(1)} = \frac{1}{2} + \frac{3}{4} \sum_{n=o}^{\infty} \left[\frac{C_n}{\lambda_n^2} \left(Y_n'(-1) - Y_n'(1) \right) e^{-\frac{32}{3}\lambda_n^2 \bar{x}} \right]$$

The last three fundamental solutions are presented in Figure III.C.1 and Table III.C.1.

2. Case two

Combining (III.B.40) and (III.C.1), the case two temperature profile is found to be

$$\theta^{(2)} = \frac{1}{8} \left[16\bar{x} - \frac{39}{280} + \bar{y} + \frac{3}{4}\bar{y}^2 - \frac{1}{8}\bar{y}^4 \right] + \sum_{n=o}^{\infty} C_n Y_n e^{-\frac{32}{3}\lambda_n^2 \bar{x}} \qquad \text{(III.C.8)}$$

At the walls the above becomes

$$\theta_{oo}^{(2)} = \theta_{ii}^{(2)} = 2\bar{x} + \frac{13}{70} + \sum_{n=o}^{\infty} C_n Y_n(1) e^{-\frac{32}{3}\lambda_n^2 \bar{x}} \qquad \text{(III.C.9)}$$

$$\theta_{oi}^{(2)} = \theta_{io}^{(2)} = 2\bar{x} - \frac{9}{140} + \sum_{n=o}^{\infty} C_n Y_n(-1) e^{-\frac{32}{3}\lambda_n^2 \bar{x}} \qquad \text{(III.C.10)}$$

By definition for case two

$$\Phi_{oo}^{(2)} = \Phi_{oi}^{(2)} = 1$$

$$\Phi_{oi}^{(2)} = \Phi_{io}^{(2)} = 0$$

And from energy balance considerations

$$\theta_m^{(2)} = 2\bar{x} \qquad \text{(III.C.11)}$$

The fundamental solutions of the second kind are summarized below.

$$\theta_{oo}^{(2)} = \theta_{ii}^{(2)} = 2\bar{x} + \frac{13}{70} + \sum_{n=o}^{\infty} C_n Y_n(1) e^{-\frac{32}{3}\lambda_n^2 \bar{x}}$$

$$\theta_{oi}^{(2)} = \theta_{io}^{(2)} = 2\bar{x} - \frac{9}{140} + \sum_{n=o}^{\infty} C_n Y_n(-1) e^{-\frac{32}{3}\lambda_n^2 \bar{x}}$$

$$\Phi_{oo}^{(2)} = \Phi_{ii}^{(2)} = 1$$

$$\Phi_{oi}^{(2)} = \Phi_{io}^{(2)} = 0$$

$$\theta_{mo}^{(2)} = \theta_{mi}^{(2)} = 2\bar{x}$$

The first two fundamental solutions are presented in Figure III.C.2 and Table III.C.1.

3. Case three

Combining (III.B.41) and (III.C.1), one obtains for the case three temperature profile

$$\theta^{(3)} = 1 + \sum_{n=o}^{\infty} C_n Y_n e^{-\frac{32}{3}\lambda_n^2 \bar{x}} \qquad \text{(III.C.12)}$$

At the upper wall the above becomes, by definition

$$\theta_{oo}^{(3)} = \theta_{ii}^{(3)} = 1$$

and at the lower wall it becomes

$$\theta_{oi}^{(s)} = \theta_{io}^{(s)} = 1 + \sum_{n=o}^{\infty} C_n Y_n(-1) e^{-\frac{32}{3}\lambda_n^2 \bar{x}} \qquad \text{(III.C.13)}$$

Differentiating (III.C.12) and employing the definition (II.B.12)

$$\Phi_{oo}^{(s)} = \Phi_{ii}^{(s)} = 4\left(\frac{\partial\theta^{(s)}}{\partial\bar{y}}\right)_{\bar{y}=1} = 4\sum_{n=o}^{\infty} C_n Y_n'(1) e^{-\frac{32}{3}\lambda_n^2 \bar{x}}$$

(III.C.14)

And by definition for case three

$$\Phi_{oi}^{(s)} = \Phi_{io}^{(s)} = 0$$

From an energy balance between the thermal entry ($\bar{x} = 0$) and any $\bar{x}$

$$\theta_m^{(s)} = 2\int_o^{\bar{x}} \Phi_{oo}^{(s)}\, d\bar{x} \qquad \text{(III.C.15)}$$

Combining (III.C.14) and (III.C.15) and performing the integration

$$\theta_m^{(s)} = -\frac{3}{4}\sum_{n=o}^{\infty}\left[\frac{C_n}{\lambda_n^2} Y_n'(1)\left(e^{-\frac{32}{3}\lambda_n^2\bar{x}} - 1\right)\right] \qquad \text{(III.C.16)}$$

But as $\bar{x} \to \infty$, $e^{-\frac{32}{3}\lambda_n^2\bar{x}} \to 0$, and also, from the fully developed temperature profile, $\theta_m^{(s)} \to 1$. Hence

$$1 = \frac{3}{4}\sum_{n=o}^{\infty}\frac{C_n}{\lambda_n^2} Y_n'(1) \qquad \text{(III.C.17)}$$

Combining (III.C.16) and (III.C.17) yields

$$\theta_m^{(3)} = 1 - \frac{3}{4} \sum_{n=0}^{\infty} \frac{C_n}{\lambda_n^2} Y_n'(1) e^{-\frac{32}{3}\lambda_n^2 \bar{x}} \qquad \text{(III.C.18)}$$

The fundamental solutions of the third kind are summarized below.

$$\theta_{oo}^{(3)} = \theta_{ii}^{(3)} = 1$$

$$\theta_{oi}^{(3)} = \theta_{io}^{(3)} = 1 + \sum_{n=0}^{\infty} C_n Y_n(-1) e^{-\frac{32}{3}\lambda_n^2 \bar{x}}$$

$$\Phi_{oo}^{(3)} = \Phi_{ii}^{(3)} = 4 \sum_{n=0}^{\infty} C_n Y_n'(1) e^{-\frac{32}{3}\lambda_n^2 \bar{x}}$$

$$\Phi_{oi}^{(3)} = \Phi_{io}^{(3)} = 0$$

$$\theta_{mo}^{(3)} = \theta_{mi}^{(3)} = 1 - \frac{3}{4} \sum_{n=0}^{\infty} \frac{C_n}{\lambda_n^2} Y_n'(1) e^{-\frac{32}{3}\lambda_n^2 \bar{x}}$$

The three fundamental solutions that are functions of $\bar{x}$ are presented in Figure III.C.3 and Table III.C.1.

4. Case four

The case four temperature profile is obtained by combining (III.B.42) and (III.C.1).

$$\theta^{(4)} = \frac{1}{4}(1 + \bar{y}) + \sum_{n=0}^{\infty} C_n Y_n e^{-\frac{32}{3}\lambda_n^2 \bar{x}} \qquad \text{(III.C.19)}$$

At the upper wall the above becomes

$$\theta_{oo}^{(4)} = \theta_{ii}^{(4)} = \frac{1}{2} + \sum_{n=0}^{\infty} C_n Y_n(1) e^{-\frac{32}{3}\lambda_n^2 \bar{x}} \qquad \text{(III.C.20)}$$

and at the lower wall, by definition

$$\theta_{oi}^{(4)} = \theta_{io}^{(4)} = 0$$

Since the heat flux is specified at the upper wall in case four

$$\Phi_{oo}^{(4)} = \Phi_{ii}^{(4)} = 1$$

Differentiating, and combining (III.C.19) with (II.B.17)

$$\Phi_{oi}^{(4)} = \Phi_{io}^{(4)} = -1 - 4 \sum_{n=o}^{\infty} C_n Y_n'(-1) e^{-\frac{32}{3}\lambda_n^2 \bar{x}} \qquad \text{(III.C.21)}$$

From energy balance considerations

$$\theta_m^{(4)} = 2 \int_o^{\bar{x}} \left(\Phi_{oo}^{(4)} + \Phi_{io}^{(4)} \right) d\bar{x} \qquad \text{(III.C.22)}$$

From the preceding three equations, one obtains

$$\theta_m^{(4)} = \frac{3}{4} \sum_{n=o}^{\infty} \left[\frac{C_n}{\lambda_n^2} Y_n'(-1) \left(e^{-\frac{32}{3}\lambda_n^2 \bar{x}} - 1 \right) \right] \qquad \text{(III.C.23)}$$

But as $\bar{x} \to \infty$, $e^{-\frac{32}{3}\lambda_n^2 \bar{x}} \to 0$, and from the fully developed temperature profile, $\theta_m^{(4)} \to \frac{1}{4}$. Hence

$$\frac{1}{4} = -\frac{3}{4} \sum_{n=o}^{\infty} \frac{C_n}{\lambda_n^2} Y_n'(-1) \qquad \text{(III.C.24)}$$

Combining the preceding two equations yields

$$\theta_m^{(4)} = \frac{1}{4} + \frac{3}{4} \sum_{n=o}^{\infty} \frac{C_n}{\lambda_n^2} Y_n'(-1) e^{-\frac{32}{3}\lambda_n^2 \bar{x}} \qquad \text{(III.C.25)}$$

The fundamental solutions of the fourth kind are summarized below.

$$\theta_{oo}^{(4)} = \theta_{ii}^{(4)} = \frac{1}{2} + \sum_{n=o}^{\infty} C_n Y_n(1) e^{-\frac{32}{3}\lambda_n^2 \bar{x}}$$

$$\theta_{oi}^{(4)} = \theta_{io}^{(4)} = 0$$

$$\Phi_{oo}^{(4)} = \Phi_{ii}^{(4)} = 1$$

$$\Phi_{oi}^{(4)} = \Phi_{io}^{(4)} = -1 - 4 \sum_{n=o}^{\infty} C_n Y_n'(-1) e^{-\frac{32}{3}\lambda_n^2 \bar{x}}$$

$$\theta_{mo}^{(4)} = \theta_{mi}^{(4)} = \frac{1}{4} + \frac{3}{4} \sum_{n=o}^{\infty} \frac{C_n}{\lambda_n^2} Y_n'(-1) e^{-\frac{32}{3}\lambda_n^2 \bar{x}}$$

The three fundamental solutions that are functions of $\bar{x}$ are presented in Figure III.C.4 and Table III.C.1.

Let it be noted at this point that the infinite series appearing in this section converge very slowly at small values of $\bar{x}$. Hence it is desirable to seek another form of the solutions in this region; such a form is discussed in Section III.E.

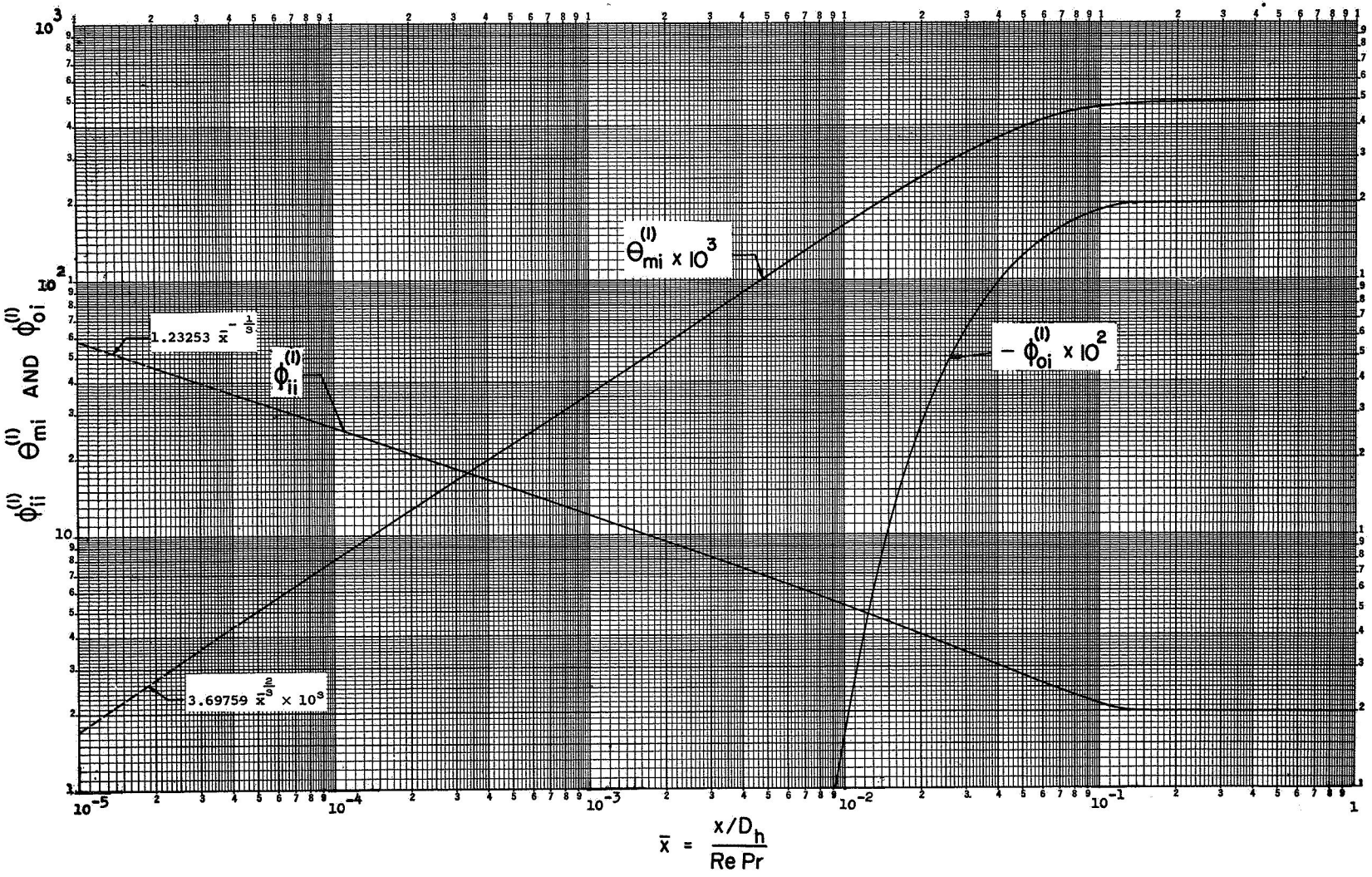

LAMINAR FUNDAMENTAL SOLUTIONS OF THE FIRST KIND

FIGURE III.C.1

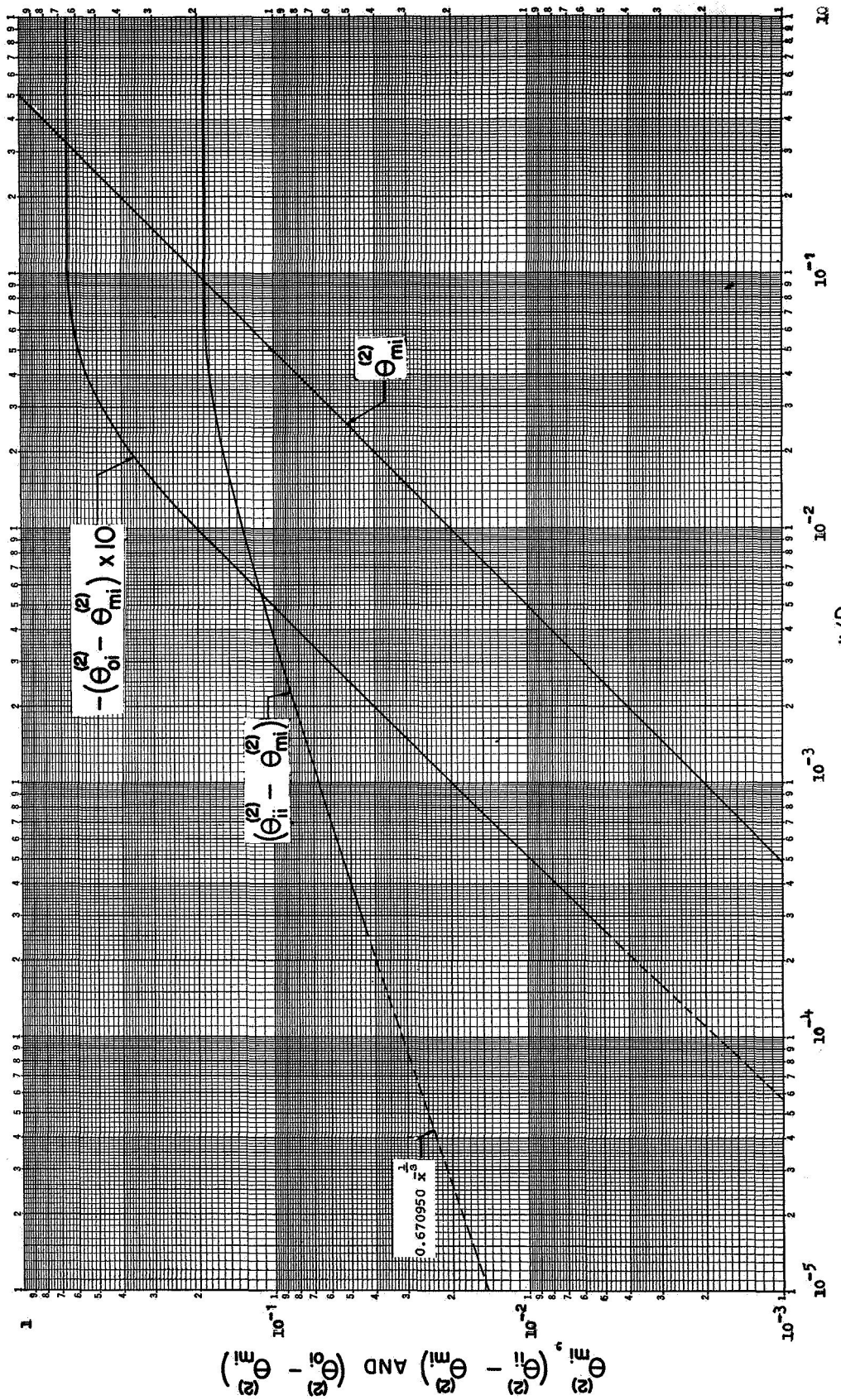

LAMINAR FUNDAMENTAL SOLUTIONS OF THE SECOND KIND

FIGURE III.C.2

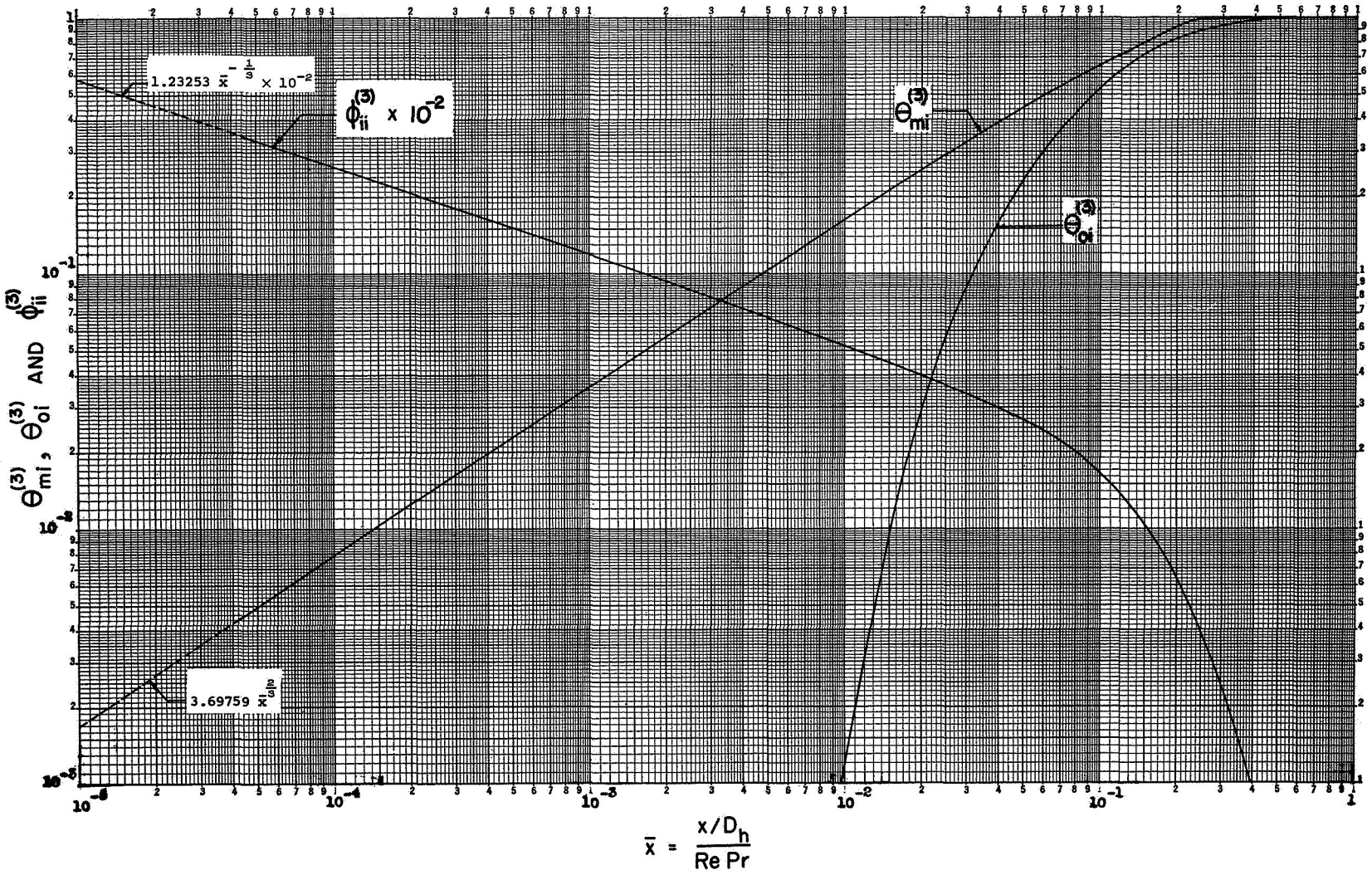

LAMINAR FUNDAMENTAL SOLUTIONS OF THE THIRD KIND

FIGURE III.C.3

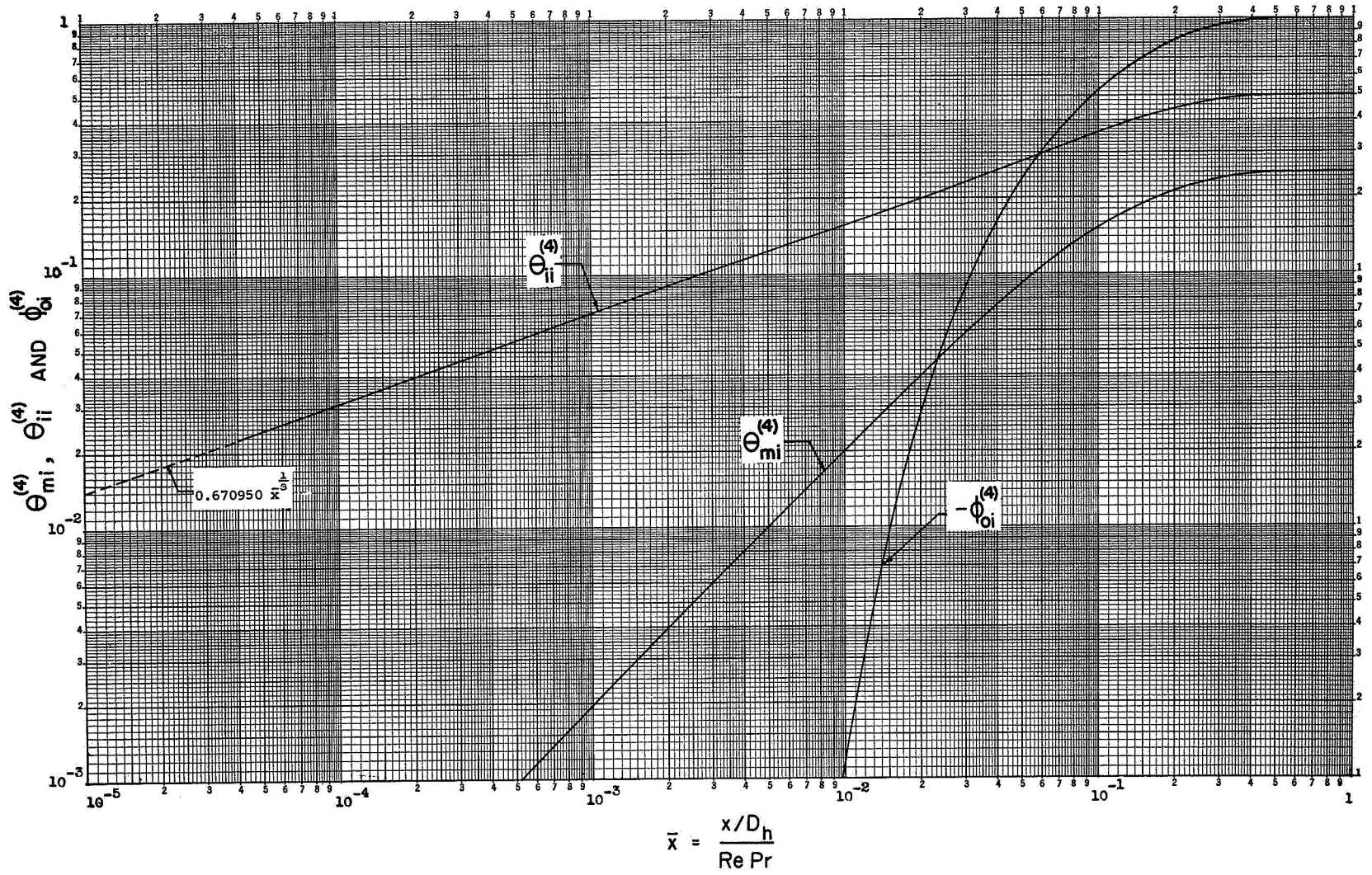

LAMINAR FUNDAMENTAL SOLUTIONS OF THE FOURTH KIND

FIGURE III.C.4

TABLE III.C.1

THE LAMINAR FUNDAMENTAL SOLUTIONS

First Kind

$\bar{x}$	$\Phi_{ii}^{(1)}$	$\Phi_{oi}^{(1)}$	$\theta_{mi}^{(1)}$
2.5×10^{-4}	19.145	-	0.01447
2.5×10^{-3}	8.638	-	0.06596
1.0×10^{-2}	5.242	-0.01704	0.1625
1.5×10^{-2}	4.501	-0.1084	0.2103
2.5×10^{-2}	3.687	-0.4572	0.2859
5.0×10^{-2}	2.762	-1.242	0.3993
7.5×10^{-2}	2.357	-1.643	0.4526
1.0×10^{-1}	2.168	-1.832	0.4777
1.25×10^{-1}	2.079	-1.921	0.4895
1.5×10^{-1}	2.037	-1.963	0.4951
2.5×10^{-1}	2.002	-1.998	0.4997
5.0×10^{-1}	2.000	-1.999	0.4999
∞	2.000	-2.000	0.5000

Second Kind

$\bar{x}$	$\theta_{ii}^{(2)}-\theta_{mi}^{(2)}$	$\theta_{oi}^{(2)}-\theta_{mi}^{(2)}$	$\theta_{mi}^{(2)}$
2.5×10^{-4}	0.04251	-0.00050	0.00050
2.5×10^{-3}	0.08935	-0.00500	0.00500
1.0×10^{-2}	0.1335	-0.01992	0.02000
1.5×10^{-2}	0.1476	-0.02915	0.03000
2.5×10^{-2}	0.1643	-0.04331	0.05000
5.0×10^{-2}	0.1803	-0.05888	0.1000
7.5×10^{-2}	0.1843	-0.06291	0.1500
1.25×10^{-1}	0.1856	-0.06420	0.2500
2.5×10^{-1}	0.1857	-0.06429	0.5000
5.0×10^{-1}	0.1857	-0.06429	1.000
∞	0.1857	-0.06429	∞

TABLE III.C.1 (Continued)

Third Kind

$\bar{x}$	$\Phi_{ii}^{(3)}$	$\theta_{oi}^{(3)}$	$\theta_{mi}^{(3)}$
2.5×10^{-4}	19.140	-	0.01449
2.5×10^{-3}	8.638	-	0.06597
1.0×10^{-2}	5.242	0.001194	0.1625
1.5×10^{-2}	4.501	0.009819	0.2109
2.5×10^{-2}	3.687	0.05685	0.2919
5.0×10^{-2}	2.703	0.2356	0.4487
7.5×10^{-2}	2.102	0.3982	0.5680
1.25×10^{-1}	1.291	0.6297	0.7343
2.5×10^{-1}	0.3831	0.8901	0.9212
5.0×10^{-1}	0.0337	0.9903	0.9931
∞	0	1.000	1.000

Fourth Kind

$\bar{x}$	$\theta_{ii}^{(4)}$	$\Phi_{oi}^{(4)}$	$\theta_{mi}^{(4)}$
2.5×10^{-4}	0.04299	-	0.00050
2.5×10^{-3}	0.09434	-	0.00500
1.0×10^{-2}	0.01535	-0.00120	0.0200
1.5×10^{-2}	0.1776	-0.00982	0.0299
2.5×10^{-2}	0.2143	-0.0568	0.0493
5.0×10^{-2}	0.279	-0.2356	0.0921
7.5×10^{-2}	0.327	-0.398	0.1261
1.25×10^{-1}	0.3938	-0.6297	0.1738
2.5×10^{-1}	0.4685	-0.8901	0.2274
5.0×10^{-1}	0.497	-0.9903	0.248
∞	0.5000	-1.000	0.5000

III. D. The Nusselt Number Relations

As a matter of interest for workers used to dealing with the Nusselt modulus for internal flow geometries, some of the expressions formulated in Section I.E. have been combined with the laminar fundamental solutions given in the previous section. The Nusselt numbers for the two most commonly treated cases, that of uniform and equal wall temperatures and that of uniform and equal wall heat fluxes, are presented in Figure III.D.1 and Table III.D.1.

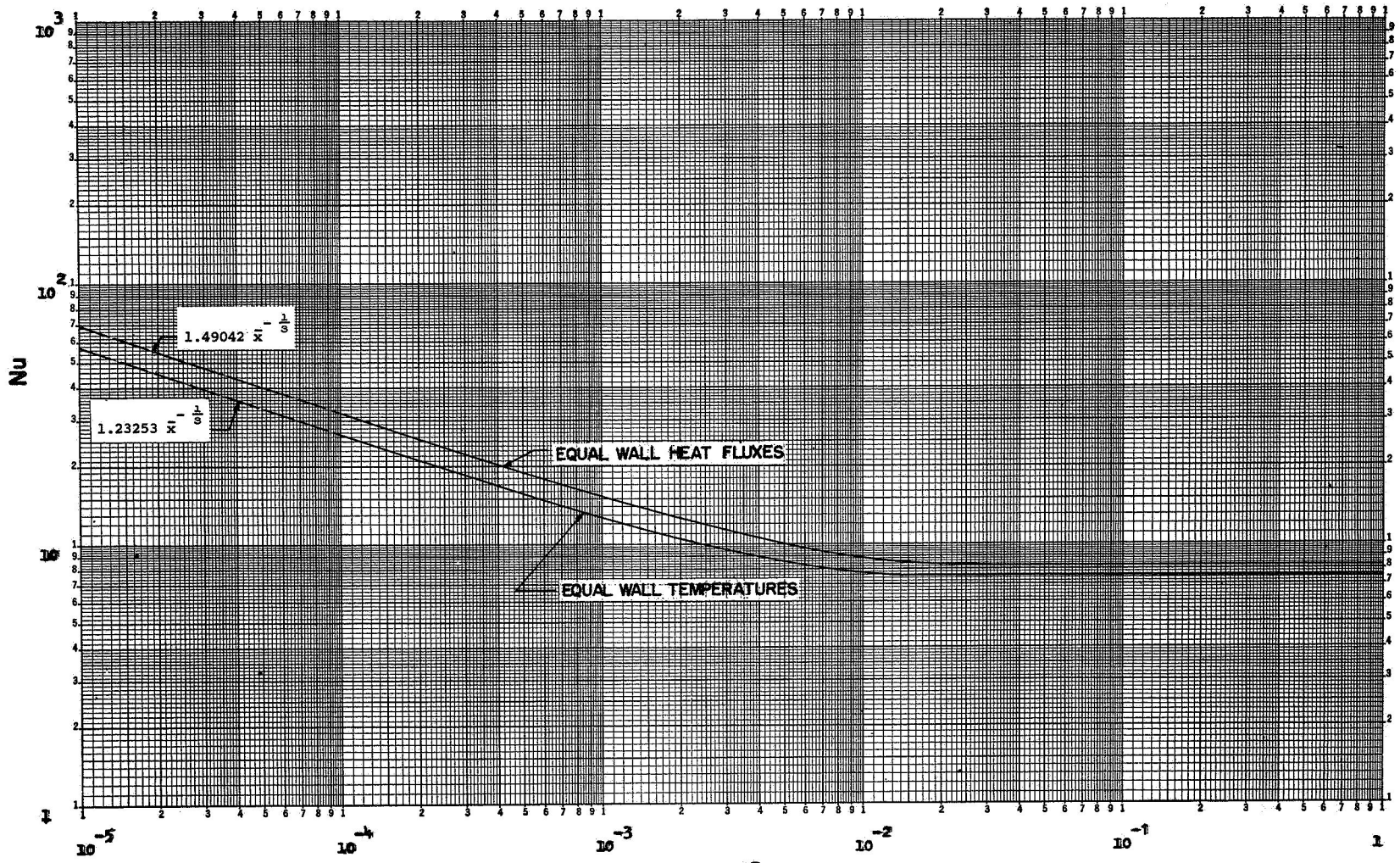

NUSSELT NUMBERS FOR UNIFORM AND EQUAL WALL TEMPERATURES AND HEAT FLUXES

FIGURE III.D.1

TABLE III.D.1

LAMINAR NUSSELT NUMBERS FOR UNIFORM AND EQUAL WALL BOUNDARY CONDITIONS

Equal Wall Temperatures

$\bar{x}$	Nu
2.5×10^{-4}	19.72
2.5×10^{-3}	9.951
1.0×10^{-2}	7.741
1.5×10^{-2}	7.582
2.5×10^{-2}	7.543
5.0×10^{-2}	7.541
7.5×10^{-2}	7.541
1.0×10^{-1}	7.541
1.25×10^{-1}	7.541
1.5×10^{-1}	7.541
2.5×10^{-1}	7.541
5.0×10^{-1}	7.541
∞	7.54072

Equal Wall Heat Fluxes

$\bar{x}$	Nu
2.5×10^{-4}	23.79
2.5×10^{-3}	11.86
1.0×10^{-2}	8.803
1.5×10^{-2}	8.439
2.5×10^{-2}	8.263
5.0×10^{-2}	8.236
7.5×10^{-2}	8.235
1.25×10^{-1}	8.235
2.5×10^{-1}	8.235
5.0×10^{-1}	8.235
∞	8.23529

III. E. Relations Valid at Small $\bar{x}$

It was pointed out at the end of Section III.C that the infinite series appearing in the fundamental solution expressions converge very slowly for small values of $\bar{x}$. Thus, in order to shorten the time of computation, it is natural to seek a limiting type of solution valid in the small $\bar{x}$ region. Leveque[35] has obtained such a solution for a uniform temperature wall, and others, for example, Eckert and Drake,[21] have derived the counterpart for a uniform heat-flux wall. These derivations will be presented here for the sake of completeness.

1. The differential equation

Recall from (III.B.1) and (III.B.2) that the energy equation for the entire region between the two planes is

$$\frac{\partial^2 \theta}{\partial \bar{y}^2} = \frac{u}{16 u_m} \frac{\partial \theta}{\partial \bar{x}} \qquad \text{(III.E.1)}$$

where

$$\frac{u}{u_m} = \frac{3}{2}\left(1 - \bar{y}^2\right) \qquad \text{(III.E.2)}$$

Now, very close to the thermal entry (very small $\bar{x}$) the temperature profile growing from the heated wall penetrates only a very short distance into the flow field; that is, the thermal boundary layer is extremely thin. Thus, focusing attention on the upper wall, the entire region of the problem is that area near $\bar{x} = 0$ and $\bar{y} = 1$. In this region very close to the wall the velocity profile is nearly linear, and this suggests the possibility of replacing (III.E.2) with a straight line of the same slope at the wall.

Thus

$$\frac{u}{u_m} = -3\bar{y} + 3 \qquad \text{(III.E.3)}$$

for $\bar{y} \approx 1$. Converting to an ordinate whose origin is at the upper wall, let

$$\bar{\eta} \triangleq 1 - \bar{y} \qquad \text{(III.E.4)}$$

Then the velocity profile becomes

$$\frac{u}{u_m} = 3\bar{\eta} \qquad \text{(III.E.5)}$$

And (III.E.1) becomes

$$\frac{\partial^2\theta}{\partial\bar{\eta}^2} = \frac{u}{16u_m}\,\frac{\partial\theta}{\partial\bar{x}} \qquad \text{(III.E.6)}$$

Combining the preceding two equations

$$\frac{\partial^2\theta}{\partial\bar{\eta}^2} = \frac{3}{16}\,\bar{\eta}\,\frac{\partial\theta}{\partial\bar{x}} \qquad \text{(III.E.7)}$$

This is the energy equation valid in the region under consideration.

Since the problem here resembles that of heat transfer from a flat plate, the possibility of the existence of a similarity solution suggests itself. Such a solution does indeed exist, and it will be derived in the following two sections for the two wall boundary conditions of interest.

2. <u>The uniform wall temperature case</u>

Here the wall boundary condition is

$$\theta_{\bar{\eta}=o} = 1 \qquad \text{(III.E.8)}$$

The similarity solution to be sought is of the form

$$\theta = \psi(\xi) \qquad \text{(III.E.9)}$$

where

$$\xi = \bar{\eta}\, \bar{x}^{-\frac{1}{3}} \qquad \text{(III.E.10)}$$

Combining (III.E.7), (III.E.9), and (III.E.10) one obtains the ordinary differential equation

$$\psi'' + \frac{1}{16}\, \xi^2 \psi' = 0 \qquad \text{(III.E.11)}$$

The solution of this equation is

$$\psi = \theta = C_1 \int e^{-\frac{\xi^3}{48}}\, d\xi + C_2 \qquad \text{(III.E.12)}$$

where C_1 and C_2 are constants. From the boundary condition (III.E.8), and from (III.E.10) one obtains

$$\theta_{\xi=o} = 1$$

Hence (III.E.12) becomes

$$1 = C_1 \left(\int e^{-\frac{\xi^3}{48}}\, d\xi \right)_{\xi=o} + C_2$$

at the wall. The integral above vanishes, as can be seen by expanding the exponential in a series and integrating term by term. Thus

$$C_2 = 1$$

Now, by definition $\theta = 0$ at $\bar{x} = 0$ ($\xi = \infty$). So (III.E.12) becomes

$$0 = C_1 \left(\int e^{-\frac{\xi^3}{48}} d\xi \right)_{\xi=\infty} + 1$$

Since the integral vanishes at $\xi = 0$, this can be written as

$$0 = C_1 \int_0^\infty e^{-\frac{\xi^3}{48}} d\xi + 1 \qquad \text{(III.E.13)}$$

From Jahnke-Emde[27]

$$\int_0^\infty e^{-\frac{\xi^3}{48}} d\xi = \frac{48^{\frac{1}{3}}}{3} \Gamma\left(\frac{1}{3}\right) \qquad \text{(III.E.14)}$$

Combining the preceding two equations, one obtains

$$C_1 = \frac{-3}{48^{\frac{1}{3}} \Gamma\left(\frac{1}{3}\right)}$$

Thus (III.E.12) becomes

$$\theta = -\frac{3}{48^{\frac{1}{3}} \Gamma\left(\frac{1}{3}\right)} \int_0^\xi e^{-\frac{\sigma^3}{48}} d\sigma + 1 \qquad \text{(III.E.15)}$$

where σ is a dummy variable.

The fundamental solutions sought are Φ_{oo} and θ_m. Turning first to Φ_{oo}, (II.B.10) yields here

$$\Phi_{oo} = -4 \left(\frac{\partial \theta}{\partial \bar{\eta}} \right)_{\bar{\eta}=o} \qquad \text{(III.E.16)}$$

Combining (III.E.10), (III.E.15), and (III.E.16) then produces

$$\Phi_{oo} = \frac{12}{48^{\frac{1}{3}}\,\Gamma\left(\frac{1}{3}\right)}\,\bar{x}^{-\frac{1}{3}} \qquad \text{(III.E.17)}$$

Evaluating the constant yields

$$\Phi_{oo} = 1.23253\,\bar{x}^{-\frac{1}{3}} \qquad \text{(III.E.18)}$$

This fundamental solution holds for both cases one and three in the region near $\bar{x} = 0$ and a unity temperature wall.

θ_m is now found by performing the integration indicated in both (III.C.4) and (III.C.15).

$$\theta_m = 2\int_o^{\bar{x}} \Phi_{oo}\, d\bar{x} \qquad \text{(III.E.19)}$$

So in this case

$$\theta_m = \frac{24}{48^{\frac{1}{3}}\,\Gamma\left(\frac{1}{3}\right)}\int_o^{\bar{x}} \bar{x}^{-\frac{1}{3}}\, d\bar{x} \qquad \text{(III.E.20)}$$

Thus

$$\theta_m = \frac{36}{48^{\frac{1}{3}}\,\Gamma\left(\frac{1}{3}\right)}\,\bar{x}^{\frac{2}{3}} \qquad \text{(III.E.21)}$$

Evaluating the constant yields

$$\theta_m = 3.69759\,\bar{x}^{\frac{2}{3}} \qquad \text{(III.E.22)}$$

This fundamental solution, like the one preceding, holds for both cases one and three.

3. The uniform wall heat flux case

In this case the wall boundary condition is

$$\Phi_{\bar{\eta}=o} = 1 \qquad \text{(III.E.23)}$$

From (II.B.15) it is seen that this is equivalent to

$$\left(\frac{\partial\theta}{\partial\bar{\eta}}\right)_{\bar{\eta}=o} = -\frac{1}{4} \qquad \text{(III.E.24)}$$

Here the similarity solution assumes the form

$$\theta = \bar{x}^{\frac{1}{3}}\,\psi(\xi) \qquad \text{(III.E.25)}$$

where

$$\xi = \bar{\eta}\,\bar{x}^{-\frac{1}{3}} \qquad \text{(III.E.26)}$$

Combining (III.E.7), (III.E.25), and (III.E.26), the following ordinary differential equation is obtained

$$\psi'' + \frac{1}{16}\,\xi^2\psi' - \frac{1}{16}\,\xi\psi = 0 \qquad \text{(III.E.27)}$$

The solution of this equation is

$$\psi = C_1\xi \int \frac{e^{-\frac{\xi^3}{48}}}{\xi^2}\,d\xi + C_2\xi \qquad \text{(III.E.28)}$$

where C_1 and C_2 are constants. Integrating by parts, the above becomes

$$\psi = C_2\xi - C_1 e^{-\frac{\xi^3}{48}} - \frac{1}{16} C_1 \xi \int \xi\, e^{-\frac{\xi^3}{48}}\, d\xi \qquad \text{(III.E.29)}$$

Introducing (III.E.25) yields

$$\theta = \bar{x}^{\frac{1}{3}} \left(C_2\xi - C_1 e^{-\frac{\xi^3}{48}} - \frac{1}{16} C_1 \xi \int \xi\, e^{-\frac{\xi^3}{48}}\, d\xi \right) \qquad \text{(III.E.30)}$$

Applying the boundary condition (III.E.24), and employing (III.E.26)

$$\left(\frac{\partial\theta}{\partial\bar{\eta}}\right)_{\bar{\eta}=0} = \bar{x}^{-\frac{1}{3}} \left(\frac{\partial\theta}{\partial\xi}\right)_{\xi=0} = C_2 = -\frac{1}{4} \qquad \text{(III.E.31)}$$

In arriving at this condition use was made of the fact that

$$\left(\int \xi\, e^{-\frac{\xi^3}{48}}\, d\xi \right)_{\xi=0} = 0$$

as can be seen by expanding the exponential in a series and integrating term by term.

Now, by definition $\theta = 0$ at $\bar{x} = 0$ $(\xi = \infty)$. Thus (III.E.30) becomes

$$0 = -\frac{1}{4}\bar{\eta} - \frac{1}{16} C_1 \bar{\eta} \int_0^\infty \xi\, e^{-\frac{\xi^3}{48}}\, d\xi$$

So

$$C_1 = \frac{-4}{\int_0^\infty \xi\, e^{-\frac{\xi^3}{48}}\, d\xi} \qquad \text{(III.E.32)}$$

From Jahnke-Emde

$$\int_0^\infty \xi\, e^{-\frac{\xi^3}{48}}\, d\xi = \frac{48^{\frac{2}{3}}}{3}\,\Gamma\left(\frac{2}{3}\right) \qquad \text{(III.E.33)}$$

Hence

$$C_1 = \frac{-12}{48^{\frac{2}{3}}\,\Gamma\left(\frac{2}{3}\right)}$$

And (III.E.30) becomes

$$\theta = \bar{x}^{\frac{1}{3}}\left[-\frac{1}{4}\,\xi + \frac{12}{48^{\frac{2}{3}}\,\Gamma\left(\frac{2}{3}\right)}\left(e^{-\frac{\xi^3}{48}} + \frac{3}{48}\,\xi\int_0^\xi \sigma\, e^{-\frac{\sigma^3}{48}}\, d\sigma\right)\right] \qquad \text{(III.E.34)}$$

where σ is a dummy variable.

Since θ_{oo} occurs at $\bar{\eta} = 0$ ($\xi = 0$), the fundamental solution is

$$\theta_{oo} = \frac{12}{48^{\frac{2}{3}}\,\Gamma\left(\frac{2}{3}\right)}\,\bar{x}^{\frac{1}{3}} \qquad \text{(III.E.35)}$$

Evaluating the constant yields

$$\theta_{oo} = 0.670950\,\bar{x}^{\frac{1}{3}} \qquad \text{(III.E.36)}$$

θ_m for this case follows directly from energy balance considerations (see (III.C.11)).

$$\theta_m = 2\bar{x} \qquad \text{(III.E.37)}$$

These fundamental solutions hold for both cases two and four in the region near $\bar{x} = 0$ and a unity Φ heat-flux wall.

The limiting fundamental solutions derived in this section are indicated by the dashed lines on the fundamental solution curves in Section III.C.

4. The Nusselt number relations

The Nusselt number relations for very small $\bar{x}$ are readily obtained by combining the preceding results of this section with those of Section II.E. This will be done here for the four fundamental cases.

a. Case one

At very small values of $\bar{x}$ the temperature profile has not yet propagated to the opposite wall, so $\Phi_{oi}^{(1)} = 0$. Hence (II.E.5) becomes

$$Nu_o = \frac{\Phi_{oo}^{(1)}}{1 - \theta_{mo}^{(1)} \left[1 + \left(\frac{t_{wi} - t_e}{t_{wo} - t_e} \right) \right]} \qquad \text{(III.E.38)}$$

Introducing (III.E.17) and (III.E.21) one obtains

$$Nu_o = \frac{1}{\frac{48^{\frac{1}{3}} \Gamma\left(\frac{1}{3}\right)}{12} \bar{x}^{-\frac{1}{3}} - 3 \left[1 + \left(\frac{t_{wi} - t_e}{t_{wo} - t_e} \right) \right] \bar{x}} \qquad \text{(III.E.39)}$$

Thus

$$Nu_o = \frac{1}{0.811339\, \bar{x}^{-\frac{1}{3}} - 3 \left[1 + \left(\frac{t_{wi} - t_e}{t_{wo} - t_e} \right) \right] \bar{x}} \qquad \text{(III.E.40)}$$

For most wall temperature ratios, the second term in the denominator is negligibly small compared with the first.

b. Case two

Here $\theta_{oi}^{(2)} = 0$ at very small $\bar{x}$, so (II.E.7) becomes

$$Nu_o = \frac{1}{\theta_{oo}^{(2)} - \theta_{mo}^{(2)} \left(1 + \frac{q''_{wi}}{q''_{wo}}\right)} \qquad \text{(III.E.41)}$$

Combining the above with (III.E.35) and (III.E.37)

$$Nu_o = \frac{1}{\frac{12}{48^{\frac{2}{3}} \Gamma\left(\frac{2}{3}\right)} \bar{x}^{\frac{1}{3}} - 2 \left(1 + \frac{q''_{wi}}{q''_{wo}}\right) \bar{x}} \qquad \text{(III.E.42)}$$

Or

$$Nu_o = \frac{1}{0.670950\ \bar{x}^{\frac{1}{3}} - 2 \left(1 + \frac{q''_{wi}}{q''_{wo}}\right) \bar{x}} \qquad \text{(III.E.43)}$$

Again, for most wall heat-flux ratios the second term is negligibly small.

c. Case three

In this case $\Phi_{oi}^{(4)} = 0$, and (II.E.9) becomes

$$Nu_o = \frac{\Phi_{oo}^{(3)}}{1 - \theta_{mo}^{(3)} - \theta_{mi}^{(4)} \left(\frac{q''_{wi} \frac{D_h}{k}}{t_{wo} - t_e}\right)} \qquad \text{(III.E.44)}$$

Introducing (III.E.17), (III.E.21), and (III.E.37)

$$Nu_o = \frac{\frac{12}{48^{\frac{1}{3}}\,\Gamma\left(\frac{1}{3}\right)}\,\bar{x}^{-\frac{1}{3}}}{1 - \frac{36}{48^{\frac{1}{3}}\,\Gamma\left(\frac{1}{3}\right)}\,\bar{x}^{\frac{2}{3}} - 2\left(\frac{q''_{wi}\,\frac{D_h}{k}}{t_{wo} - t_e}\right)\bar{x}} \qquad \text{(III.E.45)}$$

Or

$$Nu_o = \frac{1.23253\,\bar{x}^{-\frac{1}{3}}}{1 - 3.69759\,\bar{x}^{\frac{2}{3}} - 2\left(\frac{q''_{wi}\,\frac{D_h}{k}}{t_{wo} - t_e}\right)\bar{x}} \qquad \text{(III.E.46)}$$

d. Case four

Here $\theta_{oi}^{(3)} = 0$ at very small $\bar{x}$, so (II.E.11) becomes

$$Nu_o = \frac{1}{\theta_{oo}^{(4)} - \theta_{mo}^{(4)} - \theta_{mo}^{(3)}\left(\frac{t_{wi} - t_e}{q''_{wo}\,\frac{D_h}{k}}\right)} \qquad \text{(III.E.47)}$$

Combining the above with (III.E.35), (III.E.37), and (III.E.21)

$$Nu_o = \frac{1}{\frac{12}{48^{\frac{2}{3}}\,\Gamma\left(\frac{2}{3}\right)}\,\bar{x}^{\frac{1}{3}} - 2\bar{x} - \frac{36}{48^{\frac{1}{3}}\,\Gamma\left(\frac{1}{3}\right)}\left(\frac{t_{wi} - t_e}{q''_{wo}\,\frac{D_h}{k}}\right)\bar{x}^{\frac{2}{3}}} \qquad \text{(III.E.48)}$$

Hence

$$Nu_o = \frac{1}{0.670950\,\bar{x}^{\frac{1}{3}} - 2\bar{x} - 3.69759\left(\frac{t_{wi} - t_e}{q''_{wo}\frac{D_h}{k}}\right)\bar{x}^{\frac{2}{3}}} \qquad \text{(III.E.49)}$$

III. F. Relations Valid at Large $\bar{x}$

It can be seen from the fundamental solution expressions in Section III.C that at very large values of $\bar{x}$ the infinite series become negligibly small and the solutions take on a much simpler form. Since in some applications $\bar{x}$ will be large, this section is included to set forth the fundamental solutions and Nusselt number relations valid in this region. These are the fully developed solutions, applying downstream of the thermal entry length.

1. The fully developed fundamental solutions

These expressions are obtained in each case by setting the infinite series in the corresponding fundamental solution in Section III.C equal to zero.

a. Case one

$$\theta_{oo}^{(1)} = \theta_{ii}^{(1)} = 1$$

$$\theta_{oi}^{(1)} = \theta_{io}^{(1)} = 0$$

$$\Phi_{oo}^{(1)} = \Phi_{ii}^{(1)} = 2$$

$$\Phi_{oi}^{(1)} = \Phi_{io}^{(1)} = -2$$

$$\theta_{mo}^{(1)} = \theta_{mi}^{(1)} = \frac{1}{2}$$

b. Case two

$$\theta_{oo}^{(2)} = \theta_{ii}^{(2)} = 2\bar{x} + \frac{13}{70}$$

$$\theta_{oi}^{(2)} = \theta_{io}^{(2)} = 2\bar{x} - \frac{9}{140}$$

$$\Phi_{oo}^{(2)} = \Phi_{ii}^{(2)} = 1$$

$$\Phi_{oi}^{(2)} = \Phi_{io}^{(2)} = 0$$

$$\theta_{mo}^{(2)} = \theta_{mi}^{(2)} = 2\bar{x}$$

c. Case three

$$\theta_{oo}^{(3)} = \theta_{ii}^{(3)} = 1$$

$$\theta_{oi}^{(3)} = \theta_{io}^{(3)} = 1$$

$$\Phi_{oo}^{(3)} = \Phi_{ii}^{(3)} = 0$$

$$\Phi_{oi}^{(3)} = \Phi_{io}^{(3)} = 0$$

$$\theta_{mo}^{(3)} = \theta_{mi}^{(3)} = 1$$

d. Case four

$$\theta_{oo}^{(4)} = \theta_{ii}^{(4)} = \frac{1}{2}$$

$$\theta_{oi}^{(4)} = \theta_{io}^{(4)} = 0$$

$$\Phi_{oo}^{(4)} = \Phi_{ii}^{(4)} = 1$$

$$\Phi_{oi}^{(4)} = \Phi_{io}^{(4)} = -1$$

$$\theta_{mo}^{(4)} = \theta_{mi}^{(4)} = \frac{1}{4}$$

2. The fully developed Nusselt number relations

The fully developed Nusselt number relations follow from the preceding results and those of Section II.E. It should be pointed out that the shape of the temperature profiles becomes fully established long before the profiles become fully developed in the sense outlined in Section III.B, and for this reason the Nusselt number relations become fully developed, or invarient with $\bar{x}$, at $\bar{x}$ values approximately an order of magnitude smaller than do the fundamental solutions.

a. Case one

Here one obtains

$$Nu_o = \frac{2 - 2\left(\frac{t_{wi} - t_e}{t_{wo} - t_e}\right)}{1 - \frac{1}{2}\left[1 + \left(\frac{t_{wi} - t_e}{t_{wo} - t_e}\right)\right]} \qquad \text{(III.F.1)}$$

Thus

$$Nu_o = 4\left[\frac{1 - \left(\frac{t_{wi} - t_e}{t_{wo} - t_e}\right)}{1 - \left(\frac{t_{wi} - t_e}{t_{wo} - t_e}\right)}\right] \qquad \text{(III.F.2)}$$

Therefore, when $t_{wi} \neq t_{wo}$, $Nu_o = 4$. (III.F.3)

When $t_{wi} = t_{wo}$, (III.F.2) is indeterminate and other means must be employed to evaluate Nu_o. Combining the appropriate Nusselt number expression of Section II.E with the appropriate general fundamental solutions of Section III.C yields

$$Nu_o = \frac{8}{3} \frac{\left[\sum_{n=o}^{\infty} C_n Y_n'(1) e^{-\frac{32}{3}\lambda_n^2 \bar{x}} - \sum_{n=o}^{\infty} C_n Y_n'(-1) e^{-\frac{32}{3}\lambda_n^2 \bar{x}} \right]}{\left[\sum_{n=o}^{\infty} \frac{C_n}{\lambda_n^2} Y_n'(1) e^{-\frac{32}{3}\lambda_n^2 \bar{x}} - \sum_{n=o}^{\infty} \frac{C_n}{\lambda_n^2} Y_n'(-1) e^{-\frac{32}{3}\lambda_n^2 \bar{x}} \right]}$$

As $\bar{x}$ becomes large this expression approaches

$$Nu_o = \frac{8}{3} \frac{\left[C_o Y_o'(1) - C_o Y_o'(-1) \right]}{\left[\frac{C_o}{\lambda_o^2} Y_o'(1) - \frac{C_o}{\lambda_o^2} Y_o'(-1) \right]}$$

Thus

$$Nu_o = \frac{8}{3} \lambda_o^2 \quad \text{when} \quad t_{wi} = t_{wo} \tag{III.F.4}$$

In Section III.G it is found that $\lambda_o^2 = 2.82777$, so

$$Nu_o = 7.54072 \quad \text{when} \quad t_{wi} = t_{wo} \tag{III.F.5}$$

b. Case two

Combining (II.E.7) with the appropriate fully developed fundamental solutions in Section III.F.1

$$Nu_o = \frac{1}{2\bar{x} + \frac{13}{70} + \left(2\bar{x} - \frac{9}{140}\right)\left(\frac{q''_{wi}}{q''_{wo}}\right) - 2\bar{x}\left(1 + \frac{q''_{wi}}{q''_{wo}}\right)} \tag{III.F.6}$$

Thus

$$Nu_o = \frac{140}{26 - 9\frac{q''_{wi}}{q''_{wo}}} \tag{III.F.7}$$

Note that when $q''_{wi} = q''_{wo}$, $Nu_o = 8.23529$ (III.F.8)

and when $q''_{wi} = 0$, $Nu_o = 5.38462$ (III.F.9)

For convenience, (III.F.7) is plotted in Figure III.F.1. By referring to the curve one can see the strong influence of heat flux ratio on the laminar case two Nusselt number.

c. Case three

For this case

$$Nu_o = \frac{-\left(\frac{q''_{wi}\frac{D_h}{k}}{t_{wo} - t_e}\right)}{1 - 1 - \frac{1}{4}\left(\frac{q''_{wi}\frac{D_h}{k}}{t_{wo} - t_e}\right)} \qquad \text{(III.F.10)}$$

Hence, when $q''_{wi} \neq 0$, $Nu_o = 4$ (III.F.11)

When $q''_{wi} = 0$ (III.F.10) is indeterminate, and, as in case one, the entry length expressions must be used. From (II.E.9) and the fundamental solution expressions of Section III.C

$$Nu_o = \frac{4\sum_{n=o}^{\infty} C_n Y'_n(1) e^{-\frac{32}{3}\lambda_n^2 \bar{x}}}{1 - 1 + \frac{3}{4}\sum_{n=o}^{\infty} \frac{C_n}{\lambda_n^2} Y'_n(1) e^{-\frac{32}{3}\lambda_n^2 \bar{x}}} \qquad \text{(III.F.12)}$$

for the case of $q''_{wi} = 0$. And as $\bar{x}$ becomes large this expression approaches

$$Nu_o = \frac{4C_o Y'_o(1)}{\frac{3}{4}\frac{C_o}{\lambda_o^2} Y'_o(1)}$$

Hence, when $q''_{wi} = 0$, $Nu_o = \frac{16}{3}\lambda_o^2$ (III.F.13)

In Section III.G it is found that $\lambda_o^2 = 0.91140$, so when $q''_{wi} = 0$, $Nu_o = 4.8608$ (III.F.14)

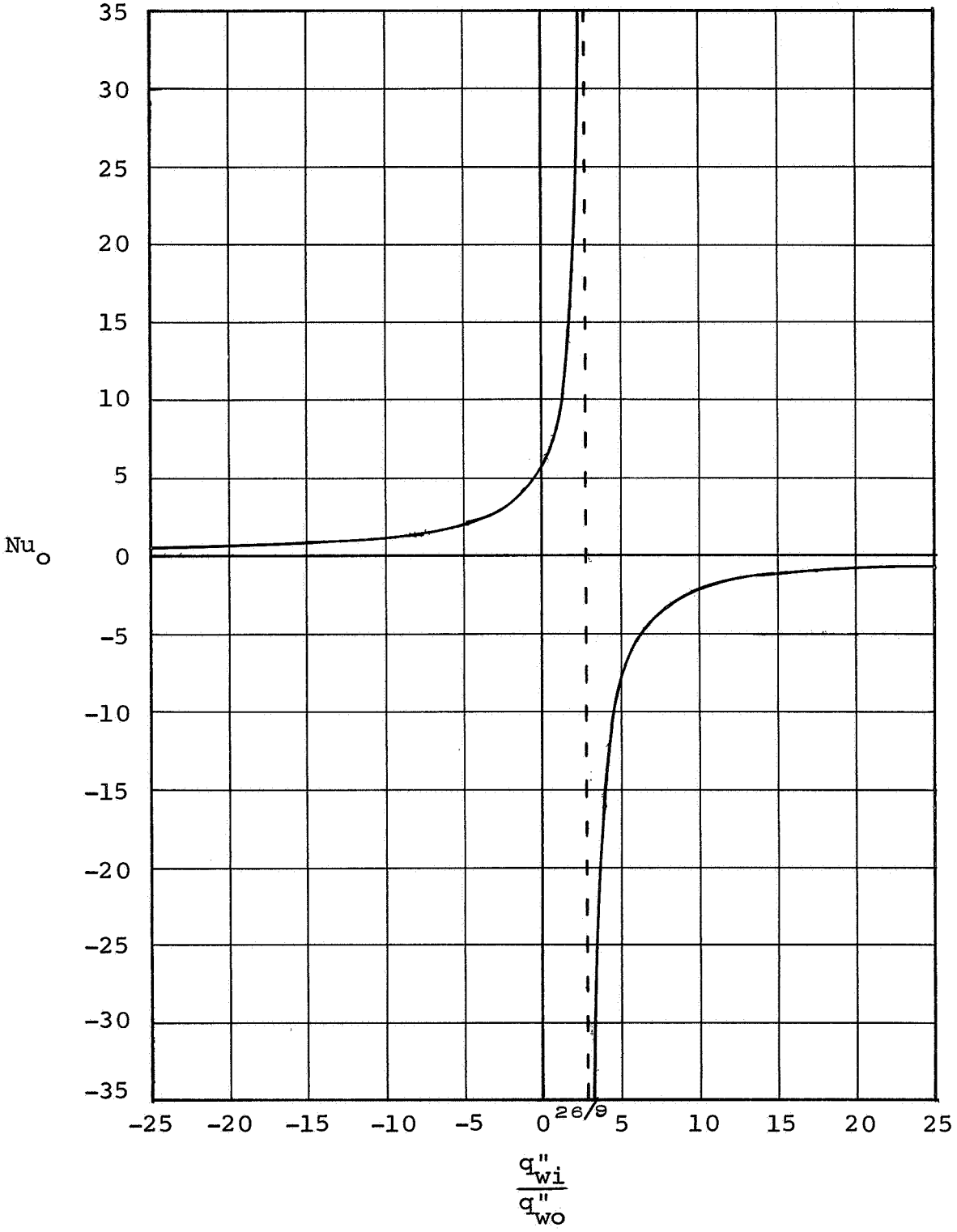

Figure III.F.1. Laminar Fully Developed Constant Heat Flux Nusselt Number

d. Case four

Here one obtains

$$Nu_o = \frac{1}{\frac{1}{2} - \frac{1}{4} + (1 - 1)\left(\frac{t_{wi} - t_e}{q''_{wo}\frac{D_h}{k}}\right)} \qquad \text{(III.F.15)}$$

Thus, when $q''_{wo} \neq 0$, $Nu_o = 4$ (III.F.16)

And when $q''_{wo} = 0$, $Nu_o = 0$ (III.F.17)

III. G. Solution of the Sturm-Liouville Equation

1. General considerations

It will be recalled from Section III.B.2 that the following Sturm-Liouville equation results from the separation of variables in the energy equation

$$Y''_n + \lambda_n^2 (1 - \bar{y}^2) Y_n = 0 \qquad \text{(III.G.1)}$$

Up to this point it has been tacitly assumed that the eigenfunctions, Y_n, are known quantities, but no mention was made of the means by which these numbers were obtained. And to be sure, the reader interested only in obtaining answers to a particular practical problem need not concern himself with such details; the previous sections along with Table III.C.1 and Figures III.C.1 through III.C.4 should suffice for his purposes. However, since the bulk of the effort involved in preparing the aforementioned figures is centered on the solution of (III.G.1), it is only proper that this solution be discussed.

For the lower values of λ_n the equation must be solved numerically, and the method used for this is set forth in the succeeding section. But for the higher values of λ_n

it is possible to obtain an analytic asymptotic solution valid near the walls, and this is done in Section III.G.3.

2. Solution at the lower eigenvalues

As mentioned in Section III.B.2, the eigenfunctions sought are confluent hypergeometric functions, and, were these sufficiently well tabulated, the problem at hand would be reduced to nothing more than opening the proper book of tables. Unfortunately, they are not tabulated for the arguments involved here.

The historical approach to problems of this sort has been to employ the method of Frobenius. This was attempted by the author, but it was found that the series coefficients (which are functions of λ) diverge before diminishing, thus posing a severe accuracy problem.

The advent of the electronic digital computer has made feasible an alternative to the above procedure consisting of an iterative method proposed by Berry and de Prima.[5] The essentials of this method are summarized here.

If $(\lambda_n^2)_k$ is the kth approximation of the desired value, λ_n^2, and $(Y_n(\bar{y}))_k$ is a solution to (III.G.1) with $\lambda^2 = (\lambda_n^2)_k$ such that $(Y_n)_k$ satisfies the requisite boundary condition only at $\bar{y} = -1$; and further if

$$\int_{-1}^{+1} w(\bar{y}) \left(Y_n\right)_k^2 d\bar{y} = 1 \qquad \text{(III.G.2)}$$

($w(\bar{y})$, the weight function, is $(1 - \bar{y}^2)$ here) then the next approximation is given by

$$\left(\lambda_n^2\right)_{k+1} = \left(\lambda_n^2\right)_k \pm \left(Y_n(1)\right)_k \cdot \left(Y_n'(1)\right)_k \qquad \text{(III.G.3)}$$

This sequence of approximations converges monotonically to λ_n^2, the value that permits satisfaction of the boundary condition at $\bar{y} = 1$. In (III.G.3) the plus (+) sign is associated with the condition of $Y_n'(1) = 0$, and the minus (-) sign with $Y_n(1) = 0$.

Computationally, the method consists of assuming a value for λ_n^2 and a value for $Y_n(-1)$ or $Y_n'(-1)$ (whichever is not specified as zero by the boundary condition), and integrating (III.G.1) numerically as an initial value problem. In general, the resulting solution will not be normalized, that is

$$\int_{-1}^{+1} (1 - \bar{y}^2) \left(Y_n\right)^2 d\bar{y} \neq 1$$

But noting that (III.B.16) is linear, it follows that

$$\left(Y_n\right)_k = K_n Y_n$$

where

$$K_n^2 = \frac{1}{\int_{-1}^{+1} (1 - \bar{y}^2) \left(Y_n\right)^2 d\bar{y}}$$

So the factor K_n is then computed and applied to satisfy condition (III.G.2). Next the assumed value of λ_n^2 is corrected by (III.G.3), and the process is repeated until the boundary condition at $\bar{y} = 1$ is satisfied. The last iteration determines λ_n and yields $Y_n(\bar{y})$. Since values for $Y_n(\bar{y})$ were stored in the computer after the final iteration it was a simple matter to calculate the eigenconstant, C_n, from (III.B.22) by a Simpson's rule integration.

The computations were performed on a Burroughs 220 Electronic Digital Computer at the Stanford University Computation Center. Further details of the computational procedure are contained in Appendix B.

The eigenvalues and pertinent combinations of constants are presented in Table III.G.1, and sketches of some lower eigenfunctions are given in Figures III.G.1 through III.G.3. It should be pointed out that results are not given for $n = 0$ for case two since the eigenfunction in that instance is a constant and the eigenconstant is zero.

3. Solution at the higher eigenvalues

It is possible to find an asymptotic solution to (III.B.16) that obviates the need for carrying out the numerical integration discussed in the preceding section for all but the first few eigenvalues. This asymptotic solution employs the WKBJ approximation (after Wentzel, Kramers, Brillouin, and Jefferies), and was first used in convective heat-transfer work by Sellars, Tribus, and Klein.[57] Applying this method, one proceeds as follows.

Let

$$Y_n = e^{g(\bar{y})} \qquad \text{(III.G.4)}$$

Then from (III.B.16)

$$g''(\bar{y}) + \left(g'(\bar{y})\right)^2 + \lambda_n^2 \, (1 - \bar{y}^2) = 0 \qquad \text{(III.G.5)}$$

Seeking an asymptotic solution of the form

$$g = \lambda_n g_o + g_1 + \lambda_n^{-1} g_2 + \cdots \qquad \text{(III.G.6)}$$

this equation is substituted into (III.G.5).

To satisfy the equation for all n the coefficients of each power of λ_n must vanish; thus one obtains

$$g_o' = \pm i \sqrt{1 - \bar{y}^2} \qquad \text{(III.G.7)}$$

and

$$g_1 = - \ln \left(\sqrt{g_o'} \right) \qquad \text{(III.G.8)}$$

Since the solution is to apply for large λ_n, the remaining terms in (III.G.6) are neglected. Combining (III.G.4), (III.G.6), (III.G.7), and (III.G.8)

$$Y_n = \frac{G\, e^{i\lambda_n \int_o^{\bar{y}} \sqrt{1-\bar{y}^2}\, dy} + H\, e^{-i\lambda_n \int_o^{\bar{y}} \sqrt{1-\bar{y}^2}\, d\bar{y}}}{\left(1 - \bar{y}^2\right)^{\frac{1}{4}}} \qquad \text{(III.G.9)}$$

This is the WKBJ approximation. Changing to a more tractable form

$$Y_n = \frac{\left[G_o \cos \lambda_n \int_o^{\bar{y}} \sqrt{1 - \bar{y}^2} - \phi \right]}{\left(1 - \bar{y}^2\right)^{\frac{1}{4}}} \qquad \text{(III.G.10)}$$

This equation will be patched into another approximate solution of (III.B.16) valid only near a wall.

a. <u>The inner wall</u>

Near the inner wall $\bar{y} \to -1$. Letting $\bar{y} = -1 + z$, $1 - \bar{y}^2 = 2z$ near the wall. Thus (III.B.16) becomes

$$Y_n'' + \lambda_n^2\, 2z\, Y_n = 0$$

where $Y = Y(z)$. This is a form of Bessel's equation having the solution

$$Y_n = G_1 z^{\frac{1}{2}} J_{\frac{1}{3}}\left(\frac{\sqrt{8}}{3}\lambda_n z^{\frac{3}{2}}\right) + H_1 z^{\frac{1}{2}} J_{-\frac{1}{3}}\left(\frac{\sqrt{8}}{3}\lambda_n z^{\frac{3}{2}}\right) \quad \text{(III.G.11)}$$

For large λ_n this has the asymptotic form

$$Y_n = \sqrt{\frac{3}{\pi\lambda_n}}\left[\frac{G_1 \cos\left(\frac{\sqrt{8}}{3}\lambda_n z^{\frac{3}{2}} - \frac{5\pi}{12}\right) + H_1 \cos\left(\frac{\sqrt{8}}{3}\lambda_n z^{\frac{3}{2}} - \frac{\pi}{12}\right)}{2^{\frac{1}{4}} z^{\frac{1}{4}}}\right]$$

(III.G.12)

Directing attention back to the WKBJ form (III.G.10), note that

$$\int_0^{\bar{y}} \sqrt{1 - \bar{y}^2}\, d\bar{y} = \int_0^{-1} \sqrt{1 - \bar{y}^2}\, d\bar{y} + \int_{-1}^{\bar{y}} \sqrt{1 - \bar{y}^2}\, d\bar{y}$$

$$= -\frac{\pi}{4} + \int_0^z \sqrt{2z - z^2}\, dz$$

So near the inner wall (for small z)

$$\int_0^{\bar{y}} \sqrt{1 - \bar{y}^2}\, d\bar{y} = -\frac{\pi}{4} + \frac{\sqrt{8}}{3} z^{\frac{3}{2}}$$

Hence (III.G.10) becomes

$$Y_n = \frac{G_o \cos\left[\frac{\sqrt{8}}{3}\lambda_n z^{\frac{3}{2}} - \left(\frac{\pi}{4}\lambda_n + \phi\right)\right]}{2^{\frac{1}{4}} z^{\frac{1}{4}}} \quad \text{(III.G.13)}$$

In order to patch (III.G.12) and (III.G.13) it is apparent that one must take

$$G_o = \sqrt{\frac{3}{\pi\lambda_n}} \qquad \text{(III.G.14)}$$

and

$$G_1 \cos\frac{5\pi}{12} + H_1 \cos\frac{\pi}{12} = \cos\left(\frac{\pi}{4}\lambda_n + \phi\right) \qquad \text{(III.G.15)}$$

$$G_1 \sin\frac{5\pi}{12} + H_1 \sin\frac{\pi}{12} = \sin\left(\frac{\pi}{4}\lambda_n + \phi\right) \qquad \text{(III.G.16)}$$

ϕ, and thus G_1 and H_1, will be determined later when the appropriate boundary conditions are brought into consideration.

b. <u>The outer wall</u>

Near the outer wall $\bar{y} \to 1$. Letting $\bar{y} = 1 - \zeta$, $1 - \bar{y}^2 = 2\zeta$ near the wall. Then (III.B.16) becomes

$$Y_n'' + \lambda_n^2 2\zeta\, Y_n = 0$$

where $Y = Y(\zeta)$. As before, the solution of this equation is

$$Y_n = G_2\zeta^{\frac{1}{2}}J_{\frac{1}{3}}\left(\frac{\sqrt{8}}{3}\lambda_n\zeta^{\frac{3}{2}}\right) + H_2\zeta^{\frac{1}{2}}J_{-\frac{1}{3}}\left(\frac{\sqrt{8}}{3}\lambda_n\zeta^{\frac{3}{2}}\right) \qquad \text{(III.G.17)}$$

And again, for large λ_n

$$Y_n = \sqrt{\frac{3}{\pi\lambda_n}}\left[\frac{G_2\cos\left(\frac{\sqrt{8}}{3}\lambda_n\zeta^{\frac{3}{2}} - \frac{5\pi}{12}\right) + H_1\cos\left(\frac{\sqrt{8}}{3}\lambda_n\zeta^{\frac{3}{2}} - \frac{\pi}{12}\right)}{2^{\frac{1}{4}}\,\zeta^{\frac{1}{4}}}\right]$$

(III.G.18)

Here the integral appearing in (III.G.10) becomes

$$\int_0^{\bar{y}} \sqrt{1 - \bar{y}^2}\, d\bar{y} = \int_0^1 \sqrt{1 - \bar{y}^2}\, d\bar{y} + \int_1^{\bar{y}} \sqrt{1 - \bar{y}^2}\, d\bar{y}$$

$$= \frac{\pi}{4} - \int_0^{\zeta} \sqrt{2\zeta - \zeta^2}\, d\zeta$$

$$= \frac{\pi}{4} - \frac{\sqrt{8}}{3} \zeta^{\frac{3}{2}}$$

So (III.G.10) becomes

$$Y_n = \sqrt{\frac{3}{\pi \lambda_n}}\ \frac{\cos\left[\frac{\sqrt{8}}{3} \lambda_n \zeta^{\frac{3}{2}} - \left(\frac{\pi}{4} \lambda_n - \phi\right)\right]}{2^{\frac{1}{4}}\ \zeta^{\frac{1}{4}}} \qquad \text{(III.G.19)}$$

And patching (III.G.18) and (III.G.19) requires that

$$G_2 \cos \frac{5\pi}{12} + H_2 \cos \frac{\pi}{12} = \cos\left(\frac{\pi}{4} \lambda_n - \phi\right) \qquad \text{(III.G.20)}$$

$$G_2 \sin \frac{5\pi}{12} + H_2 \sin \frac{\pi}{12} = \sin\left(\frac{\pi}{4} \lambda_n - \phi\right) \qquad \text{(III.G.21)}$$

Now the four sets of boundary conditions will be discussed.

c. Case one

Here the boundary conditions are

$$Y(-1) = 0$$

$$Y(1) = 0$$

Applying (III.G.11) at the inner wall it is found that $H_1 = 0$ since $z^{\frac{1}{2}} J_{-\frac{1}{3}}\left(\frac{\sqrt{8}}{3} \lambda_n z^{\frac{3}{2}}\right)$ does not approach zero

with z. Then from (III.G.15) and (III.G.16)

$$\cos\frac{5\pi}{12}\sin\left(\frac{\pi}{4}\lambda_n+\phi\right)-\sin\frac{5\pi}{12}\cos\left(\frac{\pi}{4}\lambda_n+\phi\right)=0$$

So

$$\sin\left(\frac{\pi}{4}\lambda_n+\phi-\frac{5\pi}{12}\right)=0 \qquad \text{(III.G.22)}$$

This demands

$$\frac{\pi}{4}\lambda_n+\phi-\frac{5\pi}{12}=\pm n\pi,\quad n=0,1,2,\cdots \qquad \text{(III.G.23)}$$

No generality is sacrificed if $n = 0$. And from (III.G.16) and (III.G.23)

$$G_1=1 \qquad \text{(III.G.24)}$$

Thus near the inner wall

$$Y_n=z^{\frac{1}{2}}J_{\frac{1}{3}}\left(\frac{\sqrt{8}}{3}\lambda_n z^{\frac{3}{2}}\right) \qquad \text{(III.G.25)}$$

At the outer wall $H_2 = 0$ for the same reason that $H_1 = 0$ at the inner. So

$$\sin\left(\frac{\pi}{4}\lambda_n-\phi-\frac{5\pi}{12}\right)=0 \qquad \text{(III.G.26)}$$

Combining this with (III.G.23) yields

$$\lambda_n=2n+\frac{5}{3},\quad n=0,1,2,\cdots \qquad \text{(III.G.27)}$$

Also

$$G_2=(-1)^n \qquad \text{(III.G.28)}$$

So near the outer wall

$$Y_n = (-1)^n \zeta^{\frac{1}{2}} J_{\frac{1}{3}}\left(\frac{\sqrt{8}}{3}\lambda_n \zeta^{\frac{3}{2}}\right) \qquad \text{(III.G.29)}$$

The asymptotic eigenvalue expression is now in hand, but the eigenconstants have yet to be determined; they are given by (A.9). From (III.G.25)

$$\left(\frac{\partial Y_n}{\partial \bar{y}}\right)_{\bar{y}\to -1} = z^{-\frac{1}{2}} J_{\frac{1}{3}}\left(\frac{\sqrt{8}}{3}\lambda_n z^{\frac{3}{2}}\right) - \frac{\sqrt{8}}{2}\lambda_n z\, J_{\frac{4}{3}}\left(\frac{\sqrt{8}}{3}\lambda_n z^{\frac{3}{2}}\right) \qquad \text{(III.G.30)}$$

As $z \to 0$, $z J_{\frac{4}{3}} \to 0$ and $z^{-\frac{1}{2}} J_{\frac{1}{3}} \to \dfrac{2^{\frac{1}{6}} \lambda_n^{\frac{1}{3}}}{3^{\frac{1}{3}} \Gamma\left(\frac{4}{3}\right)}$

So

$$\left(\frac{\partial Y_n}{\partial \bar{y}}\right)_{\bar{y}=-1} = \frac{2^{\frac{1}{6}} \lambda_n^{\frac{1}{3}}}{3^{\frac{1}{3}} \Gamma\left(\frac{4}{3}\right)} \qquad \text{(III.G.31)}$$

Noting from (III.G.25) that at $\bar{y} = -1$, Y_n vanishes for all values of λ

$$\left(\frac{\partial Y_n}{\partial \lambda_n}\right)_{\bar{y}=-1} = 0 \qquad \text{(III.G.32)}$$

Passing to the outer wall, from (III.G.29)

$$\left(\frac{\partial Y_n}{\partial \bar{y}}\right)_{\bar{y}\to 1} = (-1)^{n+1}\left[\zeta^{-\frac{1}{2}} J_{\frac{1}{3}}\left(\frac{\sqrt{8}}{3}\lambda_n \zeta^{\frac{3}{2}}\right) - \frac{\sqrt{8}}{2}\lambda_n \zeta J_{\frac{4}{3}}\left(\frac{\sqrt{8}}{3}\lambda_n \zeta^{\frac{3}{2}}\right)\right] \qquad \text{(III.G.33)}$$

So at the outer wall

$$\left(\frac{\partial Y_n}{\partial \bar{y}}\right)_{\bar{y}=1} = (-1)^{n+1} \frac{2^{\frac{1}{6}} \lambda_n^{\frac{1}{3}}}{3^{\frac{1}{3}} \Gamma\left(\frac{4}{3}\right)} \qquad \text{(III.G.34)}$$

Note that at this wall $Y_n = 0$ only for $\lambda = \lambda_n$, so $\frac{\partial Y_n}{\partial \lambda_n}$ must be computed from (III.G.17).

$$\left(\frac{\partial Y_n}{\partial \lambda_n}\right)_{\bar{y}\to 1} = G_2 \frac{\partial}{\partial \lambda_n}\left(\zeta^{\frac{1}{2}} J_{\frac{1}{3}}\right) + H_2 \frac{\partial}{\partial \lambda_n}\left(\zeta^{\frac{1}{2}} J_{-\frac{1}{3}}\right)$$

$$+ \zeta^{\frac{1}{2}} J_{\frac{1}{3}} \frac{\partial G_2}{\partial \lambda_n} + \zeta^{\frac{1}{2}} J_{-\frac{1}{3}} \frac{\partial H_2}{\partial \lambda_n}$$

As $\zeta \to 0$ the first three terms vanish, but since

$$H_2 = \frac{\sin\left(\frac{\pi}{4}\lambda_n - \phi - \frac{5\pi}{12}\right)}{\sin\left(-\frac{\pi}{3}\right)}$$

(from (III.G.20) and (III.G.21)), then

$$\frac{\partial H_2}{\partial \lambda_n} = (-1)^{n+1} \frac{\pi}{\sqrt{3}} \qquad \text{(III.G.35)}$$

So

$$\left(\frac{\partial Y_n}{\partial \lambda_n}\right)_{\bar{y}=1} = \frac{(-1)^{n+1}\pi}{6^{\frac{1}{6}} \Gamma\left(\frac{2}{3}\right)} \lambda_n^{-\frac{1}{3}} \qquad \text{(III.G.36)}$$

Employing (A.9) yields

$$C_n = (-1)^{n+1} \frac{2}{\pi} 6^{\frac{1}{6}} \Gamma\left(\frac{2}{3}\right) \lambda_n^{-\frac{2}{3}}$$

Also

$$C_n Y'_n(-1) = (-1)^{n+1} \frac{2^{\frac{4}{3}}}{3^{\frac{1}{6}}\pi} \frac{\Gamma\left(\frac{2}{3}\right)}{\Gamma\left(\frac{4}{3}\right)} \lambda_n^{-\frac{1}{3}}$$

$$= (-1)^{n+1} \, 1.012788 \, \lambda_n^{-\frac{1}{3}}$$

and

$$C_n Y'_n(1) = \frac{2^{\frac{4}{3}}}{3^{\frac{1}{6}}\pi} \frac{\Gamma\left(\frac{2}{3}\right)}{\Gamma\left(\frac{4}{3}\right)} \lambda_n^{-\frac{1}{3}}$$

$$= 1.012788 \, \lambda_n^{-\frac{1}{3}}$$

d. Case two

Here the boundary conditions are

$$Y'(-1) = 0$$

$$Y'(1) = 0$$

Differentiation of (III.G.11) gives

$$\left(\frac{\partial Y_n}{\partial \bar{y}}\right)_{\bar{y} \to -1} = G_1 \frac{\sqrt{8}}{2} \lambda_n z \, J_{-\frac{2}{3}}\left(\frac{\sqrt{8}}{3} \lambda_n z^{\frac{3}{2}}\right)$$

$$- H_1 \frac{\sqrt{8}}{2} \lambda_n z \, J_{\frac{2}{3}}\left(\frac{\sqrt{8}}{3} \lambda_n z^{\frac{3}{2}}\right) \qquad \text{(III.G.37)}$$

To satisfy the boundary condition at the inner wall

$$G_1 = 0$$

Then from (III.G.15) and (III.G.16)

$$\sin\left(\frac{\pi}{4}\lambda_n + \phi - \frac{\pi}{12}\right) = 0$$

from which

$$\phi = \frac{\pi}{12} - \frac{\pi}{4}\lambda_n \pm n\pi, \quad n = 0, 1, 2, \cdots \qquad \text{(III.G.38)}$$

Again n is taken to be zero. It follows that

$$H_1 = 1 \qquad \text{(III.G.39)}$$

So near the inner wall

$$Y_n = z^{\frac{1}{2}} J_{-\frac{1}{3}}\left(\frac{\sqrt{8}}{3}\lambda_n z^{\frac{3}{2}}\right) \qquad \text{(III.G.40)}$$

A similar condition exists at the outer wall, resulting in

$$\sin\left(\frac{\pi}{4}\lambda_n - \phi - \frac{\pi}{12}\right) = 0$$

$$\lambda_n = 2n + \frac{1}{3}, \quad n = 0, 1, 2, \cdots \qquad \text{(III.G.41)}$$

As before, this result leads to

$$H_2 = (-1)^n \qquad \text{(III.G.42)}$$

So near the outer wall

$$Y_n = (-1)^n \zeta^{\frac{1}{2}} J_{-\frac{1}{3}}\left(\frac{\sqrt{8}}{3}\lambda_n \zeta^{\frac{3}{2}}\right) \qquad \text{(III.G.43)}$$

Now, in order to find the expression for the eigenconstants, $\frac{\partial}{\partial \bar{y}}\left(\frac{\partial Y_n}{\partial \lambda_n}\right)$ must be determined at both walls.

Differentiating (III.G.40) yields

$$\frac{\partial}{\partial \bar{y}}\left(\frac{\partial Y_n}{\partial \lambda_n}\right)_{\bar{y}\to -1} = -\frac{5}{6}\sqrt{8}\, z\, J_{\frac{2}{3}}\left(\frac{\sqrt{8}}{3}\lambda_n z^{\frac{3}{2}}\right) + \frac{4}{3}\lambda_n z^{\frac{5}{2}} J_{\frac{5}{3}}\left(\frac{\sqrt{8}}{3}\lambda_n z^{\frac{3}{2}}\right) \tag{III.G.44}$$

At $z = 0$ both of the above terms vanish, so

$$\frac{\partial}{\partial \bar{y}}\left(\frac{\partial Y_n}{\partial \lambda_n}\right)_{\bar{y}=-1} = 0$$

Near the outer wall $G_2 = G_2(\lambda)$, so

$$\frac{\partial}{\partial \bar{y}}\left(\frac{\partial Y_n}{\partial \lambda_n}\right)_{\bar{y}\to 1} = -\left(\frac{dG_2}{d\lambda_n}\right)\left\{\frac{d}{d\zeta}\left[\zeta^{\frac{1}{2}} J_{\frac{1}{3}}\left(\frac{\sqrt{8}}{3}\lambda_n \zeta^{\frac{3}{2}}\right)\right]\right\}$$

Now since

$$G_2 = \frac{\sin\left(\frac{\pi}{12} - \frac{\pi}{4}\lambda_n + \phi\right)}{\sin\left(-\frac{\pi}{3}\right)} \tag{III.G.45}$$

it follows that

$$\frac{dG_2}{d\lambda_n} = (-1)^n \frac{\pi}{\sqrt{3}} \tag{III.G.46}$$

Thus, at the outer wall

$$\frac{\partial}{\partial \bar{y}}\left(\frac{\partial Y_n}{\partial \lambda_n}\right)_{\bar{y}=1} = (-1)^{n+1} \frac{\pi\, 2^{\frac{1}{6}}}{3^{\frac{5}{6}}\,\Gamma\left(\frac{4}{3}\right)} \lambda_n^{\frac{1}{3}} \tag{III.G.47}$$

And from (III.G.40) and (III.G.43)

$$Y_n(-1) = \frac{3^{\frac{1}{3}}}{2^{\frac{1}{6}}\,\Gamma\left(\frac{2}{3}\right)}\,\lambda_n^{-\frac{1}{3}} \qquad \text{(III.G.48)}$$

$$Y_n(1) = (-1)^n\,\frac{3^{\frac{1}{3}}}{2^{\frac{1}{6}}\,\Gamma\left(\frac{2}{3}\right)}\,\lambda_n^{-\frac{1}{3}} \qquad \text{(III.G.49)}$$

So employing (A.10) yields

$$C_n = (-1)^{n+1}\,\frac{3^{\frac{5}{6}}}{\pi\,2^{\frac{7}{6}}}\,\Gamma\left(\frac{4}{3}\right)\lambda_n^{-\frac{4}{3}} \qquad \text{(III.G.50)}$$

Also

$$C_nY_n(-1) = (-1)^{n+1}\,\frac{3^{\frac{7}{6}}}{2^{\frac{4}{3}}\,\pi}\,\frac{\Gamma\left(\frac{4}{3}\right)}{\Gamma\left(\frac{2}{3}\right)}\,\lambda_n^{-\frac{5}{3}}$$

$$= (-1)^{n+1}\;0.3001255\;\lambda_n^{-\frac{5}{3}}$$

and

$$C_nY_n(1) = -\,\frac{3^{\frac{7}{6}}}{2^{\frac{4}{3}}\,\pi}\,\frac{\Gamma\left(\frac{4}{3}\right)}{\Gamma\left(\frac{2}{3}\right)}\,\lambda_n^{-\frac{5}{3}}$$

$$= -\;0.3001255\;\lambda_n^{-\frac{5}{3}}$$

e. Case three

Here the boundary conditions are

$$Y'(-1) = 0$$

$$Y(1) = 0$$

Proceeding as before it is found that at the inner wall

$$G_1 = 0$$

$$\phi = \frac{\pi}{12} - \frac{\pi}{4}\lambda_n$$

$$H_1 = 1$$

Thus

$$Y_n = z^{\frac{1}{2}} J_{-\frac{1}{3}}\left(\frac{\sqrt{8}}{3}\lambda_n z^{\frac{3}{2}}\right) \qquad \text{(III.G.51)}$$

The conditions at the outer wall demand that

$$\sin\left(\frac{\pi}{4}\lambda_n - \phi - \frac{5\pi}{12}\right) = 0$$

So

$$\lambda_n = 2n + 1, \quad n = 0, 1, 2, \cdots \qquad \text{(III.G.52)}$$

And for the region near the outer wall it is found that

$$Y_n = (-1)^n \zeta^{\frac{1}{2}} J_{\frac{1}{3}}\left(\frac{\sqrt{8}}{3}\lambda_n \zeta^{\frac{3}{2}}\right) \qquad \text{(III.G.53)}$$

Now, $Y_n'(1)$ is given by (III.G.34), $Y_n(-1)$ by (III.G.48), and $\left(\frac{\partial Y_n}{\partial \lambda_n}\right)_{\bar{y}=1}$ by (III.G.36); so from (A.11)

there results

$$C_n = (-1)^{n+1} \frac{2 \cdot 6^{\frac{1}{6}}}{\pi} \Gamma\left(\frac{2}{3}\right) \lambda_n^{-\frac{2}{3}} \qquad \text{(III.G.54)}$$

Also

$$C_n Y_n(-1) = (-1)^{n+1} \frac{2}{\pi} 3^{\frac{1}{2}} \lambda_n^{-1}$$

$$= (-1)^{n+1} \, 1.102658 \, \lambda_n^{-1}$$

and

$$C_n Y_n'(1) = \frac{2^{\frac{4}{3}}}{3^{\frac{1}{6}} \pi} \frac{\Gamma\left(\frac{2}{3}\right)}{\Gamma\left(\frac{4}{3}\right)} \lambda_n^{-\frac{1}{3}}$$

$$= 1.012788 \, \lambda_n^{-\frac{1}{3}}$$

f. Case four

Here the boundary conditions are

$$Y(-1) = 0$$

$$Y'(1) = 0$$

At the inner wall there obtains

$$H_1 = 0$$

$$\phi = \frac{5\pi}{12} - \frac{\pi}{4} \lambda_n$$

$$G_1 = 1$$

So

$$Y_n = z^{\frac{1}{2}} J_{\frac{1}{3}}\left(\frac{\sqrt{8}}{3}\lambda_n z^{\frac{3}{2}}\right)$$

From the conditions at the outer wall

$$\sin\left(\frac{\pi}{4}\lambda_n - \phi - \frac{\pi}{12}\right) = 0$$

So

$$\lambda_n = 2n + 1, \quad n = 0, 1, 2, \cdots$$

Note that the eigenvalues for cases three and four are identical; indeed, this is to be expected since the wall boundary conditions for the two cases are symmetrical.

For the region near the outer wall it is found that

$$Y_n = (-1)^n \zeta^{\frac{1}{2}} J_{-\frac{1}{3}}\left(\frac{\sqrt{8}}{3}\lambda_n \zeta^{\frac{3}{2}}\right)$$

Now, $Y_n'(-1)$ is given by (III.G.31), $Y_n(1)$ by (III.G.49), and $\frac{\partial}{\partial \bar{y}}\left(\frac{\partial Y_n}{\partial \lambda_n}\right)_{\bar{y}=1}$ by (III.G.47), so (A.12) yields

$$C_n = (-1)^{n+1} \frac{3^{\frac{5}{6}}}{\pi\, 2^{\frac{7}{6}}} \Gamma\left(\frac{4}{3}\right) \lambda_n^{-\frac{4}{3}}$$

Also

$$C_n Y_n'(-1) = (-1)^{n+1} \frac{3^{\frac{1}{2}}}{2\pi} \lambda_n^{-1}$$

$$= (-1)^{n+1}\ 0.2756644\ \lambda_n^{-1}$$

and

$$C_n Y_n(1) = - \frac{3^{\frac{7}{6}}}{\pi\, 2^{\frac{4}{3}}} \frac{\Gamma\left(\frac{4}{3}\right)}{\Gamma\left(\frac{2}{3}\right)} \lambda_n^{-\frac{5}{3}}$$

$$= - 0.3001255\ \lambda_n^{-\frac{5}{3}}$$

The numerical results of this section are to be found in Table III.G.1. Note that the actual values rapidly approach these asymptotic results.

It should be pointed out that the eigenfunctions in this section are not normalized in the sense discussed in the preceding section, so the individual values of C_n, Y_n, and Y_n' differ by a multiplier from those found in Section III.G.2; however, this factor enters in such a manner that the actual products used, $C_n Y_n$ and $C_n Y_n'$, are identical to those in Section III.G.2.

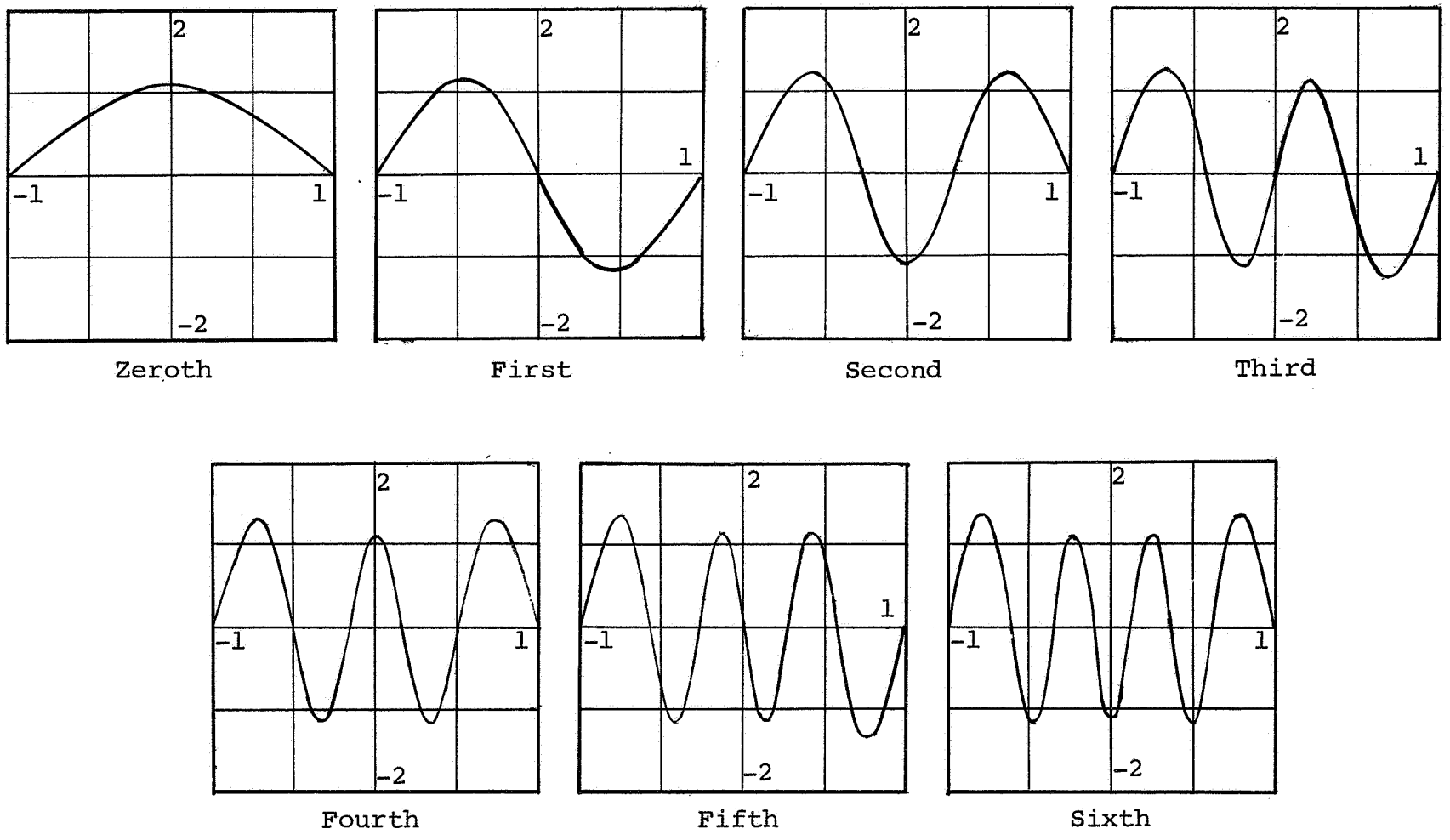

Figure III.G.1. The Eigenfunctions of the Laminar Case One

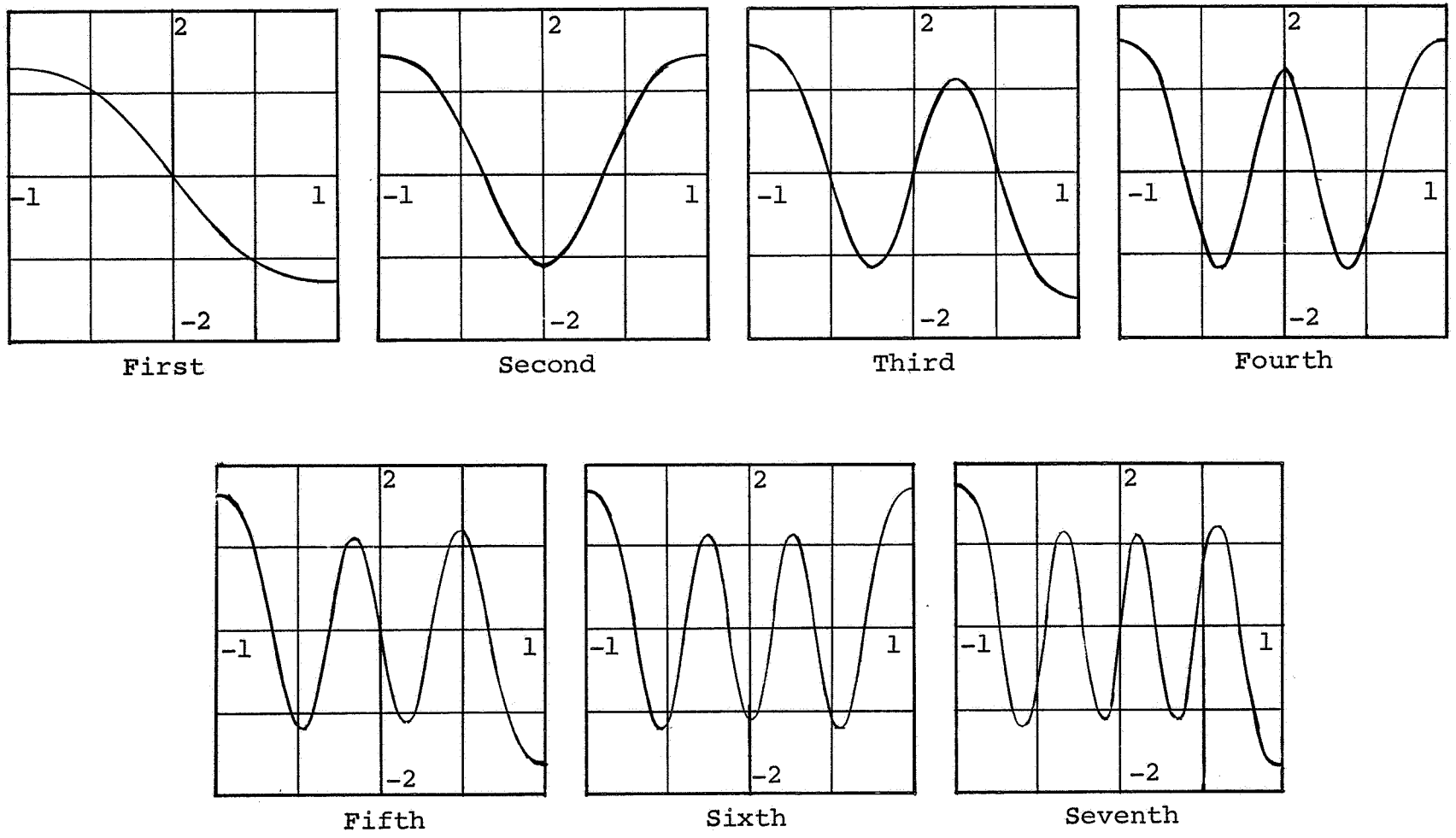

Figure III.G.2. The Eigenfunctions of the Laminar Case Two

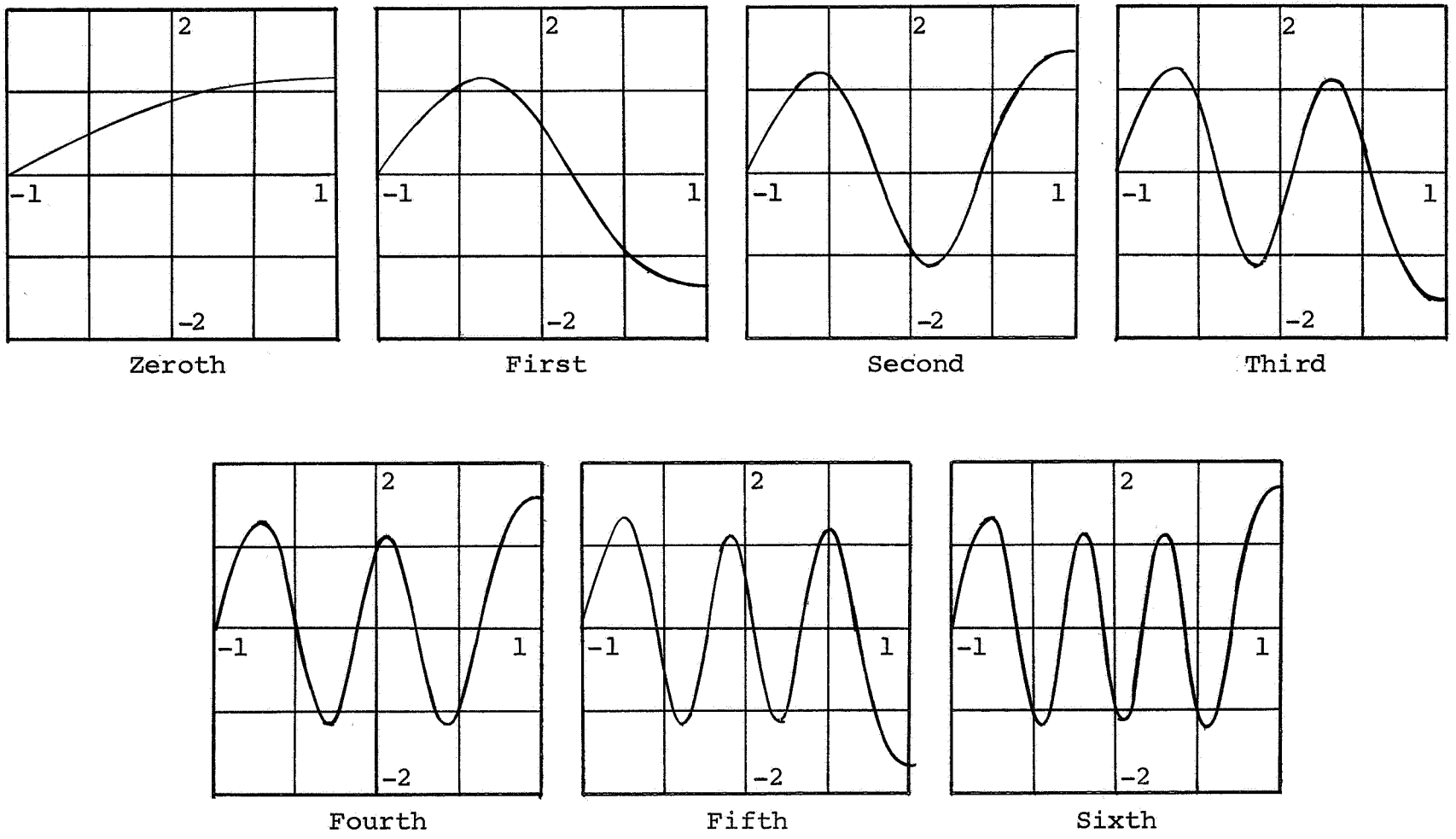

Figure III.G.3. The Eigenfunctions of the Laminar Cases Three and Four

TABLE III.G.1

LAMINAR EIGENVALUES AND CONSTANTS

Case	n	λ_n	$C_nY_n(-1)$	$C_nY_n(1)$	$C_nY_n'(-1)$	$C_nY_n'(1)$
One	0	1.6815970	0	0	-0.8580872	0.8580872
	1	3.6722938	0	0	0.6592196	0.6592196
	2	5.6698605	0	0	-0.5694625	0.5694625
	3	7.6688115	0	0	0.5145220	0.5145220
	4	9.6682450	0	0	-0.4760651	0.4760651
	5	11.667897	0	0	0.4470182	0.4470182
	6	13.667663	0	0	-0.4239725	0.4239725
	⋮					
	n	$2n + \frac{5}{3}$	0	0	$(-1)^{n+1}\,1.012788\lambda_n^{-\frac{1}{3}}$	$1.012788\lambda_n^{-\frac{1}{3}}$
Two	1	2.2631436	0.08301404	-0.08301404	0	0
	2	4.2872967	-0.02777773	-0.02777773	0	0
	3	6.2978075	0.01446840	-0.01446840	0	0
	4	8.3038990	-0.009067103	-0.009067103	0	0
	5	10.307957	0.006301757	-0.006301757	0	0
	6	12.310897	-0.004672453	-0.004672453	0	0
	7	14.313147	0.003630631	-0.003630631	0	0
	⋮					
	n	$2n + \frac{7}{3}$	$(-1)^{n+1}\,0.3001255\lambda_n^{-\frac{5}{3}}$	$-0.3001255\lambda_n^{-\frac{5}{3}}$	0	0

TABLE III.G.1 (Continued)

Case	n	λ_n	$C_nY_n(-1)$	$C_nY_n(1)$	$C_nY_n'(-1)$	$C_nY_n'(1)$
Three	0	0.95467395	-1.248417	0	0	1.088276
	1	2.9743338	0.3831966	0	0	0.7135820
	2	4.9810820	-0.2263228	0	0	0.5968426
	3	6.9846555	0.1605502	0	0	0.5318198
	4	8.9869280	-0.1244455	0	0	0.4885228
	5	10.988527	0.1015356	0	0	0.4563589
	6	12.989729	-0.08581344	0	0	0.4316344
	⋮					
	n	2n + 1	$(-1)^{n+1}1.102658\lambda_n^{-1}$	0	0	$1.012788\lambda_n^{-\frac{1}{3}}$
Four	0	0.95467395	0	-0.3580357	-0.3121086	0
	1	2.9743338	0	-0.05145435	0.09581739	0
	2	4.9810820	0	-0.02146264	-0.05659978	0
	3	6.9846555	0	-0.01212839	0.04017510	0
	4	8.9869280	0	-0.007934564	-0.03114790	0
	5	10.988527	0	-0.005660338	0.02544079	0
	6	12.989729	0	-0.004275930	-0.02150757	0
	⋮					
	n	2n + 1	0	$-0.3001255\lambda_n^{-\frac{5}{3}}$	$(-1)^{n+1}0.2756644\lambda_n^{-1}$	0

IV. TURBULENT FLOW

IV. A. Survey of Previous Studies

In comparison with its laminar counterpart, the parallel plane thermal entrance length problem for turbulent flow has received little attention in the literature. Although it is perhaps the more interesting from the standpoint of practical application, the turbulent solution requires the use of more complex velocity and diffusivity relations, and thus is a less attractive vehicle for exploring new mathematical techniques.

The work that appears can be divided into three general categories, distinguished by the method of solution employed:

(1) integral methods

(2) direct solution of the governing partial differential equation on an analog or digital computer

(3) computer solution of the eigenvalue problem resulting from separating the variables of the governing differential equation

Examples of these methods occurring in the literature are briefly discussed below; a more detailed treatment can be found in the excellent survey of Cess.[10]

Integral Methods

Deissler[15] has treated the circular tube geometry with uniform wall heat flux and with uniform wall temperature, and the parallel planes geometry with uniform and equal wall heat fluxes. Cess[11] also dealt with the latter problem. He employed the Nikuradse velocity profile and Martinelli temperature profile, and assumed equal diffusivities of momentum and heat transfer.

Direct Computer Solution of Differential Equation

Jenkins, et al.[29] solved the circular tube with uniform wall heat-flux problem, assuming $\epsilon_H/\epsilon_M = 1$.

Schlinger, et al.[54] treated the parallel planes case with uniform, but unequal, wall temperatures.

Eigenvalue Problem

Latzko[32] presented the first treatment of the turbulent thermal entrance length problem. He dealt with the uniform wall temperature circular tube case, and employed a 1/7-power velocity profile. Beckers[3] extended this work, as did Sleicher and Tribus,[60] who also considered the uniform wall heat-flux case. Sparrow, Hallman, and Siegel[61] presented a solution for this latter problem. Both Berry[4] and Poppendick[45] treated the parallel planes with uniform and equal wall temperatures, but they do not present the eigenvalues and constants.

Cess,[9] and Sternling and Sleicher[64] demonstrated the utility of the WKBJ approximation for finding the higher eigenvalues and constants for turbulent tube flow.

Finally, several fully developed temperature profile solutions should be mentioned. Harrison and Menke[24] extended Martinelli's work to the uniform, but unequal, wall heat-flux case for parallel planes, and Barrow[2] also dealt with this problem. Seban[56] treated the case of uniform and equal wall temperatures.

IV. B. Mathematical Formulation and Method of Solution

In this section the general solution of the energy equation will be developed for turbulent flow between parallel planes in a manner directly parallel to that for the laminar case in Section III. Some of the mathematical steps that have identical counterparts in Section III are omitted to avoid repetition.

1. The differential equation and boundary conditions

From (II.B.5), the energy equation for turbulent flow between parallel planes is

$$\frac{\partial}{\partial \bar{y}}\left[\left(1 + \frac{\epsilon_H}{\nu} \mathrm{Pr}\right)\frac{\partial \theta}{\partial \bar{y}}\right] = \frac{u}{16u_m}\frac{\partial \theta}{\partial \bar{x}} \qquad \text{(IV.B.1)}$$

For computational purposes the equation is henceforth written as

$$\frac{\partial}{\partial \bar{y}}\left[\left(1 + \frac{\epsilon_M}{\nu}\frac{\epsilon_H}{\epsilon_M} \mathrm{Pr}\right)\frac{\partial \theta}{\partial \bar{y}}\right] = \frac{u}{16u_m}\frac{\partial \theta}{\partial \bar{x}} \qquad \text{(IV.B.2}$$

Unlike the laminar case, an expression for $\frac{u}{u_m}$ as a function of $\bar{y}$ cannot be derived from analysis alone, but rather is obtained from experimental investigations. Similarly, the presence of $\frac{\epsilon_M}{\nu}$ and $\frac{\epsilon_H}{\epsilon_M}$ in the equation imposes complications over the laminar solution. These matters will be dealt with later in this section. Let it suffice at this point to say that the diffusivity expressions employed are valid only in certain Reynolds and Prandtl number ranges, and that numerical computations are performed only for $\mathrm{Re} = 2\times10^4$, 3×10^4, and 5×10^4, and $\mathrm{Pr} = 0.01$ and 0.70. The $\mathrm{Pr} = 0.01$ calculations are limited to the fully developed temperature profile cases.

The boundary conditions on (IV.B.2) for the four fundamental cases are given by (III.B.4) through (III.B.7). Again, these boundary conditions must be made homogeneous, and this is accomplished by the same change of variables.

$$\bar{\theta} \triangleq \theta - \theta_{fd} \qquad \text{(IV.B.3)}$$

This yields the equation

$$\frac{\partial}{\partial \bar{y}}\left[\left(1 + \frac{\epsilon_M}{\nu}\frac{\epsilon_H}{\epsilon_M} \mathrm{Pr}\right)\frac{\partial \bar{\theta}}{\partial \bar{y}}\right] = \frac{u}{16u_m}\frac{\partial \bar{\theta}}{\partial \bar{x}} \qquad \text{(IV.B.4)}$$

and the homogeneous boundary conditions (III.B.10) through (III.B.13).

2. Eddy diffusivity for momentum transfer

Before solving (IV.B.4) one must have in hand a relationship between $\frac{\epsilon_M}{\nu}$ and $\bar{y}$ suitable for the Reynolds number range of interest. The expression used for this work is a modified form of the expression suggested by Cess,[10] which is itself a combination of Van Driest's expression near the wall and Reichardt's middle law. The attractiveness of Cess's expression lies in the fact that it is a single equation applicable over the entire flow field; thus, the usual patching of equations is obviated. In Cess's nomenclature his expression is

$$\frac{\epsilon_M}{\nu} = \frac{1}{2}\left\{1 + \frac{K^2\left(r_o^+\right)^2}{9}\left[1 - \left(\frac{r}{r_o}\right)^2\right]^2 \cdot \left[1 + 2\left(\frac{r}{r_o}\right)^2\right]^2\left[1 - \exp\left(-\frac{1 - \frac{r}{r_o}}{A^+/r_o^+}\right)\right]^2\right\}^{\frac{1}{2}} - \frac{1}{2} \qquad \text{(IV.B.5)}$$

where K and A^+ are constants with values of 0.4 and 26, respectively. This equation was developed for application to circular tubes, hence the radius terms.

Applying the expression to the parallel planes geometry, there results

$$\frac{\epsilon_M}{\nu} = \frac{1}{2}\left\{1 + \left[\frac{K\, y_o^+}{3}\left(1 - \bar{y}^2\right)\left(1 + 2\bar{y}^2\right)\left(1 - \exp\frac{\bar{y} - 1}{A^+/y_o^+}\right)\right]^2\right\}^{\frac{1}{2}} - \frac{1}{2}$$

(IV.B.6)

To determine the suitability of the equation for parallel planes application, it was compared with the experimental data for air reported by Page, et al.[41,42,55] In so doing it was found that a "bumping factor" modification provided a better fit to the data for the 20,000 to 50,000 Reynolds number range studied herein. The resulting expression is

$$\frac{\epsilon_M}{\nu} = \frac{1}{2}\left\{1 + \left[\frac{K\, y_o^+}{3}\left(1 - \bar{y}^2\right)\left(1 + 2\bar{y}^2\right)\right.\right.$$

$$\left.\left.\cdot\left(1 + 1400\, y_o^{+-1.2}\left(\bar{y} - \bar{y}^2\right)\right)\left(1 - \exp\frac{\bar{y} - 1}{A^+/y_o^+}\right)\right]^2\right\}^{\frac{1}{2}} - \frac{1}{2} \qquad \text{(IV.B.7)}$$

where $K = 0.4$ and $A^+ = 26$. Figure IV.B.1 shows the shape of this diffusivity profile.

In order to use this expression it is necessary to have a relation between y_o^+ and Re. It follows from the definition of y^+ and y_o^+

$$y^+ \triangleq \frac{n}{\nu}\sqrt{\frac{g_c \tau_o}{\rho}} = n\,\mathrm{Re}\,\sqrt{\frac{f}{32}}$$

$$y_o^+ \triangleq \frac{y_o}{\nu}\sqrt{\frac{g_c \tau_o}{\rho}} \qquad \text{(IV.B.8)}$$

and from the defining equation for f

$$\tau_o \triangleq f\rho\,\frac{u_m^2}{2g_c} \qquad \text{(IV.B.9)}$$

that

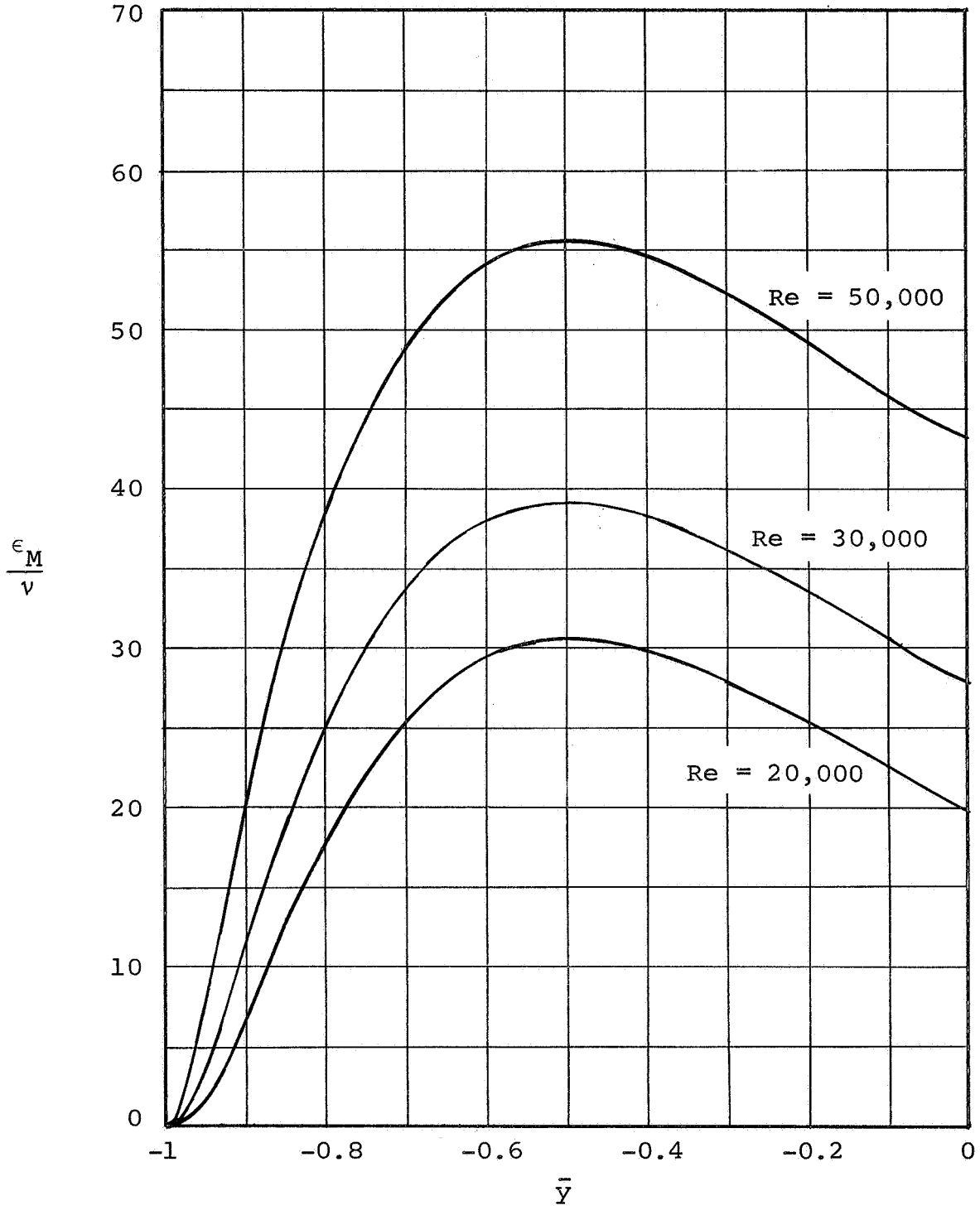

Figure IV.B.1. Eddy Diffusivity for Momentum Transfer

$$y_o^+ = Re \sqrt{\frac{f}{32}} \qquad \text{(IV.B.10)}$$

The experimentally determined friction factor expression given by Schlichting[53]

$$\frac{1}{\sqrt{f}} = 4.0 \log_{10} \left(Re \sqrt{f} \right) - 0.40 \qquad \text{(IV.B.11)}$$

can be used to provide the link between f and Re. This equation is plotted in Figure IV.B.2.

In many studies the Deissler[16] expression is employed for $\frac{\epsilon_M}{\nu}$ near a wall, so it is of interest to note the close agreement between it and the Van Driest relation (to which the Cess relation reduces in the wall region) as shown in Figure IV.B.3.

3. Velocity profiles

The velocity profile expression, $\frac{u}{u_m}$, used in (IV.B.4) is obtained from the $\frac{\epsilon_M}{\nu}$ relation (IV.B.7) and the shear stress distribution. From force balance considerations it is simple to show that

$$\tau = - \tau_o \frac{y}{y_o} \qquad \text{(IV.B.12)}$$

in the passage between the parallel planes. And from the definition of ϵ_M

$$\frac{\rho}{g_c} \left(\epsilon_M + \nu \right) \frac{du}{dy} = \tau \qquad \text{(IV.B.13)}$$

Thus

$$\frac{\rho}{g_c} \left(\epsilon_M + \nu \right) \frac{du}{dy} = - \tau_o \frac{y}{y_o}$$

Combining with (IV.B.9) and rearranging

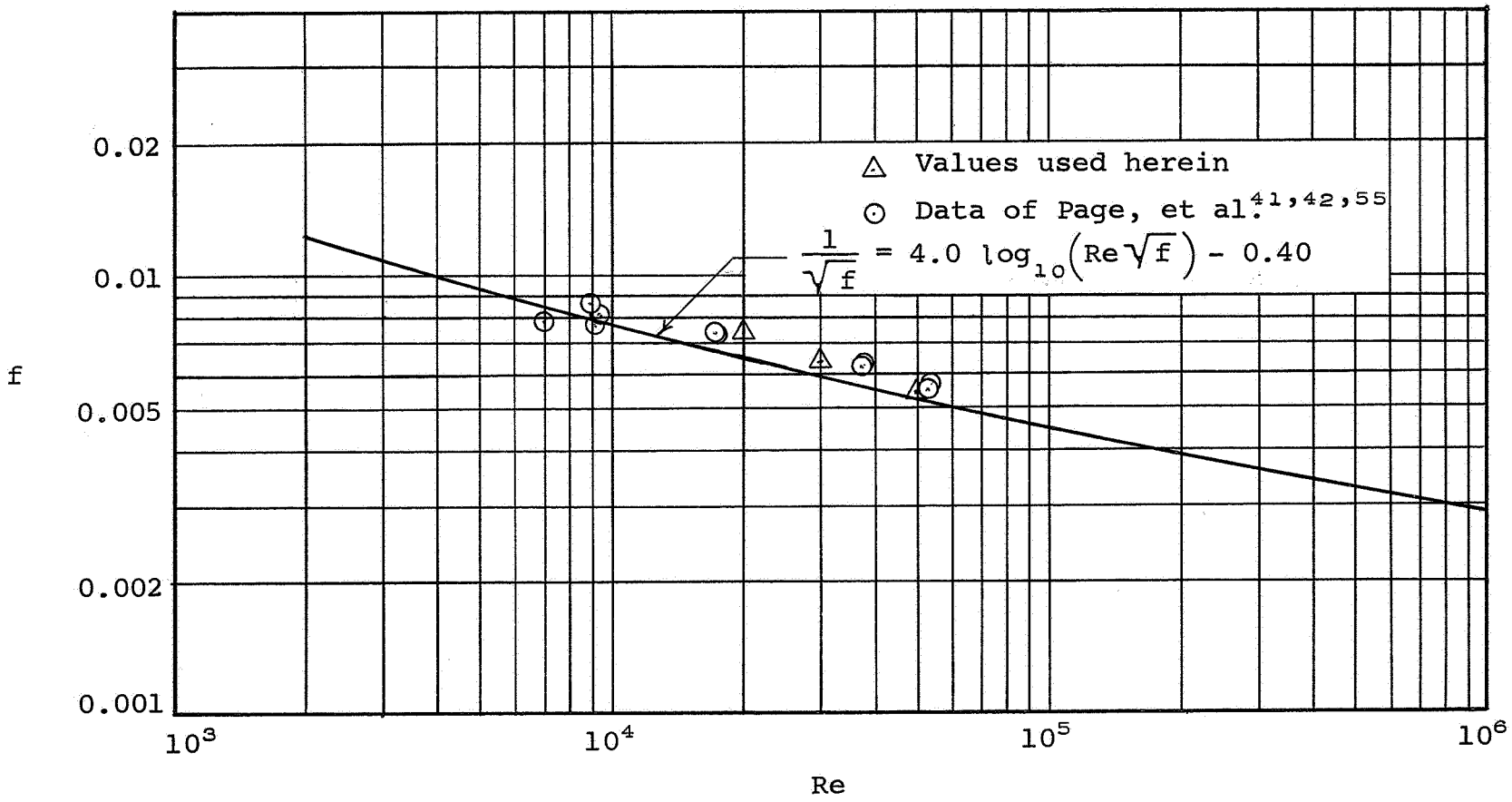

Figure IV.B.2. Parallel Planes Turbulent Flow Friction Factor

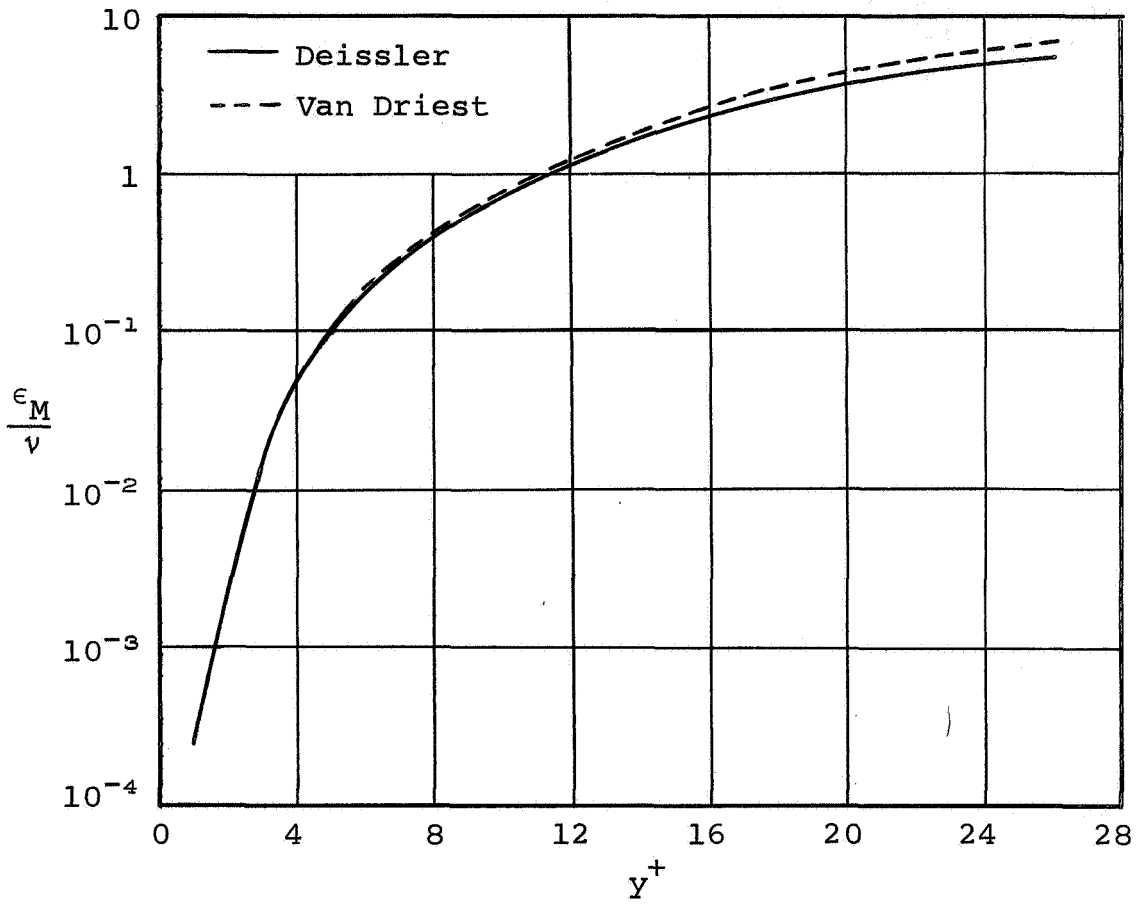

Figure IV.B.3. Comparison of the Van Driest and Deissler Eddy Diffusivity Expressions Near a Wall

$$\left(\frac{\epsilon_M}{\nu} + 1\right) \frac{d\bar{u}}{d\bar{y}} = - \frac{\bar{y}}{8} f \, Re$$

where

$$\bar{u} \triangleq \frac{u}{u_m} \qquad \text{(IV.B.14)}$$

Changing coordinates so that the independent variable is zero at the lower wall, let

$$\eta = 1 + \bar{y}$$

Then

$$\left(\frac{\epsilon_M}{\nu} + 1\right) \frac{d\bar{u}}{d\eta} = (1 - \eta) \frac{f \, Re}{8}$$

So

$$\bar{u} - \bar{u}_{\eta=o} = \frac{f \, Re}{8} \int_o^\eta \frac{(1 - \eta)}{\frac{\epsilon_M}{\nu} + 1} \, d\eta$$

But at the wall, $\bar{u} = 0$. Thus

$$\bar{u}(\eta) = \frac{f \, Re}{8} \int_o^\eta \frac{(1 - \eta)}{\frac{\epsilon_M}{\nu} + 1} \, d\eta \qquad \text{(IV.B.15)}$$

Numerical integration of this simple quadrature provides the necessary relation for $\bar{u}$.

The velocity profiles calculated in this manner are several values of Reynolds number are plotted in Figure IV.B.4 in the form of u^+, where

$$u^+ \triangleq u \sqrt{\frac{\rho}{g_c \tau_o}} = \bar{u} \sqrt{\frac{2}{f}} \qquad \text{(IV.B.16)}$$

Good agreement with the data of Page, et al. is shown.

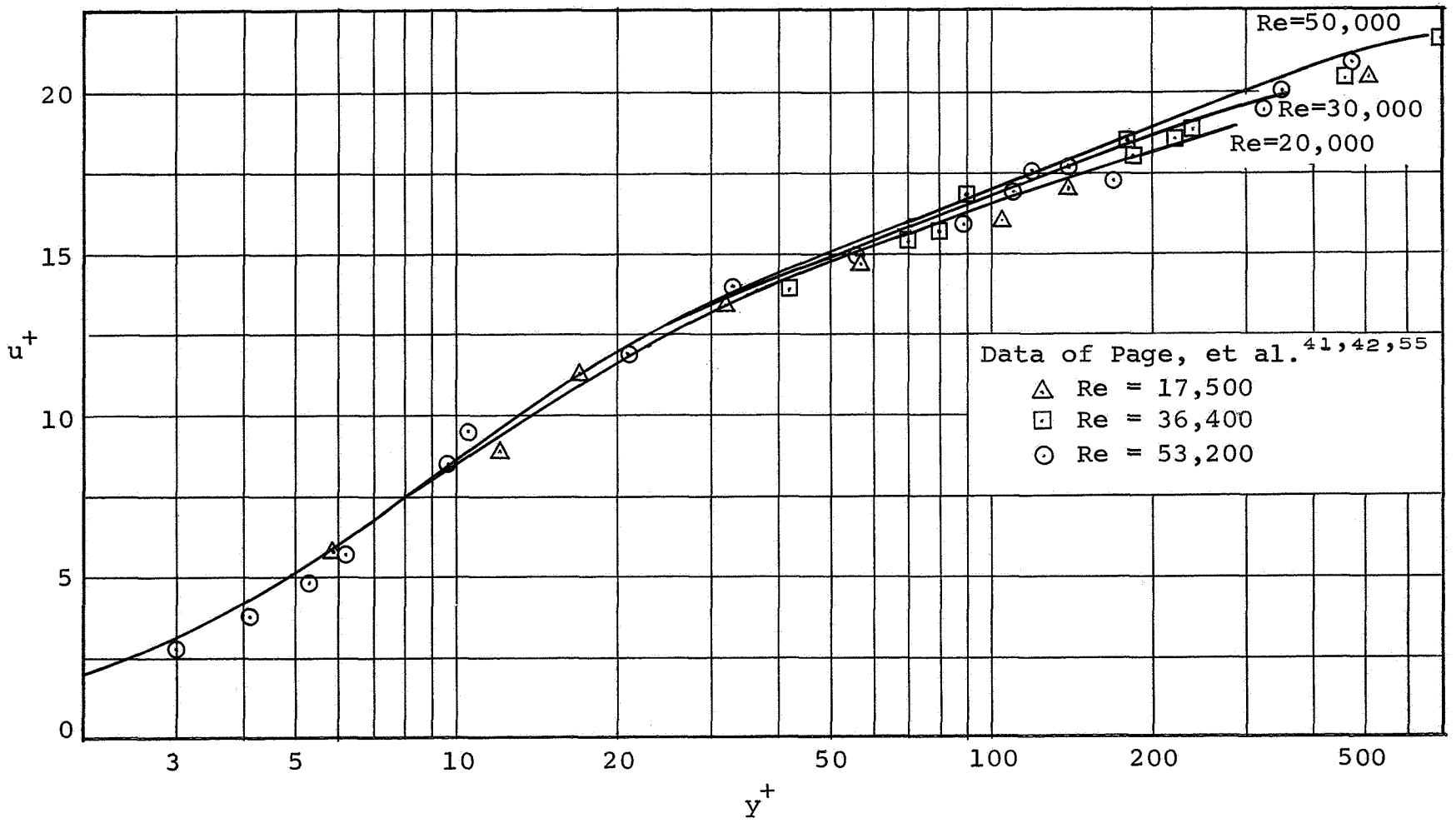

Figure IV.B.4. Parallel Planes Turbulent Velocity Profiles

Actually, the use of (IV.B.11) for friction factor calculation is not completely consistent with the use of (IV.B.7) for $\frac{\epsilon_M}{\nu}$, since one expression should follow from the other. Herein it was elected to choose (IV.B.7) as the "standard," and the friction factor was then calculated in the following manner.

For a given Reynolds number, a trial f was obtained from (IV.B.11) and this was used with (IV.B.10) and (IV.B.7) to obtain an expression for $\frac{\epsilon_M}{\nu}(\bar{y})$. Then (IV.B.15) led to $\bar{u}(\bar{y})$. From Section II.B it is known that

$$\int_{-1}^{1} \bar{u}\, d\bar{y} = 2$$

This integral was computed numerically and found to differ from 2 for the first f trial; however, the computation suggested the next trial, and the process was completed until convergence was obtained. Several friction factors calculated in this manner, and hence consistent with (IV.B.7), are plotted on Figure IV.B.2.

4. Eddy diffusivity for heat transfer

In addition to the $\frac{\epsilon_M}{\nu}$ and $\bar{u}$ relations, an expression is needed for $\frac{\epsilon_H}{\epsilon_M}$ before the solution of (IV.B.4) can proceed. The analysis of Jenkins[28] is employed for this purpose herein. Figure IV.B.5 indicates the results of his analysis.

For the 0.01 Pr case Jenkins' results were applied without modification. However, to facilitate numerical computation his diffusivity ratio expression was approximated by more simple algebraic relations. These relations, first employed by Leung,[34] are set forth below.

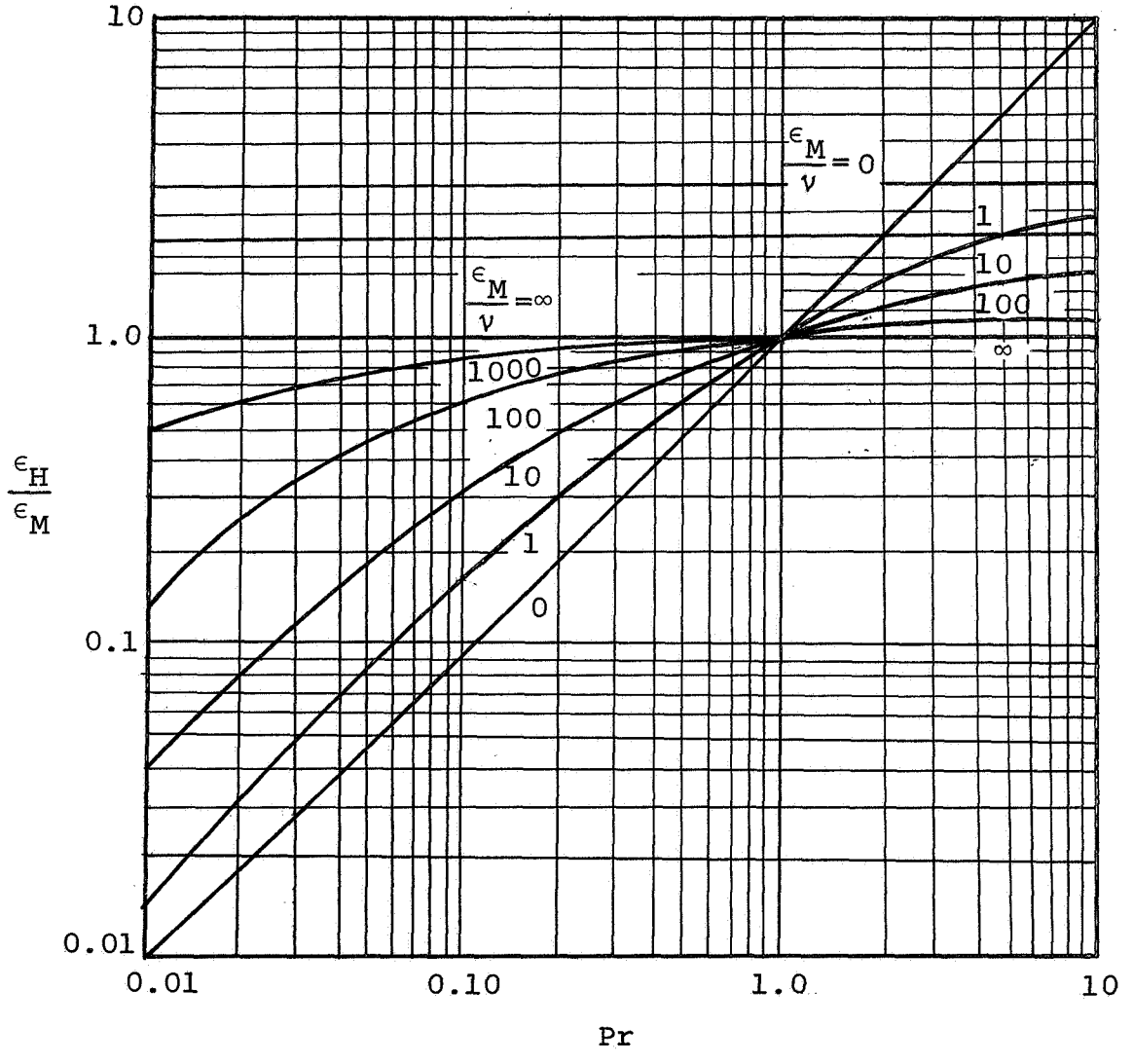

Figure IV.B.5. The Jenkins Eddy Diffusivity Ratio

Pr = 0.01

range of application	relation
$\ln \frac{\epsilon_M}{\nu} < 0.6$	$\frac{\epsilon_H}{\epsilon_M} = 0.010$
$0.6 \leq \ln \frac{\epsilon_M}{\nu} < 3.0$	$\frac{\epsilon_H}{\epsilon_M} = 0.018 + 0.016(\ln \frac{\epsilon_M}{\nu} - 1.0)$
$3.0 \leq \ln \frac{\epsilon_M}{\nu} < 4.0$	$\frac{\epsilon_H}{\epsilon_M} = 0.05 + 0.05(\ln \frac{\epsilon_M}{\nu} - 3.0)$
$4.0 \leq \ln \frac{\epsilon_M}{\nu} < 10.0$	$\frac{\epsilon_H}{\epsilon_M} = 0.10 + 0.15(\ln \frac{\epsilon_M}{\nu} - 4.0)$
$\ln \frac{\epsilon_M}{\nu} \geq 10.0$	$\frac{\epsilon_H}{\epsilon_M} = 1.0$

For the 0.7 Pr case the data of Page, et al. indicates that the Jenkins analysis underpredicts the magnitude of the diffusivity ratio. Hence a correction factor was applied to Jenkins' results in the region $y^+ > 26$. In the region $0 \leq y^+ \leq 26$ the diffusivity ratio was taken as unity since Deissler[16] demonstrated that this assumption yields heat-transfer results in good agreement with experimental data for this Prandtl number. Deissler used ϵ_M in place of ϵ_H, and the ϵ_M used herein in the sublayers is substantially that of Deissler's (see Fig. IV.B.3).

The turbulent core diffusivity ratio used is

$$\frac{\epsilon_H}{\epsilon_M} = -\left[0.216 \ln \left(0.0000865 \frac{\epsilon_M}{\nu}\right)\right]\left(\frac{\epsilon_H}{\epsilon_M}\right)_{\text{Jenkins}} \qquad \text{(IV.B.17)}$$

The correction factor, together with the Page, et al. data from which it was derived, is plotted in Figure IV.B.6.

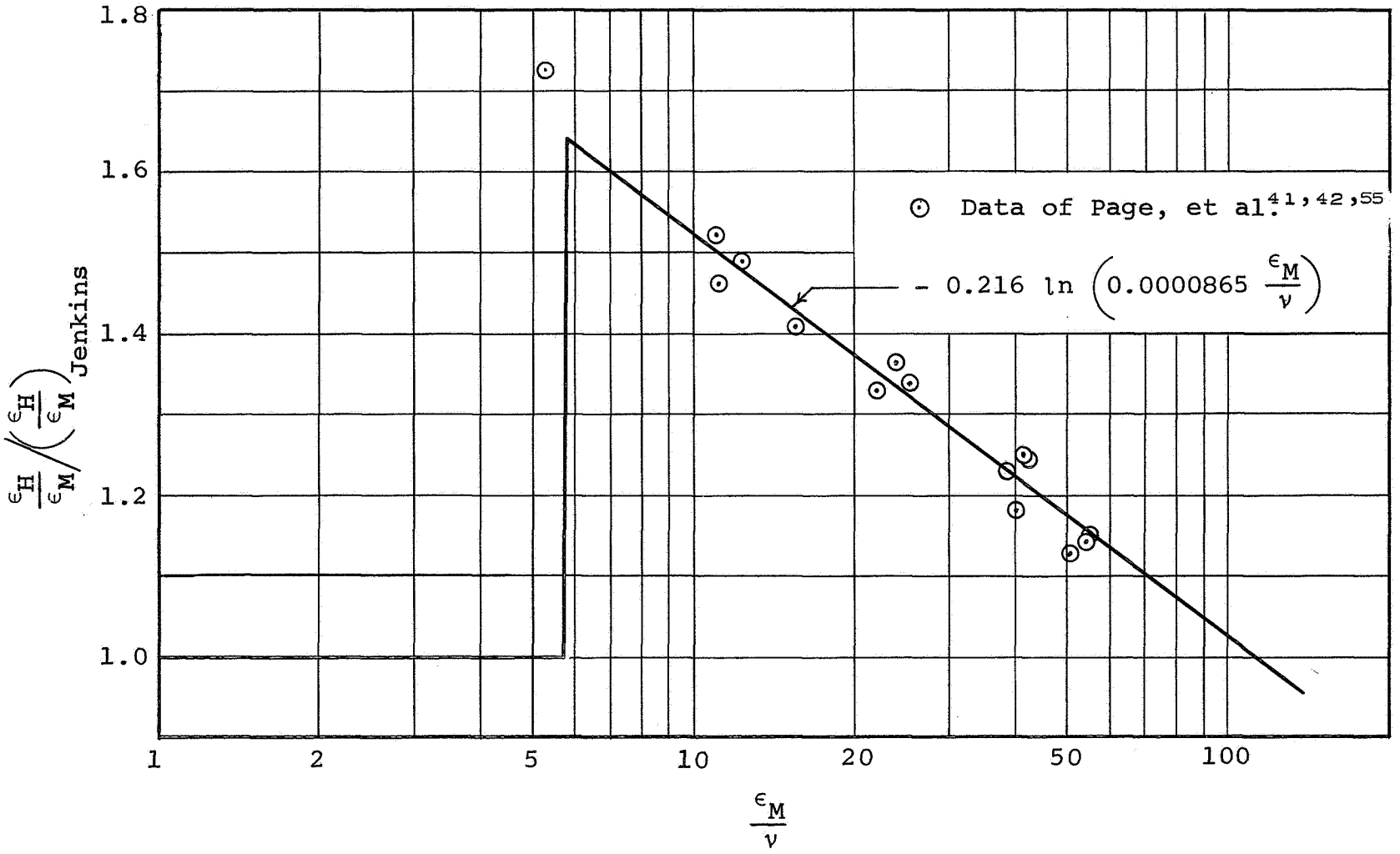

Figure IV.B.6. Eddy Diffusivity Ratio Correction Factor for Pr = 0.70

Here again Jenkins' expression was approximated by algebraic relations.

Pr = 0.70

range of application	relation
$\ln \frac{\epsilon_M}{\nu} < -1.5$	$\frac{\epsilon_H}{\epsilon_M} = 0.70$
$-1.5 \leq \ln \frac{\epsilon_M}{\nu} < 4.0$	$\frac{\epsilon_H}{\epsilon_M} = 0.775 + 0.05 \ln \frac{\epsilon_M}{\nu}$
$4.0 \leq \ln \frac{\epsilon_M}{\nu} < 10.0$	$\frac{\epsilon_H}{\epsilon_M} = 0.975 + 0.0025 (\ln \frac{\epsilon_M}{\nu} - 4.0)$
$\ln \frac{\epsilon_M}{\nu} \geq 10.0$	$\frac{\epsilon_H}{\epsilon_M} = 1.0$

5. Solution of the four fundamental problems - general considerations

Attempting to separate the variables of (IV.B.4), let

$$\bar{\theta}(\bar{x},\bar{y}) = X(\bar{x}) \cdot Y(\bar{y}) \qquad \text{(IV.B.18)}$$

Then

$$\frac{1}{\bar{u}Y} \frac{d}{d\bar{y}} \left[\left(1 + \frac{\epsilon_M}{\nu} \frac{\epsilon_H}{\epsilon_M} Pr \right) Y' \right] = \frac{1}{16} \frac{X'}{X} = -\lambda^2 \qquad \text{(IV.B.19)}$$

Hence the two following ordinary differential equations result.

$$X' + 16\lambda^2 X = 0 \qquad \text{(IV.B.20)}$$

$$\frac{d}{d\bar{y}} \left[\left(1 + \frac{\epsilon_M}{\nu} \frac{\epsilon_H}{\epsilon_M} Pr \right) Y' \right] + \lambda^2 \bar{u} Y = 0 \qquad \text{(IV.B.21)}$$

A solution of (IV.B.20) is

$$X = e^{-16\lambda^2\bar{x}} \tag{IV.B.22}$$

As was its counterpart in the laminar case, (III.B.16), (IV.B.21) is a differential equation of the Sturm-Liouville type. The weight function in this case is $\bar{u}$. Thus, as in Section III.B, the problem solution can be represented by

$$\bar{\theta}(\bar{x},\bar{y}) = \sum_{n=0}^{\infty} C_n Y_n(\bar{y}) e^{-16\lambda_n^2\bar{x}} \tag{IV.B.23}$$

where

$$C_n = \frac{-\int_{-1}^{+1} \theta_{fd}\bar{u}Y_n \, d\bar{y}}{\int_{-1}^{+1} \bar{u}Y_n^2 \, d\bar{y}} \tag{IV.B.24}$$

And again, the boundary conditions on $Y(\bar{y})$ are given by (III.B.23) through (III.B.26).

6. The fully developed temperature profiles

The fully developed temperature profiles are needed to compute the eigenconstants, C_n. In addition, of course, they form the fundamental solutions themselves at distances far downstream from the thermal entry. It will be recalled that in the laminar case these profiles could be ascertained from physical reasoning as well as by direct solution of the appropriate governing energy equation; unfortunately, for turbulent flow such is not the situation (with the exception of case three). Here the equations must be solved. In this section the pertinent equations will be set forth and their solutions presented.

a. Case one

Here the temperature profile is fully developed when all the energy transferred into the channel at the upper wall is transferred out at the lower. Thus there is no change in temperature with $\bar{x}$, and (IV.B.2) becomes

$$\frac{d}{d\bar{y}}\left[\left(1 + \frac{\epsilon_M}{\nu}\ \frac{\epsilon_H}{\epsilon_M}\ Pr\right)\frac{d\theta_{fd}}{d\bar{y}}\right] = 0 \qquad \text{(IV.B.25)}$$

And the accompanying boundary conditions are

$$\theta_{fd}^{(1)}(1) = 1$$

$$\theta_{fd}^{(1)}(-1) = 0$$

This equation has been solved numerically for several values of Re and Pr, and the required results are presented in Figure IV.B.7 and Table IV.B.1. The method of computation is the same as that discussed in Section IV.G.

b. Case two

As shown in Section III.B.3.b, for this case $\frac{\partial\theta}{\partial\bar{x}} = 2$; hence (IV.B.2) becomes

$$\frac{d}{d\bar{y}}\left[\left(1 + \frac{\epsilon_M}{\nu}\ \frac{\epsilon_H}{\epsilon_M}\ Pr\right)\frac{d\theta_{fd}}{d\bar{y}}\right] = \frac{\bar{u}}{8} \qquad \text{(IV.B.26)}$$

The boundary conditions are

$$\frac{d\theta_{fd}^{(2)}}{d\bar{y}}(1) = \frac{1}{4}$$

$$\frac{d\theta_{fd}^{(2)}}{d\bar{y}}(-1) = 0$$

Solution of (IV.B.26) provides the shape of the fully developed temperature profile, but the magnitude of $\theta_{fd}^{(2)}$ continually increases with $\bar{x}$. In fact

$$\theta_{m_{fd}}^{(2)} = 2\bar{x}$$

from (III.B.31). Thus the magnitude of the solution to (IV.B.26) is chosen such that when integrated over the channel as in (II.C.1) the result is identically zero. This shape profile is called $S(\bar{y})$. And

$$\theta_{fd}^{(2)} = 2\bar{x} + S(\bar{y}) \qquad \text{(IV.B.27)}$$

Results of numerical computation of $S(\bar{y})$ can be found in Figure IV.B.8 and Table IV.B.1.

c. Case three

This case requires no solution of an equation; rather the fully developed temperature profile is evident from physical reasoning alone, as it was for its laminar counterpart. Referring to Section III.B.3.c it is seen that

$$\theta_{fd}^{(3)} = 1 \qquad \text{(IV.B.28)}$$

d. Case four

The equation governing the temperature profile here is the same as that in case one, namely

$$\frac{d}{d\bar{y}}\left[\left(1 + \frac{\epsilon_M}{\nu}\,\frac{\epsilon_H}{\epsilon_M}\,Pr\right)\frac{d\theta_{fd}}{d\bar{y}}\right] = 0 \qquad \text{(IV.B.29)}$$

The boundary conditions are

$$\frac{d\theta_{fd}^{(4)}}{d\bar{y}}(1) = \frac{1}{4}$$

$$\theta_{fd}^{(4)}(-1) = 0$$

Again, the required constants for selected values of Re and Pr are presented in Figure IV.B.9 and Table IV.B.1.

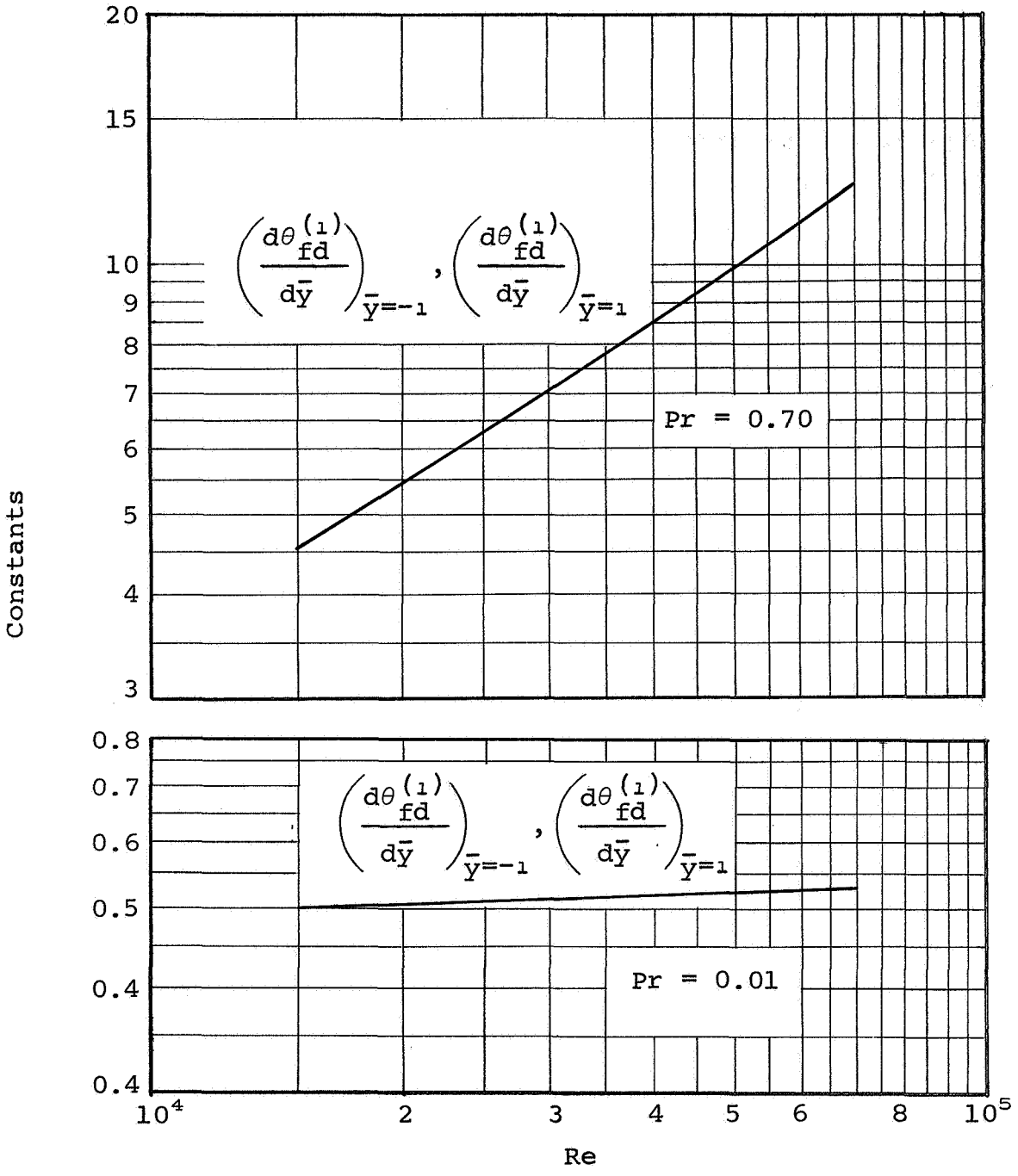

Figure IV.B.7. Turbulent Case One Fully Developed Solution Constants

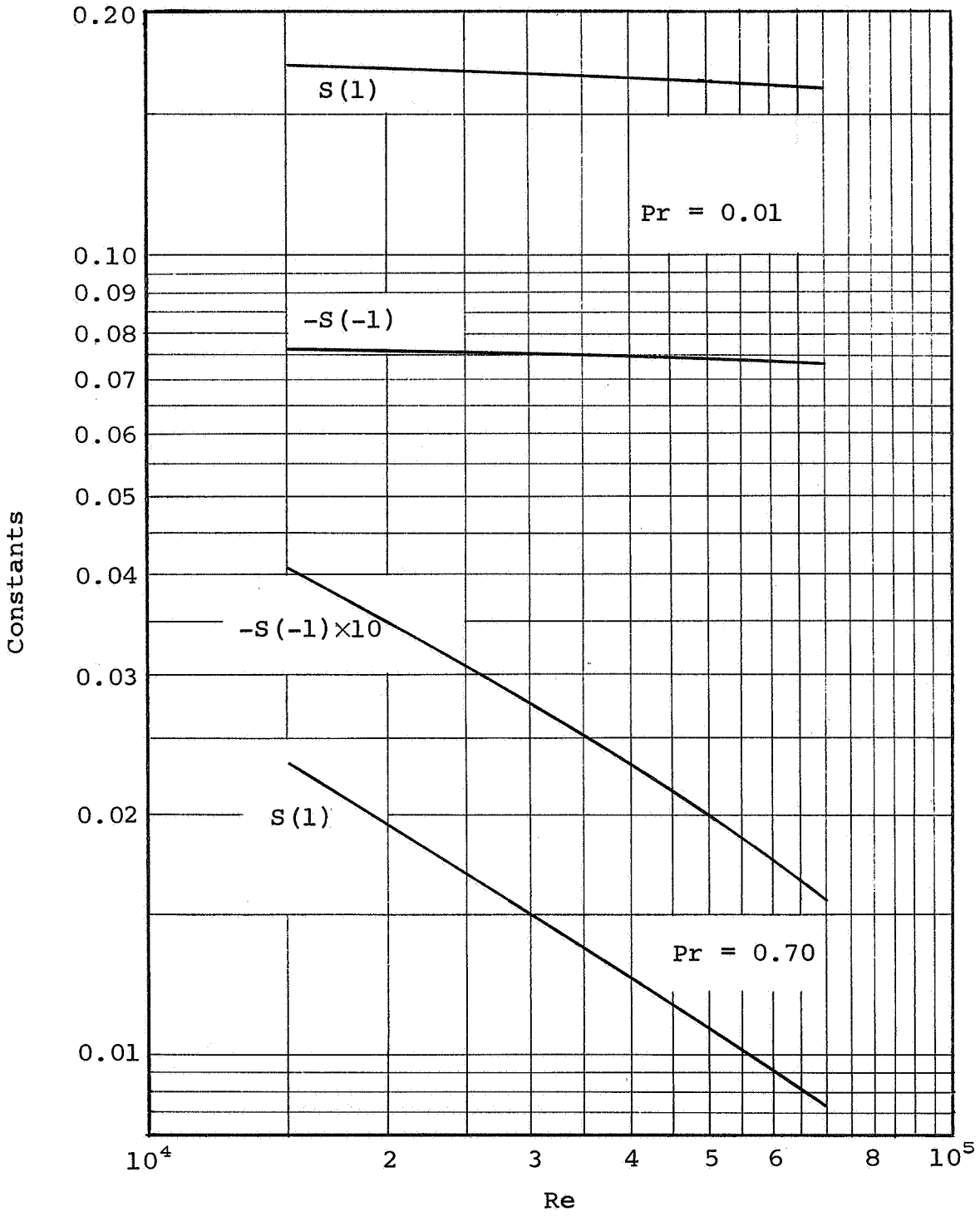

Figure IV.B.8. Turbulent Case Two Fully Developed Solution Constants

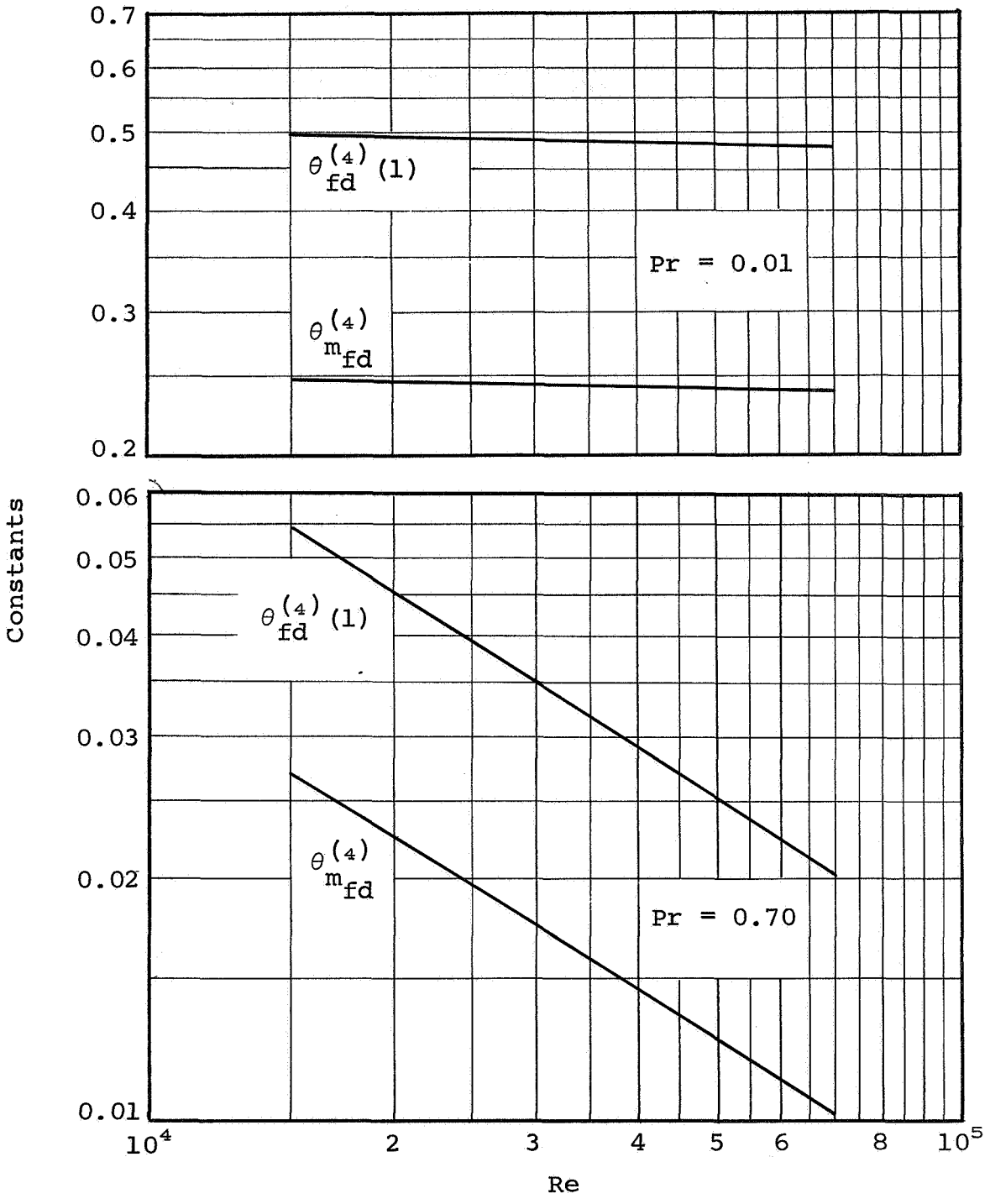

Figure IV.B.9. Turbulent Case Four Fully Developed Solution Constants

TABLE IV.B.1

TURBULENT FULLY DEVELOPED SOLUTION CONSTANTS

Pr	Re	$\left(\frac{d\theta_{fd}^{(1)}}{d\bar{y}}\right)_{\bar{y}=-1}$	$\left(\frac{d\theta_{fd}^{(1)}}{d\bar{y}}\right)_{\bar{y}=1}$	S(-1)	S(1)	$\theta_{fd}^{(4)}(1)$	$\theta_{m_{fd}}^{(4)}$
0.01	20,000	0.507140	0.507140	-0.07588	0.1706	0.49296	0.24648
0.01	30,000	0.511312	0.511312	-0.07552	0.1689	0.48894	0.24447
0.01	50,000	0.520567	0.520567	-0.07435	0.1657	0.48024	0.24012
0.70	20,000	5.48	5.48	-0.00348	0.0194	0.0453	0.02265
0.70	30,000	7.05	7.05	-0.00275	0.0150	0.0352	0.0176
0.70	50,000	9.91	9.91	-0.00199	0.0107	0.0251	0.01255

IV. C. The Four Fundamental Solutions

The temperature profiles for the four fundamental cases in turbulent flow are given by

$$\theta = \theta_{fd} + \sum_{n=o}^{\infty} C_n Y_n e^{-16\lambda_n^2 \bar{x}} \qquad \text{(IV.C.1)}$$

This is obtained from (IV.B.3) and (IV.B.23), and is the turbulent counterpart of (III.C.1). In this section this equation will be applied to each of the four fundamental cases.

1. Case one

Here the temperature profile is

$$\theta^{(1)} = \theta_{fd}^{(1)} + \sum_{n=o}^{\infty} C_n Y_n e^{-16\lambda_n^2 \bar{x}} \qquad \text{(IV.C.2)}$$

By definition, at the walls

$$\theta_{oo}^{(1)} = \theta_{ii}^{(1)} = 1$$

$$\theta_{oi}^{(1)} = \theta_{io}^{(1)} = 0$$

Differentiating (IV.C.2) and employing the definition (II.B.10)

$$\Phi_{oo}^{(1)} = \Phi_{ii}^{(1)} = 4\left(\frac{\partial\theta^{(1)}}{\partial\bar{y}}\right)_{\bar{y}=1} = 4\left(\frac{d\theta_{fd}^{(1)}}{d\bar{y}}\right)_{\bar{y}=1} + 4\sum_{n=o}^{\infty} C_n Y_n'(1) e^{-16\lambda_n^2 \bar{x}} \qquad \text{(IV.C.3)}$$

and

$$\Phi_{oi}^{(1)} = \Phi_{io}^{(1)} = -4\left(\frac{\partial\theta^{(1)}}{\partial\bar{y}}\right)_{\bar{y}=-1} = -4\left(\frac{d\theta_{fd}^{(1)}}{d\bar{y}}\right)_{\bar{y}=-1}$$

$$-4\sum_{n=o}^{\infty} C_n Y_n'(-1)e^{-16\lambda_n^2\bar{x}} \qquad \text{(IV.C.4)}$$

From energy balance considerations

$$\theta_m^{(1)} = 2\int_o^{\bar{x}} \left(\Phi_{oo}^{(1)} + \Phi_{io}^{(1)}\right) d\bar{x} \qquad \text{(IV.C.5)}$$

Performing the indicated integration yields

$$\theta_m^{(1)} = \frac{1}{2}\sum_{n=o}^{\infty}\left[\frac{C_n}{\lambda_n^2}\left(Y_n'(-1) - Y_n'(1)\right)\left(e^{-16\lambda_n^2\bar{x}} - 1\right)\right] \qquad \text{(IV.C.6)}$$

But as $\bar{x} \to \infty$, $e^{-16\lambda_n^2\bar{x}} \to 0$, and also, from the symmetry of the fully developed profile, $\theta_m^{(1)} \to \frac{1}{2}\,\theta_{fd}^{(1)}(1)$. And since $\theta_{fd}^{(1)}(1) = 1$ by definition, $\theta_m^{(1)} \to \frac{1}{2}$. Hence

$$\frac{1}{2} = -\frac{1}{2}\sum_{n=o}^{\infty}\left[\frac{C_n}{\lambda_n^2}\left(Y_n'(-1) - Y_n'(1)\right)\right] \qquad \text{(IV.C.7)}$$

Combining (IV.C.6) and (IV.C.7) yields

$$\theta_m^{(1)} = \frac{1}{2} + \frac{1}{2}\sum_{n=o}^{\infty}\left[\frac{C_n}{\lambda_n^2}\left(Y_n'(-1) - Y_n'(1)\right)e^{-16\lambda_n^2\bar{x}}\right] \qquad \text{(IV.C.8)}$$

The fundamental solutions of the first kind are summarized below.

$$\theta_{oo}^{(1)} = \theta_{ii}^{(1)} = 1$$

$$\theta_{oi}^{(1)} = \theta_{io}^{(1)} = 0$$

$$\Phi_{oo}^{(1)} = \Phi_{ii}^{(1)} = 4\left(\frac{d\theta_{fd}^{(1)}}{d\bar{y}}\right)_{\bar{y}=1} + 4\sum_{n=0}^{\infty} C_n Y_n'(1) e^{-16\lambda_n^2 \bar{x}}$$

$$\Phi_{oi}^{(1)} = \Phi_{io}^{(1)} = -4\left(\frac{d\theta_{fd}^{(1)}}{d\bar{y}}\right)_{\bar{y}=-1} - 4\sum_{n=0}^{\infty} C_n Y_n'(-1) e^{-16\lambda_n^2 \bar{x}}$$

$$\theta_{mo}^{(1)} = \theta_{mi}^{(1)} = \frac{1}{2} + \frac{1}{2}\sum_{n=0}^{\infty}\left[\frac{C_n}{\lambda_n^2}\left(Y_n'(-1) - Y_n'(1)\right)e^{-16\lambda_n^2 \bar{x}}\right]$$

The last three fundamental solutions are presented in Figure IV.C.1 and Tables IV.C.1, 2, and 3 for Pr = 0.70.

2. Case two

Combining (IV.B.27) and (IV.C.1), the case two temperature profile is

$$\theta^{(2)} = 2\bar{x} + S(\bar{y}) + \sum_{n=0}^{\infty} C_n Y_n e^{-16\lambda_n^2 \bar{x}} \qquad \text{(IV.C.9)}$$

At the walls this becomes

$$\theta_{oo}^{(2)} = \theta_{ii}^{(2)} = 2\bar{x} + S(1) + \sum_{n=0}^{\infty} C_n Y_n(1) e^{-16\lambda_n^2 \bar{x}} \qquad \text{(IV.C.10)}$$

$$\theta_{oi}^{(2)} = \theta_{io}^{(2)} = 2\bar{x} + S(-1) + \sum_{n=0}^{\infty} C_n Y_n(-1) e^{-16\lambda_n^2 \bar{x}} \qquad \text{(IV.C.11)}$$

And by definition

$$\Phi_{oo}^{(2)} = \Phi_{ii}^{(2)} = 1$$

$$\Phi_{oi}^{(2)} = \Phi_{io}^{(2)} = 0$$

And from energy balance considerations

$$\theta_m^{(2)} = 2\bar{x} \qquad \text{(IV.C.12)}$$

The fundamental solutions of the second kind are summarized below.

$$\theta_{oo}^{(2)} = \theta_{ii}^{(2)} = 2\bar{x} + S(1) + \sum_{n=o}^{\infty} C_n Y_n(1) e^{-16\lambda_n^2 \bar{x}}$$

$$\theta_{oi}^{(2)} = \theta_{io}^{(2)} = 2\bar{x} + S(-1) + \sum_{n=o}^{\infty} C_n Y_n(-1) e^{-16\lambda_n^2 \bar{x}}$$

$$\Phi_{oo}^{(2)} = \Phi_{ii}^{(2)} = 1$$

$$\Phi_{oi}^{(2)} = \Phi_{io}^{(2)} = 0$$

$$\theta_{mo}^{(2)} = \theta_{mi}^{(2)} = 2\bar{x}$$

The first two of these fundamental solutions are presented in Figure IV.C.2 and Tables IV.C.1, 2, and 3 for Pr = 0.70.

3. Case three

Combining (IV.B.28) and (IV.C.1), the case three temperature profile is seen to be

$$\theta^{(3)} = 1 + \sum_{n=o}^{\infty} C_n Y_n e^{-16\lambda_n^2 \bar{x}} \qquad \text{(IV.C.13)}$$

At the upper wall, by definition

$$\theta_{oo}^{(3)} = \theta_{ii}^{(3)} = 1$$

and at the lower wall

$$\theta_{oi}^{(s)} = \theta_{io}^{(s)} = 1 + \sum_{n=o}^{\infty} C_n Y_n(-1) e^{-16\lambda_n^2 \bar{x}} \qquad \text{(IV.C.14)}$$

Differentiating (IV.C.13) and employing the definition (II.B.12)

$$\Phi_{oo}^{(s)} = \Phi_{ii}^{(s)} = 4\left(\frac{\partial\theta^{(s)}}{\partial\bar{y}}\right)_{\bar{y}=1} = 4\sum_{n=o}^{\infty} C_n Y_n'(1) e^{-16\lambda_n^2 \bar{x}} \qquad \text{(IV.C.15)}$$

By definition

$$\Phi_{oi}^{(s)} = \Phi_{io}^{(s)} = 0$$

Now, from energy balance considerations

$$\theta_m^{(s)} = 2\int_o^{\bar{x}} \Phi_{oo}^{(s)}\, d\bar{x} \qquad \text{(IV.C.16)}$$

Combining (IV.C.15) and (IV.C.16), and integrating

$$\theta_m^{(s)} = -\frac{1}{2}\sum_{n=o}^{\infty}\left[\frac{C_n}{\lambda_n^2} Y_n'(1)\left(e^{-16\lambda_n^2\bar{x}} - 1\right)\right] \qquad \text{(IV.C.17)}$$

But as $\bar{x} \to \infty$, $e^{-16\lambda_n^2\bar{x}} \to 0$, and $\theta_m^{(s)} \to 1$. Hence

$$1 = \frac{1}{2}\sum_{n=o}^{\infty}\frac{C_n}{\lambda_n^2} Y_n'(1) \qquad \text{(IV.C.18)}$$

Combining the preceding two equations yields

$$\theta_m^{(s)} = 1 - \frac{1}{2}\sum_{n=o}^{\infty}\frac{C_n}{\lambda_n^2} Y_n'(1) e^{-16\lambda_n^2\bar{x}} \qquad \text{(IV.C.19)}$$

The fundamental solutions of the third kind are summarized below.

$$\theta_{oo}^{(3)} = \theta_{ii}^{(3)} = 1$$

$$\theta_{oi}^{(3)} = \theta_{io}^{(3)} = 1 + \sum_{n=o}^{\infty} C_n Y_n(-1) e^{-16\lambda_n^2 \bar{x}}$$

$$\Phi_{oo}^{(3)} = \Phi_{ii}^{(3)} = 4 \sum_{n=o}^{\infty} C_n Y_n'(1) e^{-16\lambda_n^2 \bar{x}}$$

$$\Phi_{oi}^{(3)} = \Phi_{io}^{(3)} = 0$$

$$\theta_{mo}^{(3)} = \theta_{mi}^{(3)} = 1 - \frac{1}{2} \sum_{n=o}^{\infty} \frac{C_n}{\lambda_n^2} Y_n'(1) e^{-16\lambda_n^2 \bar{x}}$$

The three fundamental solutions that are functions of $\bar{x}$ are presented in Figure IV.C.3 and Tables IV.C.1, 2, and 3 for Pr = 0.70.

4. Case four

The case four temperature profile follows from (IV.C.1).

$$\theta^{(4)} = \theta_{fd}^{(4)} + \sum_{n=o}^{\infty} C_n Y_n e^{-16\lambda_n^2 \bar{x}} \qquad \text{(IV.C.20)}$$

At the upper wall this becomes

$$\theta_{oo}^{(4)} = \theta_{ii}^{(4)} = \theta_{fd}^{(4)}(1) + \sum_{n=o}^{\infty} C_n Y_n(1) e^{-16\lambda_n^2 \bar{x}} \qquad \text{(IV.C.21)}$$

and at the lower wall, by definition

$$\theta_{oi}^{(4)} = \theta_{io}^{(4)} = 0$$

Also by definition, at the upper wall

$$\Phi_{oo}^{(4)} = \Phi_{ii}^{(4)} = 1$$

Differentiating (IV.C.20)

$$\Phi_{oi}^{(4)} = \Phi_{io}^{(4)} = -1 - 4 \sum_{n=o}^{\infty} C_n Y_n'(-1) e^{-16\lambda_n^2 \bar{x}} \qquad \text{(IV.C.22)}$$

$$\left(\text{Note that } \left(\frac{d\theta_{fd}^{(4)}}{d\bar{y}} \right)_{\bar{y}=1} = \frac{1}{4} . \right)$$

From energy balance considerations

$$\theta_m^{(4)} = 2 \int_o^{\bar{x}} \left(\Phi_{oo}^{(4)} + \Phi_{io}^{(4)} \right) d\bar{x} \qquad \text{(IV.C.23)}$$

So from the preceding equations

$$\theta_m^{(4)} = \frac{1}{2} \sum_{n=o}^{\infty} \left[\frac{C_n}{\lambda_n^2} Y_n'(-1) \left(e^{-16\lambda_n^2 \bar{x}} - 1 \right) \right] \qquad \text{(IV.C.24)}$$

But as $\bar{x} \to \infty$, $e^{-16\lambda_n^2 \bar{x}} \to 0$, and $\theta_m^{(4)} \to \theta_{m_{fd}}^{(4)}$

Hence

$$\theta_{m_{fd}}^{(4)} = -\frac{1}{2} \sum_{n=o}^{\infty} \frac{C_n}{\lambda_n^2} Y_n'(-1) \qquad \text{(IV.C.25)}$$

and

$$\theta_m^{(4)} = \theta_{m_{fd}}^{(4)} + \frac{1}{2} \sum_{n=o}^{\infty} \frac{C_n}{\lambda_n^2} Y_n'(-1) e^{-16\lambda_n^2 \bar{x}} \qquad \text{(IV.C.26)}$$

Actually, (IV.C.26) has little computational advantage here over (IV.C.24).

The fundamental solutions of the fourth kind are summarized below.

$$\theta_{oo}^{(4)} = \theta_{ii}^{(4)} = \theta_{fd}^{(4)}(1) + \sum_{n=o}^{\infty} C_n Y_n(1) e^{-16\lambda_n^2 \bar{x}}$$

$$\theta_{oi}^{(4)} = \theta_{io}^{(4)} = 0$$

$$\Phi_{oo}^{(4)} = \Phi_{ii}^{(4)} = 1$$

$$\Phi_{oi}^{(4)} = \Phi_{io}^{(4)} = -1 - 4 \sum_{n=o}^{\infty} C_n Y_n'(-1) e^{-16\lambda_n^2 \bar{x}}$$

$$\theta_{mo}^{(4)} = \theta_{mi}^{(4)} = \theta_{m_{fd}}^{(4)} + \frac{1}{2} \sum_{n=o}^{\infty} \frac{C_n}{\lambda_n^2} Y_n'(-1) e^{-16\lambda_n^2 \bar{x}}$$

The three fundamental solutions that are functions of $\bar{x}$ are presented in Figure IV.C.4 and Tables IV.C.1, 2, and 3 for $Pr = 0.70$.

As discussed in Section IV.G.1, the fundamental solutions are not presented for small values of $\bar{x}$ because numerical calculations were not performed for $n > 2$, and the first three terms are insufficient for adequate convergence of the series in the small $\bar{x}$ range. The $\bar{x}$ values at which the small $\bar{x}$ solutions become valid are calculated in Appendix E to aid the reader in estimating the mid-range fundamental solutions.

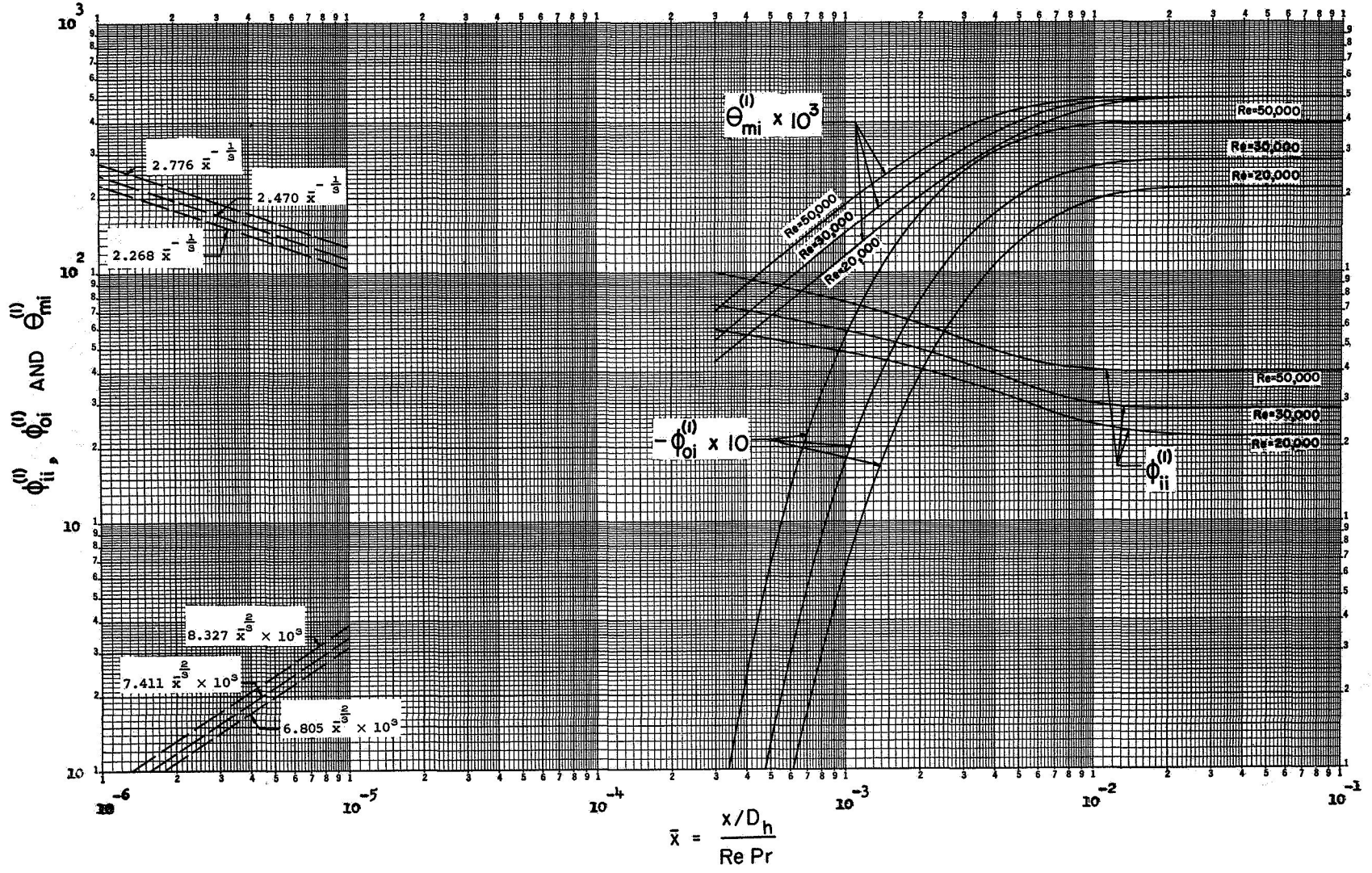

TURBULENT FUNDAMENTAL SOLUTIONS OF THE FIRST KIND

FIGURE IV.C.1

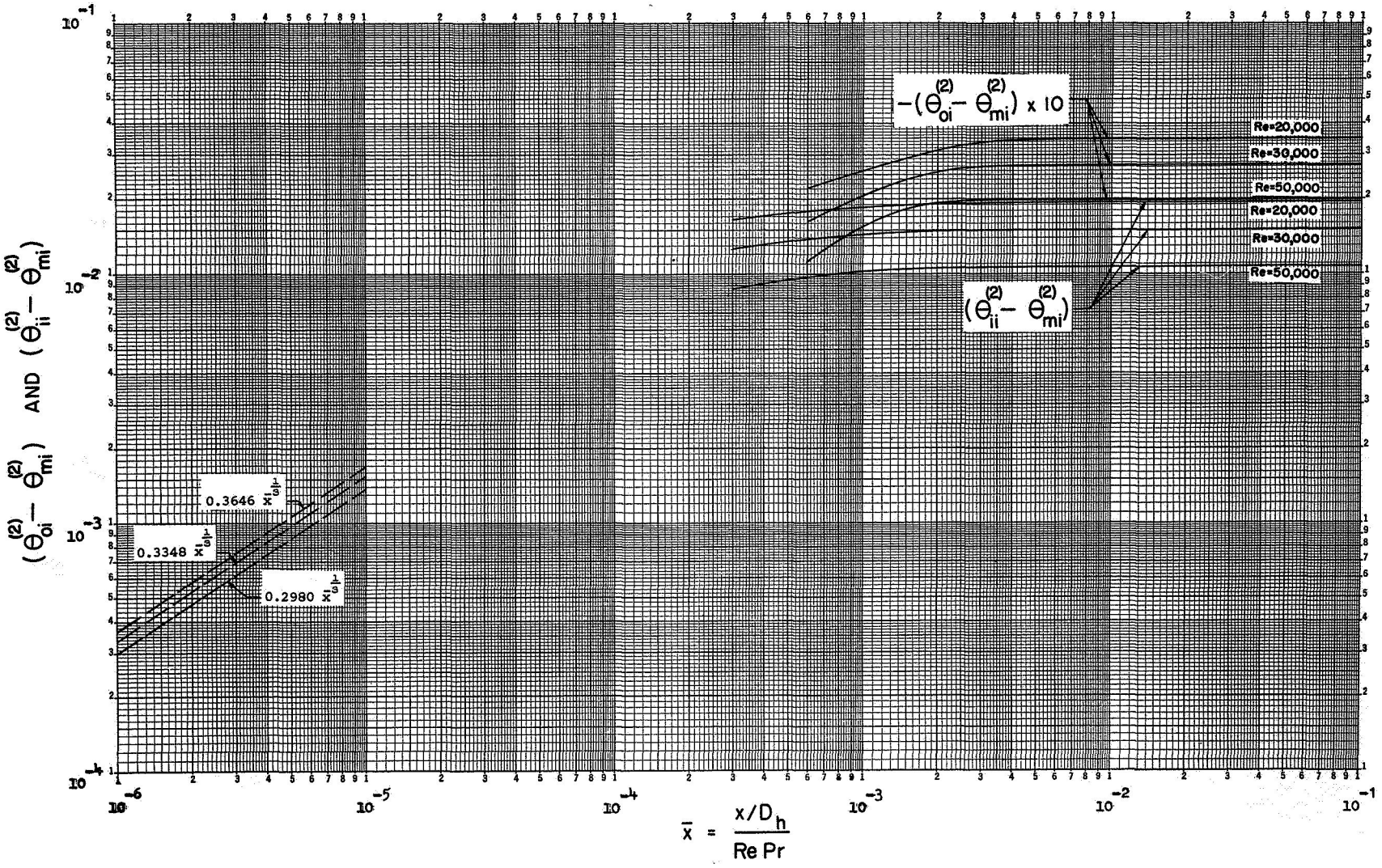

TURBULENT FUNDAMENTAL SOLUTIONS OF THE SECOND KIND

FIGURE IV.C.2

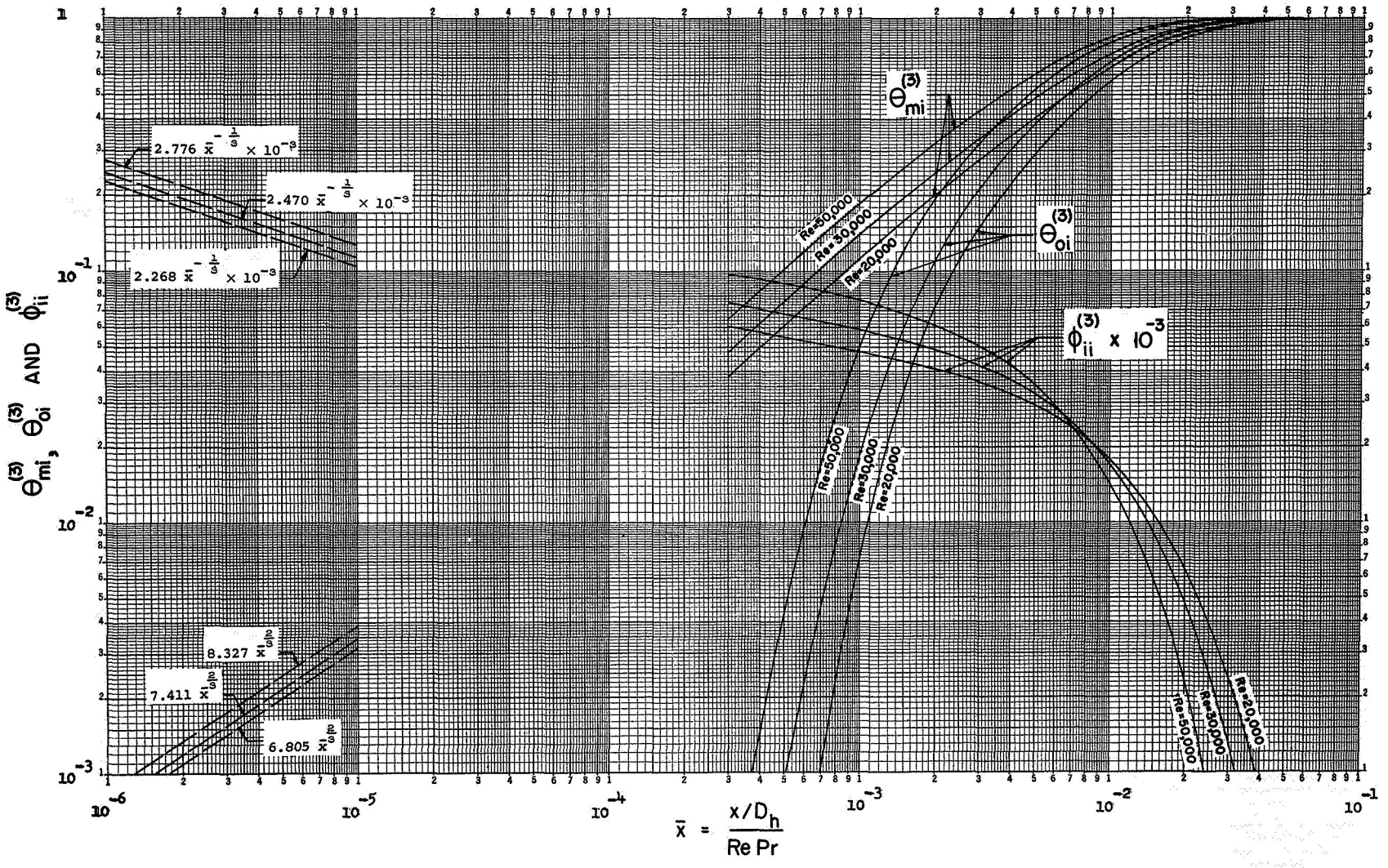

TURBULENT FUNDAMENTAL SOLUTIONS OF THE THIRD KIND

FIGURE IV.C.3

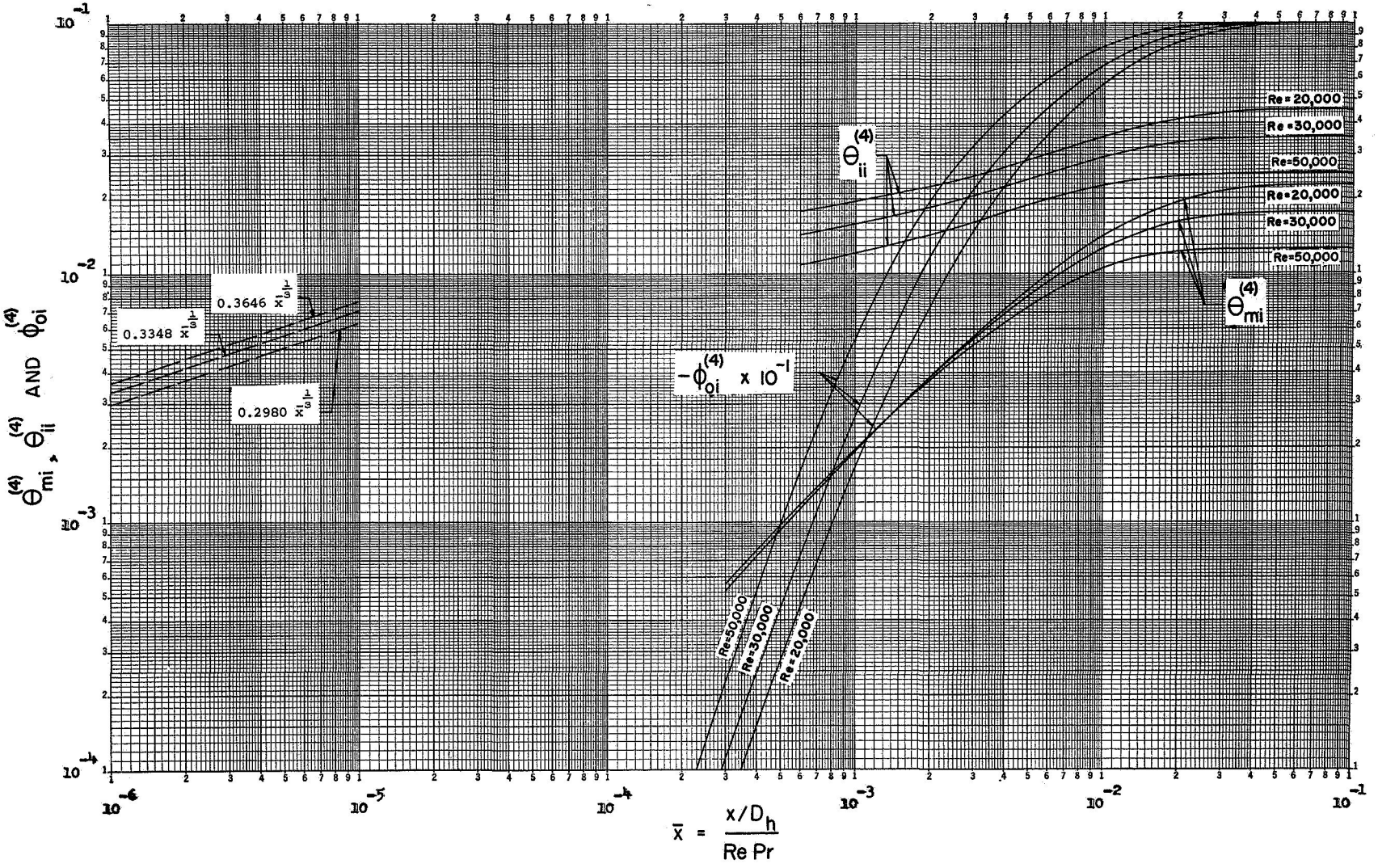

TURBULENT FUNDAMENTAL SOLUTIONS OF THE FOURTH KIND

FIGURE IV.C.4

TABLE IV.C.1

THE TURBULENT FUNDAMENTAL SOLUTIONS
FOR Pr = 0.70, Re = 20,000

First Kind

$\bar{x}$	$\Phi_{ii}^{(1)}$	$\Phi_{oi}^{(1)}$	$\theta_{mi}^{(1)}$
6.0×10^{-4}	53.1	-0.112	0.0775
8.0×10^{-4}	50.3	-0.292	0.0981
1.0×10^{-3}	48.1	-0.644	0.118
2.0×10^{-3}	40.9	-3.92	0.202
4.0×10^{-3}	33.2	-10.8	0.318
6.0×10^{-3}	28.8	-15.1	0.389
1.0×10^{-2}	24.5	-19.4	0.459
2.0×10^{-2}	22.1	-21.7	0.497
4.0×10^{-2}	21.9	-21.9	0.500
6.0×10^{-2}	21.9	-21.9	0.500
∞	21.9	-21.9	0.500

Second Kind

$\bar{x}$	$\theta_{ii}^{(2)}-\theta_{mi}^{(2)}$	$\theta_{oi}^{(2)}-\theta_{mi}^{(2)}$	$\theta_{mi}^{(2)}$
6.0×10^{-4}	0.0180	-0.00220	0.00120
8.0×10^{-4}	0.0183	-0.00241	0.00160
1.0×10^{-3}	0.0185	-0.00259	0.00200
2.0×10^{-3}	0.0191	-0.00315	0.00400
4.0×10^{-3}	0.0193	-0.00344	0.00800
6.0×10^{-3}	0.0194	-0.00348	0.0120
1.0×10^{-2}	0.0194	-0.00348	0.0200
2.0×10^{-2}	0.0194	-0.00348	0.0400
4.0×10^{-2}	0.0194	-0.00348	0.0800
6.0×10^{-2}	0.0194	-0.00348	0.120
∞	0.0194	-0.00348	∞

TABLE IV.C.1 (Continued)

Third Kind

$\bar{x}$	$\Phi_{ii}^{(3)}$	$\theta_{oi}^{(3)}$	$\theta_{mi}^{(3)}$
6.0×10^{-4}	53.2	-	0.0715
8.0×10^{-4}	50.4	0.002	0.0925
1.0×10^{-3}	48.2	0.0072	0.112
2.0×10^{-3}	41.0	0.0725	0.201
4.0×10^{-3}	32.8	0.223	0.347
6.0×10^{-3}	26.8	0.363	0.466
1.0×10^{-2}	17.9	0.573	0.642
2.0×10^{-2}	6.59	0.843	0.868
4.0×10^{-2}	0.888	0.979	0.982
6.0×10^{-2}	0.120	0.997	0.998
∞	0	1.00	1.00

Fourth Kind

$\bar{x}$	$\theta_{ii}^{(4)}$	$\Phi_{oi}^{(4)}$	$\theta_{mi}^{(4)}$
6.0×10^{-4}	0.0179	-0.0092	0.00113
8.0×10^{-4}	0.0188	-0.0116	0.00152
1.0×10^{-3}	0.0196	-0.0164	0.00192
2.0×10^{-3}	0.0226	-0.0732	0.00384
4.0×10^{-3}	0.0269	-0.229	0.00723
6.0×10^{-3}	0.0303	-0.368	0.0100
1.0×10^{-2}	0.0352	-0.576	0.0142
2.0×10^{-2}	0.0416	-0.844	0.0195
4.0×10^{-2}	0.0448	-0.979	0.0222
6.0×10^{-2}	0.0452	-0.997	0.0226
∞	0.0453	-1.00	0.0227

TABLE IV.C.2

THE TURBULENT FUNDAMENTAL SOLUTIONS
FOR Pr = 0.70, Re = 30,000

First Kind

$\bar{x}$	$\Phi_{ii}^{(1)}$	$\Phi_{oi}^{(1)}$	$\theta_{mi}^{(1)}$
6.0×10^{-4}	65.6	-0.30	0.0954
8.0×10^{-4}	61.9	-0.868	0.121
1.0×10^{-3}	58.9	-1.74	0.144
2.0×10^{-3}	49.2	-7.76	0.242
4.0×10^{-3}	39.1	-17.3	0.364
6.0×10^{-3}	33.9	-22.5	0.429
1.0×10^{-2}	29.8	-26.6	0.480
2.0×10^{-2}	28.2	-28.1	0.499
4.0×10^{-2}	28.2	-28.2	0.500
6.0×10^{-2}	28.2	-28.2	0.500
∞	28.2	-28.2	0.500

Second Kind

$\bar{x}$	$\theta_{ii}^{(2)}-\theta_{mi}^{(2)}$	$\theta_{oi}^{(2)}-\theta_{mi}^{(2)}$	$\theta_{mi}^{(2)}$
6.0×10^{-4}	0.0138	-0.00162	0.00120
8.0×10^{-4}	0.0141	-0.00186	0.00160
1.0×10^{-3}	0.0143	-0.00205	0.00200
2.0×10^{-3}	0.0148	-0.00255	0.00400
4.0×10^{-3}	0.0150	-0.00273	0.00800
6.0×10^{-3}	0.0150	-0.00275	0.0120
1.0×10^{-2}	0.0150	-0.00275	0.0200
2.0×10^{-2}	0.0150	-0.00275	0.0400
4.0×10^{-2}	0.0150	-0.00275	0.0800
6.0×10^{-2}	0.0150	-0.00275	0.120
∞	0.0150	-0.00275	∞

TABLE IV.C.2 (Continued)

Third Kind

$\bar{x}$	$\Phi_{ii}^{(3)}$	$\theta_{oi}^{(3)}$	$\theta_{mi}^{(3)}$
6.0×10^{-4}	66.0	-	0.089
8.0×10^{-4}	62.0	0.0082	0.115
1.0×10^{-3}	59.0	0.019	0.139
2.0×10^{-3}	49.3	0.109	0.246
4.0×10^{-3}	37.6	0.305	0.418
6.0×10^{-3}	29.0	0.463	0.551
1.0×10^{-2}	17.3	0.680	0.732
2.0×10^{-2}	4.76	0.912	0.926
4.0×10^{-2}	0.361	0.993	0.994
6.0×10^{-2}	0.0272	1.00	1.00
∞	0	1.00	1.00

Fourth Kind

$\bar{x}$	$\theta_{ii}^{(4)}$	$\Phi_{oi}^{(4)}$	$\theta_{mi}^{(4)}$
6.0×10^{-4}	0.0144	-0.01	0.00112
8.0×10^{-4}	0.0152	-0.016	0.00152
1.0×10^{-3}	0.0159	-0.0264	0.00190
2.0×10^{-3}	0.0186	-0.115	0.00377
4.0×10^{-3}	0.0224	-0.310	0.00691
6.0×10^{-3}	0.0253	-0.467	0.00934
1.0×10^{-2}	0.0293	-0.682	0.0127
2.0×10^{-2}	0.0336	-0.912	0.0162
4.0×10^{-2}	0.0351	-0.993	0.0175
6.0×10^{-2}	0.0352	-1.00	0.0176
∞	0.0352	-1.00	0.0176

TABLE IV.C.3

THE TURBULENT FUNDAMENTAL SOLUTIONS
FOR Pr = 0.70, Re = 50,000

First Kind

$\bar{x}$	$\Phi_{ii}^{(1)}$	$\Phi_{oi}^{(1)}$	$\theta_{mi}^{(1)}$
6.0×10^{-4}	86.6	-1.32	0.125
8.0×10^{-4}	81.0	-3.20	0.158
1.0×10^{-3}	76.5	-5.53	0.188
2.0×10^{-3}	62.3	-17.2	0.302
4.0×10^{-3}	48.7	-30.6	0.420
6.0×10^{-3}	43.3	-36.0	0.468
1.0×10^{-2}	40.2	-39.1	0.495
2.0×10^{-2}	39.6	-39.6	0.500
4.0×10^{-2}	39.6	-39.6	0.500
6.0×10^{-2}	39.6	-39.6	0.500
∞	39.6	-39.6	0.500

Second Kind

$\bar{x}$	$\theta_{ii}^{(2)}-\theta_{mi}^{(2)}$	$\theta_{oi}^{(2)}-\theta_{mi}^{(2)}$	$\theta_{mi}^{(2)}$
6.0×10^{-4}	0.00976	-0.00112	0.00120
8.0×10^{-4}	0.0100	-0.00137	0.00160
1.0×10^{-3}	0.0102	-0.00155	0.00200
2.0×10^{-3}	0.0106	-0.00191	0.00400
4.0×10^{-3}	0.0107	-0.00199	0.00800
6.0×10^{-3}	0.0107	-0.00199	0.0120
1.0×10^{-2}	0.0107	-0.00199	0.0200
2.0×10^{-2}	0.0107	-0.00199	0.0400
4.0×10^{-2}	0.0107	-0.00199	0.0800
6.0×10^{-2}	0.0107	-0.00199	0.120
∞	0.0107	-0.00199	∞

TABLE IV.C.3 (Continued)

Third Kind

$\bar{x}$	$\Phi_{ii}^{(3)}$	$\theta_{oi}^{(3)}$	$\theta_{mi}^{(3)}$
6.0×10^{-4}	86.8	0.0094	0.121
8.0×10^{-4}	81.2	0.0265	0.155
1.0×10^{-3}	76.8	0.0495	0.186
2.0×10^{-3}	61.9	0.191	0.323
4.0×10^{-3}	42.8	0.436	0.530
6.0×10^{-3}	29.7	0.608	0.674
1.0×10^{-2}	14.4	0.811	0.842
2.0×10^{-2}	2.32	0.969	0.974
4.0×10^{-2}	0.0608	0.999	0.999
6.0×10^{-2}	0.00160	1.00	1.00
∞	0	1.00	1.00

Fourth Kind

$\bar{x}$	$\theta_{ii}^{(4)}$	$\Phi_{oi}^{(4)}$	$\theta_{mi}^{(4)}$
6.0×10^{-4}	0.0109	-0.016	0.00116
8.0×10^{-4}	0.0116	-0.0328	0.00156
1.0×10^{-3}	0.0122	-0.0552	0.00194
2.0×10^{-3}	0.0144	-0.195	0.00369
4.0×10^{-3}	0.0177	-0.439	0.00639
6.0×10^{-3}	0.0200	-0.610	0.00827
1.0×10^{-2}	0.0226	-0.812	0.0105
2.0×10^{-2}	0.0247	-0.970	0.0122
4.0×10^{-2}	0.0251	-0.999	0.0125
6.0×10^{-2}	0.0251	-1.00	0.0126
∞	0.0251	-1.00	0.0126

IV. D. The Nusselt Number Relations

As with the laminar case, several of the general Nusselt number relations presented in Section I.E have been combined with the appropriate fundamental solutions. The results are presented in Table IV.D.1.

IV. E. Relations Valid at Small $\bar{x}$

At very small values of $\bar{x}$ the temperature profile reaching out from the heated wall has not yet penetrated beyond the laminar sublayer. Hence the region of interest is purely laminar, as it was, of course, in Section II.E., and the development in that section is applicable here with only minor modification.

1. The differential equation

Recall from (IV.B.1) that the energy equation for the entire region between the two planes is

$$\frac{\partial}{\partial \bar{y}} \left[\left(1 + \frac{\epsilon_H}{\nu} \mathrm{Pr} \right) \frac{\partial \theta}{\partial \bar{y}} \right] = \frac{\bar{u}}{16} \frac{\partial \theta}{\partial \bar{x}} \qquad \text{(IV.E.1)}$$

where $\bar{u} \triangleq \frac{u}{u_m}$. (IV.E.2)

Now in the region of interest here, the laminar sublayer very close to a wall, $\frac{\epsilon_H}{\nu} \mathrm{Pr} \ll 1$. So the energy equation for this region reduces to

$$\frac{\partial^2 \theta}{\partial \bar{y}^2} = \frac{\bar{u}}{16} \frac{\partial \theta}{\partial \bar{x}} \qquad \text{(IV.E.3)}$$

This is precisely the equation (III.E.1) used in the laminar section. But there is an important different here; $\bar{u}$ no longer assumes the parabolic laminar form. Rather, as can be seen from (IV.B.15) when $\frac{\epsilon_M}{\nu} \ll 1$ and $\eta^2 \ll \eta$,

TABLE IV.D.1

TURBULENT NUSSELT NUMBERS FOR UNIFORM AND EQUAL WALL BOUNDARY CONDITIONS, Pr = 0.70

Equal Wall Temperatures

$\bar{x}$	Nusselt Number		
	Re = 20,000	Re = 30,000	Re = 50,000
6.0×10^{-4}	62.7	80.7	114
8.0×10^{-4}	62.2	80.4	114
1.0×10^{-3}	62.1	80.3	114
2.0×10^{-3}	62.0	80.3	114
∞	62.0	80.3	114

Equal Wall Heat Fluxes

$\bar{x}$	Nusselt Number		
	Re = 20,000	Re = 30,000	Re = 50,000
6.0×10^{-4}	63.5	82.0	116
8.0×10^{-4}	63.1	81.6	115
1.0×10^{-3}	63.0	81.5	115
2.0×10^{-3}	62.9	81.4	115
∞	62.9	81.4	115

$$\bar{u} = \frac{Re\ f}{8}\,\eta \qquad (\eta \triangleq 1 + \bar{y})$$

at the lower wall. At the upper wall this becomes

$$\bar{u} = \frac{Re\ f}{8}\,\bar{\eta} \qquad (\bar{\eta} \triangleq 1 - \bar{y}) \qquad \text{(IV.E.4)}$$

This relation is the familiar $u^+ = y^+$ equation in a form more convenient for the purpose at hand. Thus the energy equation becomes

$$\frac{\partial^2\theta}{\partial\bar{\eta}^2} = \frac{Re\ f}{128}\,\bar{\eta}\,\frac{\partial\theta}{\partial\bar{x}} \qquad \text{(IV.E.5)}$$

for the region under consideration. It is identical in form to (III.E.7) of the laminar section, differing only in the magnitude of the constant coefficient; hence the same similarity solution approach is applicable.

2. The uniform wall temperature case

Here the wall boundary condition is

$$\theta_{\bar{\eta}=0} = 1 \qquad \text{(IV.E.6)}$$

The similarity solution sought is of the form

$$\theta = \psi(\xi) \qquad \text{(IV.E.7)}$$

where

$$\xi = \bar{\eta}\,\bar{x}^{-\frac{1}{3}} \qquad \text{(IV.E.8)}$$

Combining (IV.E.5), (IV.E.7), and (IV.E.8) yields the ordinary differential equation

$$\psi'' + \frac{Re\ f}{384}\,\xi^2\psi' = 0 \qquad \text{(IV.E.9)}$$

The solution of this equation is

$$\psi = \theta = C_1 \int e^{-\frac{Re\ f}{1152}\xi^3}\, d\xi + C_2 \qquad \text{(IV.E.10)}$$

where C_1 and C_2 are constants. From the boundary condition (IV.E.6), and from (IV.E.8) one obtains

$$\theta_{\xi=0} = 1 \qquad \text{(IV.E.11)}$$

Hence, from (IV.E.10)

$$1 = C_1 \left(\int e^{-\frac{Re\ f}{1152}\xi^3}\, d\xi \right)_{\xi=0} + C_2$$

The integral in this equation vanishes, as can be seen by expanding the exponential in a series and integrating term by term. Thus

$$C_2 = 1 \qquad \text{(IV.E.12)}$$

Since $\theta = 0$ at $\bar{x} = 0$ $(\xi = \infty)$ by definition, (IV.E.10) becomes

$$0 = C_1 \left(\int e^{-\frac{Re\ f}{1152}\xi^3}\, d\xi \right)_{\xi=\infty} + 1$$

Since the integral vanishes at $\xi = 0$, this can be written as

$$0 = C_1 \int_0^\infty e^{-\frac{Re\ f}{1152}\xi^3}\, d\xi + 1 \qquad \text{(IV.E.13)}$$

From Jahnke-Emde[27]

$$\int_0^\infty e^{-\frac{Re\ f}{1152}\xi^3}\, d\xi = \left(\frac{1152}{Re\ f}\right)^{\frac{1}{3}} \frac{1}{3}\,\Gamma\left(\frac{1}{3}\right) \qquad \text{(IV.E.14)}$$

Combining the preceding two equations yields

$$C_1 = -\frac{3}{\Gamma\left(\frac{1}{3}\right)}\left(\frac{Re\ f}{1152}\right)^{\frac{1}{3}}$$

Thus (IV.E.10) becomes

$$\theta = -\frac{3}{\Gamma\left(\frac{1}{3}\right)}\left(\frac{Re\ f}{1152}\right)^{\frac{1}{3}}\int_0^{\xi} e^{-\frac{Re\ f}{1152}\sigma^3}\, d\sigma + 1 \qquad \text{(IV.E.15)}$$

where σ is a dummy variable.

The fundamental solutions sought are Φ_{oo} and θ_m. Considering first Φ_{oo}, (II.B.10) yields

$$\Phi_{oo} = -4\left(\frac{\partial\theta}{\partial\bar{\eta}}\right)_{\bar{\eta}=o} \qquad \text{(IV.E.16)}$$

Combining this with (IV.E.8) and (IV.E.15) gives

$$\Phi_{oo} = \frac{12}{\Gamma\left(\frac{1}{3}\right)}\left(\frac{Re\ f}{1152}\right)^{\frac{1}{3}}\bar{x}^{-\frac{1}{3}} \qquad \text{(IV.E.17)}$$

Hence

$$\Phi_{oo} = 4.479\left(\frac{Re\ f}{1152}\right)^{\frac{1}{3}}\bar{x}^{-\frac{1}{3}} \qquad \text{(IV.E.18)}$$

This fundamental solution holds for both cases one and three in the region near $\bar{x} = 0$ and a unity temperature wall.

θ_m is now found by performing the integration indicated in both (IV.C.5) and (IV.C.16).

$$\theta_m = 2\int_0^{\bar{x}} \Phi_{oo}\, d\bar{x} \qquad \text{(IV.E.19)}$$

So in this case

$$\theta_m = \frac{36}{\Gamma\left(\frac{1}{3}\right)} \left(\frac{Re\ f}{1152}\right)^{\frac{1}{3}} \bar{x}^{\frac{2}{3}} \qquad \text{(IV.E.20)}$$

Thus

$$\theta_m = 13.44 \left(\frac{Re\ f}{1152}\right)^{\frac{1}{3}} \bar{x}^{\frac{2}{3}} \qquad \text{(IV.E.21)}$$

This fundamental solution, like the one preceding, holds for both cases one and three.

3. The uniform wall heat flux case

In this case the wall boundary condition is

$$\Phi_{\bar{\eta}=0} = 1 \qquad \text{(IV.E.22)}$$

From (II.B.15) it is seen that this is equivalent to

$$\left(\frac{\partial\theta}{\partial\bar{\eta}}\right)_{\bar{\eta}=0} = -\frac{1}{4} \qquad \text{(IV.E.23)}$$

Here the similarity solution is of the form

$$\theta = \bar{x}^{\frac{1}{3}} \psi(\xi) \qquad \text{(IV.E.24)}$$

where

$$\xi = \bar{\eta}\ \bar{x}^{-\frac{1}{3}} \qquad \text{(IV.E.25)}$$

Combining the above two equations with (IV.E.5) yields the following ordinary differential equation

$$\psi'' + \frac{Re\ f}{384}\ \xi^2\psi' - \frac{Re\ f}{384}\ \xi\psi = 0 \qquad \text{(IV.E.26)}$$

The solution of this equation is

$$\psi = C_1 \xi \int \frac{e^{-\frac{Re\ f}{1152}\xi^3}}{\xi^2} d\xi + C_2 \xi \qquad \text{(IV.E.27)}$$

where C_1 and C_2 are constants. Integrating by parts, the above becomes

$$\psi = C_2 \xi - C_1 e^{-\frac{Re\ f}{1152}\xi^3} - \frac{Re\ f}{384} C_1 \xi \int \xi\ e^{-\frac{Re\ f}{1152}\xi^3} d\xi \qquad \text{(IV.E.28)}$$

Introducing (IV.E.24) yields

$$\theta = \bar{x}^{\frac{1}{3}} \left[C_2 \xi - C_1 e^{-\frac{Re\ f}{1152}\xi^3} - \frac{Re\ f}{384} C_1 \xi \int \xi\ e^{-\frac{Re\ f}{1152}\xi^3} d\xi \right] \qquad \text{(IV.E.29)}$$

Applying the boundary condition (IV.E.23), and employing (IV.E.25)

$$\left(\frac{\partial\theta}{\partial\bar{\eta}}\right)_{\bar{\eta}=0} = \bar{x}^{-\frac{1}{3}} \left(\frac{\partial\theta}{\partial\xi}\right)_{\xi=0} = C_2 = -\frac{1}{4} \qquad \text{(IV.E.30)}$$

In arriving at this condition, use is made of the fact that the integral in (IV.E.29) vanishes at $\xi = 0$, as can be seen by expanding the exponential in a series and integrating term by term.

By definition $\theta = 0$ at $\bar{x} = 0$ ($\xi = \infty$), so (IV.E.29) becomes

$$0 = -\frac{1}{4}\bar{\eta} - \frac{Re\ f}{384} C_1 \bar{\eta} \int_0^\infty \xi\ e^{-\frac{Re\ f}{1152}\xi^3} d\xi$$

So

$$C_1 = - \frac{96}{\text{Re } f \int_0^\infty \xi \, e^{- \frac{\text{Re } f}{1152} \xi^3} \, d\xi} \qquad \text{(IV.E.31)}$$

From Jahnke-Emde

$$\int_0^\infty \xi \, e^{- \frac{\text{Re } f}{1152} \xi^3} \, d\xi = \left(\frac{1152}{\text{Re } f}\right)^{\frac{2}{3}} \frac{1}{3} \Gamma\left(\frac{2}{3}\right) \qquad \text{(IV.E.32)}$$

Hence

$$C_1 = - \frac{1}{4 \left(\frac{\text{Re } f}{1152}\right)^{\frac{1}{3}} \Gamma\left(\frac{2}{3}\right)} \qquad \text{(IV.E.33)}$$

And (IV.E.29) becomes

$$\theta = \bar{x}^{\frac{1}{3}} \left[- \frac{1}{4} \xi + \frac{1}{4 \left(\frac{\text{Re } f}{1152}\right)^{\frac{1}{3}} \Gamma\left(\frac{2}{3}\right)} \left(e^{- \frac{\text{Re } f}{1152} \xi^3} + \frac{\text{Re } f}{384} \xi \int_0^\xi \sigma \, e^{- \frac{\text{Re } f}{1152} \sigma^3} \, d\sigma \right) \right] \qquad \text{(IV.E.34)}$$

where σ is a dummy variable.

Since θ_∞ occurs at $\bar{\eta} = 0$ ($\xi = 0$), the fundamental solution is

$$\theta_{oo} = \frac{1}{4 \left(\frac{\text{Re } f}{1152}\right)^{\frac{1}{3}} \Gamma\left(\frac{2}{3}\right)} \bar{x}^{\frac{1}{3}} \qquad \text{(IV.E.35)}$$

Evaluating the constant yields

$$\theta_{oo} = 0.1846 \left(\frac{Re\ f}{1152}\right)^{-\frac{1}{3}} \bar{x}^{\frac{1}{3}} \qquad \text{(IV.E.36)}$$

θ_m for this case follows directly from energy balance considerations (see (IV.C.12)).

$$\theta_m = 2\bar{x} \qquad \text{(IV.E.37)}$$

These fundamental solutions hold for both cases two and four in the region near $\bar{x} = 0$ and a unity Φ heat-flux wall.

The limiting fundamental solutions derived in this section are indicated by the dashed lines on the fundamental solution curves in Section IV.G.

4. The Nusselt number relations

The Nusselt number relations for very small values of $\bar{x}$ follow from the preceding developments of this section and the results of Section II.E.

a. Case one

At very small $\bar{x}$ the temperature profile has not propagated to the opposite wall, so $\Phi_{oi}^{(1)} = 0$. Hence (II.E.5) becomes

$$Nu_o = \frac{\Phi_{oo}^{(1)}}{1 - \theta_{mo}^{(1)} \left[1 + \left(\frac{t_{wi} - t_e}{t_{wo} - t_e}\right)\right]} \qquad \text{(IV.E.38)}$$

Introducing (IV.E.17) and (IV.E.20) there follows

$$Nu_o = \frac{1}{\frac{\Gamma\left(\frac{1}{3}\right)}{12\left(\frac{Re\ f}{1152}\right)^{\frac{1}{3}}} \bar{x}^{\frac{1}{3}} - 3\left[1 + \left(\frac{t_{wi} - t_e}{t_{wo} - t_e}\right)\right]\bar{x}} \qquad \text{(IV.E.39)}$$

So

$$Nu_o = \frac{1}{0.2232\left(\frac{Re\ f}{1152}\right)^{-\frac{1}{3}} \bar{x}^{-\frac{1}{3}} - 3\left[1 + \left(\frac{t_{wi} - t_e}{t_{wo} - t_e}\right)\right]\bar{x}} \qquad \text{(IV.E.40)}$$

For most wall temperature ratios, the second term in the denominator is negligible compared to the first.

b. Case two

Here $\theta_{oi}^{(2)} = 0$ at very small $\bar{x}$, so (II.E.7) becomes

$$Nu_o = \frac{1}{\theta_{oo}^{(2)} - \theta_{mo}^{(2)}\left(1 + \frac{q''_{wi}}{q''_{wo}}\right)} \qquad \text{(IV.E.41)}$$

Combining this with (IV.E.35) and (IV.E.37) yields

$$Nu_o = \frac{1}{\frac{1}{4\left(\frac{Re\ f}{1152}\right)^{\frac{1}{3}}\Gamma\left(\frac{2}{3}\right)} \bar{x}^{-\frac{1}{3}} - 2\left(1 + \frac{q''_{wi}}{q''_{wo}}\right)\bar{x}} \qquad \text{(IV.E.42)}$$

Or

$$Nu_o = \frac{1}{0.1846\left(\frac{Re\ f}{1152}\right)^{-\frac{1}{3}} \bar{x}^{-\frac{1}{3}} - 2\left(1 + \frac{q''_{wi}}{q''_{wo}}\right)\bar{x}} \qquad \text{(IV.E.43)}$$

Again, the second term in the denominator is normally negligible.

c. Case three

In this case $\Phi_{oi}^{(4)} = 0$, and (II.E.9) becomes

$$Nu_o = \frac{\Phi_{oo}^{(3)}}{1 - \theta_{mo}^{(3)} - \theta_{mi}^{(4)} \left(\frac{q''_{wi} \frac{D_h}{k}}{t_{wo} - t_e} \right)} \qquad \text{(IV.E.44)}$$

Introducing (IV.E.17), (IV.E.20), and (IV.E.37) yields

$$Nu_o = \frac{\frac{12}{\Gamma\left(\frac{1}{3}\right)} \left(\frac{Re\ f}{1152} \right)^{\frac{1}{3}} \bar{x}^{-\frac{1}{3}}}{1 - \frac{36}{\Gamma\left(\frac{1}{3}\right)} \left(\frac{Re\ f}{1152} \right)^{\frac{1}{3}} \bar{x}^{\frac{2}{3}} - 2 \left(\frac{q''_{wi} \frac{D_h}{k}}{t_{wo} - t_e} \right) \bar{x}} \qquad \text{(IV.E.45)}$$

Or

$$Nu_o = \frac{4.479 \left(\frac{Re\ f}{1152} \right)^{\frac{1}{3}} \bar{x}^{-\frac{1}{3}}}{1 - 13.44 \left(\frac{Re\ f}{1152} \right)^{\frac{1}{3}} \bar{x}^{\frac{2}{3}} - 2 \left(\frac{q''_{wi} \frac{D_h}{k}}{t_{wo} - t_e} \right) \bar{x}} \qquad \text{(IV.E.46)}$$

d. Case four

Here $\theta_{oi}^{(3)} = 0$ at very small $\bar{x}$, so (II.E.11) becomes

$$Nu_o = \frac{1}{\theta_{oo}^{(4)} - \theta_{mo}^{(4)} - \theta_{mo}^{(3)} \left(\frac{t_{wi} - t_e}{q''_{wo} \frac{D_h}{k}} \right)} \qquad \text{(IV.E.47)}$$

Combining this with (IV.E.35), (IV.E.37), and (IV.E.20) gives

$$Nu_o = \frac{1}{\frac{1}{4\left(\frac{Re\ f}{1152}\right)^{\frac{1}{3}}\Gamma\left(\frac{2}{3}\right)}\bar{x}^{-\frac{1}{3}} - 2\bar{x} - \frac{36}{\Gamma\left(\frac{1}{3}\right)}\left(\frac{Re\ f}{1152}\right)^{\frac{1}{3}}\left(\frac{t_{wi} - t_e}{q''_{wo}\frac{D_h}{k}}\right)\bar{x}^{\frac{2}{3}}} \qquad \text{(IV.E.48)}$$

Thus

$$Nu_o = \frac{1}{0.1846\left(\frac{Re\ f}{1152}\right)^{-\frac{1}{3}}\bar{x}^{-\frac{1}{3}} - 2\bar{x} - 13.44\left(\frac{Re\ f}{1152}\right)^{\frac{1}{3}}\left(\frac{t_{wi} - t_e}{q''_{wo}\frac{D_h}{k}}\right)\bar{x}^{\frac{2}{3}}} \qquad \text{(IV.E.49)}$$

IV. F. Relations Valid at Large $\bar{x}$

As was the case for the laminar flow counterparts, at large values of $\bar{x}$ the infinite series in the turbulent fundamental solution expressions vanish. The term remaining in these expressions is the fully developed solution; it is the subject of treatment in the present section.

1. The fully developed fundamental solutions

These expressions are obtained in each case by setting the infinite series in the corresponding fundamental solution in Section IV.C equal to zero.

a. Case one

$$\theta^{(1)}_{oo} = \theta^{(1)}_{ii} = 1$$

$$\theta^{(1)}_{oi} = \theta^{(1)}_{io} = 0$$

$$\Phi^{(1)}_{oo} = \Phi^{(1)}_{ii} = 4\left(\frac{d\theta^{(1)}_{fd}}{d\bar{y}}\right)_{\bar{y}=1}$$

$$\Phi_{oi}^{(1)} = \Phi_{io}^{(1)} = -4\left(\frac{d\theta_{fd}^{(1)}}{d\bar{y}}\right)_{\bar{y}=-1}$$

$$\left(\text{Note: } \left(\frac{d\theta_{fd}^{(1)}}{d\bar{y}}\right)_{\bar{y}=-1} = \left(\frac{d\theta_{fd}^{(1)}}{d\bar{y}}\right)_{\bar{y}=1}\right)$$

$$\theta_{mo}^{(1)} = \theta_{mi}^{(1)} = \frac{1}{2}$$

b. Case two

$$\theta_{oo}^{(2)} = \theta_{ii}^{(2)} = 2\bar{x} + S(1)$$

$$\theta_{oi}^{(2)} = \theta_{io}^{(2)} = 2\bar{x} + S(-1)$$

$$\Phi_{oo}^{(2)} = \Phi_{ii}^{(2)} = 1$$

$$\Phi_{oi}^{(2)} = \Phi_{io}^{(2)} = 0$$

$$\theta_{mo}^{(2)} = \theta_{mi}^{(2)} = 2\bar{x}$$

c. Case three

$$\theta_{oo}^{(3)} = \theta_{ii}^{(3)} = 1$$

$$\theta_{oi}^{(3)} = \theta_{io}^{(3)} = 1$$

$$\Phi_{oo}^{(3)} = \Phi_{ii}^{(3)} = 0$$

$$\Phi_{oi}^{(3)} = \Phi_{io}^{(3)} = 0$$

$$\theta_{mo}^{(3)} = \theta_{mi}^{(3)} = 1$$

d. Case four

$$\theta_{oo}^{(4)} = \theta_{ii}^{(4)} = \theta_{fd}^{(4)} \quad (1)$$

$$\theta_{oi}^{(4)} = \theta_{io}^{(4)} = 0$$

$$\Phi_{oo}^{(4)} = \Phi_{ii}^{(4)} = 1$$

$$\Phi_{oi}^{(4)} = \Phi_{io}^{(4)} = -1$$

$$\theta_{mo}^{(4)} = \theta_{mi}^{(4)} = \theta_{m_{fd}}^{(4)}$$

The preceding fundamental solutions for which no numerical values have been assigned are functions of Reynolds number and Prandtl number. They were evaluated numerically by the method discussed in Section IV.G, and are presented in Figures IV.B.7, 8, and 9 and Table IV.B.1.

2. The fully developed Nusselt number relations

The fully developed Nusselt number relations for turbulent flow follow from the preceding results and those of Section II.E. As in the laminar case, the fully developed Nusselt number relations are valid at smaller values of $\bar{x}$ than are the fully developed fundamental solutions.

a. Case one

Here one obtains

$$Nu_o = \frac{4\left(\frac{d\theta_{fd}^{(1)}}{d\bar{y}}\right)_{\bar{y}=1}\left[1 - \left(\frac{t_{wi} - t_e}{t_{wo} - t_e}\right)\right]}{1 - \frac{1}{2}\left[1 + \left(\frac{t_{wi} - t_e}{t_{wo} - t_e}\right)\right]} \qquad \text{(IV.F.1)}$$

Thus

$$Nu_o = 8\left(\frac{d\theta_{fd}^{(1)}}{d\bar{y}}\right)_{\bar{y}=1}\left[\frac{1 - \left(\frac{t_{wi} - t_e}{t_{wo} - t_e}\right)}{1 - \left(\frac{t_{wi} - t_e}{t_{wo} - t_e}\right)}\right] \qquad \text{(IV.F.2)}$$

Therefore, when $t_{wi} \neq t_{wo}$,

$$Nu_o = 8\left(\frac{d\theta_{fd}^{(1)}}{d\bar{y}}\right)_{\bar{y}=1} \qquad \text{(IV.F.3)}$$

This Nusselt number is plotted against Reynolds number for a Prandtl number of 0.70 in Figure IV.F.1.

When $t_{wi} = t_{wo}$ (IV.F.2) is indeterminate and the Nusselt number must be evaluated by a limiting process, as was carried out for the corresponding laminar case. Combining the appropriate Nusselt number expression of Section II.E with the appropriate general fundamental solutions of Section IV.C, one obtains

$$Nu_o = 4\frac{\left[\sum_{n=o}^{\infty} C_n Y_n'(1)e^{-16\lambda_n^2\bar{x}} - \sum_{n=o}^{\infty} C_n Y_n'(-1)e^{-16\lambda_n^2\bar{x}}\right]}{\left[\sum_{n=o}^{\infty} \frac{C_n}{\lambda_n^2} Y_n'(1)e^{-16\lambda_n^2\bar{x}} - \sum_{n=o}^{\infty} \frac{C_n}{\lambda_n^2} Y_n'(-1)e^{-16\lambda_n^2\bar{x}}\right]}$$

As $\bar{x}$ becomes large this expression approaches

$$Nu_o = 4\frac{\left[C_o Y_o'(1) - C_o Y_o'(-1)\right]}{\left[\frac{C_o}{\lambda_o^2} Y_o'(1) - \frac{C_o}{\lambda_o^2} Y_o'(-1)\right]}$$

Thus

$$Nu_o = 4\lambda_o^2 \quad \text{when} \quad t_{wi} = t_{wo} \qquad \text{(IV.F.4)}$$

A plot of this Nusselt number is given in Figure IV.F.1.

b. Case two

Combining (II.E.7) with the appropriate fully developed fundamental solutions in Section IV.F.1 yields

$$Nu_o = \frac{1}{2\bar{x} + S(1) + \left[2\bar{x} + S(-1)\right]\left(\frac{q''_{wi}}{q''_{wo}}\right) - 2\bar{x}\left(1 + \frac{q''_{wi}}{q''_{wo}}\right)} \qquad \text{(IV.F.5)}$$

Thus

$$Nu_o = \frac{1}{S(1) + S(-1)\left(\frac{q''_{wi}}{q''_{wo}}\right)} \qquad \text{(IV.F.6)}$$

This fully developed Nusselt number is plotted versus Reynolds number for equal wall heat fluxes in Figure IV.F.1.

c. Case three

For this case

$$Nu_o = \frac{-\left(\frac{q''_{wi}\,\frac{D_h}{k}}{t_{wo} - t_e}\right)}{1 - 1 - \theta^{(4)}_{m_{fd}}\left(\frac{q''_{wi}\,\frac{D_h}{k}}{t_{wo} - t_e}\right)} \qquad \text{(IV.F.7)}$$

Hence, when $q''_{wi} \neq 0$, $Nu_o = \frac{1}{\theta^{(4)}_{m_{fd}}}$ (IV.F.8)

When $q''_{wi} = 0$ (IV.F.10) is indeterminate and the entry length expressions must be employed. From (II.E.9) and the fundamental solution expressions of Section IV.C

$$Nu_o = \frac{4 \sum_{n=o}^{\infty} C_n Y'_n(1) e^{-16\lambda_n^2 \bar{x}}}{1 - 1 + \frac{1}{2} \sum_{n=o}^{\infty} \frac{C_n}{\lambda_n^2} Y'_n(1) e^{-16\lambda_n^2 \bar{x}}} \qquad \text{(IV.F.9)}$$

for the case of $q''_{wi} = 0$. As $\bar{x}$ becomes large this expression approaches

$$Nu_o = \frac{4 C_o Y'_o(1)}{\frac{1}{2} \frac{C_o}{\lambda_o^2} Y'_o(1)}$$

Hence, when $q''_{wi} = 0$, $Nu_o = 8 \lambda_o^2$ (IV.F.10)

d. Case four

Here one obtains

$$Nu_o = \frac{1}{\theta_{fd}^{(4)}(1) - \theta_{m_{fd}}^{(4)} + (1 - 1)\left(\frac{t_{wi} - t_e}{q''_{wo} \frac{D_h}{k}}\right)} \qquad \text{(IV.F.11)}$$

Hence, when $q''_{wo} \neq 0$, $Nu_o = \frac{1}{\theta_{fd}^{(4)}(1) - \theta_{m_{fd}}^{(4)}}$ (IV.F.12)

And when $q''_{wo} = 0$, $Nu_o = 0$ (IV.F.13)

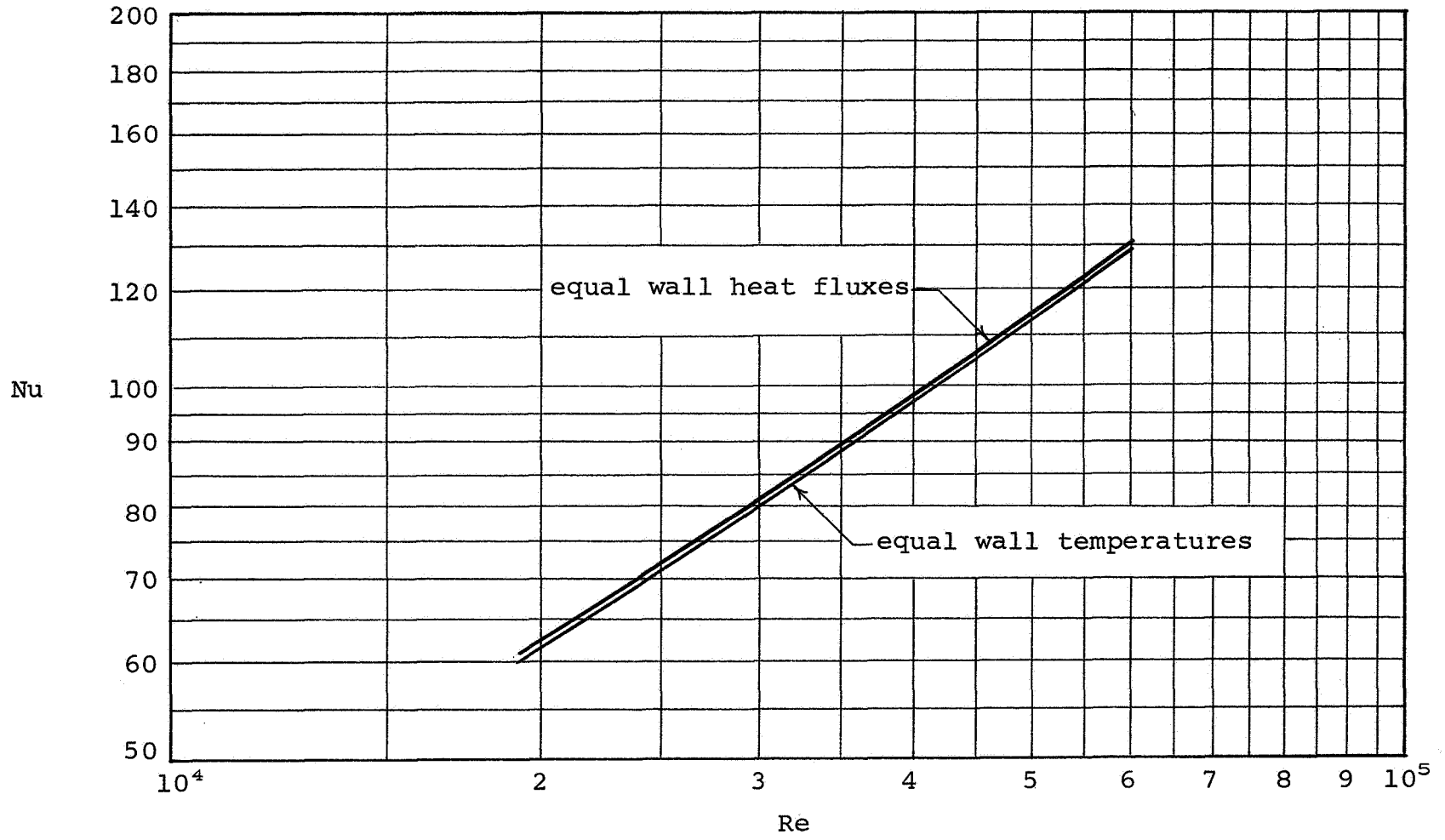

Figure IV.F.1. Turbulent Fully Developed Nusselt Numbers

IV. G. Solution of the Sturm-Liouville Equation

1. General considerations

Recall from Section IV.B.5 that the Sturm-Liouville equation resulting from the separation of variables in the energy equation is

$$\frac{d}{d\bar{y}}\left[\left(1+\frac{\epsilon_M}{\nu}\,\frac{\epsilon_H}{\epsilon_M}\,Pr\right)Y_n'\right]+\lambda_n^2\bar{u}Y_n=0 \qquad \text{(IV.G.1)}$$

For the calculation of the fundamental solutions it is necessary to solve this equation along with the appropriate boundary conditions to obtain λ_n, $Y_n(-1)$, $Y_n'(-1)$, $Y_n(1)$, $Y_n'(1)$, and C_n for the four fundamental cases. As in the laminar study, the equation is attacked in two different manners, depending on the value of the index n.

For the lower values of n the equation is solved numerically, and the eigenfunctions are determined throughout the interval between the planes. For the higher n range the WKBJ asymptotic solution is again employed, and only the values at the walls are obtained; but of course, these are sufficient for the calculation of the fundamental solutions.

Unfortunately, it was found that the asymptotic solutions are not valid at the very low values of n as they were for the laminar case. It appears as though the numerical solution must be employed for n less than about ten. Thus, since the present study was limited to calculations for $n \leq 2$ for most cases, it was not possible to use the asymptotic solution results in the calculation of the fundamental solutions, and the series converged satisfactorily only for relatively large values of $\bar{x}$, as evidenced by Figures IV.C.1, 2, 3, and 4.

2. Solution at the lower eigenvalues

Here again, the iterative procedure based on the method of Berry and de Prima is employed. The eigenvalue correction is carried out precisely as described in Section III.G.2, except that in this case the weight function appearing in the Sturm-Liouville equation and the normalization expression is the turbulent velocity profile represented by $\bar{u}(\bar{y})$. The fact that it is not available as an analytic expression is immaterial in the numerical computations.

Because the widely differing flow characteristics in various regions of the interval make attractive a numerical integration scheme employing variable step-widths (as discussed in Appendix C), Simpson's rule is not used in the normalization factor and eigenconstant calculations. Rather, the same predictor - corrector scheme used in the eigenfunction calculations is employed.

The computations were performed on a Burroughs 220 Electronic Digital Computer at the Stanford University Computation Center. Further details of the computational procedure are given in Appendix C.

The eigenvalues and pertinent combination of constants are presented in Table IV.G.1.

3. Solution at the higher eigenvalues

As with the laminar case, the WKBJ approximation may fruitfully be applied to determine asymptotic expressions for the higher eigenvalues and eigenconstants. The development proceeds along the same lines as that in Section III.G.3.

From (IV.B.21) the differential equation of interest here is

$$\frac{d}{d\bar{y}}\left(hY_n'\right) + \lambda_n^2 \bar{u} Y_n = 0 \qquad \text{(IV.G.2)}$$

where $h \triangleq 1 + \frac{\epsilon_M}{\nu}\,\frac{\epsilon_H}{\epsilon_M}\,Pr$ (IV.G.3)

Now letting $Y_n = e^{g(\bar{y})}$ (IV.G.4)

one obtains from (IV.G.2)

$$hg'' + hg'^2 + h'g' + \lambda_n^2 \bar{u} = 0 \qquad \text{(IV.G.5)}$$

Seeking a solution of the form

$$g = \lambda_n g_o + g_1 + \lambda_n^{-1} g_2 + \cdots \qquad \text{(IV.G.6)}$$

this expression is combined with its predecessor, and coefficients of like powers of λ_n are equated, yielding

$$g_o' = \pm i \sqrt{\frac{\bar{u}}{h}} \qquad \text{(IV.G.7)}$$

and

$$g_1 = -\ln\left(\sqrt{hg_o'}\right) \qquad \text{(IV.G.8)}$$

Proceeding as in Section III.G.3, there follows

$$Y_n = \frac{G\, e^{i\lambda_n \int_o^{\bar{y}} \sqrt{\frac{\bar{u}}{h}}\, d\bar{y}} + H\, e^{-i\lambda_n \int_o^{\bar{y}} \sqrt{\frac{\bar{u}}{h}}\, d\bar{y}}}{h^{\frac{1}{2}}\left(\frac{\bar{u}}{h}\right)^{\frac{1}{4}}} \qquad \text{(IV.G.9)}$$

Changing this WKBJ approximation to a more convenient form

$$Y_n = \frac{G_o \cos\left[\lambda_n \int_o^{\bar{y}} \sqrt{\frac{\bar{u}}{h}}\, d\bar{y} - \phi\right]}{h^{\frac{1}{2}}\left(\frac{\bar{u}}{h}\right)^{\frac{1}{4}}} \qquad \text{(IV.G.10)}$$

Since these expressions are going to be used near the walls of the channel, it is advantageous at this time to exploit the fact that certain simplifications occur in the behavior of $\bar{u}$ and h in these laminar sublayer regions.

Rewriting (IV.B.7) in terms of y^+ rather than $\bar{y}$, it can be seen that for small y^+

$$\frac{\epsilon_M}{\nu} = \left(\frac{K}{A^+}\right)^2 y^{+4} \qquad \text{(IV.G.11)}$$

Hence

$$\frac{\epsilon_M}{\nu} = \left(\frac{K}{A^+}\right)^2 y_o^{+4} z^4 \qquad (\text{or } \zeta^4) \qquad \text{(IV.G.12)}$$

Utilizing (IV.B.10)

$$\frac{\epsilon_M}{\nu} = \left[\left(\frac{K\, f}{A^+ 16}\right)^2 \frac{Re^4}{4}\right] z^4 \qquad (\text{or } \zeta^4) \qquad \text{(IV.G.13)}$$

Thus $\frac{\epsilon_M}{\nu}$ approaches zero near the walls. To establish a feeling for the manner in which it does so, note the curve in Figure IV.B.3. Now since $\frac{\epsilon_H}{\epsilon_M}$ and Pr are of the order of unity or less, it follows that h approaches unity at the walls.

Directing attention now to $\bar{u}$, it can be seen from (IV.B.15) that in the wall region where $\frac{\epsilon_M}{\nu} \ll 1$ and $z^2 \ll z$

$$\bar{u} = \frac{Re\ fz}{8} \quad (\text{or } \frac{Re\ f\zeta}{8}, \text{ depending on the wall}) \qquad (IV.G.14)$$

a. The inner wall

Near the inner wall $\bar{y} \to -1$. As in the laminar case the substitution $\bar{y} = -1 + z$ is made. The differential equation, (IV.G.2), thus becomes

$$\frac{d}{dz}\left(hY_n'\right) + \lambda_n^2 \bar{u} Y_n = 0$$

which, in the light of the preceding development, reduces near the walls to

$$Y_n'' + \lambda_n^2 \frac{Re\ f}{8} zY_n = 0$$

Letting

$$\delta \triangleq \sqrt{\frac{Re\ f}{8}} \qquad (IV.G.15)$$

this becomes

$$Y_n'' + \lambda_n^2 \delta^2 z Y_n = 0 \qquad (IV.G.16)$$

where $Y_n = Y_n(z)$. This is a form of Bessel's equation having the solution

$$Y_n = G_1 z^{\frac{1}{2}} J_{\frac{1}{3}}\left(\frac{2}{3}\delta\lambda_n z^{\frac{3}{2}}\right) + H_1 z^{\frac{1}{2}} J_{-\frac{1}{3}}\left(\frac{2}{3}\delta\lambda_n z^{\frac{3}{2}}\right) \qquad (IV.G.17)$$

For large λ_n this has the asymptotic form

$$Y_n = \sqrt{\frac{3}{\pi\lambda_n}}\left[\frac{G_1 \cos\left(\frac{2}{3}\delta\lambda_n z^{\frac{3}{2}} - \frac{5\pi}{12}\right) + H_1 \cos\left(\frac{2}{3}\delta\lambda_n z^{\frac{3}{2}} - \frac{\pi}{12}\right)}{\delta^{\frac{1}{2}} z^{\frac{1}{4}}}\right]$$

(IV.G.18)

Returning now to the WKBJ form (IV.G.10), note that

$$\int_0^{\bar{y}} \sqrt{\frac{\bar{u}}{\bar{h}}}\, d\bar{y} = \int_0^{-1} \sqrt{\frac{\bar{u}}{\bar{h}}}\, d\bar{y} + \int_{-1}^{\bar{y}} \sqrt{\frac{\bar{u}}{\bar{h}}}\, d\bar{y}$$

$$= -\gamma + \int_0^z \delta z^{\frac{1}{2}}\, dz$$

where

$$\gamma \triangleq - \int_0^{-1} \sqrt{\frac{\bar{u}}{\bar{h}}}\, d\bar{y} \qquad \text{(IV.G.19)}$$

Thus

$$\int_0^{\bar{y}} \sqrt{\frac{\bar{u}}{\bar{h}}}\, d\bar{y} = -\gamma + \frac{2}{3}\delta z^{\frac{3}{2}}$$

Note that γ must be evaluated numerically for each particular value of Reynolds and Prandtl numbers. The results of such an evaluation are to be found in Table IV.G.2.

The equation (IV.G.10) then becomes near the inner wall

$$Y_n = \frac{G_o \cos\left[\lambda_n \frac{2}{3}\delta z^{\frac{3}{2}} - \left(\lambda_n \gamma + \phi\right)\right]}{\delta^{\frac{1}{2}} z^{\frac{1}{4}}} \qquad \text{(IV.G.20)}$$

In order to patch the two expressions (IV.G.18) and (IV.G.20), it is apparent that

$$G_o = \sqrt{\frac{3}{\pi \lambda_n}} \qquad \text{(IV.G.21)}$$

and

$$G_1 \cos \frac{5\pi}{12} + H_1 \cos \frac{\pi}{12} = \cos\left(\gamma\lambda_n + \phi\right) \qquad \text{(IV.G.22)}$$

$$G_1 \sin \frac{5\pi}{12} + H_1 \sin \frac{\pi}{12} = \sin\left(\gamma\lambda_n + \phi\right) \qquad \text{(IV.G.23)}$$

As in the laminar case, ϕ, G_1, and H_1 will be determined later from boundary condition considerations.

b. The outer wall

Near the outer wall $\bar{y} \to 1$. Making the substitution $\bar{y} = 1 - \zeta$, the differential equation becomes

$$Y_n'' + \lambda_n^2 \delta^2 \zeta Y_n = 0$$

where $Y_n = Y_n(\zeta)$. Again, this has the solution

$$Y_n = G_2 \zeta^{\frac{1}{2}} J_{\frac{1}{3}}\left(\frac{2}{3}\delta\lambda_n \zeta^{\frac{3}{2}}\right) + H_2 \zeta^{\frac{1}{2}} J_{-\frac{1}{3}}\left(\frac{2}{3}\delta\lambda_n \zeta^{\frac{3}{2}}\right) \qquad \text{(IV.G.24)}$$

And for large λ_n

$$Y_n = \sqrt{\frac{3}{\pi\lambda_n}}\left[\frac{G_2 \cos\left(\frac{2}{3}\delta\lambda_n\zeta^{\frac{3}{2}} - \frac{5\pi}{12}\right) + H_2 \cos\left(\frac{2}{3}\delta\lambda_n\zeta^{\frac{3}{2}} - \frac{\pi}{12}\right)}{\delta^{\frac{1}{2}}\zeta^{\frac{1}{4}}}\right] \qquad \text{(IV.G.25)}$$

Here the integral appearing in (IV.G.10) becomes

$$\int_0^{\bar{y}} \sqrt{\frac{\bar{u}}{h}}\, d\bar{y} = \int_0^1 \sqrt{\frac{\bar{u}}{h}}\, d\bar{y} + \int_1^{\bar{y}} \sqrt{\frac{\bar{u}}{h}}\, d\bar{y}$$

$$= \gamma - \int_0^{\zeta} \delta\zeta^{\frac{1}{2}}\, d\zeta$$

$$= \gamma - \frac{2}{3}\delta\zeta^{\frac{3}{2}}$$

So

$$Y_n = \sqrt{\frac{3}{\pi\lambda_n}} \frac{\cos\left[\lambda_n \frac{2}{3}\delta\zeta^{\frac{3}{2}} - \left(\lambda_n\gamma - \phi\right)\right]}{\delta^{\frac{1}{2}}\zeta^{\frac{1}{4}}} \qquad \text{(IV.G.26)}$$

Then from the above and (IV.G.25)

$$G_2 \cos\frac{5\pi}{12} + H_2 \cos\frac{\pi}{12} = \cos\left(\gamma\lambda_n - \phi\right) \qquad \text{(IV.G.27)}$$

$$G_2 \sin\frac{5\pi}{12} + H_2 \sin\frac{\pi}{12} = \sin\left(\gamma\lambda_n - \phi\right) \qquad \text{(IV.G.28)}$$

Now the four sets of boundary conditions will be introduced.

c. Case one

Here the boundary conditions are

$$Y(-1) = 0$$

$$Y(1) = 0$$

Applying (IV.G.17) at the inner wall it is found that $H_1 = 0$ since

$$z^{\frac{1}{2}} J_{-\frac{1}{3}}\left(\frac{2}{3}\delta\lambda_n z^{\frac{3}{2}}\right)$$

does not approach zero with z. Then from (IV.G.22) and (IV.G.23)

$$\cos\frac{5\pi}{12}\sin\left(\gamma\lambda_n + \phi\right) - \sin\frac{5\pi}{12}\cos\left(\gamma\lambda_n + \phi\right) = 0$$

So

$$\sin\left(\gamma\lambda_n + \phi - \frac{5\pi}{12}\right) = 0 \qquad \text{(IV.G.29)}$$

This requires that

$$\gamma\lambda_n + \phi - \frac{5\pi}{12} = \pm\ n\pi, \qquad n = 0, 1, 2, \cdots \qquad \text{(IV.G.30)}$$

Without losing generality, n is taken to be zero. Then from (IV.G.23) and (IV.G.30)

$$G_1 = 1 \qquad \text{(IV.G.31)}$$

Thus, in the region near the inner wall

$$Y_n = z^{\frac{1}{2}} J_{\frac{1}{3}}\left(\frac{2}{3}\,\delta\lambda_n z^{\frac{3}{2}}\right) \qquad \text{(IV.G.32)}$$

At the outer wall $H_2 = 0$ for the same reason that $H_1 = 0$ at the inner. Thus

$$\sin\left(\gamma\lambda_n - \phi - \frac{5\pi}{12}\right) = 0 \qquad \text{(IV.G.33)}$$

Combining this result with (IV.G.30) yields

$$\lambda_n = \left(2n + \frac{5}{3}\right)\frac{\pi}{4\gamma}, \qquad n = 0, 1, 2, \cdots \qquad \text{(IV.G.34)}$$

Also

$$G_2 = (-1)^n \qquad \text{(IV.G.35)}$$

So near the outer wall

$$Y_n = (-1)^n\, \zeta^{\frac{1}{2}} J_{\frac{1}{3}}\left(\frac{2}{3}\,\delta\lambda_n \zeta^{\frac{3}{2}}\right) \qquad \text{(IV.G.36)}$$

Now the expressions needed for the determination of the asymptotic eigenconstants must be derived. From (IV.G.32)

$$\left(\frac{\partial Y_n}{\partial \bar{y}}\right)_{\bar{y}\to -1} = z^{-\frac{1}{2}} J_{\frac{1}{3}}\left(\frac{2}{3}\delta\lambda_n z^{\frac{3}{2}}\right) - \delta\lambda_n z J_{\frac{4}{3}}\left(\frac{2}{3}\delta\lambda_n z^{\frac{3}{2}}\right) \qquad \text{(IV.G.37)}$$

As $z \to 0$, $zJ_{\frac{4}{3}} \to 0$ and $z^{-\frac{1}{2}} J_{\frac{1}{3}} \to \left(\frac{\delta\lambda_n}{3}\right)^{\frac{1}{3}} \frac{1}{\Gamma\left(\frac{4}{3}\right)}$

So

$$\left(\frac{\partial Y_n}{\partial \bar{y}}\right)_{\bar{y}=-1} = \frac{(\delta/3)^{\frac{1}{3}}}{\Gamma\left(\frac{4}{3}\right)} \lambda_n^{\frac{1}{3}} \qquad \text{(IV.G.38)}$$

Noting from (IV.G.32) that at $\bar{y} = -1$, Y_n vanishes for all values of λ

$$\left(\frac{\partial Y_n}{\partial \lambda_n}\right)_{\bar{y}=-1} = 0 \qquad \text{(IV.G.39)}$$

Shifting attention to the outer wall, from (IV.G.36)

$$\left(\frac{\partial Y_n}{\partial \bar{y}}\right)_{\bar{y}\to 1} = (-1)^{n+1}\left[\zeta^{-\frac{1}{2}} J_{\frac{1}{3}}\left(\frac{2}{3}\delta\lambda_n \zeta^{\frac{3}{2}}\right) - \delta\lambda_n \zeta J_{\frac{4}{3}}\left(\frac{2}{3}\delta\lambda_n \zeta^{\frac{3}{2}}\right)\right] \qquad \text{(IV.G.40)}$$

So at the outer wall

$$\left(\frac{\partial Y_n}{\partial \bar{y}}\right)_{\bar{y}=1} = (-1)^{n+1} \frac{(\delta/3)^{\frac{1}{3}}}{\Gamma\left(\frac{4}{3}\right)} \lambda_n^{\frac{1}{3}} \qquad \text{(IV.G.41)}$$

Note that at this wall $Y_n = 0$ only for $\lambda = \lambda_n$, so $\frac{\partial Y_n}{\partial \lambda_n}$ must be computed from (IV.G.24).

$$\left(\frac{\partial Y_n}{\partial \lambda_n}\right)_{\bar{y}\to 1} = G_2 \frac{\partial}{\partial \lambda_n}\left(\zeta^{\frac{1}{2}} J_{\frac{1}{3}}\right) + H_2 \frac{\partial}{\partial \lambda_n}\left(\zeta^{\frac{1}{2}} J_{-\frac{1}{3}}\right)$$

$$+ \zeta^{\frac{1}{2}} J_{\frac{1}{3}} \frac{\partial G_2}{\partial \lambda_n} + \zeta^{\frac{1}{2}} J_{-\frac{1}{3}} \frac{\partial H_2}{\partial \lambda_n}$$

The first three terms vanish as $\zeta \to 0$. Then since

$$H_2 = \frac{\sin\left(\gamma\lambda_n - \phi - \frac{5\pi}{12}\right)}{\sin\left(-\frac{\pi}{3}\right)}$$

(from (IV.G.27) and (IV.G.28)),

$$\frac{\partial H_2}{\partial \lambda_n} = (-1)^{n+1} \frac{4\gamma}{\sqrt{3}} \qquad \text{(IV.G.42)}$$

So

$$\left(\frac{\partial Y_n}{\partial \lambda_n}\right)_{\bar{y}=1} = (-1)^{n+1} \frac{4\gamma}{3^{\frac{1}{6}}\delta^{\frac{1}{3}}\,\Gamma\left(\frac{2}{3}\right)} \lambda_n^{-\frac{1}{3}} \qquad \text{(IV.G.43)}$$

Inserting the above expressions into (A.9) yields

$$C_n = (-1)^{n+1} \frac{3^{\frac{1}{6}}\delta^{\frac{1}{3}}\,\Gamma\left(\frac{2}{3}\right)}{2\gamma} \lambda_n^{-\frac{2}{3}}$$

Also

$$C_n Y_n'(-1) = (-1)^{n+1} \frac{\delta^{\frac{2}{3}}}{3^{\frac{1}{6}} 2\gamma} \frac{\Gamma\left(\frac{2}{3}\right)}{\Gamma\left(\frac{4}{3}\right)} \lambda_n^{-\frac{1}{3}}$$

$$= (-1)^{n+1}\ 0.63134\ \gamma^{-1}\delta^{\frac{2}{3}} \lambda_n^{-\frac{1}{3}} \qquad \text{(IV.G.44)}$$

and

$$C_n Y_n'(1) = \frac{\delta^{\frac{2}{3}}}{3^{\frac{1}{6}} 2\gamma} \frac{\Gamma\left(\frac{2}{3}\right)}{\Gamma\left(\frac{4}{3}\right)} \lambda_n^{-\frac{1}{3}}$$

$$= 0.63134\ \gamma^{-1}\delta^{\frac{2}{3}}\lambda_n^{-\frac{1}{3}} \qquad \text{(IV.G.45)}$$

d. Case two

Here the boundary conditions are

$$Y_n'(-1) = 0$$

$$Y_n'(1) = 0$$

Differentiation of (IV.G.17) gives

$$\left(\frac{\partial Y_n}{\partial \bar{y}}\right)_{\bar{y}\to -1} = G_1\ \delta\lambda_n z J_{-\frac{2}{3}}\left(\frac{2}{3}\delta\lambda_n z^{\frac{3}{2}}\right) - H_1\ \delta\lambda_n z J_{\frac{2}{3}}\left(\frac{2}{3}\delta\lambda_n z^{\frac{3}{2}}\right)$$

(IV.G.46)

To satisfy the inner wall boundary condition

$$G_1 = 0$$

Then from (IV.G.22) and (IV.G.23)

$$\sin\left(\gamma\lambda_n + \phi - \frac{\pi}{12}\right) = 0$$

from which

$$\phi = \frac{\pi}{12} - \gamma\lambda_n \pm n\pi, \qquad n = 0, 1, 2, \cdots \qquad \text{(IV.G.47)}$$

Again n is set equal to zero. It follows that

$$H_1 = 1 \tag{IV.G.48}$$

So near the inner wall

$$Y_n = z^{\frac{1}{2}} J_{-\frac{1}{3}}\left(\frac{2}{3}\delta\lambda_n z^{\frac{3}{2}}\right) \tag{IV.G.49}$$

A similar condition exists at the outer wall, resulting in

$$\sin\left(\gamma\lambda_n - \phi - \frac{\pi}{12}\right) = 0$$

Hence

$$\lambda_n = \left(2n + \frac{1}{3}\right)\frac{\pi}{4\gamma}, \qquad n = 0, 1, 2, \cdots \tag{IV.G.50}$$

As before, this result leads to

$$H_2 = (-1)^n \tag{IV.G.51}$$

So near the outer wall

$$Y_n = (-1)^n \zeta^{\frac{1}{2}} J_{-\frac{1}{3}}\left(\frac{2}{3}\delta\lambda_n \zeta^{\frac{3}{2}}\right) \tag{IV.G.52}$$

In order to determine the expression for the eigenconstants, $\frac{\partial}{\partial\bar{y}}\left(\frac{\partial Y_n}{\partial\lambda_n}\right)$ must be evaluated at both walls. Differentiating (IV.G.49) yields

$$\frac{\partial}{\partial\bar{y}}\left(\frac{\partial Y_n}{\partial\lambda_n}\right)_{\bar{y}\to -1} = -\frac{5}{3}\delta z J_{\frac{2}{3}}\left(\frac{2}{3}\delta\lambda_n z^{\frac{3}{2}}\right) + \frac{2}{3}\delta^2\lambda_n z^{\frac{5}{2}} J_{\frac{5}{3}}\left(\frac{2}{3}\delta\lambda_n z^{\frac{3}{2}}\right) \tag{IV.G.53}$$

At $z = 0$ both of these terms vanish, so

$$\frac{\partial}{\partial \bar{y}}\left(\frac{\partial Y_n}{\partial \lambda_n}\right)_{\bar{y}=-1} = 0$$

Near the outer wall G_2 is a function of λ; thus

$$\frac{\partial}{\partial \bar{y}}\left(\frac{\partial Y_n}{\partial \lambda_n}\right)_{\bar{y}\to 1} = -\left(\frac{dG_2}{d\lambda_n}\right)\left\{\frac{d}{d\zeta}\left[\zeta^{\frac{1}{2}} J_{\frac{1}{3}}\left(\frac{2}{3}\,\delta\lambda_n \zeta^{\frac{3}{2}}\right)\right]\right\}$$

Now since

$$G_2 = \frac{\sin\left(\frac{\pi}{12} - \gamma\lambda_n + \phi\right)}{\sin\left(-\frac{\pi}{3}\right)} \qquad \text{(IV.G.54)}$$

it follows that

$$\frac{dG_2}{d\lambda_n} = (-1)^n \frac{4\gamma}{\sqrt{3}} \qquad \text{(IV.G.55)}$$

Thus, at the outer wall

$$\frac{\partial}{\partial \bar{y}}\left(\frac{\partial Y_n}{\partial \lambda_n}\right)_{\bar{y}=1} = (-1)^{n+1} \frac{4\gamma\delta^{\frac{1}{3}}}{3^{\frac{5}{6}}\,\Gamma\left(\frac{4}{3}\right)}\,\lambda_n^{\frac{1}{3}} \qquad \text{(IV.G.56)}$$

Now from (IV.G.49) and (IV.G.52)

$$Y_n(-1) = \frac{3^{\frac{1}{3}}}{\delta^{\frac{1}{3}}\,\Gamma\left(\frac{2}{3}\right)}\,\lambda_n^{-\frac{1}{3}} \qquad \text{(IV.G.57)}$$

$$Y_n(1) = (-1)^n \frac{3^{\frac{1}{3}}}{\delta^{\frac{1}{3}}\,\Gamma\left(\frac{2}{3}\right)}\,\lambda_n^{-\frac{1}{3}} \qquad \text{(IV.G.58)}$$

Thus employing (A.10) yields

$$C_n = (-1)^{n+1} \frac{3^{\frac{5}{6}}}{8\gamma\delta^{\frac{1}{3}}} \Gamma\left(\frac{4}{3}\right) \lambda_n^{-\frac{4}{3}}$$

Also

$$C_n Y_n(-1) = (-1)^{n+1} \frac{3^{\frac{7}{6}}}{8\gamma\delta^{\frac{2}{3}}} \frac{\Gamma\left(\frac{4}{3}\right)}{\Gamma\left(\frac{2}{3}\right)} \lambda_n^{-\frac{5}{3}}$$

$$= (-1)^{n+1} \; 0.29699 \; \gamma^{-1}\delta^{-\frac{2}{3}} \lambda_n^{-\frac{5}{3}} \qquad \text{(IV.G.59)}$$

and

$$C_n Y_n(-1) = - \frac{3^{\frac{7}{6}}}{8\gamma\delta^{\frac{2}{3}}} \frac{\Gamma\left(\frac{4}{3}\right)}{\Gamma\left(\frac{2}{3}\right)} \lambda_n^{-\frac{5}{3}}$$

$$= - \; 0.29699 \; \gamma^{-1}\delta^{-\frac{2}{3}} \lambda_n^{-\frac{5}{3}} \qquad \text{(IV.G.60)}$$

e. Case three

Here the boundary conditions are

$$Y'(-1) = 0$$

$$Y(1) = 0$$

Proceeding as before it is found that at the inner wall

$$G_1 = 0$$

$$\phi = \frac{\pi}{12} - \gamma\lambda_n$$

$$H_1 = 1$$

Thus

$$Y_n = z^{\frac{1}{2}} J_{-\frac{1}{3}}\left(\frac{2}{3}\,\delta\lambda_n z^{\frac{3}{2}}\right) \qquad \text{(IV.G.61)}$$

The conditions at the outer wall lead to

$$\sin\left(\gamma\lambda_n - \phi - \frac{5\pi}{12}\right) = 0$$

So

$$\lambda_n = (2n + 1)\,\frac{\pi}{4\gamma}\,, \qquad n = 0,\ 1,\ 2,\ \cdots \qquad \text{(IV.G.62)}$$

For the region near the outer wall it is found that

$$Y_n = (-1)^n\,\zeta^{\frac{1}{2}} J_{\frac{1}{3}}\left(\frac{2}{3}\,\delta\lambda_n\zeta^{\frac{3}{2}}\right) \qquad \text{(IV.G.63)}$$

Now, $Y_n'(1)$ is given by (IV.G.41), $Y_n(-1)$ by (IV.G.57), and $\left(\frac{\partial Y_n}{\partial\lambda_n}\right)_{\bar{y}=1}$ by (IV.G.43); thus from (A.11) there results

$$C_n = (-1)^{n+1}\,\frac{3^{\frac{1}{6}}\delta^{\frac{1}{3}}}{2\gamma}\,\Gamma\left(\frac{2}{3}\right)\lambda_n^{-\frac{2}{3}}$$

Also

$$C_n Y_n(-1) = (-1)^{n+1}\,\frac{3^{\frac{1}{2}}}{2\gamma}\,\lambda_n^{-1}$$

$$= (-1)^{n+1}\ 0.86603\ \gamma^{-1}\lambda_n^{-1} \qquad \text{(IV.G.64)}$$

and

$$C_n Y_n'(1) = \frac{\delta^{\frac{2}{3}}}{2\gamma 3^{\frac{1}{6}}} \frac{\Gamma\left(\frac{2}{3}\right)}{\Gamma\left(\frac{4}{3}\right)} \lambda_n^{-\frac{1}{3}}$$

$$= 0.63134\ \delta^{\frac{2}{3}} \gamma^{-1} \lambda_n^{-\frac{1}{3}} \qquad \text{(IV.G.65)}$$

f. Case four

Here the boundary conditions are

$$Y(-1) = 0$$

$$Y'(1) = 0$$

At the inner wall it is found that

$$H_1 = 0$$

$$\phi = \frac{5\pi}{12} - \gamma\lambda_n$$

$$G_1 = 1$$

Hence

$$Y_n = z^{\frac{1}{2}} J_{\frac{1}{3}}\left(\frac{2}{3}\,\delta\lambda_n z^{\frac{3}{2}}\right) \qquad \text{(IV.G.66)}$$

From the conditions at the outer wall

$$\sin\left(\gamma\lambda_n - \phi - \frac{\pi}{12}\right) = 0$$

So

$$\lambda_n = (2n + 1)\,\frac{\pi}{4\gamma}, \qquad n = 0, 1, 2, \cdots \qquad \text{(IV.G.67)}$$

In the region near the outer wall there obtains

$$Y_n = (-1)^n \zeta^{\frac{1}{2}} J_{-\frac{1}{3}}\left(\frac{2}{3}\delta\lambda_n\zeta^{\frac{3}{2}}\right) \qquad \text{(IV.G.68)}$$

Now, $Y_n'(-1)$ is given by (IV.G.38), $Y_n(1)$ by (IV.G.58), and $\frac{\partial}{\partial\bar{y}}\left(\frac{\partial Y_n}{\partial\lambda_n}\right)_{\bar{y}=1}$ by (IV.G.56); so (A.12) yields

$$C_n = (-1)^{n+1} \frac{3^{\frac{5}{6}}}{8\gamma\delta^{\frac{1}{3}}} \Gamma\left(\frac{4}{3}\right) \lambda_n^{-\frac{4}{3}}$$

Also

$$C_n Y_n'(-1) = (-1)^{n+1} \frac{3^{\frac{1}{2}}}{8\gamma} \lambda_n^{-1}$$

$$= (-1)^{n+1} \; 0.21651 \; \gamma^{-1}\lambda_n^{-1} \qquad \text{(IV.G.69)}$$

and

$$C_n Y_n(1) = -\frac{3^{\frac{7}{6}}}{8\gamma\delta^{\frac{2}{3}}} \frac{\Gamma\left(\frac{4}{3}\right)}{\Gamma\left(\frac{2}{3}\right)} \lambda_n^{-\frac{5}{3}}$$

$$= -\; 0.29699 \; \gamma^{-1}\delta^{-\frac{2}{3}}\lambda_n^{-\frac{5}{3}} \qquad \text{(IV.G.70)}$$

The numerical results of this section are presented in Table IV.G.1. The cautioning remark on page 90 in the laminar section regarding the normalization of the eigenfunctions also applies to this section.

TABLE IV.G.1

TURBULENT EIGENVALUES AND CONSTANTS FOR Pr = 0.70

Case	n	λ_n	$C_nY_n(-1)$	$C_nY_n(1)$	$C_nY_n'(-1)$	$C_nY_n'(1)$
One Re=20,000	0	3.935	0	0	-7.590	7.590
	1	9.99	0	0	3.040	3.040
	2	17.82	0	0	-1.678	1.678
	3	24.62	0	0	1.438	1.438
	4	31.5	0	0	-1.375	1.375
	⋮					
	n	$3.257\left(2n + \frac{5}{3}\right)$	0	0	$(-1)^{n+1}6.949\lambda_n^{-\frac{1}{3}}$	$6.949\lambda_n^{-\frac{1}{3}}$
One Re=30,000	0	4.48	0	0	-9.842	9.842
	1	11.28	0	0	4.041	4.041
	2	19.8	0	0	-2.194	2.194
	⋮					
	n	$3.698\left(2n + \frac{5}{3}\right)$	0	0	$(-1)^{n+1}8.592\lambda_n^{-\frac{1}{3}}$	$8.592\lambda_n^{-\frac{1}{3}}$
One Re=50,000	0	5.33	0	0	-13.98	13.98
	1	13.32	0	0	5.923	5.923
	2	23.1	0	0	-3.195	3.195
	⋮					
	n	$4.386\left(2n + \frac{5}{3}\right)$	0	0	$(-1)^{n+1}11.45\lambda_n^{-\frac{1}{3}}$	$11.45\lambda_n^{-\frac{1}{3}}$

TABLE IV.G.1 (Continued)

Case	n	λ_n	$C_nY_n(-1)$	$C_nY_n(1)$	$C_nY_n'(-1)$	$C_nY_n'(1)$
Two	1	7.916	2.472×10^{-3}	-2.472×10^{-3}	0	0
	2	15.98	-8.882×10^{-4}	-8.882×10^{-4}	0	0
	3	22.51	6.601×10^{-4}	-6.601×10^{-4}	0	0
Re=20,000	⋮					
	n	$3.257\left(2n+\frac{1}{3}\right)$	$(-1)^{n+1}0.4640\lambda_n^{-\frac{5}{3}}$	$-0.4640\lambda_n^{-\frac{5}{3}}$	0	0
Two	1	8.896	2.488×10^{-3}	-2.488×10^{-3}	0	0
	2	17.84	-8.683×10^{-4}	-8.683×10^{-4}	0	0
	3	25.4	6.090×10^{-4}	-6.090×10^{-4}	0	0
Re=30,000	⋮					
	n	$3.698\left(2n+\frac{1}{3}\right)$	$(-1)^{n+1}0.4837\lambda_n^{-\frac{5}{3}}$	$-0.4837\lambda_n^{-\frac{5}{3}}$	0	0
Two	1	10.44	2.502×10^{-3}	-2.502×10^{-3}	0	0
	2	20.79	-8.573×10^{-4}	-8.573×10^{-4}	0	0
	3	29.89	5.674×10^{-4}	-5.674×10^{-4}	0	0
Re=50,000	⋮					
	n	$4.386\left(2n+\frac{1}{3}\right)$	$(-1)^{n+1}0.5107\lambda_n^{-\frac{5}{3}}$	$-0.5107\lambda_n^{-\frac{5}{3}}$	0	0

TABLE IV.G.1 (Continued)

Case	n	λ_n	$C_nY_n(-1)$	$C_nY_n(1)$	$C_nY_n'(-1)$	$C_nY_n'(1)$
Three	0	2.502	-1.162	0	0	12.20
	1	9.03	0.2179	0	0	3.689
	2	16.9	-0.1044	0	0	1.644
Re=20,000	⋮					
	n	$3.257(2n+1)$	$(-1)^{n+1}3.591\lambda_n^{-1}$	0	0	$6.949\lambda_n^{-\frac{1}{3}}$
Three	0	2.840	-1.164	0	0	15.72
	1	10.17	0.2235	0	0	4.928
	2	18.8	-0.1029	0	0	2.204
Re=30,000	⋮					
	n	$3.698(2n+1)$	$(-1)^{n+1}4.077\lambda_n^{-1}$	0	0	$8.592\lambda_n^{-\frac{1}{3}}$
Three	0	3.374	-1.168	0	0	22.16
	1	11.98	0.2267	0	0	7.143
	2	22.0	-0.1044	0	0	3.269
Re=50,000	⋮					
	n	$4.386(2n+1)$	$(-1)^{n+1}4.837\lambda_n^{-1}$	0	0	$11.45\lambda_n^{-\frac{1}{3}}$

TABLE IV.G.1 (Concluded)

Case	n	λ_n	$C_nY_n(-1)$	$C_nY_n(1)$	$C_nY_n'(-1)$	$C_nY_n'(1)$
Four	0	2.502	0	-2.743×10^{-2}	-2.881×10^{-1}	0
	1	9.03	0	-3.269×10^{-3}	5.534×10^{-2}	0
	2	16.9	0	-1.637×10^{-3}	-2.578×10^{-2}	0
Re=20,000	⋮					
	n	$3.257(2n+1)$	0	$-0.4640\lambda_n^{-\frac{5}{3}}$	$(-1)^{n+1}0.8978\lambda_n^{-1}$	0
Four	0	2.840	0	-2.140×10^{-2}	-2.890×10^{-1}	0
	1	10.17	0	-2.541×10^{-3}	5.602×10^{-2}	0
	2	18.8	0	-1.192×10^{-3}	-2.553×10^{-2}	0
Re=30,000	⋮					
	n	$3.698(2n+1)$	0	$-0.4837\lambda_n^{-\frac{5}{3}}$	$(-1)^{n+1}1.019\lambda_n^{-1}$	0
Four	0	3.374	0	-1.530×10^{-2}	-2.904×10^{-1}	0
	1	11.98	0	-1.839×10^{-3}	5.794×10^{-2}	0
	2	22.0	0	-8.203×10^{-4}	-2.568×10^{-2}	0
Re=50,000	⋮					
	n	$4.386(2n+1)$	0	$-0.5107\lambda_n^{-\frac{5}{3}}$	$(-1)^{n+1}1.209\lambda_n^{-1}$	0

TABLE IV.G.2

TURBULENT WKBJ PARAMETERS

Pr	Re	δ	γ
0.01	20,000	4.3246	0.98610
0.01	30,000	4.9143	0.98294
0.01	50,000	5.8529	0.97488
0.70	20,000	4.3246	0.24116
0.70	30,000	4.9143	0.21240
0.70	50,000	5.8529	0.17906

V. EXPERIMENTAL WORK

As part of a continuing project in the area of non-isothermal wall heat transfer, a parallel plates test facility was constructed in the Stanford University Mechanical Engineering Laboratory. For the present study the facility was used to provide a check on the several assumptions embodied in the turbulent analysis, and to test the superposition technique. The test facility is described in Section V.A and the experimental results are discussed in Section V.B.

V. A. Description of Apparatus

1. General

The parallel planes test apparatus consists of two parallel copper plates which can be water heated (or cooled) from the backsides, a system to supply and meter air passing between the plates, a water heating system, and thermocouple circuitry for plate temperature and heat-flux measurements.

The plate spacing and air flow rate can be varied such that Reynolds numbers ranging from 500 to 100,000 can be achieved, and the plates can be heated such that the effects of asymmetric heating and longitudinal variations in wall heat flux or temperature can be studied.

2. The test section

The infinite parallel planes are approximated by two parallel vertically mounted plates, each 49.25 inches in the air flow (vertical) direction and 24 inches wide. The spacing between the plates can be varied between 0 and 6 inches by sliding them along their four supporting shafts, on which they are ball-bushing mounted; this not only allows the plates to be separated for polishing, but also provides flexibility for varying the hydrodynamic entry length and for future rectangular passage studies. Figure V.A.1 shows

the parallel plates rotated 90° to a horizontal position and spread apart for polishing.

The air is contained between the plates by two Plexiglas spacers running the length at each edge. These spacers are 0.5 inches wide and of a thickness equal to the desired plate spacing. A rectangular groove running the entire length is machined into the two faces of each to provide for a linear "O" ring seal.

A two-dimensional Plexiglas nozzle provides the transition between a large plenum chamber and the plate channel. Both plenum and nozzle are described in Section V.A.3.

Each plate is composed of 48 1- by 24-inch copper cells, each separated from its neighbors by a thermal insulator consisting of a 0.031- by 24-inch strip of 25-percent plasticized Kel-F plastic, as shown in Figure V.A.2. The thermal conductivity of this plastic was measured and found to be 0.08 Btu/hr-ft^2-°F/ft. The 24 cells forming one end of each plate can be heated (or cooled) individually to any desired temperature between ambient and 180° F by passing water through them. The 24 cells forming the other end cannot be heated, and constitute an adiabatic wall. The plates are mounted on the four supporting shafts such that the heated ends are always opposite each other, but the plates may be released from the nozzle, and their bearing-mounted supporting frame (see Fig. V.A.3) rotated 180°, so that tests may be conducted in either of two ways; in one, the air first passes through the adiabatic section so that the velocity profile becomes established before the heated section is reached (the thermal entrance length problem), and in the other the air flows from the nozzle directly into the heated section (the hydrodynamic entrance length problem). The present tests were confined to the former arrangement.

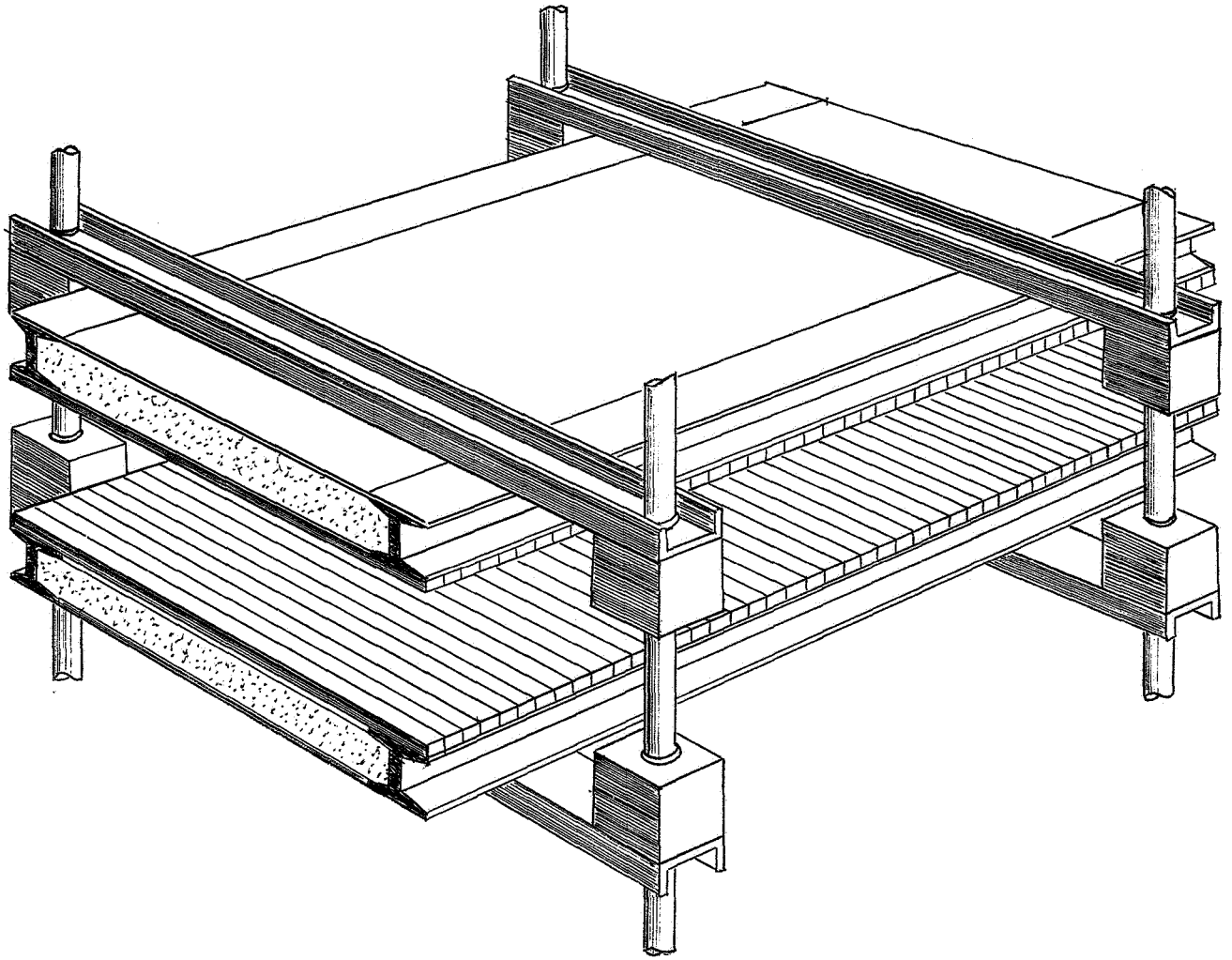

Figure V.A.1. Parallel Plates in a Horizontal Position for Polishing

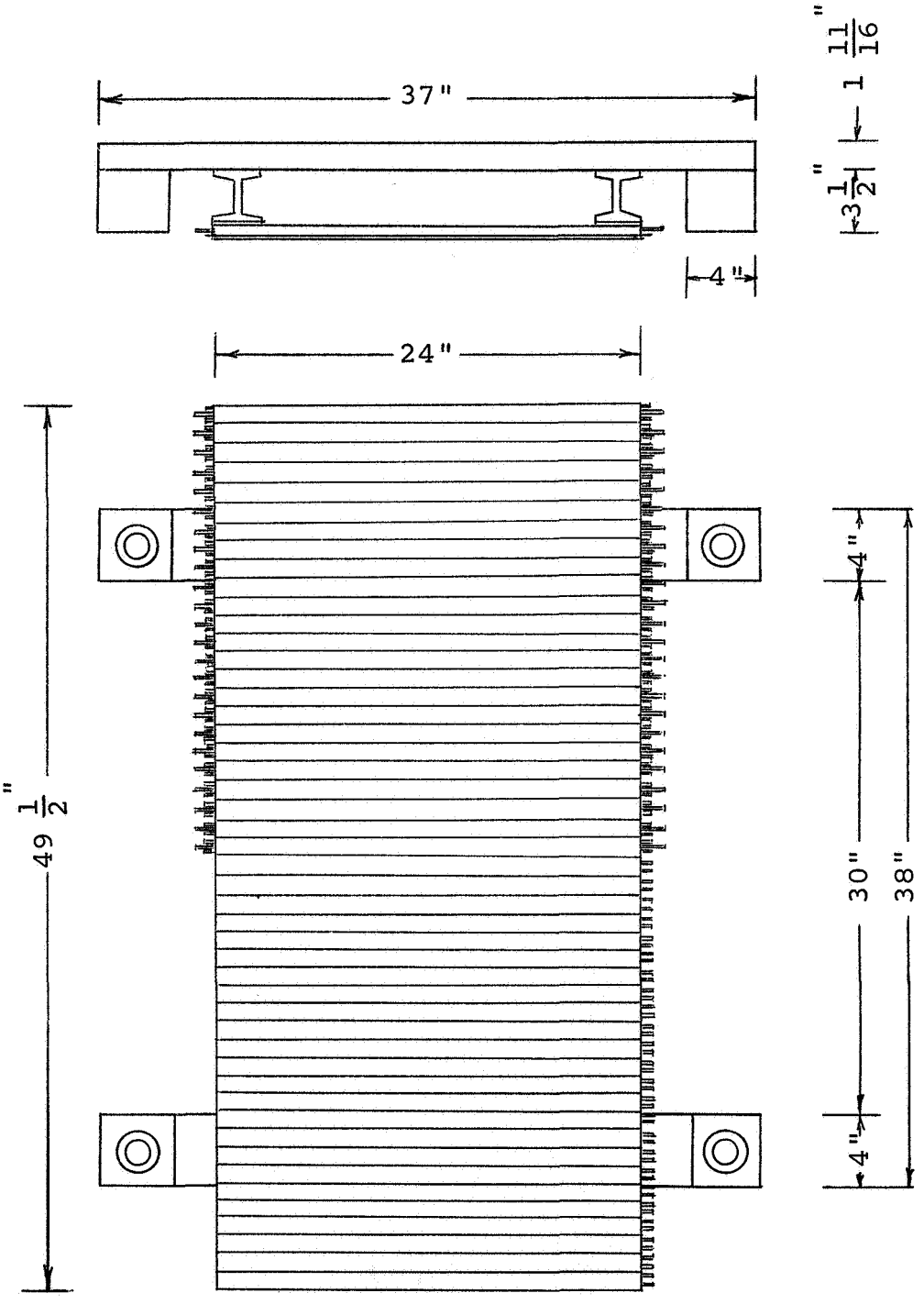

Figure V.A.2. Parallel Plate Assembly

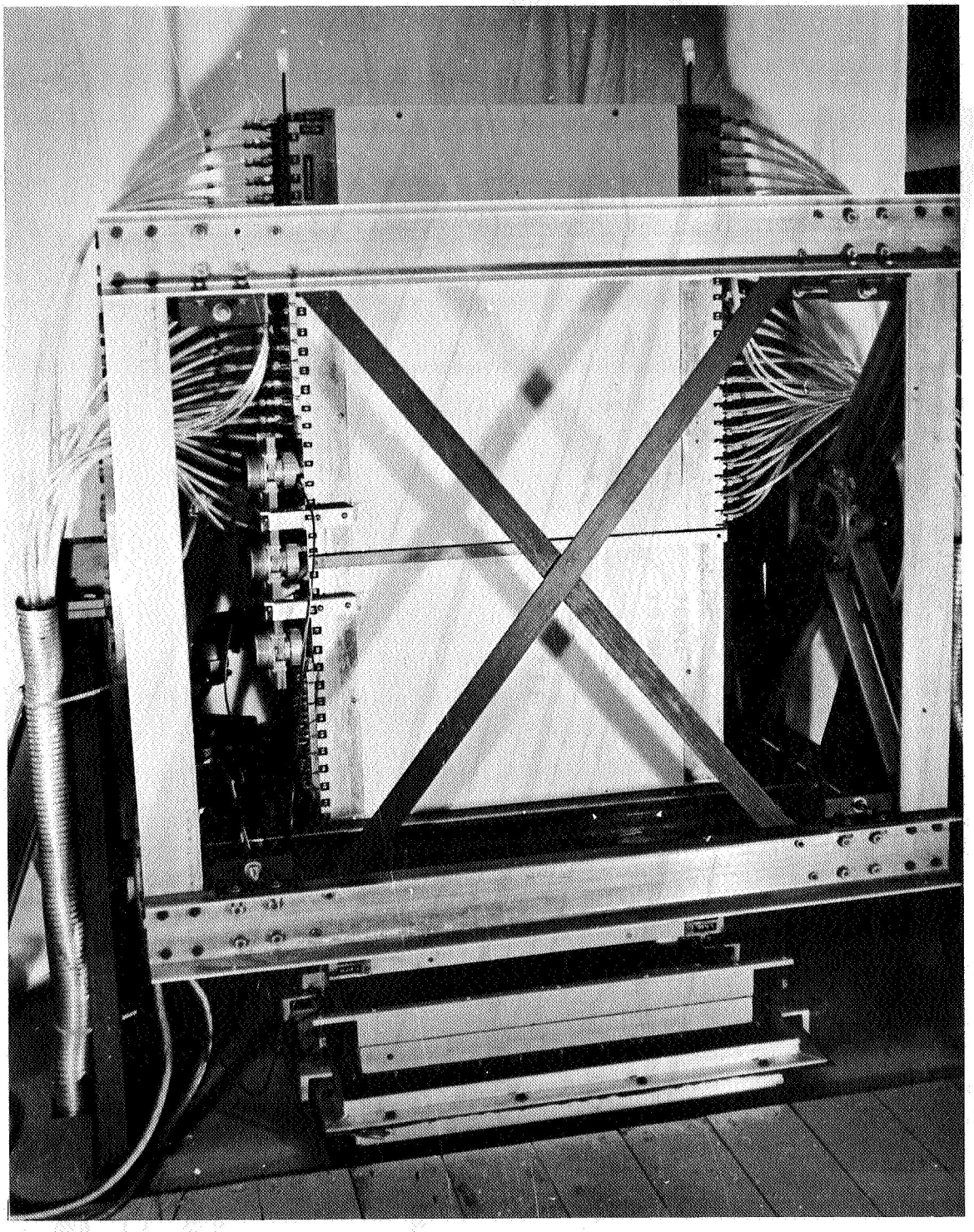

Figure V.A.3. The Test Section and Supporting Structure

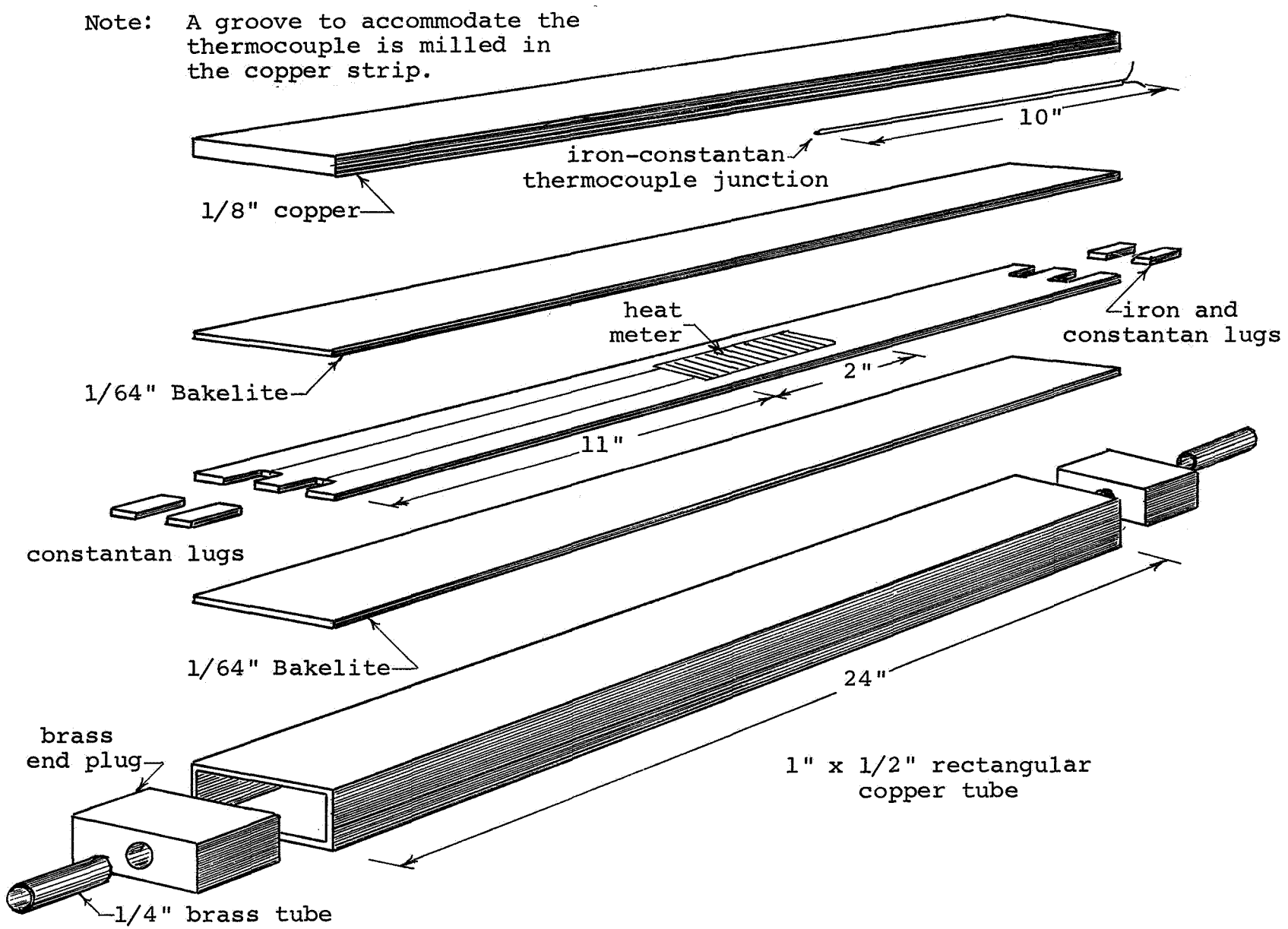

Figure V.A.4. Exploded View of a Heated Cell

Each cell is an epoxy bonded lamination of a 0.5- by 1.0-inch rectangular OFHC copper tube of 0.062-inch wall thickness, three 0.0156-inch-thick strips of Bakelite, and a 0.125-inch-thick strip of OFHC copper, as shown in Figure V.A.4. The cells are mounted so that the copper strip faces the air channel. A 30-gauge iron-constantan thermocouple is imbedded near the center of each copper strip, the lead wires being fed out to the cell end in a shallow groove milled in the internal face of the strip. Thus the plate wall temperature can be measured at 48 points along its flow length. The heated cells each have a Beckman and Whitley, Inc. thermopile type heat flow transducer mounted in the center Bakelite lamination. Since the thermal resistance network is such that essentially all the heat transferred between air and copper strip also passes through the Bakelite to (or from) the copper tubing, the heat flow transducers enable the wall heat flux to be measured at 24 points along the heated half of each plate.

During operation each copper strip is essentially isothermal, but each may be maintained at a different temperature because of the Kel-F insulation between them. The temperature levels of the heated cells are controlled by varying the temperature of water streams passing through the rectangular tube portion of them. This water is introduced to the cells through a 1/4-inch brass tube soldered in each end; the ends of the unheated cells are blanked off with brass plugs.

The back side of each plate (composed of the rectangular copper tube side of the cells) is insulated with a 3-inch-thick pad of Fiberglas. Additional insulation is packed around the plate edges during operation.

During the construction of the plates each completed bonded cell assembly was machined flat on all sides. They then were lined up on a plane table, rectangular tube side

down, and bonded together with an epoxy resin. The separating strips of Kel-F plastic were sodium etched to accept the bond. The resulting plate was then bonded to two 1/8-inch silicon rubber pads running its length, and then to two aluminum I beams, which were, in turn, bolted to two aluminum channels containing the ball bushings for shaft support. This assembly is shown in Figure V.A.2.

The resulting rigid structures were clamped to the table of a large vertical boring mill, on which the entire copper strip surface was machined flat. This suspensive process was followed by a period of hand sanding and polishing until a mirror finish was produced.

3. The air system

The air system consists of an 800 cfm. maximum flow rate, 30-inch H_2O maximum static pressure Buffalo centrifugal blower, a flow regulating valve, two parallel orifice metering sections, a screened plenum chamber, and an adjustable two-dimensional nozzle for introducing the air into the test section between the two parallel plates. After passing up between the plates the air is discharged into the laboratory. The air system is shown in schematic form in Figure V.A.5. The blower and metering section portion is shared with a companion apparatus, an annular passage, which is described by Lundberg, et al.[37]

The two metering sections with their flat plate orifices were constructed according to ASME standards. Each can be equipped with one of two orifices. The pertinent dimensions of the two alternative sections are as follows:

Duct Diameter (in.)	Orifice Diameter (in.)	$\beta = d/D$
6.367	4.225	0.664
6.367	1.910	0.300
1.498	0.824	0.550
1.498	0.375	0.250

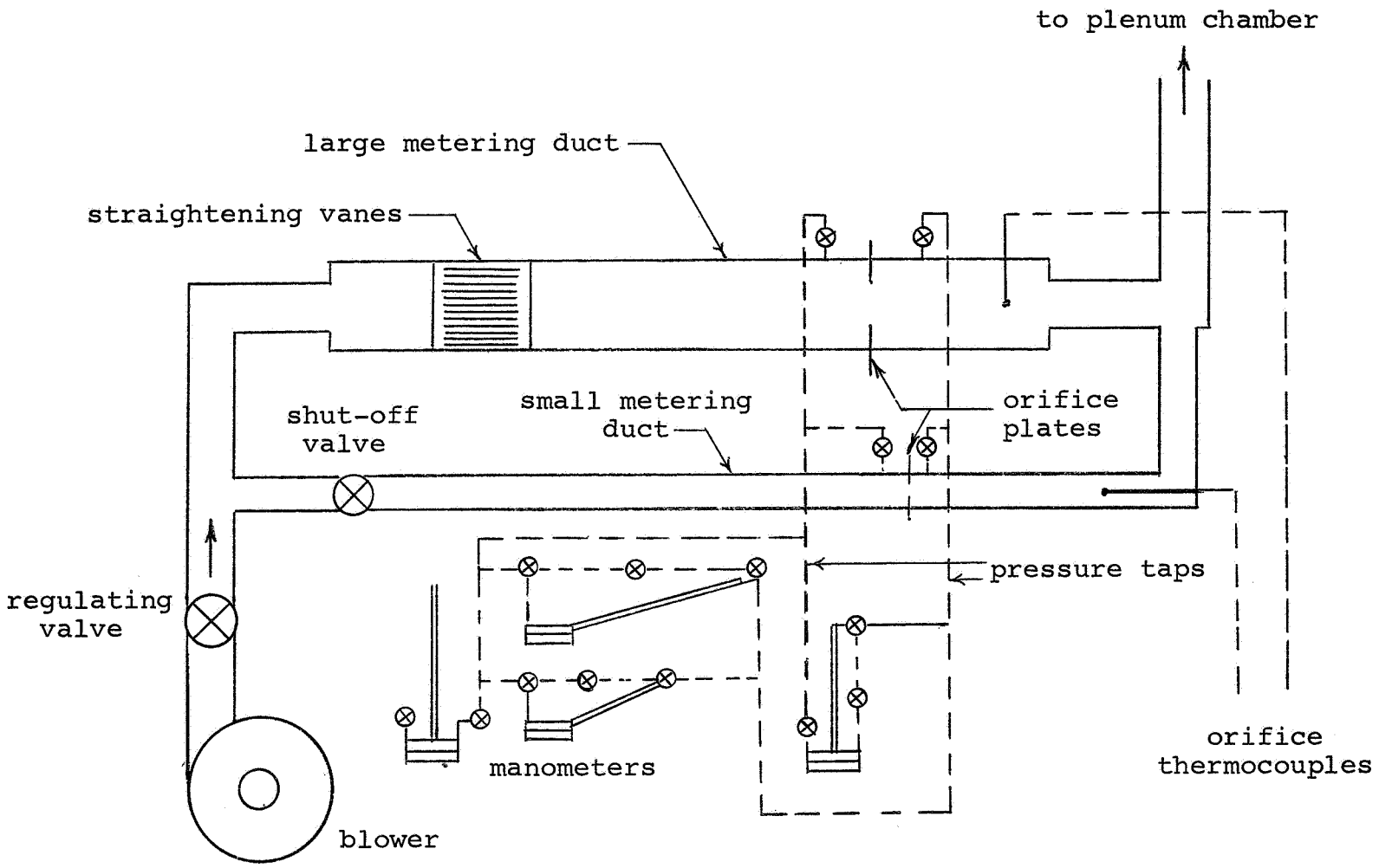

Figure V.A.5. The Air System

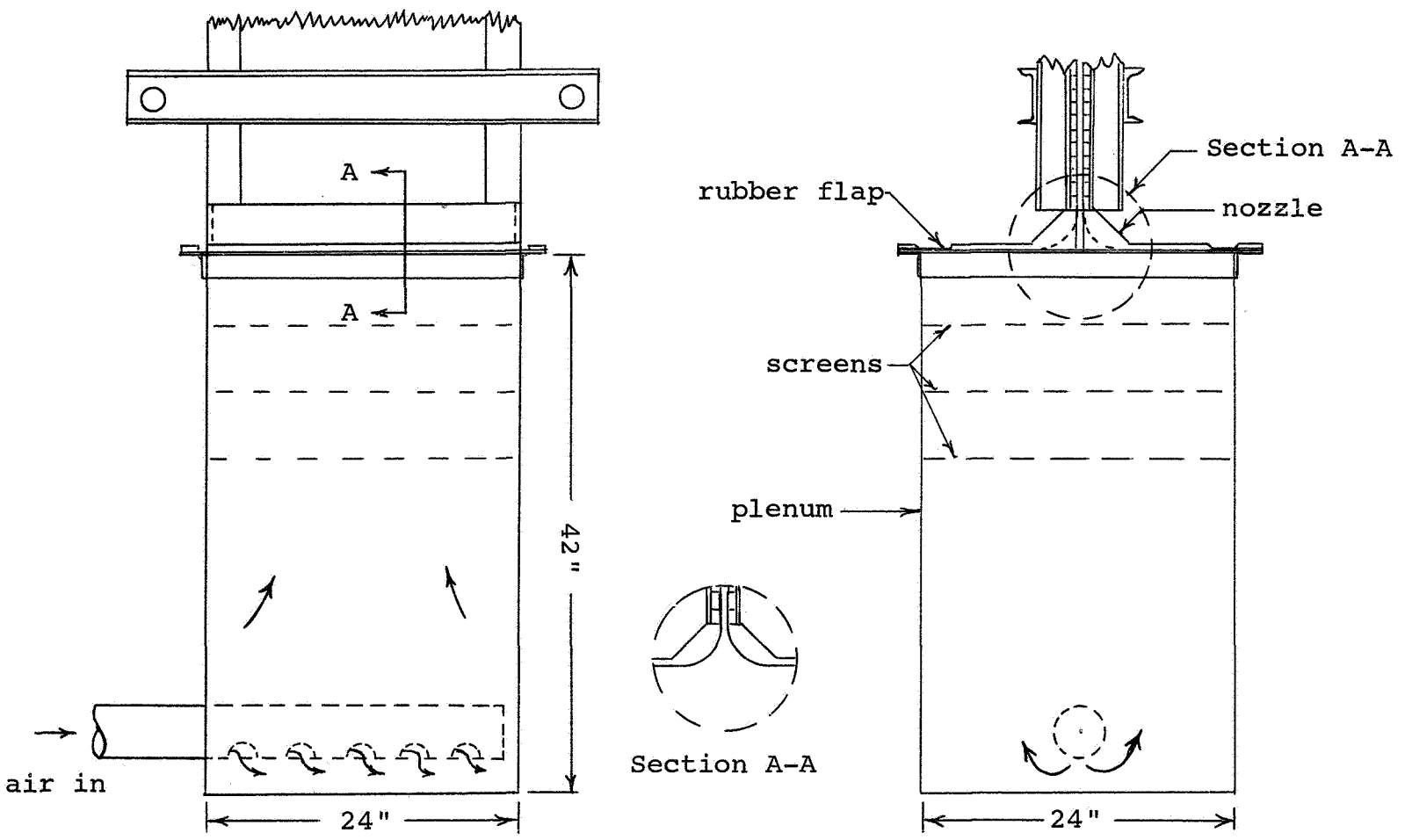

Figure V.A.6. Plenum Chamber and Nozzle Assembly

Orifice upstream static pressure is measured by a 30-inch vertical water manometer, and orifice differential pressure by one of three parallel devices, a 16-inch vertical water manometer, or an inclined oil manometer having a range of either 1 or 5 inches of water. The differential manometers were adjusted from time to time by comparison with a micro-manometer, and the entire metering system was checked out by running it in series with a laboratory portable nozzle tank with a well established calibration. A total air flow range from 1 to 750 cfm. can be measured with this metering system with a probable uncertainty of about $\pm$1 percent.

The plenum chamber and nozzle assembly is shown in Figure V.A.6. The chamber consists of a reinforced, sealed, plywood box, 24 by 24 inches, by 42 inches in the flow direction. Three screens are used to insure a uniform distribution of low turbulence air at the nozzle inlet. The two nozzle halves themselves form the top of the plenum chamber, being attached both to it and to the parallel plates.

Each nozzle half is made from a 1/2-inch plate and quarter circular cylinder of Plexiglas. The plate has a thin neoprene flap bonded around its periphery on three edges and the cylindrical nozzle piece on the fourth. During operation the flaps are clamped to the plenum chamber top, thus providing a seal. A linear "O" ring in a rectangular groove provides the seal between the top of the nozzle and the bottom edge of each parallel plate. End blocks are positioned between the nozzle halves at each end, and duct-seal putty is used to fill any remaining cracks. The entire air system was checked with soapy water for leaks before operation.

4. The water system

The heated cells of the parallel plates are heated (or cooled) by a stream of steam-heated water passing through the rectangular tubing. There are 48 such streams in the system, one for each heated cell. The heart of the system is a 48-channel temperature regulator consisting of 48 steam-water mixing sections designed to minimize vibration and hammer (see Figs. V.A.7 and V.A.8), and 48 fine-control needle valves to regulate the steam flow into each mixer and hence to regulate the water temperature leaving each mixer. The hot water is carried to the two parallel plates through 48 1/4-inch polyethylene tubes.

After passing through the heating cells of the plates the water again enters a bank of polyethylene tubes which carries it to a collector trough, into which it is ejected in 48 horizontal jets. These jets arc downward and impinge on the flat Plexiglas bottom of the trough, and, since the point of impingement is related to the flow rate in each tube, the trough serves as an effective substitute for 48 individual flow meters. The flow rate in each tube must be at least 1/2 gpm. to ensure a negligible water temperature change through the heated cells. From the collector trough, the water drains to a sewer.

On the upstream side of the temperature regulator, the cold water is supplied by a centrifugal pump. It is drawn from a 30,000-gallon sump located beneath the laboratory, and filtered before entering the mixing sections in the temperature regulator. The sump level is constantly maintained from a city water supply.

The regulator steam is supplied at 40 psig by a 45-horsepower boiler located near the test apparatus. The steam passes through a strainer and a centrifugal steam drier before being introduced to the mixing sections.

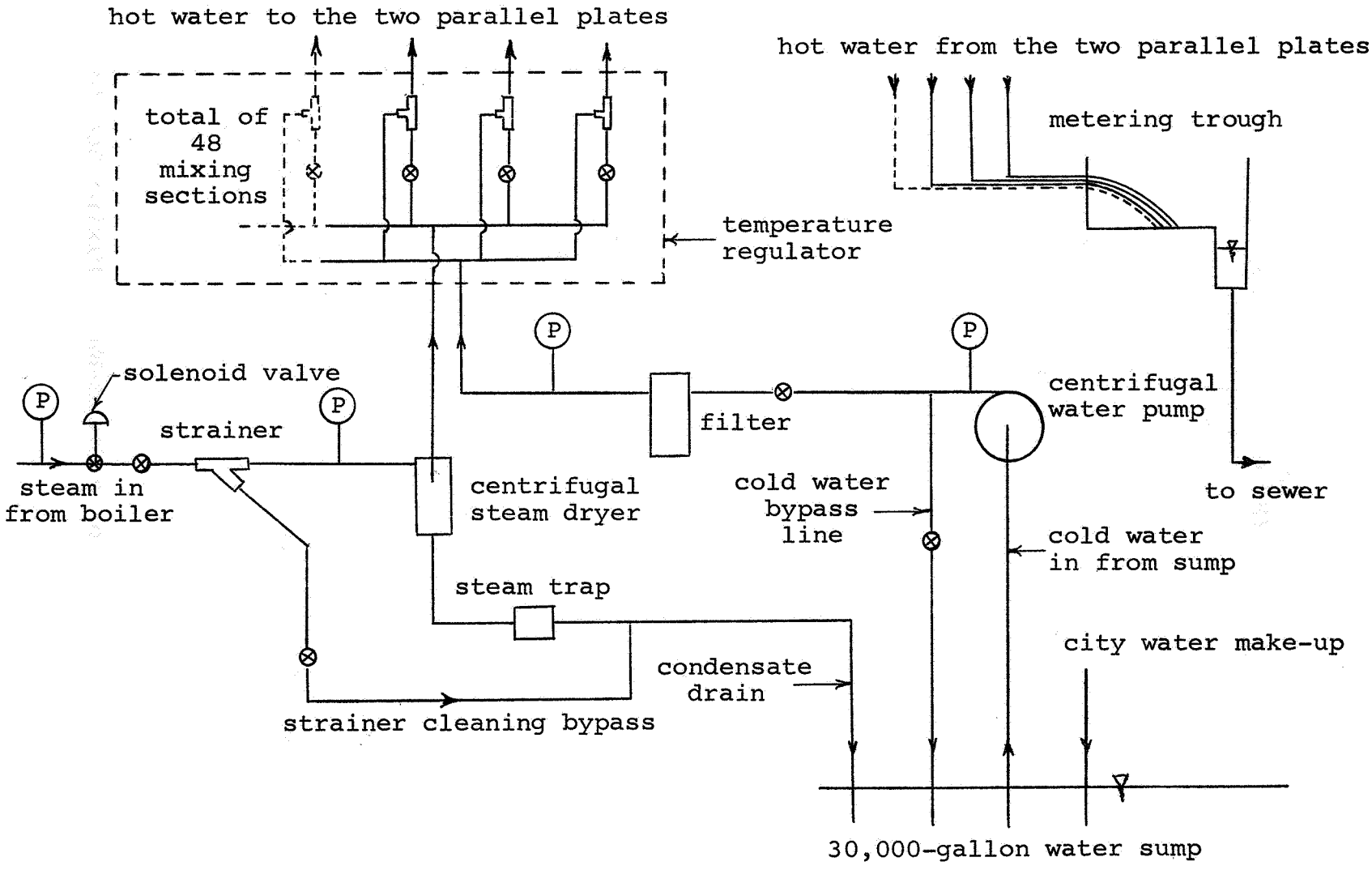

Figure V.A.7. The Steam-Water System

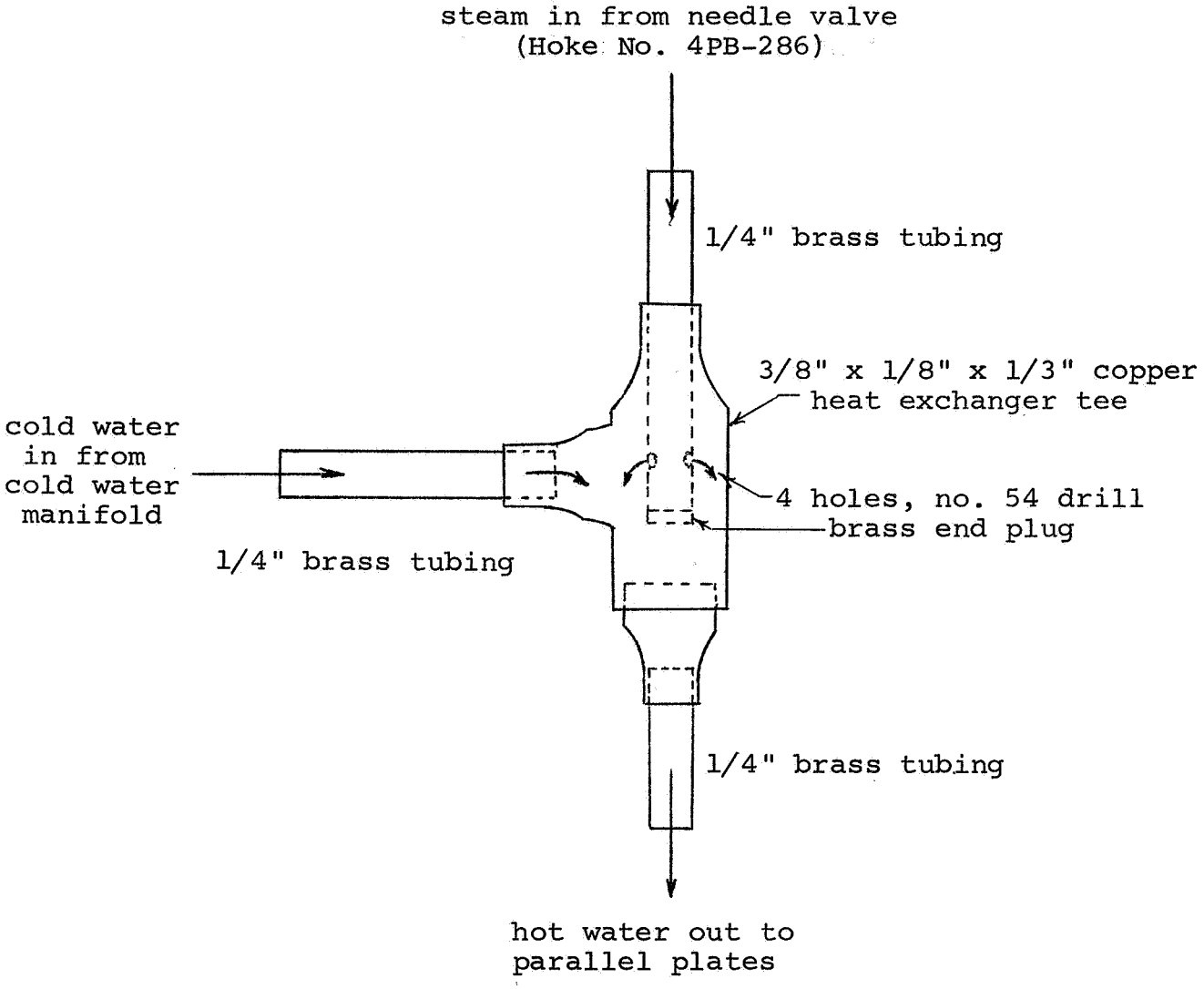

(Note: All connections are soft-soldered.)

Figure V.A.8. Detail of a Steam-Water Mixing Section

Since the epoxy resin bonds in the parallel plate structure begin to lose strength at temperatures in excess of 200° F, an automatic safety device is incorporated in the water system to insure that water (or steam) hotter than 180° F cannot reach the plates. This device consists of several thermostat switches in selected polyethylene tubes and a solenoid valve in the main steam line.

5. Electrical instrumentation

The electrical instrumentation consists of a thermocouple system to measure plate and air temperatures and a heat meter system to measure plate heat fluxes. The thermocouples used were all made from 30-gauge, glass insulated, iron-constantan wire, samples of which were calibrated against NBS thermometers and found to deviate from the standard tables by a maximum of $\pm 0.20^{\circ}$ F throughout the range of interest. Ninety-six thermocouples are used to measure plate temperatures, one being imbedded in each cell as described in Section V.A.2. Seven shielded couples are mounted in the air stream at the top of the plenum chamber to measure the inlet air temperature, and several more are used for measuring air metering section temperatures, ambient wet and dry bulb temperatures, and inlet water temperature. All thermocouples are referenced to a distilled water ice bath.

The thermocouple voltages are read with a Leeds and Northrup portable precision potentiometer. They are distributed to this instrument through a multiple selector switch arrangement shown in Figure V.A.9. Copper lead wires run from the selector switch console to isothermal zone boxes near the thermocouple installation areas, at which points they are connected to the thermocouple wires. The zone boxes for the plate thermocouples consist of multipin connectors, since it is necessary to unhook these

couples to rotate the plates or to free the selector switch console for use with the annulus apparatus. Details of the thermocouple circuit are shown in Figure V.A.10.

The wiring system for the 48 heat meters is similar to that for the plate thermocouples, except that no ice reference junction is used here since the heat meters indicate a temperature difference across a thermal resistance (the center Bakelite lamination) rather than a temperature itself. Details of the circuit are shown in Figure V.A.11.

Since the heat meter sensitivities differed somewhat, a Hewlett-Packard 412A DC VTVM was used to record their voltage outputs. It was found that the high input impedance of this instrument resulted in a negligible current flow; thus it acted essentially as a potentiometer.

All the heat meters were calibrated in place after the plates were completely constructed and mounted. This was accomplished with a nichrome ribbon heater arrangement which effected a measured heat flow through a cell into its water passage. With this procedure it is believed that the heat meter sensitivities were obtained with a probable uncertainty of ± 5 percent.

A photograph of the thermocouple and heat meter selector switch console, the manometer board, and the temperature regulator valves is presented as Figure V.A.12.

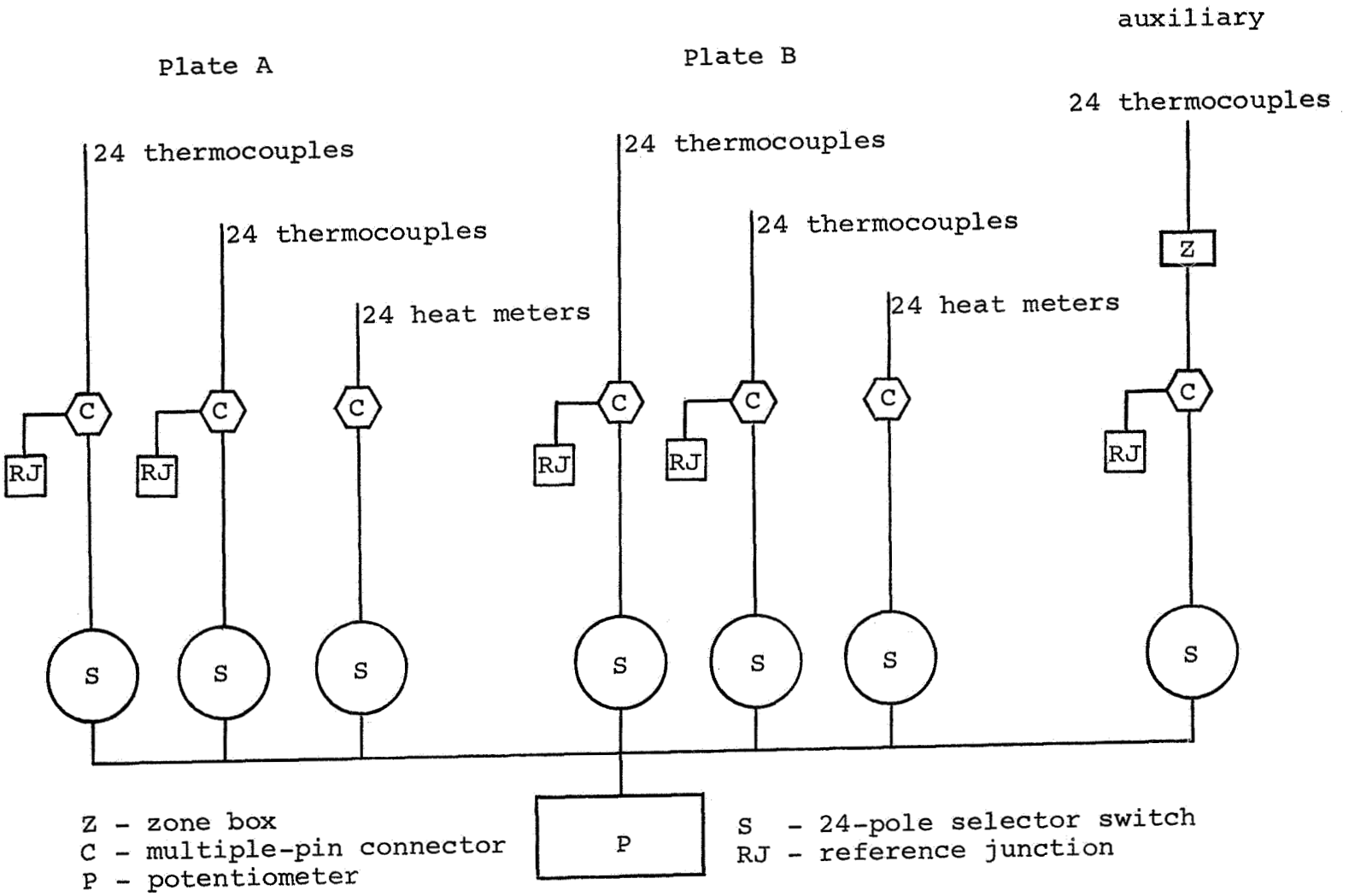

Figure V.A.9. Thermocouple and Heat Meter Selector System

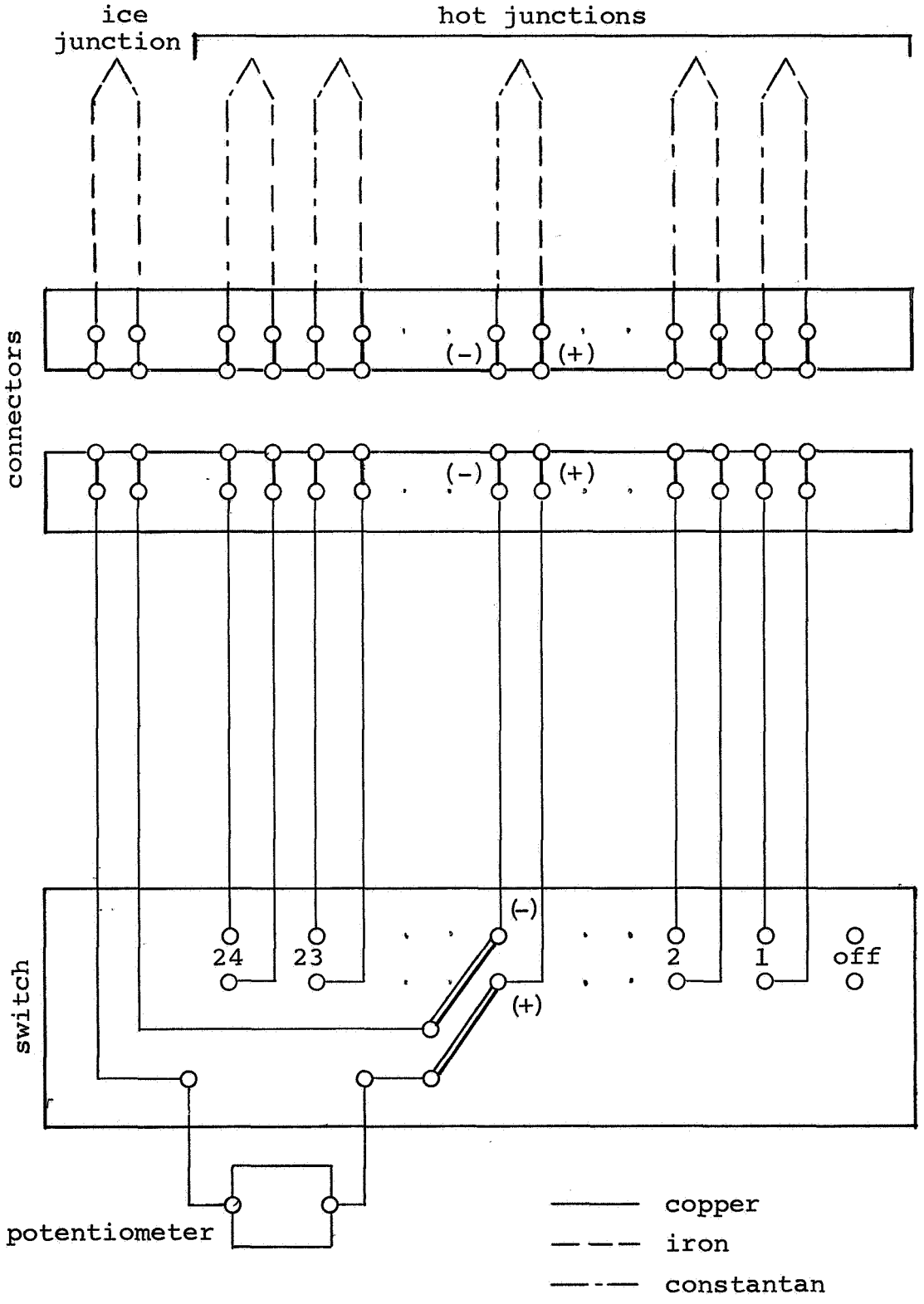

Figure V.A.10. Thermocouple Circuit

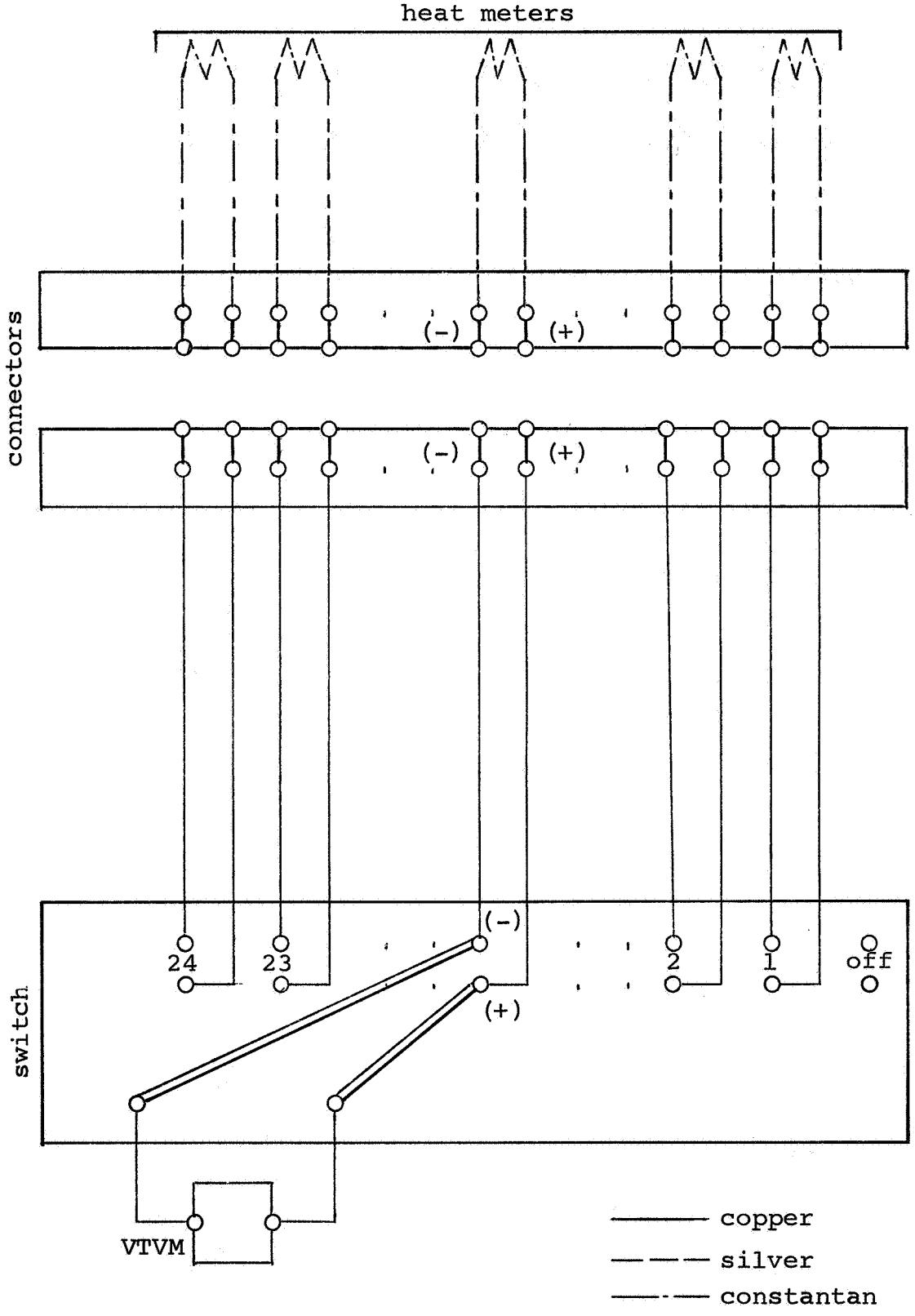

Figure V.A.11. Heat Meter Circuit

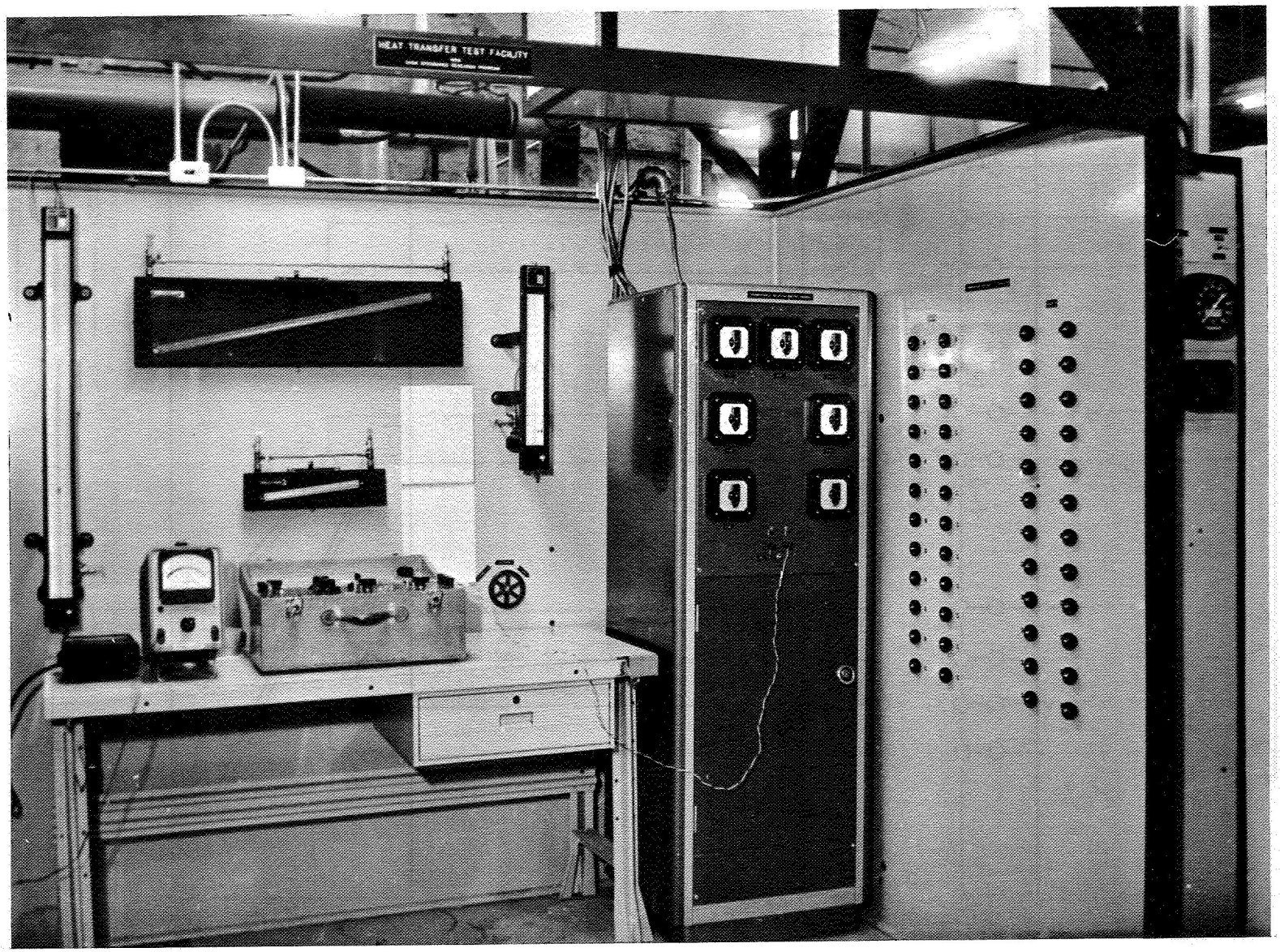

Figure V.A.12. Controls and Instrumentation

V. B. Comparison of Experimental and Theoretical Results

Several turbulent flow experimental runs were conducted at various Reynolds numbers and with several wall boundary conditions, and the resulting data are presented in Figures V.B.1-5. In all cases the plate spacing was set at 0.5 inches. In discussing the data, first some general remarks pertinent to all runs will be made, and then each run will be treated individually.

In all cases heat flux predictions resulting from the use of the fundamental solutions of the first kind are shown. Use of the solutions of the second kind was precluded by the fact that they are not known for small enough values of $\bar{x}$. In applying the fundamental solutions, the wall temperatures were approximated by steps of $\bar{x}$ length 5×10^{-5}; thus, in the cases where the wall temperature varies only slightly the comparison of theory and experiment provides a good check on the theory, but in the rapidly varying wall temperature regions errors due to the step approximation can occur.

It will be noted that wall temperatures are plotted in the negative $\bar{x}$ region; this is because heat leak near the thermal entry caused several unheated cells upstream of it to have temperatures other than the air inlet temperature, t_e, and this effect was included in the application of the theory.

By and large, the theory overpredicts the magnitude of the heat flux by about 10 percent. Since the heat flux data is felt to have an uncertainty of ±7 percent, this is a significant deviation, and, all factors considered, it is most probable that it is a result of using an eddy diffusivity ratio larger than that actually existing. The Nusselt number data of Leung[34] lends credence to this hypothesis; he finds good agreement with a theory based on a constant value of $\epsilon_H/\epsilon_M = 1.2$ outside the sublayers.

Turning now to the individual test results, Figures V.B.1 and V.B.2 present results for constant wall temperatures which bracket the inlet temperature. Here the theory predicts the general trend of the data, but overpredicts its magnitude. Figure V.B.3 treats constant wall temperatures which both lie above the inlet temperature; again, the data trend is predicted better than its magnitude.

In Figure V.B.4 the upper wall is subjected to a temperature step and then a ramp, while the lower wall temperature is uniform after the step. The comparison at the lower wall is similar to those of the preceding figures, but the upper wall comparison seems somewhat better; this is because the step approximation of the ramp tends to underpredict, or more precisely, to lag the exact prediction. It is interesting to note that at the upper wall the heat flux actually decreases for a short distance downstream of the step even though the wall temperature is increasing up the ramp.

Figure V.B.5 presents results for a more complicated step-ramp combination, and again the lag due to the step approximation is apparent. Here the heat flux downstream of the initial upper wall step does not diminish as in the previous case; this is because the step is less severe, and the ramp slope is greater.

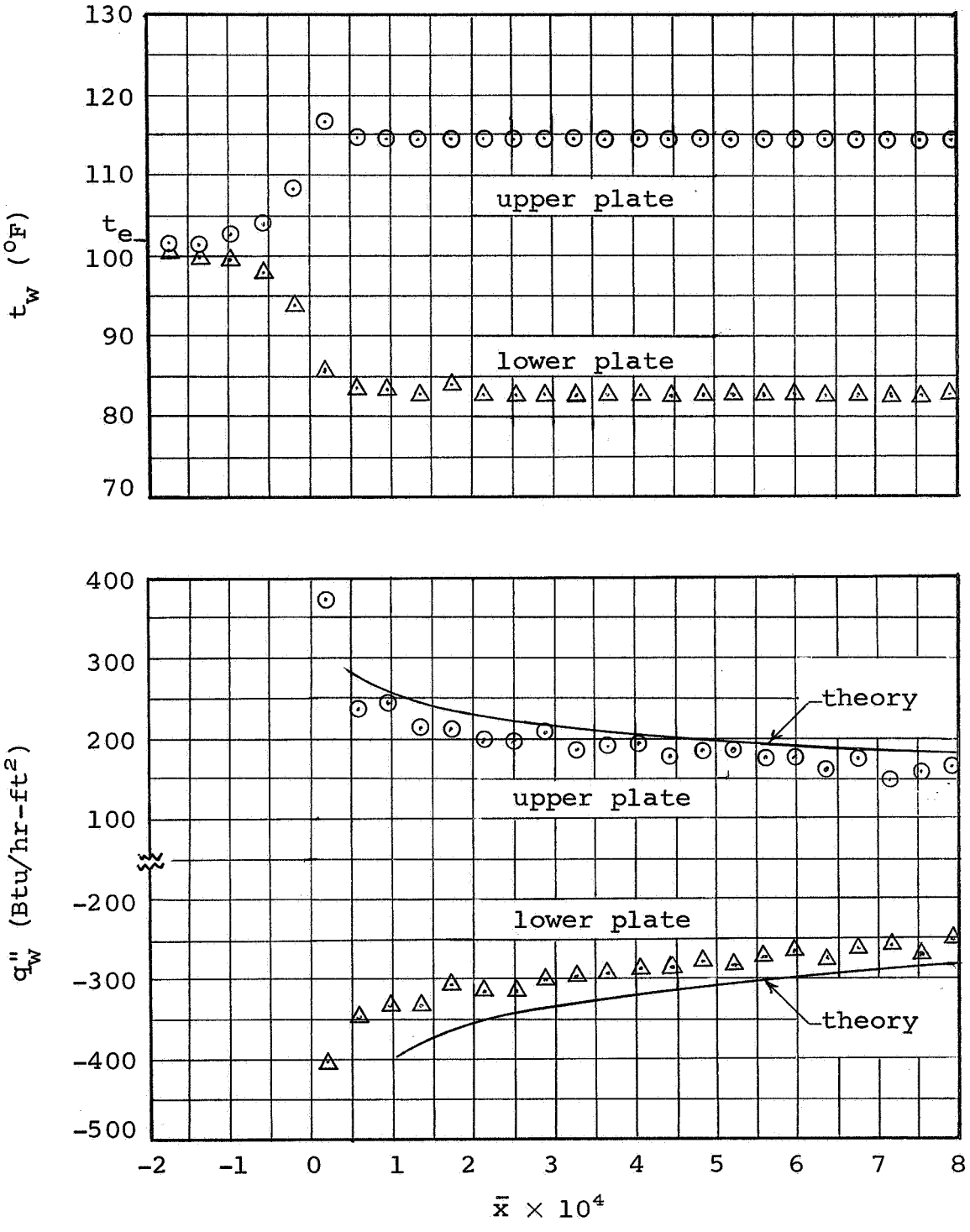

Figure V.B.1. Comparison of Experimental and Theoretical Values, Re = 39,850

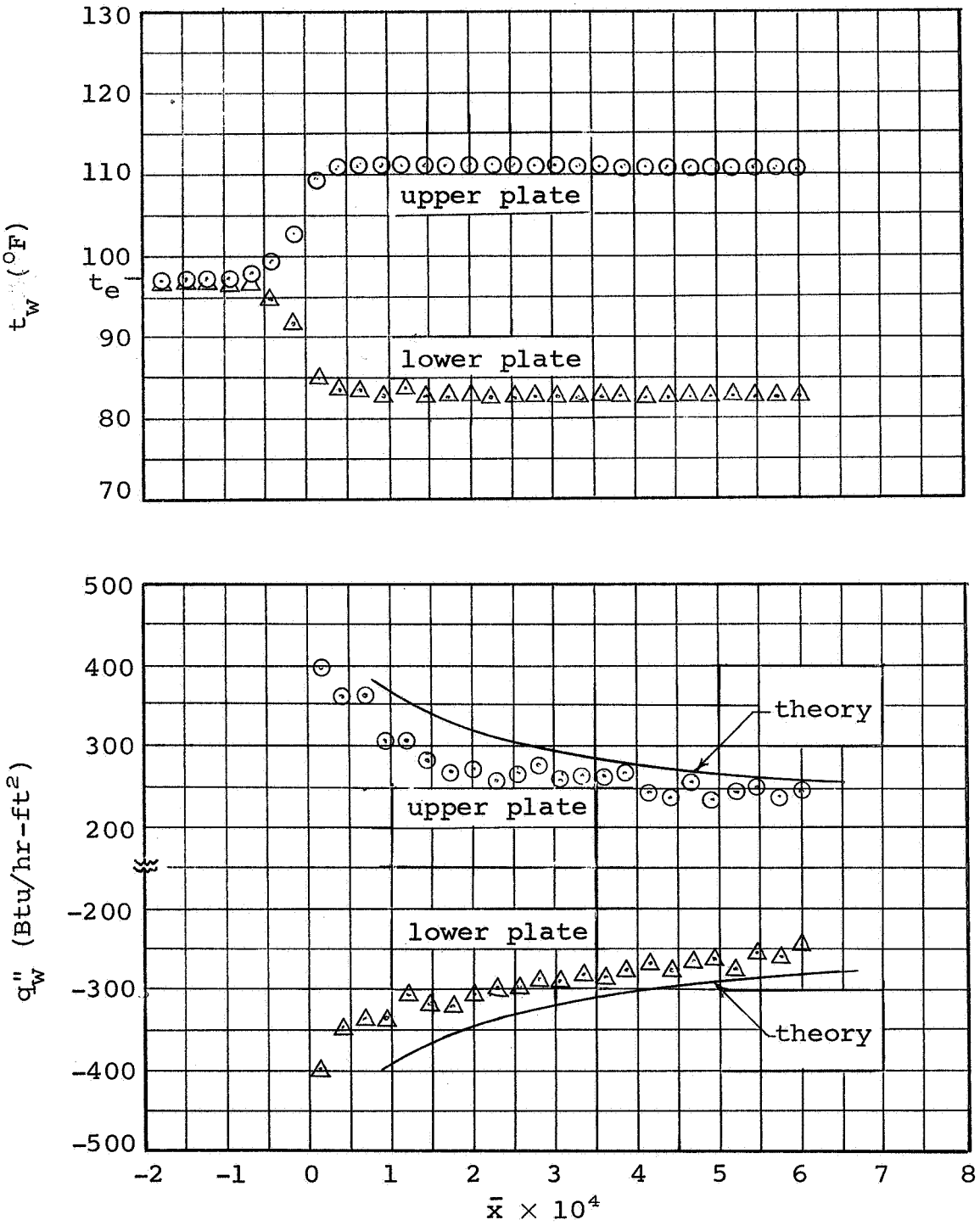

Figure V.B.2. Comparison of Experimental and Theoretical Values, Re = 57,700

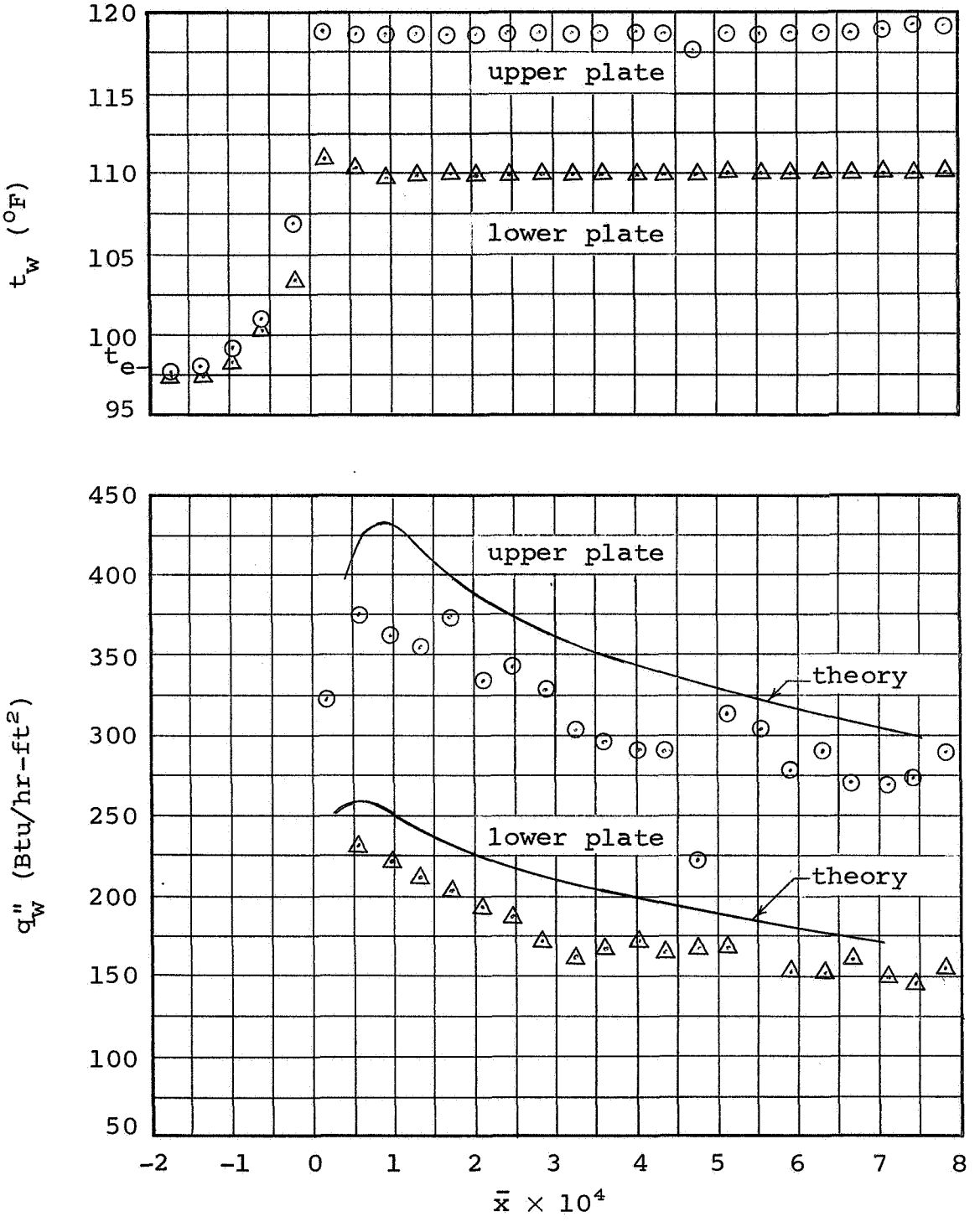

Figure V.B.3. Comparison of Experimental and Theoretical Values, Re = 40,400

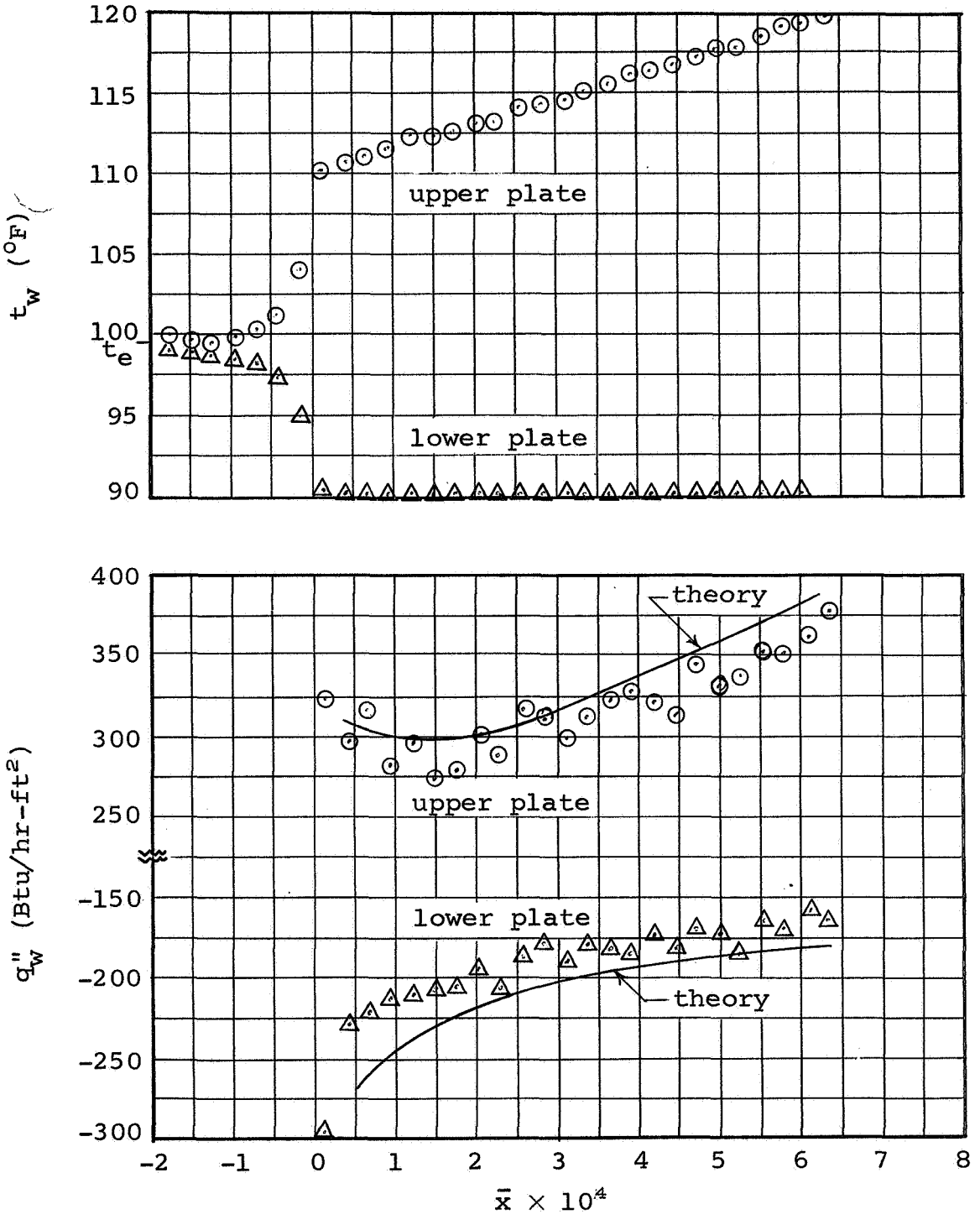

Figure V.B.4. Comparison of Experimental and Theoretical Values, Re = 57,000

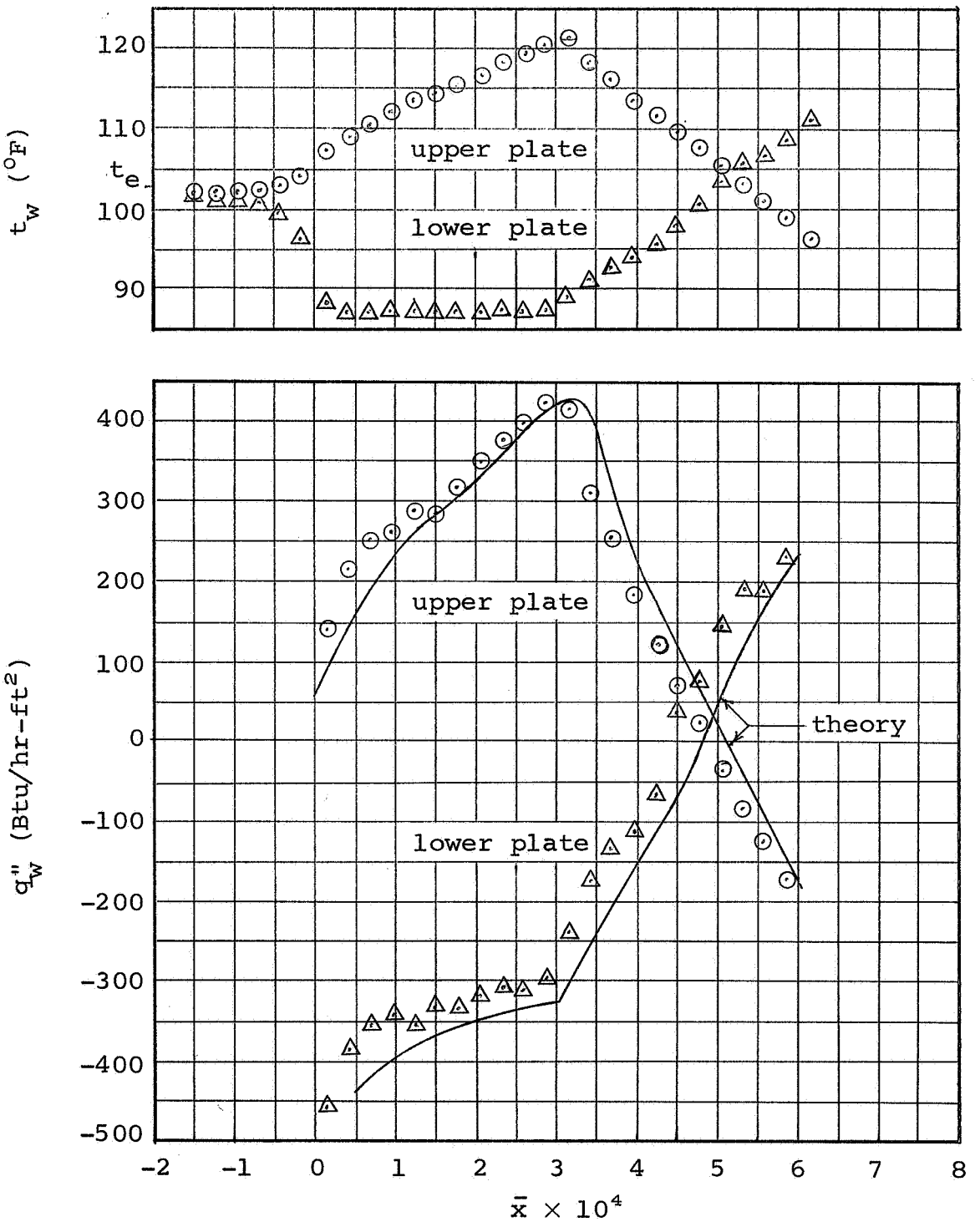

Figure V.B.5. Comparison of Experimental and Theoretical Values, Re = 56,300

VI. CONCLUSIONS

The treatment of the laminar problem in Section III is essentially complete; all wall boundary conditions of interest are discussed (with the exception of specified wall resistance and wall internal temperature), the solutions are presented with an accuracy quite sufficient for practical purposes, and the method of use of the solutions is presented. Experimental verification of the laminar theory is not included herein, but this can be found in the work of Lundberg, et al.[37], whose treatment of the circular annular passage parallels that of the present study.

As opposed to the laminar work, the treatment of the turbulent case is really little more than an introduction to the general problem, and the development of a method of approach. It cannot be considered complete in that it applies to only one Prandtl number over a limited Reynolds number range, and, as discussed in Section V.B, there is some doubt as to the suitability of the eddy diffusivity ratio employed. Hence, it is to be hoped that in the future additional fundamental diffusivity studies will be conducted, and that the results will be applied to the problem herein for a wide range of Reynolds and Prandtl numbers.

Looking back over the fundamental solution results, it is of interest to note several important $\bar{x}$ regions for non-isothermal wall heat transfer. First, it can be seen that the effects of a wall temperature (or heat flux) step are completely damped out at an $\bar{x}$ distance downstream of about 10^{-1} for laminar flow and about 10^{-2} for turbulent ($Pr = 0.70$). Recalling the definition of $\bar{x}$, it can be seen that for equal D_h and Pr the turbulent thermal entrance length is apt to be about as long, or perhaps somewhat longer, than its laminar counterpart. Examination

of the fundamental solutions also reveals that constant heat flux thermal entrance lengths tend to be about one half to one order of magnitude shorter than constant wall temperature thermal entrance lengths.

Comparing the magnitudes of the various io subscripted fundamental solutions with those with ii subscripts, it can be seen that the effects of a temperature (or heat flux) step at one wall are not apparent at the opposite wall for an $\bar{x}$ distance downstream of about 10^{-2} for laminar flow and about 10^{-3} for turbulent (Pr = 0.70). This propagation delay creates a type of "zone of silence" above the step.

APPENDIX A

DERIVATION OF EXPRESSIONS USEFUL FOR EVALUATING THE HIGHER EIGENCONSTANTS

In this appendix are derived eigenconstant relations used in Sections III.G.3 and IV.G.3 to evaluate the higher eigenconstants. These relations are valid for <u>all</u> the eigenconstants, but were found inconvenient to use for the lower ones which were calculated numerically from (III.B.22) and (IV.B.24).

Recall that the Sturm-Liouville equation resulting from the laminar treatment is

$$Y_n'' + \lambda_n^2 \left(1 - \bar{y}^2\right) Y_n = 0 \tag{A.1}$$

and that for the turbulent case is

$$\frac{d}{d\bar{y}} \left[\left(1 + \frac{\epsilon_M}{\nu} \frac{\epsilon_H}{\epsilon_M} Pr \right) Y_n' \right] + \lambda_n^2 \frac{u}{u_m} Y_n = 0 \tag{A.2}$$

These equations are of the general form

$$\frac{d}{d\bar{y}} (hY_n') + \lambda_n^2 w Y_n = 0 \tag{A.3}$$

where for the laminar case

$$h = 1$$

$$w = 1 - \bar{y}^2$$

and for the turbulent case

$$h = 1 + \frac{\epsilon_M}{\nu} \frac{\epsilon_H}{\epsilon_M} Pr$$

$$w = \frac{u}{u_m} = \bar{u}$$

Now, from (III.B.22) and (IV.B.24) the general equation for the eigenconstants is

$$C_n = - \frac{\int_{-1}^{+1} \theta_{fd} w Y_n \, d\bar{y}}{\int_{-1}^{+1} w Y_n^2 \, d\bar{y}} \qquad (A.4)$$

This expression will now be put in more convenient form for higher eigenconstant evaluation.

Consider first the numerator of (A.4). Combining with (A.3) and integrating by parts twice yields

$$- \int_{-1}^{+1} \theta_{fd} w Y_n \, d\bar{y} = \frac{1}{\lambda_n^2} \int_{-1}^{+1} \theta_{fd} \, d\left(h Y_n'\right)$$

$$= \frac{1}{\lambda_n^2} \theta_{fd} h Y_n' \Big|_{-1}^{+1} - \frac{1}{\lambda_n^2} \int_{-1}^{+1} \theta_{fd}' h \, dY_n$$

$$= \frac{1}{\lambda_n^2} \theta_{fd} h Y_n' \Big|_{-1}^{+1} - \frac{1}{\lambda_n^2} \theta_{fd}' h Y_n \Big|_{-1}^{+1}$$

$$+ \frac{1}{\lambda_n^2} \int_{-1}^{+1} Y_n \frac{d}{d\bar{y}} \left(h \theta_{fd}'\right) d\bar{y} \qquad (A.5)$$

Now from (IV.B.25) it is seen that for boundary condition cases 1, 3, and 4

$$\frac{d}{d\bar{y}} \left(h \theta_{fd}'\right) = 0$$

So for these cases the integral in (A.4) vanishes. And from (IV.B.26) the analogous expression for case 2 is

$$\frac{d}{d\bar{y}}\left(h\theta'_{fd}\right) = \frac{w}{8}$$

So for this case the integral in (A.5) becomes

$$\int_{-1}^{+1} Y_n \frac{d}{d\bar{y}}\left(h\theta'_{fd}\right) d\bar{y} = \frac{1}{8}\int_{-1}^{+1} Y_n w \, d\bar{y}$$

Introducing (A.3) this becomes

$$\int_{-1}^{+1} Y_n \frac{d}{d\bar{y}}\left(h\theta'_{fd}\right) d\bar{y} = -\frac{1}{8\lambda_n^2}\int_{-1}^{+1} \frac{d}{d\bar{y}}\left(hY'_n\right) d\bar{y}$$

$$= -\frac{1}{8\lambda_n^2} hY'_n \Big|_{-1}^{+1}$$

But the case 2 boundary conditions stipulate that $Y'_n = 0$ at both walls; hence the integral vanishes in this case too.

Thus, recognizing that $h = 1$ at both walls, it is seen from (A.5) that the numerator of (A.4) is

$$-\int_{-1}^{+1} \theta_{fd} w Y_n \, d\bar{y} = \frac{1}{\lambda_n^2}\left[\theta_{fd} Y'_n - \theta'_{fd} Y_n\right]_{-1}^{+1} \qquad (A.6)$$

Consider next the denominator of (A.4). To put it into the form sought, one operates on (A.3). Differentiation with respect to λ_n* yields

$$\frac{\partial}{\partial\lambda_n}\left[\frac{\partial}{\partial\bar{y}}\left(h\frac{\partial Y_n}{\partial\bar{y}}\right)\right] + 2\lambda_n w Y_n + \lambda_n^2 w \frac{\partial Y_n}{\partial\lambda_n} = 0$$

---

*Herein $\frac{\partial}{\partial\lambda_n}$ is used to denote $\frac{\partial}{\partial\lambda}_{\lambda=\lambda_n}$.

Interchanging the order of differentiation

$$\frac{\partial}{\partial \bar{y}}\left[h\,\frac{\partial}{\partial \bar{y}}\left(\frac{\partial Y_n}{\partial \lambda_n}\right)\right] + 2\lambda_n w Y_n + \lambda_n^2 w\,\frac{\partial Y_n}{\partial \lambda_n} = 0$$

Applying the operator $\int_{-1}^{+1} Y_n\, d\bar{y}$ and rearranging

$$\int_{-1}^{+1} w Y_n^2\, d\bar{y} = -\frac{1}{2\lambda_n}\left\{\int_{-1}^{+1} Y_n\,\frac{\partial}{\partial \bar{y}}\left[h\,\frac{\partial}{\partial \bar{y}}\left(\frac{\partial Y_n}{\partial \lambda_n}\right)\right] d\bar{y} + \int_{-1}^{+1} Y_n \lambda_n^2 w\,\frac{\partial Y_n}{\partial \lambda_n}\, d\bar{y}\right\}$$

Integrating the first term on the right-hand side by parts twice yields

$$\int_{-1}^{+1} w Y_n^2\, d\bar{y} = -\frac{1}{2\lambda_n}\left\{\left[Y_n h\,\frac{\partial}{\partial \bar{y}}\left(\frac{\partial Y_n}{\partial \lambda_n}\right) - \frac{\partial Y_n}{\partial \bar{y}}\,h\,\frac{\partial Y_n}{\partial \lambda_n}\right]_{-1}^{+1} + \int_{-1}^{+1} \frac{\partial Y_n}{\partial \lambda_n}\left[\frac{\partial}{\partial \bar{y}}\left(h\,\frac{\partial Y_n}{\partial \bar{y}}\right) + \lambda_n^2 w Y_n\right] d\bar{y}\right\}$$

But from (A.3) it is seen that the integrand on the right-hand side is identically zero. Hence, noting that $h = 1$ at both walls, one obtains

$$\int_{-1}^{+1} w Y_n^2\, d\bar{y} = -\frac{1}{2\lambda_n}\left[Y_n\,\frac{\partial}{\partial \bar{y}}\left(\frac{\partial Y_n}{\partial \lambda_n}\right) - Y_n'\,\frac{\partial Y_n}{\partial \lambda_n}\right]_{-1}^{+1} \qquad \text{(A.7)}$$

Thus, combining (A.4), (A.6), and (A.7)

$$C_n = -\frac{2}{\lambda_n}\left\{\frac{\left[\theta_{fd}Y_n' - \theta_{fd}'Y_n\right]_{-1}^{+1}}{\left[Y_n\frac{\partial}{\partial\bar{y}}\left(\frac{\partial Y_n}{\partial\lambda_n}\right) - Y_n'\frac{\partial Y_n}{\partial\lambda_n}\right]_{-1}^{+1}}\right\} \qquad (A.8)$$

Note that this equation applies for both laminar and turbulent flow.

Now the appropriate expressions for each of the four fundamental cases will be set forth.

Case One

Here the boundary conditions are

$$Y_n(-1) = 0$$

$$Y_n(1) = 0$$

so

$$C_n = \frac{2}{\lambda_n}\frac{Y_n'(1)}{Y_n'(1)\left(\frac{\partial Y_n}{\partial\lambda_n}\right)_{\bar{y}=1} - Y_n'(-1)\left(\frac{\partial Y_n}{\partial\lambda_n}\right)_{\bar{y}=-1}} \qquad (A.9)$$

Case Two

Here the boundary conditions are

$$Y_n'(-1) = 0$$

$$Y_n'(1) = 0$$

so

$$C_n = \frac{1}{2\lambda_n}\frac{Y_n(1)}{Y_n(1)\frac{\partial}{\partial\bar{y}}\left(\frac{\partial Y_n}{\partial\lambda_n}\right)_{\bar{y}=1} - Y_n(-1)\frac{\partial}{\partial\bar{y}}\left(\frac{\partial Y_n}{\partial\lambda_n}\right)_{\bar{y}=-1}} \qquad (A.10)$$

Case Three

Here the boundary conditions are

$$Y_n'(-1) = 0$$

$$Y_n(1) = 0$$

so

$$C_n = \frac{2}{\lambda_n} \frac{Y_n'(1)}{Y_n'(1)\left(\frac{\partial Y_n}{\partial \lambda_n}\right)_{\bar{y}=1} + Y_n(-1)\frac{\partial}{\partial \bar{y}}\left(\frac{\partial Y_n}{\partial \lambda_n}\right)_{\bar{y}=-1}} \qquad \text{(A.11)}$$

Case Four

Here the boundary conditions are

$$Y_n(-1) = 0$$

$$Y_n'(1) = 0$$

so

$$C_n = \frac{1}{2\lambda_n} \frac{Y_n(1)}{Y_n(1)\frac{\partial}{\partial \bar{y}}\left(\frac{\partial Y_n}{\partial \lambda_n}\right)_{\bar{y}=1} + Y_n'(-1)\left(\frac{\partial Y_n}{\partial \lambda_n}\right)_{\bar{y}=-1}} \qquad \text{(A.12)}$$

APPENDIX B

DETAILS OF THE NUMERICAL CALCULATION OF THE LAMINAR EIGENFUNCTIONS

The numerical integration technique employed is presented in Milne[38] as Method XII for linear equations of second order, and will not be repeated here. The interval from $\bar{y} = -1$ to $\bar{y} = +1$ was divided into 400 equal increments for the integration. The initial value of the λ_n^2 "guess" was that obtained from the asymptotic solution of Section III.G.3

After each integration across the interval from $y = -1$ to $\bar{y} = +1$, the eigenfunction was normalized by calculation (Simpson's rule) and application of the factor

$$\left[\int_{-1}^{+1} \left(1 - \bar{y}^2\right) \left(Y_n\right)^2 \, d\bar{y} \right]^{-\frac{1}{2}}$$

The next trial λ_n^2 was then computed by the Berry and de Prima method and the integration was repeated. Since closure is very rapid, the iterations were continued until no change occurred in λ_n^2 (the computer carries eight significant figures).

To provide a check on the accuracy of the method the calculated eigenvalues are compared with those reported by other investigators in Table B.1. The majority of the values compared were published during the preparation of the present work.

After these calculations were completed Lundberg[37] performed similar calculations for an annular passage using a more sophisticated integration scheme (a predictor-corrector method due to Hamming) and found that 250 increments provided sufficient accuracy.

The computer program is written in BALGOL language and is presented below.

```
2   COMMENT      COMPUTATION OF EIGENFUNCTIONS, EIGENVALUES,
2                AND EIGENCONSTANTS FOR THE PARALLEL PLANES
2                LAMINAR FLOW FUNDAMENTAL SOLUTIONS$
2   COMMENT      THE LIST OF FORMAT STATEMENTS$
2   FORMAT HED1 (B48,*DETERMINATION OF LAMBDA*,W3)$
2   FORMAT HED2 (B47,*RESULTS OF FINAL ITERATION,W3)$
2   FORMAT TRY (*Y0=*,F14.8,*YP0=*,F14.8,*YN=*,F14.8,*YPN=*,
2                F14.8,*LL=*,F14.8,*LLB=*,F14.8,W4)$
2   FORMAT ENDS (*CASE=*,X2.0,*Y0=*,F14.8,*YP0=*,F14.8,
2                *YN=*,F14.8,*YPN=*,F14.8,W4)$
2   FORMAT TRY2 (*LAMBDA=*,F14.8,B5,*LAMBDA SQUARED=*,
2                W4,B49,*THE VALUES OF Y FOLLOW*,W4)$
2   FORMAT TRY3 (6F20.8,W4)$
2   FORMAT TRY4 (*THE EIGENCONSTANT IS *,F14.8,W4)$
2   COMMENT      THE LIST OF ARRAY DECLARATIONS$
2   ARRAY  Y(500),Z(500),WF(500),F(500),G(500),H(500)$
2   COMMENT      SOME FURTHER DECLARATIONS AND
2                SETTING OF SOME INITIAL VALUES$
2   INPUT VALUES (L,Y0,YP0,DEL,CASE)$
28..WRITE ($$HED1)$
2   READ  ($$VALUES)$
2   N=(2.0)/(DEL)$
2   V=0$
2   X=0$
2   LL=L.L$ LLB=0$
2   FOR I=(1,1,N)$ BEGIN
```

```
2       WF(I)=(1.0-(((I)(DEL))-1.0)*2)$
2       H(I) =(DEL)(DEL)(WF(I)) END$
2NEWL..FOR I=(1,1,N)$ BEGIN
2       G(I) =(LL)(H(I))$
2       F(I) =1.0+((G(I))/(12.0))$ END$
2   COMMENT      INTEGRATION OF THE DIFFERENTIAL EQUATIONS$
2DEINT..DYO=YPO.DEL$
2       Y(1)=DYO+YO$
2       Z(1)=(F(1))(Y(1))$
2       ZO=YO$
2       DZI=Z(1)-ZO$
2   FOR I=(2,1,N)$ BEGIN
2       DDZI=-(G(I-1))(Y(I-1))$
2       DZI =DDZI+DZI$
2       Z(I)=DZI+Z(I-1)$
2       Y(I)=(Z(I))/(F(I)) END$
2   YPN=(DZI+Z(N-1))((G(N-1))/(12.0+G(N-1))))/DEL$
2   COMMENT      CALCULATION OF THE NORMALIZATION
2                FACTOR BY SIMPSONS RULE INTEGRATION$
2   P=0.0$
2   Q=0.0$
2   FOR I=(1,2,N-1)$
2       P=P+(WF(I))((Y(I))(Y(I)))$
2   FOR I=(2,2,N)$
2       Q=Q+(WF(I))((Y(I))(Y(I)))$
2   S=(2.0)(4P+2Q)/((3.0)N)$
```

```
2    FOR I=(1,1,N)$
2       Y(I)=Y(I)/S$ YO=YO/S$ YPO=YPO/S$
2    COMMENT      TEST FOR CONVERGENCE$
2    IF (LL NEQ LLB)$ GO TO BDP$
2    WRITE ($$HED2)$
2    GO QUIT$
2    COMMENT      THE BERRY AND DE PRIMA CALCULATION
2                 OF THE NEXT EIGENVALUE GUESS$
2BDP.. EITHER IF CASE EQL 1$ BEGIN
2       LLB=LL$
2       LL=LL-(Y(N))(YPN)$ END$
2       OTHERWISE$ BEGIN
2       LLB=LL$
2       LL=LL+(Y(N))(YPN) END$
2    OUTPUT TRY1(YO,YPO,Y(N),YPN,LL,LLB)$
2    WRITE ($$TRY1,TRY)$
2    GO NEWL$
2QUIT..WRITE ($$IC,ENDS)$
2    OUTPUT IC (CASE,YO,YPO,Y(N),YPN)$
2    WRITE($$LLID,TRY2)$
2    OUTPUT LLID (SQRT(LL),LL)$
2    OUTPUT ORDVAL (YO,FOR I=(1,1,N)$Y(I))$
2    WRITE ($$ORDVAL,TRY3)$
2    COMMENT      CALCULATION OF THE EIGENCONSTANT
2                 BY SIMPSONS RULE INTEGRATION$
2    P=0.0$
```

```
2   Q=0.0$
2   FOR I=(1,2,N-1)$
2      P=P+(WF(I))(Y(I))(0.5)(I)(DEL)$
2   FOR I=(2,2,N-2)$
2      Q=Q+(WF(I))(Y(I))(0.5)(I)(DEL)$
2   NUM=(2.0)(4P+2Q)/((3.0)N)$
2   P=0.0$
2   Q=0.0$
2   FOR I=(1,2,N-1)$
2      P=P+(WF(I))(Y(I))(Y(I))$
2   FOR I=(2,2,N-2)$
2      Q=Q+(WF(I))(Y(I))(Y(I))$
2   DEN=(2.0)(4P+2Q)/((3.0)N)$
2   C=NUM/DEN$
2   WRITE ($$CONST,TRY4)$
2   OUTPUT CONST (C)$
2   GO TO 8$
2   FINISH$
```

TABLE B.1

COMPARISON OF THE LAMINAR EIGENVALUES REPORTED BY SEVERAL INVESTIGATORS

Case One

n	Present Study	Prins, Mulder & Schenk[46]	Cess & Shaffer[14]	Brown[7]
0	1.681597	1.6816	1.681595	1.6815953222
1	3.672294		3.672291	
2	5.669861	5.6699	5.669857	5.6698573459
3	7.668812		7.668809	
4	9.668245	9.6678	9.66824	9.6682424625
5	11.66790		11.66791	
6	13.66766			13.6676614426 (Brown also presents the next six even λ's)

Case Two

n	Present Study	Cess & Shaffer[12]	Cess & Shaffer[13]
1	2.263144		2.263106
2	4.287297	4.287224	
3	6.297808		6.29768
4	8.303899	8.30372	
5	10.30796		10.3077
6	12.31090	12.3114	
7	14.31315		14.3141

Cases Three and Four

n	Present Study	Schenk[50]
0	0.9546740	0.9547
1	2.974334	2.9743
2	4.981082	4.9812
3	6.984656	
4	8.986928	
5	10.98853	
6	12.98973	

APPENDIX C

DETAILS OF THE NUMERICAL CALCULATION OF THE TURBULENT FULLY DEVELOPED TEMPERATURE PROFILES AND EIGENFUNCTIONS

1. The fully developed temperature profiles

The fully developed temperature profiles, discussed in Section IV.B, were all calculated in essentially the same manner, so only that of case one will be treated here. The equation requiring solution is given by (IV.B.25).

$$\frac{d}{d\bar{y}}\left[\left(1 + \frac{\epsilon_M}{\nu}\,\frac{\epsilon_H}{\epsilon_M}\,Pr\right)\frac{d\theta_{fd}}{d\bar{y}}\right] = 0 \qquad (C.1)$$

The boundary conditions are

$$\theta_{fd}(-1) = 0$$

$$\theta_{fd}(1) = 1$$

The first step in the solution involved the calculation of the $\frac{\epsilon_M}{\nu}$, $\frac{\epsilon_H}{\epsilon_M}$, and $\bar{u}$ (for case two) profiles for the Reynolds and Prandtl numbers of interest. This was accomplished in a straightforward fashion employing equations (IV.B.7) and (IV.B.15), and the expressions in Section IV.B.4. Calculations were carried out at $\bar{y}$ intervals of 0.002 and the results were stored on magnetic tape for future use.

Next (C.1) was integrated using a numerical scheme developed by Mr. I. H. Wentzien and Professor J. G. Herriot of the Stanford University Computation Center. This scheme employs a fourth order Adams predictor-corrector method (see Hildebrand[25]) in the body of the interval and the Runge-Kutta method for starting. It has the very attractive feature of automatically increasing or decreasing the

step-width size during the integration depending on the relationship between the predictor-corrector difference and prescribed relative and absolute error limits. When the step-width size is decreased the Runge-Kutta method is used again for starting. Since the method is actually set up to solve a system of first order differential equations, (C.1) was reduced for computational purposes to

$$\frac{d\theta'_{fd}}{d\bar{y}} = - \frac{\frac{d}{d\bar{y}}\left(\frac{\epsilon_M}{\nu} \frac{\epsilon_H}{\epsilon_M} Pr\right) \theta'_{fd}}{1 + \frac{\epsilon_M}{\nu} \frac{\epsilon_H}{\epsilon_M} Pr} \tag{C.2}$$

$$\frac{d\theta_{fd}}{d\bar{y}} = \theta'_{fd} \tag{C.3}$$

The integration proceeded as an initial value problem with $\theta_{fd}(-1) = 0$ and $\theta'_{fd}(-1) = 1$, and then, utilizing the linearity of the equation, the results were scaled by the factor required to make $\theta_{fd}(1) = 1$. They were stored on magnetic tape for use in the eigenconstant calculations.

2. The eigenfunctions, eigenvalues, and eigenconstants

The same predictor-corrector numerical scheme was used to integrate (IV.B.21). The equation was first reduced to two first order equations,

$$\frac{dY'_n}{d\bar{y}} = - \frac{\frac{d}{d\bar{y}}\left(\frac{\epsilon_M}{\nu} \frac{\epsilon_H}{\epsilon_M} Pr\right) Y'_n - \lambda_n^2 \bar{u} Y_n}{1 + \frac{\epsilon_M}{\nu} \frac{\epsilon_H}{\epsilon_M} Pr} \tag{C.4}$$

$$\frac{dY_n}{d\bar{y}} = Y'_n \tag{C.5}$$

A third equation,

$$\frac{dK_n^2}{d\bar{y}} = \bar{u}Y_n^2 \qquad (C.6)$$

was integrated simultaneously with the above two so that the normalization factor was obtained without a subsidiary Simpson's rule integration.

As in the laminar case, the Berry and de Prima method was employed to converge on the correct eigenvalue. Having done this, the eigenconstant was calculated from (IV.B.24).

The computer program used for the eigenfunction and eigenvalue calculations is presented below.

```
2COMMENT COMPUTATION OF EIGENFUNCTIONS AND EIGENVALUES FOR
2         THE PARALLEL PLANES TURBULENT FLOW FUNDAMENTAL
2         SOLUTIONS USING THE FOURTH ORDER ADAMS PREDICTOR-
2         CORRECTOR METHOD, THE RUNGE-KUTTA METHOD FOR
2         STARTING, AND ERROR CONTROLS$
2INTEGER I,J,AA,BB,N,M,UHH,UNO,DOS$
2INTEGER KEY1,KEY2,KEY3,KEY4,KEY5,KEY6$
2BOOLEAN SKIP,KEEPER,ZERT$
2ARRAY X(5,5),L(5,5),F(5,5),XP(5),
2      E(5),B(510),D(510),FB(510)$
2FORMAT MESSAGE (*IN THE FOLLOWING CALCULATIONS H=*,
2                X10.8,W2)$
2FORMAT FRMT1(B2,S10.8,W4)$
2FORMAT FRMT2(B10,6F16.8,W0)$
2FORMAT IDL(*CASE=*,X2.0,B5,*RE=*,X6.0,B5,*PR=*,X3.2,
2          B5,*LL=*,F14.8,B5,*LAMBDA=*,F14.8,W4)$
2FORMAT GAB2(*Y1=*,F14.8,B5,*YP1=*,F14.8,B5,*Y2=*,
2           F14.8,B5,*YP2=*,F14.8,W4)$
2FORMAT GAB4(*THE PREVIOUS VALUE OF LAMBDA SQUARED WAS *,
2           F14.8,B5,* AND LAMBDA WAS *,F14.8,W4)$
2FORMAT GAB5 (B100,W1)$
2FORMAT DONE(B47,*RESULTS OF FINAL ITERATION*,W3)$
2FORMAT GOMO(B50,*INTERMEDIATE RESULTS*,W3)$
2OUTPUT NEWH(H)$
2OUTPUT ORD(T)$
2OUTPUT RESULTS (FOR I=(1,1,EQ)$X(I,J))$
```

```
2OUTPUT ID(CNU,RE,PR,LL,LLL)$
2OUTPUT GAB(YZ.NOR,YPZ.NOR,YMN,YPN)$
2OUTPUT GAB3(LLOLD,LLLOLD)$
2COMMENT  FUNCTIONS FOR FORWARD,CENTRAL,
2         AND BACKWARD DIFFERENCE INTERPOLATION$
2FUNCTION FINT(CC,DD,EE,FF,GG,HH,II,JJ,KK)=CC+
2         HH(DD-CC)+0.5(HH)(II)(EE-2.0DD+CC)+
2         (1.0/6.0)HH.II.JJ(FF-3.0EE+3.0DD-CC)+
2         (1.0/24.0)HH.II.JJ.KK(GG-4.0FF+6.0EE-
2         4.0DD+CC)$
2FUNCTION CINT(CC,DD,EE,FF,GG,HH)=CC+0.5HH(DD-FF)
2         +0.5HH.HH(DD-2.0CC+FF)+HH(HH.HH-1.0)/12.0)
2         (EE-2.0DD+2.0FF-GG)+(HH.HH(HH.HH-1.0)/24.0)
2         (EE-4.0DD+6.0CC-4.0FF+GG)$
2FUNCTION BINT(CC,DD,EE,FF,GG,HH,II,JJ,KK)=CC+
2         H(CC-DD)+0.5HH.II(CC-2.0DD+EE)+
2         (HH.II.JJ/6.0)(CC-3.0(DD-EE)-FF)+
2         (HH.II.JJ.KK/24.0)(CC-4.0(DD+FF)+6.0EE
2         +GG)$
2COMMENT SUBROUTINE FOR COMPUTING DERIVATIVES
2        FOR EIGENVALUE DETERMINATION$
2SUBROUTINE FUNCT$ BEGIN
2   EITHER IF(T LSS 1.0)$ BEGIN
2      S=FIX(T/DEL)$
2      U=T/DEL$
2      EITHER IF (T EQL 0)$BEGIN
```

```
2          F(1,M)=0.0$
2          F(2,M)=YPZ$
2          F(3,M)=0.0 END$
2       OR IF(U EQL FLOAT(S))$ BEGIN
2          F(1,M)=(-X(1,M).D(S)-LL(FB(S))(X(2,M)))/
2                 (1.0+B(S))$
2          F(2,M)=X(1,M)$
2          F(3,M)=((FB(S))(X(2,M)))(X(2,M)) END$
2       OR IF (T LSS DEL)$ BEGIN
2          F(1,M)=((-X(1,M))(FINT(0.0,D(1),D(2),D(3),
2                 U,U-1.0,U-2.0,U-3.0))-LL(X(2,M))
2                 FINT(ZERO,FB(1),FB(2),FB(3),FB(4),
2                 U,U-1.0,U-2.0,U-3.0)))/(1.0+FINT(
2                 ZERO,B(1),B(2),B(3),B(4),U,U-1.0,
2                 U-2.0,U-3.0))$
2          F(2,M)=X(1,M)$
2          F(3,M)=(FINT(ZERO,FB(1),FB(2),FB(3),FB(4),
2                 U,U-1.0,U-2.0,U-3.0))X(2,M).X(2,M) END$
2       OR IF (T LSS 3.0DEL)$BEGIN
2          U=(T/DEL-S)$
2          F(1,M)=((-X(1,M))(FINT(D(S),D(S+1),D(S+2),
2                 D(S+3),D(S+4),U,U-1,U-2,U-3))-LL
2                 (X(2,M))(FINT(FB(S),FB(S+1),FB(S+2),
2                 FB(S+3),FB(S+4),U,U-1,U-2,U-3)))/
2                 (1.0+FINT(B(S),B(S+1),B(S+2),B(S+3),
2                 B(S+4),U,U-1,U-2,U-3))$
```

```
2          F(2,M)=X(1,M)$
2          F(3,M)=(FINT(FB(S),FB(S+1),FB(S+2),FB(S+3),
2                 FB(S+4),U,U-1,U-2,U-3))•X(2,M)•X(2,M) END$
2       OTHERWISE$ BEGIN
2          U=(1•0/DEL)(T-S•DEL)$
2          F(1,M)=((-X(1,M))(CINT(D(S),D(S+1),D(S+2),
2                 D(S-1),D(S-2),U))-LL(X(2,M))(CINT(
2                 FB(S),FB(S+1),FB(S+2),FB(S-1),FB(S-2),
2                 U)))/(1•0+CINT(B(S),B(S+1),B(S+2),B(S-1),
2                 B(S-2),U))$
2          F(2,M)=X(1,M)$
2          F(3,M)=(CINT(FB(S),FB(S+1),FB(S+2),FB(S-1),FB
2                 (S-2),U))•X(2,M)•X(2,M) END$  END$
2    OTHERWISE$BEGIN
2       S=N-FIX(T/DEL)$
2       U=(T/DEL)-FLOAT(FIX(T/DEL))$
2       EITHER IF (T EQL 2•0)$ BEGIN
2          F(1,M)=0•0$
2          F(2,M)=X(1,M)$
2          F(3,M)=0•0$ END$
2       OR IF (T/DEL EQL FLOAT(FIX(T/DEL)))$ BEGIN
2          F(1,M)=(X(1,M)•D(S)-LL•FB(S)•X(2,M))/
2                 (1•0+B(S))$
2          F(2,M)=X(1,M)$
2          F(3,M)=FB(S)•X(2,M)•X(2,M) END$
2       OR IF (T LSS (FINAL-3•0DEL))$ BEGIN
```

```
2          F(1,M)=(X(1,M).(CINT(D(S),D(S-1),D(S-2),
2                 D(S+1),D(S+2),U))-LL(X(2,M))(CINT
2                 (FB(S),FB(S-1),FB(S-2),FB(S+1),
2                 FB(S+2),U)))/(1.0+CINT(B(S),B(S-1),
2                 B(S-2),B(S+1),B(S+2),U))$
2          F(2,M)=X(1,M)$
2          F(3,M)=(CINT(FB(S),FB(S-1),FB(S-2),FB(S+1),
2                 FB(S+2),U)).X(2,M).X(2,M) END$
2       OTHERWISE$ BEGIN
2          F(1,M)=((X(1,M))(BINT(D(S),D(S+1),D(S+2),
2                 D(S+3),D(S+4),U,U+1,U+2,U+3))-LL.
2                 X(2,M).(BINT(FB(S),FB(S+1),FB(S+2),
2                 FB(S+3),FB(S+4),U,U+1,U+2,U+3)))/
2                 (1.0+BINT(B(S),B(S+1),B(S+2),B(S+3),
2                 B(S+4),U,U+1,U+2,U+3))$
2          F(2,M)=X(1,M)$
2          F(3,M)=(BINT(FB(S),FB(S+1),FB(S+2),FB(S+3),
2                 FB(S+4),U,U+1,U+2,U+3)).X(2,M).X(2,M)
2          END$ END$ RETURN END$
2UHH=900$
2UNO=1$
2DOS=2$
2ZERT=0$
2OUT..READ($$GUESSIN)$
2       READ($$NEWVAL)$
2       INPUT GUESSIN(YZ,YPZ,LLL,KEY1,CNU,ZERLIT)$
```

```
2      INPUT NEWVAL(EXPOREL,EXPOABS)$
2      READ($$CASENU)$
2      INPUT CASENU(SKIP,EQ)$
2N=510$
2REWIND(UHH)$
2YPY..FINDM(UHH,KEY1)$
2      READM(UHH$ZERT$FLIST)$
2      READM(UHH$ZERT$DLIST)$
2      READM(UHH$ZERT$BLIST)$
2      MOVEM(UHH$DOS)$
2      READM(UHH$ZERT$REPR)$
2      INPUT FLIST(KEY1,FOR I=(1,1,N)$FB(I))$
2      INPUT DLIST(KEY2,FOR I=(1,1,N)$D(I))$
2      INPUT BLIST(KEY3,FOR I=(1,1,N)$B(I))$
2      INPUT REPR (KEY6,RE,PR,FR)$
2N=1000$
2COMMENT SET UP INITIAL VALUES$
2       LL=LLL.LLL$
2       KEEPER=SKIP$
2NEWL..X(1,1)=YPZ$
2       X(2,1)=YZ$
2       X(3,1)=0.0$
2       SKIP=KEEPER$
2       N=1000$
2       TEMP=0$
2       T=0$
```

```
2       CODE=0$
2       ZERO=0$
2       DEL=(2.0/N)$
2       INITIAL=0$
2       FINAL=2.0$
2       DEL=(2.0/N)$
2       H=DEL$
2       COUNT=20$
2COMMENT BEGIN  PROGRAM
2         SET UP ACCURACY TESTS$
2    IF SKIP$ BEGIN
2       AA=2$
2       BB=4$
2       GO TO 2222 END$
2    RELTEST=14.2.(10.0*EXPOREL)$
2    ABSTEST=14.2.(10.0*EXPOABS)$
2    FACTOR=10.0*(EXPOREL-EXPOABS)$
2    LB=14.2(10.0*(EXPOREL-2.3))$
2    H=H+H$
2COMMENT  RUNGE KUTTA STARTING METHOD$
21111..AA=2$
2       BB=2$
22222..FOR J=(AA,1,BB)$ BEGIN
2          M=J-1$
2          ENTER FUNCT$
2       FOR I=(1,1,EQ)$ BEGIN
```

```
2          L(I,1)=H.F(I,M)$
2          X(I,J)=X(I,M)+0.5L(I,1) END$
2          T=T+0.5H$
2          M=J$
2          ENTER FUNCT$
2       FOR I=(1,1,EQ)$ BEGIN
2          L(I,2)=H.F(I,J)$
2          X(I,J)=X(I,J-1)+0.5L(I,2) END$
2          ENTER FUNCT$
2       FOR I=(1,1,EQ)$ BEGIN
2          L(I,3)=H.F(I,J)$
2          X(I,J)=X(I,J-1)+L(I,3) END$
2          T=T-0.5H+H$
2          ENTER FUNCT$
2       FOR I=(1,1,EQ)$ BEGIN
2          L(I,4)=H.F(I,J)$
2          X(I,J)=X(I,J-1)+0.16666667(L(I,1)+2.0
2                   (L(I,2)+L(I,3))+L(I,4)) END$END$
2       IF BB EQL 2$ BEGIN
23333..FOR I=(1,1,EQ)$
2          XP(I)=X(I,2)$
2COMMENT   XP(I)=DOUBLE INTERVAL RESULT TO BE
2                 USED IN ERROR ANALYSIS$
2          T=T-H$
2          H=0.5H$
2          WRITE ($$NEWH,MESSAGE)$
```

```
2          BB=3$
2          GO TO 2222 END$
2       IF BB EQL 3$ BEGIN
2          J=3$
2COMMENT IS ACCURACY CRITERION MET$
24444..FOR I=(1,1,EQ)$ BEGIN
2          E(I)=ABS(XP(I)-X(I,J))$
2          EITHER IF E(I) LSS ABS(X(I,J)).RELTEST$
2             E(I)=E(I)/ABS(X(I,J))$
2          OR IF E(I) LSS ABSTEST$
2             E(I)=E(I).FACTOR$
2          OTHERWISE$BEGIN
2             T=T-H$
2             IF J EQL 5$ BEGIN
2                FOR I=(1,1,EQ)$
2                X(I,1)=X(I,4)$
2                GO TO 1111 END$
2             GO TO 3333 END$ END$
2          IF J EQL 5$
2             GO TO 6666$
2          AA=4$
2          BB=4$
2          GO TO 2222$ END$
2COMMENT SHOULD ANY OF THE STARTING VALUES
2         BE  PRINTED  OUT$
2       T=T-H-H-H$
```

```
2          IF CODE EQL 1$
2          T=FINAL-H$
2       FOR J=(2,1,4)$ BEGIN
2          T=T+H$
2          TEMP=TEMP+1$
29999..IF(T GEQ FINAL)$ BEGIN
2          IF CODE EQL 1$
2             GO ABLE$
2             GO SPEC$ END$
2ABLE..IF T GEQ FINAL$
2          GO SIMP$
2          IF TEMP EQL COUNT$ BEGIN
2          WRITE ($$ORD,FRMT1)$
2          WRITE ($$RESULTS,FRMT2)$
2          TEMP=0$ END$ END$
25555..IF T GEQ FINAL$
2          GO SIMP$
2COMMENT BEGIN ADAMS METHOD$
2          M=4$
2          ENTER FUNCT$
2          FOR I=(1,1,EQ)$ BEGIN
2             XP(I)=X(I,4)+0.041666667H.(55.0F(I,4)-
2                   59.0F(I,3)+37.0F(I,2)-9.0F(I,1))$
2             X(I,5)=XP(I) END$
2          T=T+H$
2          M=5$
```

```
2          ENTER FUNCT$
2          FOR I=(1,1,EQ)$
2             X(I,5)=X(I,4)+0.041666667H.(9.0F(I,5)+
2                    19.0F(I,4)-5.0F(I,3)+F(I,2))$
2          IF SKIP$
2             GO TO 6666$
2          J=5$
2          GO TO 4444$
26666..FOR J=(2,1,5)$
2          FOR I=(1,1,EQ)$ BEGIN
2             F(I,J-1)=F(I,J)$
2             X(I,J-1)=X(I,J) END$
2       TEMP=TEMP+1$
2          IF T GEQ FINAL$ BEGIN
2             IF CODE EQL 1$
2             GO BAKER$
2             GO SPEC$ END$
2BAKER..IF T GE@ FINAL$
2          GO SIMP$
2        IF TEMP EQL COUNT$ BEGIN
2          J=4$
2          WRITE ($$ORD,FRMT1)$
2          WRITE ($$RESULTS,FRMT2)$
2          TEMP=0$END$
2        IF SKIP$
2          GO TO 5555$
```

```
2COMMENT TEST WHETHER INTERVAL CAN
2         BE DOUBLED$
2          FOR I=(1,1,EQ)$ BEGIN
2              IF (E(I) GTR LB)$
2                 GO TO 5555$ END$
2              IF T+H+H GEQ FINAL$
2                 GO TO 5555$
2          FOR I=(1,1,EQ)$
2              X(I,1)=I(I,4)$
2              H=H+H+H+H$
2          GO TO 1111$
2SPEC..IF T EQL FINAL$
2          GO SIMP$
2       T=T-H$
2       FOR I=(1,1,EQ)$
2          X(I,1)=X(I,J-1)$
2       H=FINAL-T$
2       KEEPER=SKIP$
2       AA=2$
2       BB=4$
2       SKIP=1$
2       CODE=1.0$
2       GO 2222$
2SIMP..YMN=X(2,J)$
2       YPN=X(1,J)$
2       NOR=(1.0/SQRT(X(3,J)))$
```

```
2       YMN=YMN.NOR$
2       YPN=YPN.NOR$
2       LLOLD=LL$
2       LLLOLD=LLL$
2       EITHER IF CNU EQL 1$
2          LL=LL-YMN.YPN$
2       OTHERWISE$
2          LL=LL+YMN.YPN$
2       LLL=SQRT(LL)$
2       EITHER IF LL LSS 10.0$
2          ZERLIM=ZERLIT.(0.0005)$
2       OTHERWISE$
2          ZERLIM=ZERLIT.(0.005)$
2       IF ABS(LLOLD-LL) LEQ ZERLIM$
2          GO COMPLETE$
2          GO REDO$
2COMPLETE..WRITE ($$DONE)$
2       WRITE($$ID,IDL)$
2       WRITE($$GAB,GAB2)$
2       WRITE($$GAB3,GAB4)$
2       FOR I=(1,1,5)$ BEGIN
2          FOR II=(1,1,5)$
2             X(I,II)=0.0 END$
2       WRITE ($$GAB5)$
2       GO OUT$
2REDO..WRITE ($$GOMO)$
```

```
2       WRITE ($$ID,IDL)$
2       WRITE ($$GAB,GAB2)$
2       WRITE ($$GAB3,GAB4)$
2       WRITE ($$GAB5)$
2       FOR I=(1,1,5)$BEGIN
2          FOR II=(1,1,5)$
2             X(I,II)=0.0 END$
2       GO NEWL$
2       FINISH$
```

APPENDIX D

EXAMPLE OF THE USE OF THE FUNDAMENTAL SOLUTIONS

It is convenient to use the graphs of the fundamental solutions, Figures III.C.1-4 and IV.C.1-4, for rapid calculations involving superposition of relatively simple boundary conditions to approximate more complicated ones. For illustration, a specific example will be treated in this appendix.

Consider a problem in which the wall temperatures vary axially in the manner shown in Figure G.1. The fluid is air which enters at atmospheric pressure with a fully established velocity profile and a uniform temperature of 98.1° F. The inlet Reynolds number is 40,400, the plate spacing is 0.5 inches, and $\frac{k}{D_h} = 0.20$. It is desired to determine the heat flux at each wall as a function of $\bar{x}$.

The pertinent equations are (II.D.23) and (II.D.24); these are reproduced here for convenience.

$$q''_{wo}(\bar{x}) = \frac{k}{D_h}\left\{\int_{\xi=0}^{\xi=\bar{x}} \left[\Phi_{oo}^{(1)}(\bar{x} - \xi)\right] dt_{wo}(\xi) + \int_{\xi=0}^{\xi=\bar{x}} \left[\Phi_{oi}^{(1)}(\bar{x} - \xi)\right] dt_{wi}(\xi)\right\} \qquad (D.1)$$

$$q''_{wi}(\bar{x}) = \frac{k}{D_h}\left\{\int_{\xi=0}^{\xi=\bar{x}} \left[\Phi_{io}^{(1)}(\bar{x} - \xi)\right] dt_{wo}(\xi) + \int_{\xi=0}^{\xi=\bar{x}} \left[\Phi_{ii}^{(1)}(\bar{x} - \xi)\right] dt_{wi}(\xi)\right\} \qquad (D.2)$$

Recall that the integrals are to be evaluated in the Stieltjes sense. Thus, approximating t_{wo} and t_{wi} by the steps shown in Figure G.1, (D.1) and (D.2) become

$$q''_{wo} = \frac{k}{D_h} \sum_{\substack{\text{all steps} \\ \text{before } \bar{x}}} \left[\Phi_{oo}^{(1)}(\bar{x} - \xi)\right] \delta t_{wo}(\xi) + \frac{k}{D_h} \sum_{\substack{\text{all steps} \\ \text{before } \bar{x}}} \left[\Phi_{oi}^{(1)}(\bar{x} - \xi)\right] \delta t_{wi}(\xi) \qquad \text{(D.3)}$$

$$q''_{wi} = \frac{k}{D_h} \sum_{\substack{\text{all steps} \\ \text{before } \bar{x}}} \left[\Phi_{ii}^{(1)}(\bar{x} - \xi)\right] \delta t_{wi}(\xi) + \frac{k}{D_h} \sum_{\substack{\text{all steps} \\ \text{before } \bar{x}}} \left[\Phi_{io}^{(1)}(\bar{x} - \xi)\right] \delta t_{wo}(\xi) \qquad \text{(D.4)}$$

The wall temperature steps employed are as follows.

$\bar{x}$	δt_{wo} (^{o}F)	δt_{wi} (^{o}F)
-2.0×10^{-4}	-0.5	-0.75
-1.5×10^{-4}	0.75	0.5
-1.0×10^{-4}	2.0	1.5
-0.5×10^{-4}	6.0	3.75
0	11.75	6.75
0.5×10^{-4}	0.75	0.25

The values of $\Phi_{ii}^{(1)}(\bar{x})$ and $\Phi_{io}^{(1)}(\bar{x})$ at the Reynolds number of interest are obtained by crossplotting them against Re with $\bar{x}$ as a parameter using Figure IV.C.1, and then

plotting against $\bar{x}$ at the proper Re. Recall that $\Phi_{ii}^{(1)} = \Phi_{oo}^{(1)}$ and $\Phi_{io}^{(1)} = \Phi_{oi}^{(1)}$.

As an example of the calculation procedure, consider the position at the outer (upper) plate, $\bar{x} = 5\times10^{-4}$. One obtains from (D.3) the following result.

$$q''_{wo} = 0.20 \left[(80.0)(-0.5) + (82.0)(0.75) + (83.5)(2.0) + (86.0)(6.0) + (88.5)(11.75) + (91.5)(0.75)\right] + 0.20 \left[(-0.38)(-0.75) + (-0.24)(0.5) + (-0.125)(1.5)\right]$$

Thus

$$q''_{wo} = 362.5 \ \frac{\text{Btu}}{\text{hr-ft}^2}$$

Proceeding in the above manner, the heat fluxes are calculated for several $\bar{x}$ values at each plate. The results are tabulated below, and plotted on Figure D.1.

$\bar{x}$	q''_{wo} (Btu/hr-ft^2)	q''_{wi} (Btu/hr-ft^2)
-1.5×10^{-4}	-11.5	-17.3
-1.0×10^{-4}	6.5	-4.63
-0.5×10^{-4}	52.1	30.3
0	186.5	114.3
0.5×10^{-4}	408.3	261.7
1.0×10^{-4}	432.8	250.3
1.5×10^{-4}	406.4	235.0
2.0×10^{-4}	388.0	224.5
2.5×10^{-4}	374.2	216.5
3.0×10^{-4}	362.5	209.8
3.5×10^{-4}	352.4	203.7
4.0×10^{-4}	343.2	198.1

$\bar{x}$	q''_{wo} (Btu/hr-ft^2)	q''_{wi} (Btu/hr-ft^2)
4.5×10^{-4}	337.0	193.5
5.0×10^{-4}	305.1	188.6
5.5×10^{-4}	323.1	184.4
6.0×10^{-4}	317.0	180.2
6.5×10^{-4}	311.0	176.4
7.0×10^{-4}	304.2	172.0
7.5×10^{-4}	299.1	170.5

Referring to Figure V.B.3, it can be seen that the example given here is the heat flux prediction for that particular test run.

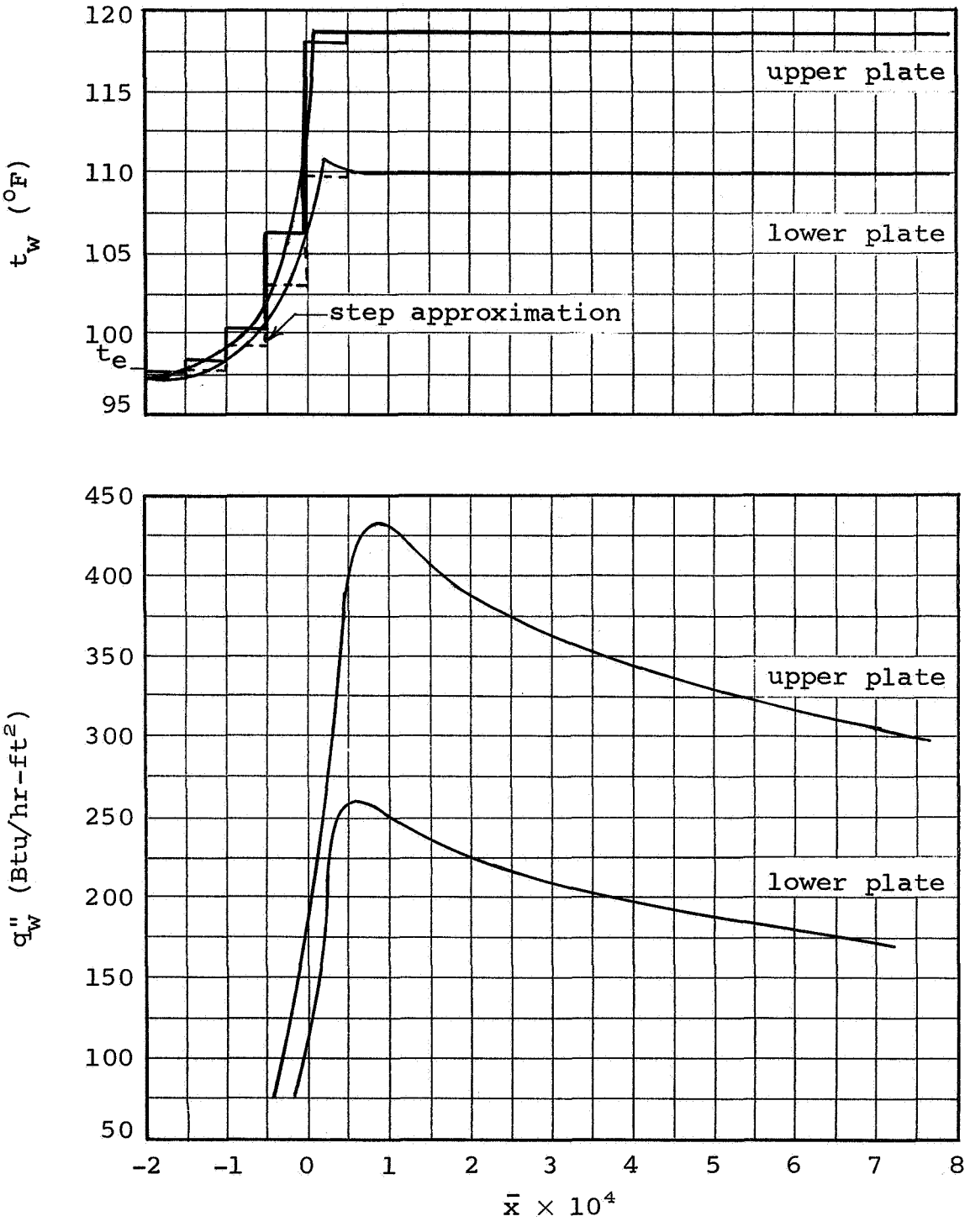

Figure D.1. Example of the Use of the Fundamental Solutions

APPENDIX E

ESTIMATE OF THE RANGE OF VALIDITY OF THE TURBULENT SMALL $\bar{x}$ SOLUTIONS

As can be seen from Figures IV.C.1, 2, 3, and 4, there is a large gap between the calculated fundamental solutions and the small $\bar{x}$ asymptotes. Thus the range of validity of the small $\bar{x}$ solutions is not apparent from the figures, as it is in the laminar case. For this reason it is desirable to use the expressions developed in Section IV.E to obtain estimates of the maximum value of $\bar{x}$ for which these solutions are valid.

Recall that the small $\bar{x}$ solutions were predicated on the fact that the temperature profile had not yet penetrated the turbulent core; that is, it was confined to the laminar sublayer. Thus the limiting $\bar{x}$ value sought can be obtained by using the temperature relations of Section IV.E to calculate the value of $\bar{x}$ at which the sublayer edge temperature has risen to, say, 1 percent of the value at the wall.

Taking the laminar sublayer edge to occur at $y^+ = 5$ (from Figure IV.B.3 it is seen that $\frac{\epsilon_M}{\nu} = 0.1$ here), (IV.B.8) indicates that

$$\bar{\eta} = \frac{5}{Re}\sqrt{\frac{32}{f}} \qquad \text{(E.1)}$$

defines the sublayer thickness. Thus, the similarity solutions of Section IV.E will be used to determine the limiting values of the variable ξ, and this, combined with (E.1) will lead to $\bar{x}_{max}$.

Cases one and three

Here the ratio of fluid to wall temperature is given by (IV.E.15) and (IV.E.6).

$$\frac{\theta}{\theta_{\bar{\eta}=0}} = -\frac{3}{\Gamma\left(\frac{1}{3}\right)}\left(\frac{\text{Re } f}{1152}\right)^{\frac{1}{3}} \int_0^{\xi} e^{-\frac{\text{Re } f}{1152}\sigma^3}\, d\sigma + 1 \qquad \text{(E.2)}$$

Setting the temperature ratio equal to 0.01, one obtains

$$\frac{3}{\Gamma\left(\frac{1}{3}\right)}\left(\frac{\text{Re } f}{1152}\right)^{\frac{1}{3}} \int_0^{\xi} e^{-\frac{\text{Re } f}{1152}\sigma^3}\, d\sigma = 0.99 \qquad \text{(E.3)}$$

Changing variables, let

$$\omega \triangleq \frac{\text{Re } f}{1152}\sigma^3 \qquad \text{(E.4)}$$

Then (E.3) becomes

$$\frac{1}{\Gamma\left(\frac{1}{3}\right)} \int_0^{\frac{\text{Re } f}{1152}\xi^3} e^{-\omega}\, \omega^{-\frac{2}{3}}\, d\omega = 0.99 \qquad \text{(E.5)}$$

From Pearson[44]

$$\frac{1}{\Gamma\left(\frac{1}{3}\right)} \int_0^{\frac{\text{Re } f}{1152}\xi^3} e^{-\omega}\, \omega^{-\frac{2}{3}}\, d\omega = I\left(\sqrt{3}\,\frac{\text{Re } f}{1152}\xi^3,\ -\frac{2}{3}\right) \qquad \text{(E.6)}$$

where I is an incomplete gamma function. Hence

$$I\left(\sqrt{3}\,\frac{\text{Re } f}{1152}\xi^3,\ -\frac{2}{3}\right) = 0.99 \qquad \text{(E.7)}$$

Pearson tabulates the incomplete gamma function, and from his book and (E.7) one obtains

$$\sqrt{3}\,\frac{\text{Re } f}{1152}\xi^3 = 4.79 \qquad \text{(E.8)}$$

Then, from (IV.E.8) and (E.1)

$$\bar{x} = \left(\frac{5}{1.4}\right)^3 32^{\frac{3}{2}} \frac{1}{1152\ Re^2\sqrt{f}} = \frac{7.12}{Re^2\sqrt{f}} \qquad (E.9)$$

The maximum value of $\bar{x}$ for which the small $\bar{x}$ solutions are valid for cases one and three are given in the following table.

Re	$\bar{x}_{max}$
20,000	2.06×10^{-7}
30,000	9.84×10^{-8}
50,000	3.85×10^{-8}

Referring to Figures IV.C.1 and IV.C.3, it can be seen that the fundamental solutions do not merge with the small $\bar{x}$ asymptotes in the $\bar{x}$ range plotted.

It is of interest to note that had the 1 percent restriction imposed on the temperature ratio been relaxed to 10 percent, the $\bar{x}_{max}$ values tabulated above would be increased by only a factor of 2.74.

Cases two and four

Here the ratio of fluid to wall temperature is given by (IV.E.34) and (IV.E.35).

$$\frac{\theta}{\theta_{\bar{\eta}=0}} = 4\left(\frac{Re\ f}{1152}\right)^{\frac{1}{3}}\Gamma\left(\frac{2}{3}\right)\left[-\frac{1}{4}\xi + \frac{1}{4\left(\frac{Re\ f}{1152}\right)^{\frac{1}{3}}\Gamma\left(\frac{2}{3}\right)}\left(e^{-\frac{Re\ f}{1152}\xi^3} + \frac{Re\ f}{384}\xi\int_0^{\xi}\sigma\, e^{-\frac{Re\ f}{1152}\sigma^3}\, d\sigma\right)\right] \qquad (E.10)$$

Setting the temperature ratio equal to 0.01 and changing variables to ω (defined by (E.4)), one obtains

$$e^{-\frac{Re\ f}{1152}\xi^3} + \left(\frac{Re\ f}{1152}\right)^{\frac{1}{3}} \xi \int_0^{\frac{Re\ f}{1152}\xi^3} e^{-\omega}\, \omega^{-\frac{1}{3}}\, d\omega$$

$$- \left(\frac{Re\ f}{1152}\right)^{\frac{1}{3}} \Gamma\left(\frac{2}{3}\right) \xi = 0.01 \qquad \text{(E.11)}$$

Now let

$$\alpha \triangleq \frac{Re\ f}{1152}\xi^3 \qquad \text{(E.12)}$$

Then

$$e^{-\alpha} + \alpha^{\frac{1}{3}} \int_0^{\alpha} e^{-\omega}\, \omega^{-\frac{1}{3}}\, d\omega - \Gamma\left(\frac{2}{3}\right) \alpha^{\frac{1}{3}} = 0.01 \qquad \text{(E.13)}$$

From Pearson

$$\int_0^{\alpha} e^{-\omega}\, \omega^{-\frac{1}{3}}\, d\omega = \Gamma\left(\frac{2}{3}\right) I\left(\sqrt{\frac{3}{2}}\,\alpha,\ -\frac{1}{3}\right) \qquad \text{(E.14)}$$

So (E.13) becomes

$$e^{-\alpha} + \alpha^{\frac{1}{3}}\, \Gamma\left(\frac{2}{3}\right) I\left(\sqrt{\frac{3}{2}}\,\alpha,\ -\frac{1}{3}\right) - \Gamma\left(\frac{2}{3}\right) \alpha^{\frac{1}{3}} = 0.01 \qquad \text{(E.15)}$$

Using Pearson's tables, it is found that

$$\alpha = 2.29$$

Then from (IV.E.25), (E.1), and (E.12)

$$\bar{x} = \frac{5^3\ 32^{\frac{3}{2}}}{2.29} \quad \frac{1}{1152\ Re^2\sqrt{f}} = \frac{8.60}{Re^2\sqrt{f}} \qquad (E.16)$$

The maximum value of $\bar{x}$ for which the small $\bar{x}$ solutions are valid for cases two and four are given in the following table.

Re	$\bar{x}_{max}$
20,000	2.48×10^{-7}
30,000	1.19×10^{-7}
50,000	4.65×10^{-8}

It can be seen that the case two and four small $\bar{x}$ solutions are valid at somewhat greater values of $\bar{x}$ than are the case one and three solutions; however, this region of validity is still off the scale of Figures IV.C.2 and IV.C.4.

APPENDIX F

EXPERIMENTAL UNCERTAINTY

The experimental uncertainty in the wall heat flux, q''_w, and the longitudinal coordinate, $\bar{x}$, can be estimated using the method described by Kline and McClintock,[31] and basing the estimates on odds of 20 to 1.

Uncertainty in $\bar{x}$

Recall the definition of $\bar{x}$.

$$\bar{x} \triangleq \frac{x}{D_h RePr} \tag{F.1}$$

The uncertainty in D_h is ± 1 percent. The longitudinal positions of the heated cells are known within $\pm \frac{1}{32}$ inch; thus x has an uncertainty of ± 6 percent at the first heated cell, ± 0.69 percent at the fifth, and a negligible uncertainty at the downstream end of the test section. The Prandtl number uncertainty is about ± 2.5 percent. The Reynolds number is evaluated from

$$Re = \frac{\dot{m} D_h}{A_c \mu} \tag{F.2}$$

where A_c is the duct cross sectional area. The uncertainty of the air mass flow rate, $\dot{m}$, is ± 1.2 percent, and those of the flow cross sectional area and air viscosity are ± 2 percent and ± 1.5 percent, respectively. Thus the probable uncertainty in Reynolds number is ± 2.8 percent, and the uncertainty in $\bar{x}$ becomes ± 7.1 percent at the first heated cell, diminishing to ± 3.9 percent down the passage.

Uncertainty in q''_w

From the repeatability of the heat meter calibrations and the accuracy of the calibrating ammeter and voltmeters, it is felt that the heat meter sensitivities are known with a probable uncertainty of ± 5 percent. Considering the accuracy of the VTVM used for monitoring the heat meters during the tests, and the ability of the operator to "average out" slight needle fluctuations, the final uncertainty in q''_w is ± 7 percent.

APPENDIX G

SOME USEFUL CONSTANTS

There are listed here for convenience certain constants that appear in several places in the body of this work.

$$\Gamma\left(\frac{1}{3}\right) = 2.678939$$

$$\Gamma\left(\frac{2}{3}\right) = 1.354119$$

$$\Gamma\left(\frac{4}{3}\right) = 0.8929796$$

$$2^{\frac{4}{3}} = 2.519842$$

$$3^{\frac{1}{6}} = 1.200937$$

$$3^{\frac{1}{2}} = 1.732051$$

$$3^{\frac{7}{6}} = 3.602811$$

REFERENCES

1. Agrawal, H. C.; "Heat Transfer in Laminar Flow Between Parallel Plates at Small Peclet Numbers"; Applied Scientific Research, vol. A9, 1960.

2. Barrow, H.; "Convective Heat Transfer Coefficients for Turbulent Flow Between Parallel Plates With Unequal Heat Fluxes"; International Journal of Heat and Mass Transfer, vol. 1, p. 306, Jan. 1961.

3. Beckers, H. L.; "Heat Transfer in Turbulent Tube Flow"; Applied Scientific Research, vol. A6, p. 147, June 1956.

4. Berry, V. J.; "Non-Uniform Heat Transfer to Fluids Flowing in Conduits"; Applied Scientific Research, vol. A4, p. 61, 1953.

5. Berry, V. J. and de Prima, C. R.; "An Iterative Method for the Solution of Eigenvalue Problems"; Jour. Appl. Phys., vol. 23, p. 195, 1952.

6. Bodnarescu, M. V.; "Zur Theorie des Warmeubergangs in Laminarer Stromung"; VDI - Forshungsheft 450, ED. B, vol. 21, p. 19, 1955.

7. Brown, G. M.; "Heat or Mass Transfer in a Fluid in Laminar Flow in a Circular or Flat Conduit"; American Institute of Chemical Engineers Journal, vol. 6, p. 179, June 1960.

8. Butler, R. M. and Plewes, A. C.; "Evaporation of Solids into Laminar Air Streams"; Chem. Engr. Progress Symposium Series No. 10, vol. 50, p. 121, 1954.

9. Cess, R. D.; "Approximation of the Eigenvalues for Heat Transfer in Turbulent Tube Flow"; Jour. of Aero. Sciences, vol. 25, p. 723, 1958.

10. Cess, R. D.; "A Survey of the Literature on Heat Transfer in Turbulent Tube Flow"; Westinghouse Research Report 8-0529-R24, Dec. 2, 1958.

11. Cess, R. D.; "Heat Transfer in a Thermal Entrance Region for Turbulent Flow Through Flat Rectangular Ducts"; Westinghouse Research Report 405FF155-R1, 1957.

12. Cess, R. D. and Shaffer, E. C.; "Heat Transfer to Laminar Flow Between Parallel Plates With a Prescribed Wall Heat Flux"; Applied Scientific Research, vol. A8, p. 339, 1958.

13. Cess, R. D. and Shaffer, E. C.; "Laminar Heat Transfer Between Parallel Plates With an Unsymmetrically Prescribed Heat Flux at the Walls"; Applied Scientific Research, vol. A9, 1960.

14. Cess, R. D. and Shaffer, E. C.; "Summary of Laminar Heat Transfer Between Parallel Plates With Unsymmetrical Wall Temperatures"; Jour. of Aero. Sciences, p. 538, August 1959.

15. Deissler, R. G.; "Analysis of Turbulent Heat Transfer and Flow in the Entrance Regions of Smooth Passages"; NACA TN 3016, 1953.

16. Deissler, R. G.; "Analysis of Turbulent Heat Transfer, Mass Transfer, and Fluid Friction in Smooth Tubes at High Prandtl and Schmidt Numbers"; NACA Report 1210, 1955.

17. Dennis, S. C. R. and Poots, G.; "An Approximate Treatment of Forced Heat Convection in Laminar Flow Between Parallel Plates"; Applied Scientific Research, vol. A5, p. 453, 1956.

18. Does De Bye, J. A. W. van der and Schenk, J.; "Heat Transfer in Laminar Flow Between Parallel Plates"; Applied Scientific Research, vol. A3, p. 308, 1953.

19. Drew, T. B.; "Mathematical Attacks on Forced Convection Problems: A Review"; Trans. AIChE, vol. 26, 1931.

20. Dzung, L. S.; "Heat Transfer in a Flat Duct With Sinusoidal Heat Flux Distribution"; 2nd U.N. Conference on Atomic Energy, A/Conf.15/pap. 254, 1958.

21. Eckert, E. R. G. and Drake, R.; "Introduction to Heat and Mass Transfer"; 2nd Edition, McGraw-Hill Book Co., New York, 1957.

22. Graetz, L.; Annalen d. Physik (N.F.), vol. 25, p. 337, 1885.

23. Gupta, S. C.; "A Variational Principle for Fully Developed Laminar Heat Transfer in Uniform Channels I"; Applied Scientific Research, vol. A10, 1961.

24. Harrison, W. B. and Menke, J. R.; "Heat Transfer to Liquid Metals Flowing in Asymmetrically Heated Channels"; Trans. ASME, vol. 71, p. 797, 1949.

25. Hildebrand, F. B.; "Introduction to Numerical Analysis"; McGraw-Hill Book Co., New York, 1956.

26. Jacob, M.; "Heat Transfer"; vol. 1, John Wiley and Sons, New York, p. 451, 1949.

27. Jahnke, E. and Emde, F.; "Tables of Functions"; Fourth Edition, Dover, New York, 1945.

28. Jenkins, E.; "Variation in the Eddy Conductivity With Prandtl Modulus and its Use in Prediction of Turbulent Heat Transfer Coefficients"; Heat Transfer and Fluid Mechanics Institute Preprints, p. 147, 1951, Stanford Univ. Press, Stanford, Calif.

29. Jenkins, R., Brough, H. W., and Sage, B. H.; "Prediction of Temperature Distribution in Turbulent Flow"; Ind. Engrg. Chem., vol. 43, p. 2483, 1951.

30. Klein, J. and Tribus, M.; "Forced Convection From Non-Isothermal Surfaces"; ASME Paper 53-SA-46, presented at the ASME Semi-Annual Meeting, Los Angeles, Calif., June 28-July 2, 1953.

31. Kline, S. J. and McClintock, E. A.; "The Description of Uncertainties in Single Sample Experiments"; Mechanical Engineering, Jan. 1953.

32. Latzko, H.; "Der Wärmeubergang in Einer Turbulenten Flüssigkeit oder Gasstrom"; Z. angew. Math. und Mech., vol. 1, 1921, translation: NACA TM 1068, 1944.

33. Lauwerier, H. A.; "The Use of Confluent Hypergeometric Functions in Mathematical Physics and the Solution of an Eigenvalue Problem"; Applied Scientific Research, vol. A2, p. 184, 1949.

34. Leung, E. Y. W., Kays, W. M., and Reynolds, W. C.; "Heat Transfer With Turbulent Flow in Concentric and Eccentric Annuli With Constant Heat Flux"; Stanford University Department of Mechanical Engineering Thermoscience Division Report No. AHT-4, April 1962.

35. Leveque, M. A.; "Les Lois de la Transmission de Chaleur par Convection"; Annales des Mines, vol. 13, p. 201, April 1928.

36. Levy, S.; "Heat Conduction Methods in Forced Convection Flow"; Trans. ASME, vol. 78, p. 1627, Nov. 1956.

37. Lundberg, R. E., Reynolds, W. C., and Kays, W. M.; "Heat Transfer With Laminar Flow in Concentric Annuli With Constant and Variable Wall Temperature and Heat Flux"; Stanford University Department of Mechanical Engineering Thermosciences Division Report No. AHT-2, Sept. 1, 1961.

38. Milne, W. E.; "Numerical Solution of Differential Equations"; John Wiley and Sons, New York, 1953.

39. Norris, R. H. and Streid, D. D.; "Laminar Flow Heat Transfer Coefficients for Ducts"; Trans. ASME, vol. 62, p. 525, August 1940.

40. Nusselt, W.; "Der Wärmeaustausch am Berieselungskühler"; Zeit. V.D.I., vol. 67, p. 206, 1923.

41. Page, F., Corcoran, W. H., Schlinger, W. G., and Sage, B. H.; "Temperature and Velocity Distributions in Uniform Flow Between Parallel Plates"; Ind. Engrg. Chem., vol. 44, p. 419, 1952.

42. Page, F., Schlinger, W. G., Breaux, D. K., and Sage, B. H.; "Temperature Gradients in Turbulent Gas Streams. Point Values of Eddy Conductivity and Viscosity in Uniform Flow Between Parallel Plates"; Ind. Engrg. Chem., vol. 44, p. 424, 1952.

43. Pahor, S. and Strnad, J.; "A Note on Heat Transfer in Laminar Flow Through a Gap"; Applied Scientific Research, vol. A10, 1961.

44. Pearson, K.; "Tables of the Incomplete Gamma Function"; Cambridge University Press, Second Re-Issue, 1951.

45. Poppendiek, H. F.; "Turbulent Liquid-Metal Heat Transfer in Channels"; Nuclear Science and Engineering, vol. 5, no. 6, p. 390, 1959.

46. Prins, J. A., Mulder, J., and Schenk, J.; "Heat Transfer in Laminar Flow Between Parallel Planes"; Applied Scientific Research, vol. A2, p. 431, 1951.

47. Purday, H. F. P.; "Streamline Flow"; Constable and Company Ltd., London, p. 146, 1949.

48. Reynolds, W. C., McCuen, P. A., Lundberg, R. E., Leung, Y. W., and Heaton, H. S.; "Heat Transfer in Annular Passages With Variable Wall Temperature and Heat Flux"; Stanford University Department of Mechanical Engineering Report No. AHT-1, May 31, 1960.

49. Rubesin, M. W.; "The Effect of an Arbitrary Surface-Temperature Variation Along a Flat Plate on the Convective Heat Transfer in an Incompressible Turbulent Boundary Layer"; NACA TN 2345, April 1951.

50. Schenk, J.; "A Problem of Heat Transfer in Laminar Flow Between Parallel Plates"; Applied Scientific Research, vol. A4, p. 241, 1955.

51. Schenk, J.; "Heat Loss of Fluids Flowing Through Conduits"; Applied Scientific Research, vol. A4, p. 222, 1953.

52. Schenk, J. and Beckers, H. L.; "Heat Transfer in Laminar Flow Between Parallel Plates"; Applied Scientific Research, vol. A4, p. 405, 1954.

53. Schlichting, H.; "Boundary Layer Theory"; First English Edition, McGraw-Hill Book Co., New York, 1955.

54. Schlinger, W. G., Berry, V. J., Mason, J. L., and Sage, B. H.; "Temperature Gradient in Turbulent Gas Streams"; Ind. Engrg. Chem., vol. 45, p. 662, 1953.

55. Schlinger, W. G., Hsu, K. T., Caver, S. D., and Sage, B. H.; "Temperature Gradients in Turbulent Gas Streams"; Ind. Engrg. Chem., vol. 45, p. 864, 1953.

56. Seban, R. A.; "Heat Transfer to Fluid Flowing Turbulently Between Parallel Walls With Asymmetric Wall Temperatures"; Trans. ASME, vol. 72, p. 789, August 1950.

57. Sellars, J. R., Tribus, M., and Klein, J. S.; "Heat Transfer to Laminar Flow in a Round Tube or Flat Conduit - The Graetz Problem Extended"; Trans. ASME, vol. 78, p. 441, Feb. 1956.

58. Siegel, R., Sparrow, E. M., and Hallman, T. M.; "Steady Laminar Heat Transfer in a Circular Tube With Prescribed Wall Heat Flux"; Applied Scientific Research, vol. A7, p. 386, 1958.

59. Singh, S. N.; "The Determination of Eigenfunctions of a Certain Sturm-Liouville Equation and its Application to Problems of Heat Transfer"; Applied Scientific Research, vol. A7, p. 237, 1958.

60. Sleicher, C. A. and Tribus, M.; "Heat Transfer in a Pipe With Turbulent Flow and Arbitrary Wall Temperature Distribution"; Heat Transfer and Fluid Mechanics Institute Preprints, p. 59, 1956, Stanford Univ. Press, Stanford, Calif.

61. Sparrow, E. M., Hallman, T. M., and Siegel, R.; "Turbulent Heat Transfer in the Thermal Entrance Region of a Pipe With Uniform Heat Flux"; Applied Scientific Research, vol. A7, p. 37, 1957.

62. Sparrow, E. M. and Siegel, R.; "Application of Variational Methods to the Thermal Entrance Region of Ducts"; International Journal of Heat and Mass Transfer, vol. 1, p. 161, August 1960.

63. Stein, R. P.; "The Dependence of the Heat Transfer Coefficient on the Ratio of the Heat Fluxes From the Walls of Parallel Plane Flow Channels"; Reactor Heat Transfer Conf., TID-7529, 1956.

64. Sternling, C. V. and Sleicher, C. A.; "Asymptotic Eigenfunctions for Turbulent Heat Transfer in a Pipe"; Jour. of Aero. Sciences, vol. 29, no. 1, Jan. 1962.

65. Yih, C. S. and Cermak, J. E.; "Laminar Heat Convection in Pipes and Ducts"; Civil Engrg. Dept., Colorado Agricultural and Mechanical College, Fort Collins, Colorado, Report No. 5, ONR Contract No. N90nr-82401, NR 063-071/1-19-49, Sept. 1951.